

**The Role Of The DOMAIN OF UNKNOWN FUNCTION
(DUF2358) In Sugar Signalling Pathways In
*Arabidopsis thaliana***

Wardah Alhoqail

A thesis submitted for the degree of Doctor of Philosophy

School of Life Sciences

University of Essex

January 2021

Abstract

Sugars play a key role as signalling molecules to regulate metabolism and development of plants but also play a critical role in response to abiotic stresses such as drought and high salinity . This study was conducted to investigate the role of DUF2358 in sugar signalling pathways under stress conditions which affect primary metabolism. For that, we investigated the role of DUF2358 in stress signaling pathways using knockout and overexpress mutants. Drought and prolonged dark treatments were carried out followed by analysis of gene expression, metabolites and plant phenotypes. Co-IP and a yeast-two-hybrid screens were performed to identify putative interacting proteins. We demonstrated that DUF258 is localised in the chloroplast likely attached to the thylakoid membrane. Changing DUF2358 expression had no effect on plant phenotype under optimal condition. However, under starvation conditions photosynthetic electron transport was affected. At the molecular level, ABA signalling pathways are induced in the knockout plants, which may be modulated through the interaction with CLPC1 and downstream induction of ABF4 and ABF1 expression. We suggest that DUF2358 may be involved in sensing the energy status of plants, triggering signaling pathways, such as dark-induced senescence. Many of the key components altered at the transcriptional level were kinases, and therefore future studies need to focus on the activity of the key kinases and their downstream targets to assess whether DUF2358 is truly involved in the communication between chloroplast energy status and well known sugar signaling pathways.

**To my husband, my mother, and my children Hailah and Abdullah,
I Love you all...**

Acknowledgments

One of the best things that has happened in my life was studying at the university of Essex and working with some wonderful groups of people in my PhD. Foremost, I would like to express my sincere gratitude and my thanks to my supervisor Dr. Ulrike Bechtold for supporting me during my research, for her patience and constant feedback. The difficult times would be harder without her support and motivation. Thanks for guiding me over the years. Also, I would like to thank Professor Philip Mullineaux for his support, encouragement, and valuable advice all the years.

I would also like to thank all the nice members of the Plant Group for their help and support and assistance in the lab.

Finally, I would like to thank my husband Abdulmohsen, for his support and thank my family for their love and constant encouragement.

Table of contents

	Abstract	i
	Dedication	ii
	Acknowledgment	iii
	Table of contents	iv
	List of figures	x
	List of tables	xvi
	List of abbreviations	xviii
1.	General Introduction	1
1.1.	Introduction	2
1.2.	Sugar sensing and signalling mechanisms	3
1.2.1.	Hexokinase (HxK)	5
1.2.2.	TOR signalling	8
1.2.3.	Snf1-Related protein Kinases (SnRK1)	12
1.2.4.	Transcriptional regulation of sugar signalling	15
1.2.5.	Transcriptional regulation of SnRK1 under stress	17
1.3.	Abiotic stress	19
1.3.1.	Drought stress	20
1.3.1.1.	Drought stress morphological effects	21
1.3.1.2.	Abscisic acid (ABA)	22
1.3.1.3.	Reactive oxygen species (ROS)	23
1.3.1.4.	The effect of drought on photosynthesis	24
1.3.2.	Dark-induced senescence	25
1.4.	Cross-talk between signalling pathways	27
1.4.1.	Cross-talk between SnRK1 and TOR signalling pathways	27
1.4.2.	Cross-Talk Between ABA and glucose	29
1.5.	Aims and Objective	31
2.	Material and Methods	32
2.1.	Molecular Biology Technique	33
2.1.1.	Plant material and growth conditions	33
2.1.2.	Primer design	35

2.1.3.	Preparation of Culture Media	39
2.1.3.1.	preparation of 0.5 MS media for screening purposes	39
2.1.3.2.	Luria-Bertani medium (LB media)	39
2.1.3.3.	Yeast media	40
2.1.3.3.1.	Yeast peptone dextrose adenine (YPDA) media	40
2.1.3.3.2.	Synthetic dropout media	40
2.1.4.	Screening for primary transgenics on MS plates	40
2.1.5.	DNA Extraction PCR and Gel Analysis	41
2.1.6.	Polymerase Chain Reaction (PCR)	42
2.1.7.	RNA Extraction, cDNA, and Qpcr	43
2.1.8.	Crossing program	43
2.1.9.	Protein Extraction	44
2.1.10.	Western Blot	45
2.1.11.	Protoplast isolation	46
2.1.12.	Protoplast transfection	47
2.1.13.	Transient expression	47
2.1.13.1.	<i>Agrobacterium</i> electro-competent cells preparation	47
2.1.13.2.	<i>Agrobacterium</i> transformation	48
2.1.13.3.	Agro infiltration	50
2.1.14.	Chloroplast isolation	51
2.1.15.	Co-immunoprecipitation and pull-down	51
2.1.16.	Proteomics	52
2.1.17.	Plasmid construction and cloning	53
2.1.18.	Preparation of <i>E. coli</i> competent cells	57
2.1.19.	Yeast Two-Hybrid system	58
2.1.19.1.	Preparation of yeast AH109 cells	59
2.1.19.2.	Yeast transformation	60
2.1.19.3.	Screening for Protein-protein interaction	61
2.2.	Plant phenotyping and growth techniques	61
2.2.1.	Drought stress	61
2.2.2.	Dark-induced senescence	62
2.2.3.	Extended night and glucose supplementation	62
2.2.4.	Growth analysis	63

2.3.	Bioinformatics techniques	64
2.3.1.	Chlorophyll fluorescence measurements	64
2.3.2.	H ₂ O ₂ measurement	65
2.3.3.	Carbohydrate assay	66
2.3.3.1.	Carbohydrate extraction	66
2.3.3.2.	Hexose sample preparations	66
2.3.3.3.	Starch sample preparations	66
2.3.3.4.	Hexose assay	67
2.3.4.	Confocal Laser Scanning Microscopy	68
2.3.5.	RNA Sequencing (RNA-Seq)	69
2.3.5.1.	RNA-Seq data analysis	69
2.3.5.2.	Gene anthology analysis	70
2.3.6.	Metabolite analysis	70
2.3.7.	Statistical analysis	71
3.	The impact of altered <i>DUF2358</i> expression on plant growth and abiotic stress responses	72
3.1.	Introduction	73
3.2.	Results	76
3.2.1.	DUF2358 and KIN10 expression under drought conditions	76
3.2.2.	Screening <i>dufko4</i> , <i>dufko5</i> , and <i>dufko6</i>	76
3.2.3.	Screening 35S:DUF2358	78
3.2.4.	Screening of native promoter: DUF:GFP (pNAT:DUF:GFP) and native promoter: DUF (pNAT:DUF) plants in a <i>dufko3</i> background	79
3.2.5.	Screening <i>kin10-2</i> mutant	80
3.2.6.	Screening crosses plant <i>dufko3</i> with <i>kin10-2</i> (<i>dufko_kin10-2</i>)	81
3.3.	Growth Analysis	82
3.4.	Localisation of DUF2358	87
3.5.	Drought stress	89
3.5.1.	Drying rate	89
3.5.2.	Gene Expression	90
3.5.2.1.	ABA-regulated gene expression during progressive drought	93
3.5.2.2.	Sugar-responsive gene-expression during progressive drought	96

3.5.3.	Carbohydrate measurement	99
3.5.4.	H ₂ O ₂ Content	100
3.6.	Prolonged dark treatment	101
3.6.1.	The maximum efficiency of photosystem II measurement	101
3.6.2.	Gene Expression	102
3.6.2.1.	Sugar responsive genes	105
3.6.2.2.	ABA signalling genes	107
3.6.2.3.	Dark inducible genes	108
3.6.2.4.	Dark-induced leaf senescence genes	108
3.6.2.5.	Other investigated genes	110
3.7.	Sugar dark treatment	111
3.7.1.	The maximum efficiency of photosystem II Fv/Fm measurement	112
3.7.2.	Gene Expression	112
3.7.3.	Carbohydrate measurement	120
3.8.	Western Blot	122
3.9.	Conclusion	123
4.	The effect of altered DUF2358 expression on Metabolite components using Metabolomics technology	128
4.1	Introduction	129
4.2.	Results	130
4.2.1.	The maximum efficiency of photosystem II measurement	130
4.2.2.	Data filtering	131
4.2.3.	Data normalisation	132
4.2.4.	Exploratory data analysis	133
4.2.4.1.	Statistical analysis	133
4.2.4.2.	Principal component analysis (PCA)	134
4.2.4.3.	Clustering	136
4.2.4.4.	Correlation analysis	141
4.3.	Conclusion	142

5.	The effect of prolonged dark treatment on the global gene expression in Col-0 and <i>dufko3</i>	144
5.1.	Introduction	145
5.2.	Results	145
5.2.1.	Data pre-processing	145
5.2.2.	Overview of the significantly expressed group of genes	147
5.2.3.	Gene Ontology (GO) analysis of all DEGs	149
5.2.3.1.	Functional analysis of upregulated genes in <i>dufko3</i> under darkness	149
5.2.3.2.	Functional analysis of genes downregulated in <i>dufko3</i> under continuous darkness	153
5.2.3.3.	Functional analysis of genes downregulated in <i>dufko3</i> under light/dark conditions	156
5.2.4.	Dark-induced leaf senescence	157
5.3.	Conclusion	163
6.	Identification of putative DUF2358 interacting proteins	164
6.1.	Introduction	165
6.2.	Result	165
6.2.1.	DUF2358 localisation and Co-Immunoprecipitation	165
6.2.2.	Yeast-2-Hybrid (Y2H) screening of putative interaction	171
6.3.	Discussion	174
6.3.1.	DUF2358 interacts with GAPDH	174
6.3.2.	DUF2358 interacts with CLPC1B	175
6.3.3.	DUF2358 interacts with CAS	176
6.3.4.	DUF2358 interacts with CA	177
6.4.	Conclusion	178
7.	Final discussion	179
7.1.	Overview of the outcomes of this study	180
7.2.	Putative involvement of DUF2358 in plant light signal transduction	182
7.3.	Involvement of DUF2358 in sugar-signalling and dark-induced senescence pathways	183

7.4.	Involvement of DUF2358 in ABA signalling pathways	186
7.5.	Conclusion	187
	References	189
	Appendices	215

List of figures

Figure 1.1.	Outline of sugar and energy-sensing and signalling models in <i>Arabidopsis</i> .	5
Figure 1.2.	TOR signalling pathway in plants (McCready et al., 2020)	11
Figure 1.3.	A starvation response gene networking in <i>Arabidopsis thaliana</i> (Bechtold et al., 2016, unpublished network).	19
Figure 1.4.	Genetic overview of interactions between Sugar and Hormone Signalling in <i>Arabidopsis</i> . Scheme resource (Ramon et al., 2008).	30
Figure 2.1.	DUF2358- Overexpression construct map (<i>DUFOE</i>).	34
Figure 2.2.	pNAT:DUF2358:GFP- construct maps.	35
Figure 2.3.	Plasmid map of pUBQ:DUF2358::GFP and pBIN61-p19.	50
Figure 2.4.	Localisation of N-terminal region of <i>starch synthase 4</i> SS4 fused to GFP in <i>Nicotiana benthamiana</i> chloroplasts. (Gámez-Arjona et al., 2014).	50
Figure 2.5.	Yeast two-hybrid vectors.	55
Figure 2.6	Overview of yeast two-hybrid (Y2H) GAL4 system (Folter and Immink, 2011).	59
Figure 3.1.	DUF2358 and KIN10 expressions under drought stress.	76
Figure 3.2.	PCR confirmation of T-DNA in <i>dufko4</i> plants.	77
Figure 3.3.	Fold change of relative gene expression of <i>DUFOE1</i> , <i>DUFOE2</i> , <i>DUFOE3</i> , and <i>DUFOE4</i> .	78
Figure 3.4.	Fold change of relative gene expression of <i>dufko3</i> , pNAT:DUF:GFP and pNAT:DUF compared with Col-0.	79
Figure 3.5.	Detection of GFP expression by Western blot analyses for pNAT:DUF:GFP protein samples, stop codon (TGA) were detected in pNAT:DUF:GFP.	80
Figure 3.6	PCR confirmation of T-DNA in <i>kin10</i> plants.	81
Figure 3.7.	PCR screening of crossed plant (<i>duf_kin10-2</i>).	82

Figure 3.8.	All germination and growth stages for all the genotypes compared with Col-0 under normal conditions.	84
Figure 3.9.	Total averages of exposed leaf area measured in mm ² .	85
Figure 3.10.	Flower stem length is measured in cm.	86
Figure 3.11.	Principal growth stage 3.	86
Figure 3.12.	Principal growth stage 5.	86
Figure 3.13.	Seed weight in gm for each genotype.	87
Figure 3.14.	Plant on the 25th day from sowing the plants.	87
Figure 3.15.	Plasmid map of pUBQ:DUF2358::GFP.	88
Figure 3.16.	Drying rates were determined as the slope of the decrease in soil water. protoplast transfection with Ct pUBQ:DUF:GFP.	90
Figure 3.17.	KIN10 expression in <i>dufko</i> under control condition.	92
Figure 3.18.	Normalised DUF2358 and KIN10 gene expressions under well-watered and drought conditions	93
Figure 3.19.	Normalised gene expressions for ABA-related genes under well-watered and drought conditions..	95
Figure 3.20.	Normalised gene expressions for sugar-responsive genes under well-watered and drought conditions for Col-0 plants and mutants.	97
Figure 3.21.	Normalised gene expression of different investigated genes (ACR5, ACR9, PLP2, and ATRRP4) in Col-0 and all mutant genotypes subjected to drought stress.	99
Figure 3.22.	Analysis of soluble sugar levels in Col-0 and mutant genotypes subjected to drought stress.	100
Figure 3.23.	Analysis of hydrogen peroxide levels in Col-0 and mutant genotypes subjected to drought stress.	101
Figure 3.24.	Time course of Fv/Fm averages of Col-0, <i>dufko3</i> , and pNAT:DUF kept in darkness for nine days, False colour image of Fv/Fm values after nine days of darkness.	102

Figure 3.25.	Normalised gene expression of DUF2358, KIN10, and sugar-responsive genes in Col-0 and all mutant genotypes subjected to 9 days of darkness.	106
Figure 3.26.	Normalised ABA signalling gene expressions after nine days of darkness	107
Figure 3.27.	Normalised DIN6 gene expressions after nine days of darkness.	108
Figure 3.28.	Normalised gene expressions involved in dark-induced leaf senescence after nine days of darkness.	110
Figure 3.29.	Normalised gene expression after nine days of darkness of ACR5, MPK5, AT1G12790, and UMAMIT33.	111
Figure 3.30.	Fv/Fm for <i>dufko3</i> mutant, <i>DUFQE</i> mutant, and Col-0 after four hours of different treatments.	112
Figure 3.31.	Normalised gene expression of DIN6, SEN5, and AXP in Col-0 and all mutant genotypes subjected to 4 hours of darkness.	114
Figure 3.32.	Normalised gene expression of AT4G25580 and ATTPS5 in Col-0 subjected to 4 hours of darkness.	115
Figure 3.33.	The content of soluble sugar and starch in Col-0, <i>dufko3</i> , <i>DUFQE3</i> under the treatments.	121
Figure 3.34.	Western blot analysis of the protein from different genotypes with different antibodies: Rubisco, the Calvin-Benson cycle proteins(CB) Transketolase 5 (TK), FBP aldolase (FBPA), the photosystem I(PS1) PsaA, Lhca1 proteins, and the electron transport (ET) cytochrome b6 Cytb6 and RieskeFeS proteins.	122
Figure 4.1.	Bars compare Fv/Fm averages between the three genotypes for four days.	131
Figure 4.2.	Box plot and kernel density plots of the top 50 features before and after normalisation.	133
Figure 4.3.	Significant features across the three genotypes and two treatments above a threshold of $p < 0.01$.	134

Figure 4.4.	Scree plot showing the five significant principal components with total accumulative variance and individual variance explained.	135
Figure 4.5.	PCA plot of Col-0 <i>dufko3</i> and pNAT:DUF significant metabolites under light and dark conditions.	136
Figure 4.6.	Heatmap generated hierarchical clustering using Euclidean distance measure and the Ward clustering algorithm.	137
Figure 4.7.	Box plots summarising the normalised sugar concentrations of (A) sucrose, (B) glucose, (C) mannose, and (D) galactose in Col-0 and mutants.	139
Figure 4.8.	Box plots summarising the normalised amino acid concentrations of (A) leucine, (B) serine, and (C) aspartic acid in Col-0 and mutant under light and dark conditions.	141
Figure 4.9.	Heat map generated using the Pearson correlation matrix of significant metabolites under both light and continuous dark treatments in Col-0 <i>dufko3</i> and pNAT:DUF.	142
Figure 5.1.	Mean-variance trend of filtered counts with a cutoff: cpm = 1 in at least 1 sample.	146
Figure 5.2.	Venn diagram illustrates the overlapping between upregulated and downregulated genes under dark and no stress conditions.	149
Figure 5.3.	Venn diagram illustrates unique and common upregulated genes under dark and light/dark conditions.	150
Figure 5.4.	The most significant gene ontology enrichment of biological processes for upregulated genes in <i>dufko3</i> under dark conditions compared to Col-0.	151
Figure 5.5.	Log ₂ fold change (<i>dufko3</i> /Col-0) unique genes under dark conditions, response to ABA-associated genes.	151
Figure 5.6.	Log ₂ fold change (<i>dufko3</i> /Col-0) genes under dark conditions, senescence-associated genes.	152
Figure 5.7.	Gene ontology enrichment map of the molecular function of upregulated genes under dark conditions.	152

Figure 5.8.	Log ₂ fold change (<i>dufko3</i> /Col-0) of chloroplast and thylakoid membrane-associated genes.	154
Figure 5.9.	Summary of biological processes significantly enriched in the downregulated group of genes in the <i>dufko3</i> under prolonged dark treatment.	155
Figure 5.10.	Summary of molecular function significantly enriched in the downregulated group of genes in the <i>dufko3</i> under dark conditions.	155
Figure 5.11.	Venn diagram illustrates unique and common downregulated genes under dark and light/dark conditions.	156
Figure 5.12.	Summary of molecular function significantly enriched in the downregulated group of genes in the <i>dufko3</i> under light/dark conditions.	157
Figure 5.13.	Dark-induced leaf senescence-associated genes expression for <i>dufko3</i> vs. Col-0 under dark conditions.	158
Figure 5.14.	Dark-induced leaf senescence-associated genes expression for <i>dufko3</i> vs. Col-0 under light/dark conditions.	159
Figure 5.15.	The molecular regulatory network under light and energy deprivation-induced leaf senescence. The graph was generated using the information from Liebsch and Keech (2016).	161
Figure 6.1.	Plasmid map of pUBQ:DUF2358::GFP and Plasmid map of pBIN61-p19.	167
Figure 6.2.	Transient expression of Ct-DUF::GFP (A-C, G-I), Nt-GFP::SS4 (D-F), and P19 (J) in <i>Nicotiana benthamiana</i> chloroplasts.	168
Figure 6.3.	GFP expression after chloroplast isolation.	169
Figure 6.4.	Yeast-two-hybrid plate screening results for different putative DUF2358 interacting proteins.	174
Figure 7.1.	The molecular regulatory network under light and energy deprivation-induced leaf senescence, including our suggestion of	188

the involvement of DUF2358 in the dark-induced senescence and regulating KIN10 activity. The graph was generated based on the information from Liebsch and Keech (2016).

List of Tables

Table 2.1.	List of T-DNA and Overexpression mutant lines that were screened to identify loss of function, overexpression and native promoter mutants.	33
Table 2.2	List of all primers and templates which were used in this study.	36
Table 2.3.	Restriction enzymes (RE) were used for cloning system in this study.	56
Table 2.4.	Generated Prey and Bait constructs of <i>Nicotiana benthamiana</i> and <i>Arabidopsis thaliana</i> proteins were used to conduct yeast-2-hybrid system.	57
Table 2.5.	Arabidopsis Growth Stages for the Soil-Based Phenotypic Analysis Platform. Table based on Boyes <i>et al.</i> , 2001.	63
Table 3.1.	Direct and indirect targets genes of DUF2358 main information.	90
Table 3.2.	Investigated genes under nine days of darkness.	103
Table 3.3.	Overlap between the drought time series dataset (Bechtold <i>et al</i> 2016) and KIN10 regulated genes (KIN10 over-expressing plants; Baena González <i>et al</i> 2007).	116
Table 3.4.	Overview of all of qRT-PCR stress treatments.	124
Table 3.5.	Overview of all of qRT-PCR control experiments.	126
Table 4.1	Summary of the initial data processing results.	132
Table 5.1.	Summary of alignments for each sample in this chapter compared to <i>Arabidopsis thaliana</i> Col-0.	147
Table 5.2.	All significant genes which were expressed under non-stress and dark conditions.	148
Table 5.3.	Summary of the cellular compartment significantly enriched in the downregulated group of genes in the <i>dufko3</i> under prolonged dark treatment.	153
Table 5.4.	GO term associated with aging and senescence-related processes for a downregulated group of genes in <i>dufko3</i> under light/dark conditions.	156
Table 5.5.	Dark-induced leaf senescence-associated gene expressions for <i>dufko3</i> vs. Col-0 under dark and light/dark conditions.	159

Table 5.6.	Comparison of the fold expression results from RNA-seq and fold expression from prolonged dark treatment gene expression using qPCR.	162
Table: 6.1.	Proteins were detected after co-immunoprecipitation with GFP antibody.	170
Table 6.2.	Yeast-two-hybrid results in putative DUF2358 interacting proteins.	172

List of abbreviations

°C	Degree Celsius
µg	Microgram
µl	Microliter
µmol	Micromoles
µmol.m ⁻² s ⁻¹	Micromole: per second and square meter
ABA	Abscisic acid
AD	Activation domain
AgriGo	GO Analysis Toolkit and Database for Agricultural Community.
BD	DNA-binding domain
BLAST	Basic Local Alignment Search Tool
Bp	base pair
cDNA	Complementary DNA
Cm	Centimeter
CO ₂	Carbon dioxide
Col-0	Columbia-0
C-terminal	Carboxy Terminal of amino acid chain of protein or polypeptide
D	Dark
DEGs	differentially expressed genes
DG	Dark with glucose treatment
DNA	Deoxyribonucleic acid
dNTPs	deoxyribonucleotide triphosphate
Dr	Drought
<i>E. coli</i>	<i>Escherichia coli</i>
FC	field capacity
Fv/Fm	The maximum efficiency of photosystem II
g	Relative centrifugal force
GFP	green fluorescent protein
gm	Gram
Go	Gene ontology
H ₂ O ₂	Hydrogen peroxide
L	Liter

L	Light
LB	Left border of T-DNA
LG	light with glucose treatment
LHCs	light-harvesting complex.
Log	Logarithm
M	Molar
ml	Milliliter
mM	Millimolar
N-terminal	start of protein or polypeptide
OD ₆₀₀	Optical density of a sample measured at a wavelength of 600 nm
PCR	Polymerase chain reaction
pH	potential of hydrogen
PPFD	Photosynthetic photon flux density
PSII	photosystem II
PSI-RC	photosystem I reaction center
p-value	probability value
PVDF membranes	Polyvinylidene fluoride membranes
qRT-PCR	Real-Time Quantitative Reverse Transcription PCR
RNA	Ribonucleic acid
RNA-seq	RNA-sequencing
ROS	Reactive oxygen species
Rpm	Revolutions per minute
rSWC	Relative soil water content
SEA	Singular enrichment analysis
T-DNA	transfer DNA
V	Volume
VBSSM	Variational Bayesian State-Space Modelling
W	Weight
WT	Wild type
ww	Well-watered
Y2H	Yeast Two-Hybrid system

Chapter 1

General Introduction

1.1. Introduction

Sugars are final products of photosynthesis and are important components in plant cells because they play multiple roles in many vital processes. They play an essential regulatory role in plant developmental processes such as germination, growth, seedling establishment, flowering, and senescence (Rolland *et al.*, 2002, 2006; Rosa *et al.*, 2009; Smeekens *et al.*, 2010; Cordoba *et al.*, 2015). Sugars also provide carbon skeletons, which are essential structural components and energy sources (Gómez-Arjona *et al.*, 2014). Moreover, they play a vital role in carbon and nitrogen metabolism, sensing and signalling in plants (Rolland *et al.*, 2006), and also play a significant role in controlling many metabolic processes such as photosynthesis (Rosa *et al.*, 2009; Lastdrager *et al.*, 2014), starch synthesis and starch dissolution (Baena-González *et al.*, 2007).

When plants are exposed to environmental stress, sugars are essential for plants to adapt and survive (Couée *et al.*, 2006; Yamada and Osakabe, 2018). It is, therefore, important to understand how plants sense and respond to different environmental stresses that compromise photosynthesis and respiration to achieve optimal use of energy supplies. In general, plants tend to control and regulate sugar consumption by suppressing plant growth and enhancing cell activities, such as respiration and basic vital processes, under stress conditions (Rolland *et al.*, 2006; Law *et al.*, 2018).

Under environmental stresses such as drought and deficiency of nutrient, sucrose and other soluble sugars accumulate. Soluble sugars acclimation accrues as a result of the reduction of carbon utilisation which caused by the decrease in the growth rate (Nuccio *et al.*, 2015; Thalmann and Santelia, 2017). Soluble sugars act as signalling molecules identified by special signal pathways and regulate anabolism and

catabolism processes to maintain the balance of energy (Li and Sheen, 2016). Different stresses affect plants in different ways; for example, drought and salinity cause an increase in sucrose concentrations (Almodares *et al.*, 2008; Henry *et al.*, 2015; Nuccio *et al.*, 2015), while high light and heavy metals cause a decrease in soluble sugar concentrations (Gill *et al.*, 2001). Different sugars play different roles in plant metabolism under stress; for example, sucrose and glucose support cellular respiration and maintain cellular homeostasis (Gupta and Kaur, 2005; Cho *et al.*, 2007) and regulate sugar metabolites, along with its interacting with ABA and ethylene signalling pathways (Cho and Yoo, 2007). Under stress condition, sugar metabolism, such as photosynthesis and respiration is a dynamic system that contains various syntheses and breaks down a wide variety of components (Rosa *et al.*, 2004; Rosa *et al.*, 2009). Changes in soluble sugar concentration under environmental stress usually include changes in CO₂ assimilation, enzyme activity, and expression of related genes (Gupta and Kaur, 2005; Rosa *et al.*, 2009).

1.2. Sugar sensing and signalling mechanisms

Plant growth and development need energy, which is produced by photosynthesis, a process that uses light to convert CO₂ into carbohydrates, which are used during a plant's vital processes or stored in the form of starch to be used at a time of need. In addition to their role as an essential source of energy, carbohydrates also play a fundamental role in plants as signalling molecules (Smeekens, 2000; Morkunas *et al.*, 2012). Different signals are produced by sugars to modify plant growth, development, productivity, and response to different stress. Environmental stresses such as drought alter the sugar levels in plants as a result of the decrease in plant growth, which

acclimates soluble sugars (glucose, fructose, and sucrose), which induce oxidative damage (Mohammadkhani and Heidari, 2008; Rosa, 2009; Arabzadeh, 2012). There is extensive interaction between sugar and hormone signalling in plants. Hexokinase (HXK) is the conserved glucose sensor. Also, Snf1-related kinases (SnRKs) play an important role as a sugar sensor and trehalose metabolism in sugar signalling (Rolland *et al.*, 2006). At the transcriptional level, it has been shown that sugar regulates the expression of many genes. More than 1,800 genes are differentially expressed (repressed or induced) in response to sugar (Cordoba *et al.*, 2015) which will be discussed in more detail below

Plant cells can sense and react to many metabolic signals, including hexoses such as glucose and fructose, utilising many different signalling pathways such as Hexokinase HXK-dependent and Hexokinase HXK-independent pathways, protein kinases KIN10/11, and Target of Rapamycin (TOR) signalling, all of which will be discussed in more detail below (Figure 1.1).

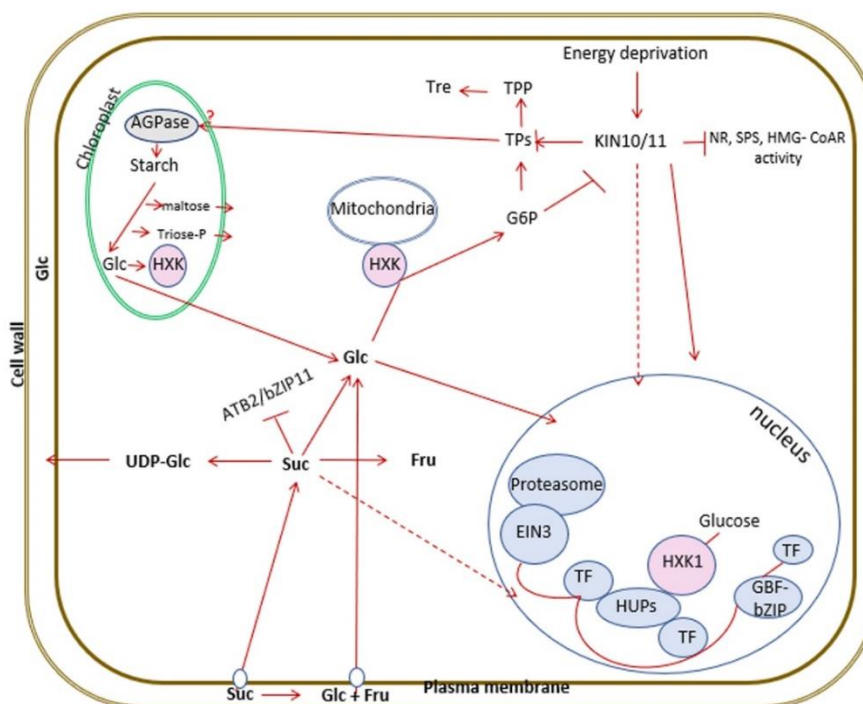


Figure 1.1. Outline of sugar and energy-sensing and signalling models in Arabidopsis. (G6P) Glucose 6-phosphate, (Tre) trehalose, (T6P) trehalose-6-phosphate, (TPP) T6P phosphatase, T6P synthase (TPS), (Glc) Glucose, (Fru) Fructose, (NR) nitrate reductase, (SPS) sucrose phosphate synthase, and (HMG-CoAR) 3-hydroxy-3-methylglutaryl-coenzyme A reductase. Glc involves in metabolism after being phosphorylated by HXK. KIN10/11 play an important role in energy signalling, regulating enormous reprogramming processes of transcription through bZIP TFs, and controlling enzymes. KIN10/11 activities are inhibited by sugar phosphates particularly by G6P. Tre metabolism play a key regulatory role intermediated by T6P synthase (TPS) and T6P phosphatase (TPP) enzymes. T6P Also play an important role as regulatory signalling molecule. G-protein coupled receptor signalling by RGS1 and GPA1 involve in the sensing of extracellular glucose and sugar signalling by THF1 which is in the plastids. Sucrose inhibits ATB2/bZIP11 TF. This role is only exaptational to transported sucrose and not triggered by sucrose hydrolysis products Glc and Fru. This scheme was drawn based on the information from Ramon *et al.* (2008).

1.2.1. Hexokinase (HxK)

Hexose sugars are phosphorylated before they can be used in metabolic processes. There are two families of enzymes that can phosphorylate glucose and fructose in plants, namely hexokinases (HXKs) and fructokinases (FRKs) (Granot *et al.*, 2013;

Aguilera-Alvarado and Sánchez-Nieto, 2017). In *Arabidopsis thaliana*, there are three HXKs, which are catalytic active (AtHXK1, AtHXK2, and AtHXK3), whereas Hexokinase-Like (AtHXL1, AtHXL2, and AtHXL3) genes do not possess catalytic activity (Karve *et al.*, 2008). Different isoforms of hexokinase in *Arabidopsis* are located in different subcellular compartments and can be found in the outer mitochondrial membrane (Karve *et al.*, 2008), in plastids (Granot, 2007), and even the nucleus as part of high-molecular-weight complexes (Cho *et al.*, 2006).

HXKs functions are evolutionarily conserved in many organisms but play different roles in plants compared to their role in heterotroph organisms (Cho *et al.*, 2010; Karve *et al.*, 2010; Kim *et al.*, 2013). In plants, HXK contributes to the breakdown of sucrose and starch into hexoses, thereby reintroducing hexoses into a hexose phosphate pool, which is constituted of three metabolic factors, namely glucose 6-phosphate, glucose 1-phosphate, and fructose 6-phosphate (Paul *et al.*, 2001). HXKs are also part of sucrose and starch synthesis processes and are considered to be part of the mechanism that senses carbohydrate status and regulates the resource allocation in plants (Paul *et al.*, 2001; Granot *et al.*, 2013). The contribution to both breakdown and synthesis of starch suggests that HXKs are closely linked to the sensing and regulating carbohydrate levels in plants (Paul *et al.*, 2001; Kunz *et al.*, 2015). Hexokinase was the first glucose sensor to be recognised to act as a multiple function protein involved in sugar sensing and regulatory functions in plants and yeast (Ramon *et al.*, 2008; Cho *et al.*, 2010; Aguilera-Alvarado and Sánchez-Nieto, 2017). For example, AtHXK1 regulates the availability of sugar during plant development and promotes cell expansion and growth under light conditions (Moore *et al.*, 2003; Rolland *et al.*, 2006; Ramon *et al.*, 2008; Cheng *et al.*, 2011). HXK1 signalling can either promote or represses plant growth, depending on the glucose concentration and plant sensitivity

for glucose (Akpinar *et al.*, 2012). Under high internal glucose concentrations, some photosynthetic gene expressions are suppressed by HXKs' dependent signalling pathways (Moore *et al.*, 2003; Rolland *et al.*, 2006).

In recent years, the enzymatic hexose-phosphorylation activity, and sugar sensing roles of HXK1, have been shown to be independent of each other (Moore *et al.*, 2003; Cho *et al.*, 2006). This knowledge was derived from studying mutant lines under specific conditions and has helped to understand the mechanisms and functions of these genes. For example, the AtHXK1 loss-of-function2 mutant (*gin2*) was identified by a mutant screen using high concentrations of glucose. Normally, high glucose concentrations inhibit plant growth by activating ABA biosynthesis and the ABA signalling pathway, which leads to vegetative stress response (Rolland *et al.*, 2002; Rolland and Sheen, 2005). However, the mutants were able to grow normally under high glucose concentration compared to the wild-type and were referred to as glucose insensitive 2 (*gin2*) (Moore *et al.*, 2003). The *gin2* mutants are catalytically inactive but still promote many signalling functions in gene expression, reproduction of the root cells, and leaf growth and senescence (Moore *et al.*, 2003). In addition, *gin2* is insensitive to auxin and hypersensitive to cytokinin (Rolland and Sheen, 2005).

On the other hand, plants that are hypersensitive to glucose (*glo*) are more strongly inhibited by glucose compared to the wild-type. It has been reported that ethylene-insensitive mutants such as *etr1-1*, *ein2*, as well as *mkk9*, showed glucose hypersensitivity, which is a *glo* phenotype (Ramon *et al.*, 2008).

AtHXK1 (S177A and G104D): two catalytically inactive alleles of HXK1 (Moore *et al.*, 2003; Feng *et al.*, 2015) restore glucose phenotype in *gin2*. S177A and G104D can mediate repression of chlorophyll accumulation by glucose and photosynthetic gene

expression (Cho *et al.*, 2010). In glucose-insensitive mutant5 (*gin5*), the characterisation of this mutant shows that glucose-specific accumulation of ABA is fundamental for the glucose response mediated by hexokinase (Gibson 2005; Karve *et al.*, 2012; Yuan *et al.*, 2014). On the other hand, glucose-insensitive mutant 6 (*gin6*) inhibit the expression of the ABA INSENSITIVE4 (ABI4) transcription factor, which is involved in seed-specific ABA responses. This suggests that ABI4 is a regulator involved in glucose and seed-specific ABA signalling pathways (Arenas-Huertero *et al.*, 2000). Together, these results prove HXK1 to be a glucose sensor in plants.

AtHXK1 is also involved in stomatal closure, either directly through ABA signalling in guard cells, or indirectly via its effect on photosynthesis. For example, AtHXK1 overexpression in guard cells of Arabidopsis caused the induction of ABA-responsive genes ARABIDOPSIS RAB GTPASE HOMOLOG B18 (RAB18) and ABA INSENSITIVE5 (ABI5), which induced stomatal closure (Kelly *et al.*, 2013). Similarly, when photosynthetic activity increased, for example, under high light, HXK induced stomatal closure as a result of sensing an excess of sugars, thus highlighting the important role of HXK in regulating photosynthetic activity (Kelly *et al.*, 2012).

1.2.2. TOR signalling

The target of rapamycin (TOR) kinase is a serine-threonine protein kinase (PK), and major regulator of plant growth by preserving energy and maintaining metabolic homeostasis in many organisms (Xiong and Sheen, 2012; Margalha *et al.*, 2019; Fu *et al.*, 2020). It is evolutionarily conserved in yeast, plants, and animals. Rapamycin is a natural antibiotic which is produced in the soil by *Streptomyces hygroscopicus* bacteria. The rapamycin antibiotic can inhibit the activity of TOR protein kinase in yeast and

mammals (Xiong and Sheen, 2015; Shi *et al.*, 2018) but not in plants when used at the same concentration, and therefore plant TOR is insensitive to rapamycin (Dobrenel *et al.*, 2011). TOR plays a role in nutrient sensing and signalling in all eukaryotes (Shi *et al.*, 2018).

In plants, TORC1 complex consists of REGULATORY-ASSOCIATED PROTEIN OF TOR (RAPTOR) and LETHAL WITH SEC THIRTEEN 8 (LST8) proteins (Ryabova *et al.*, 2019). TORC1 in *Arabidopsis thaliana* consists of one copy of TOR, two copies of Raptor (A and B), and two copies of LST8 (LST8-1 and LST8-2) (Moreau *et al.*, 2012)

TORC1 is activated by nutrients and growth factors such as phytohormones while inactivated by energy deprivation and starvation (Shi *et al.*, 2018).

TOR plays an important role in linking the energy/nutrient status of plants with environmental signalling, which gives the plant the ability to survive under stress conditions (Baena-González and Hanson, 2017; Shi *et al.*, 2018; Xiong and Sheen, 2012). In *Arabidopsis* TOR mutants, it has been suggested that there is an association between TOR signalling cell size, seed size, and yield, as well as stress resistance regulating plant growth and development under stress conditions (Ren *et al.*, 2011; Deprost *et al.*, 2007). The TOR signalling pathway plays a key role in protein synthesis by controlling translational processes through phosphorylation RIBOSOMAL S6 KINASES, which depends on the energy supplies and nutrient availability (Roux and Topisirovic, 2012; Xiong and Sheen, 2012). It is also an important part of the auxin signalling pathway, linking hormone and nutrient signalling pathways (Henriques *et al.*, 2014), although the link between auxin and TOR signalling has been debated. A study by Xiong *et al.* (2013) reported that auxin signalling is separate from TOR activation in *Arabidopsis*. However, Deng *et al.* (2016) reported that TOR affects auxin

concentration and response in plants, and therefore is crucial for auxin signalling transduction in *Arabidopsis*.

A recent study revealed that TOR signalling plays fundamental roles in the transcriptional regulation of a wide range of genes, which are involved in metabolism, cell division, and transcription, and represses many genes which are associated with responses to pathogen or defence elicitors (De Vleeschauwer *et al.*, 2018). Consequently, TOR overexpression lines show a high level of sensitivity to bacterial and fungal pathogens by reducing the activity of defence hormones, such as salicylic acid and jasmonic acid. On the other hand, when TOR signalling is reduced, it promoted plant resistance to bacterial and fungal pathogens (De Vleeschauwer *et al.*, 2018).

Utilising the rapamycin-sensitive binding protein 12-2 (BP12-2 express yeast FK506 Binding Protein12) and the active-site TOR inhibitors (asTORia), showed that combining the treatment removes the correlation of TOR activity and plant growth in *Arabidopsis* (Xiong *et al.*, 2017). Therefore, TOR signalling plays an important role during the transition stages from heterotrophic to photoautotrophic growth in *Arabidopsis thaliana* (Xiong *et al.*, 2017).

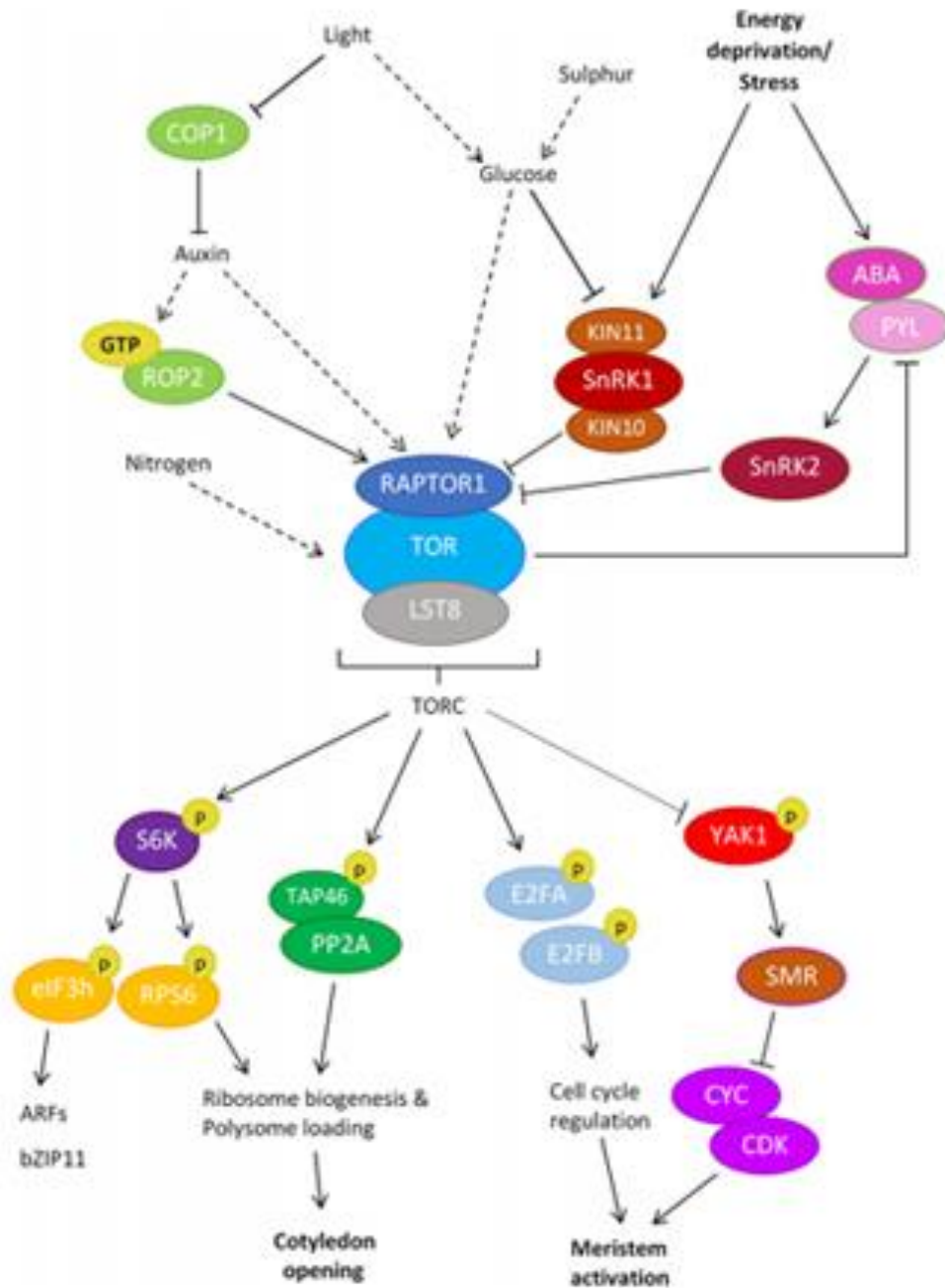


Figure 1.2. TOR signalling pathway in plants (McCready et al., 2020) The figure illustrates up- and downstream of TOR Complex (TORC) signalling in plants. Light, glucose and nutrients activate TOR pathway. Light negatively regulate COP1 which is also a negative regulator of TOR which leads to activate TOR through the activation of the auxin pathway. Light and glucose inactivate SnRK1 which lead to indirect activation of TORC. While stress induce SnRK2s through the bind ABA and PYL receptors. TORC1 phosphorylate its targets either directly for E2FA/B and S6K or indirectly for PP2A (via the subunit TAP46). The phosphorylation of TORC targets lead to the activation of cellular processes which are important for plant development .figure source (McCready *et al.*, 2020).

TOR signalling is activated when nutrient supplies, essential for protein synthesis, decrease in plant cells. TOR signalling prevents autophagy and promotes protein biosynthesis. Processes that are enhanced or inhibited through TOR signalling pathways are illustrated in Figure (1.2.) Glucose produced by photosynthesis drives (TOR) signalling relays through glycolytic processes and mitochondrial bioenergetics to control root growth and control the activity of meristem. This is separated from glucose sensing, growth hormone signalling, and stem-cell maintenance. Consequently, Glucose-TOR signalling affects a wide range of genes, which are involved in primary and secondary metabolism, signalling, transcription, transport, and protein folding (Xiong *et al.*, 2013).

1.2.3. Snf1-Related protein Kinases (SnRK1)

The second central nutrient-sensing kinase is the protein kinase complex SnRK1 (Snf1-Related protein Kinase 1), also known as KIN10 and KIN11. When carbon concentration decreases, SnRK1 is activated in order to enhance saving energy and nutrient recovery. (Baena-González and Sheen, 2008; Crozet *et al.*, 2014; Broeckx *et al.*, 2016; Hamasaki *et al.*, 2019; Margalha *et al.*, 2019). Their main role is to regulate the transcription network during sugar starvation and stress conditions (Ramon *et al.*, 2008). SnRK1 proteins are evolutionarily conserved protein kinases in plants. Protein kinase complexes composed of three subunits. the first one α subunit which has catalytic activity and perform the most activity of the protein. α subunit is encoding by three genes in Arabidopsis. The other subunits in protein kinases are β , and γ which are regulatory subunits (Jossier *et al.*, 2009). SnRK1 α 1 (KIN10/AKIN10), SnRK1 α 2

(KIN11/AKIN11), and SnRK1 α 3 (KIN12/AKIN12) (Margalha *et al.*, 2019) and they are orthologs of the yeast and mammalian (Halford *et al.*, 2003; Halford and Hey, 2009).

The SnRK1 complex contains two homologs of α -subunits, which are composed of a catalytic domain (with T-loop) and a regulatory domain, β -subunit and γ -subunit (Crozet *et al.* 2014). The catalytic α -subunit is encoded by SnRK1 α 1 (AKIN10, AT3G01090) and SnRK1 α 2 (AKIN11, AT3G29160) (Nukarinen *et al.*, 2016). Sugar phosphates regulate SnRK1 activity in plants by controlling the activity and the phosphorylation status in the T-loop of the catalytic alpha subunits by adjusting ATP production or by increasing the consumption of ATP (Crozet *et al.*, 2014; Ghillebert *et al.*, 2011). This phosphorylation is acquired by upstream kinase, post-translational modifications, various metabolites, and hormones (Crozet *et al.*, 2014). Glucose-6-phosphate (G6P), glucose-1-phosphate (G1P), trehalose, and trehalose-6-phosphate (T6P) repress the activity of SnRK1 (Baena-González *et al.*, 2007; O'Hara *et al.*, 2013). Undergrowth conditions where sugars are not limiting SnRK1 activity is suppressed (Lastdrager *et al.*, 2014).

The SnRK1 signalling network impacts many aspects of plant development from germination to senescence (Baena-González and Hanson, 2017). It also regulates the catabolism and anabolism processes of sugars and controls transcriptional responses to maintain cell homeostasis. Both KIN10 and KIN11 have been found in the nucleus and cytoplasm. However, at the molecular level, KIN10 is expressed largely in shoot and root tissues, while KIN11 is limited to a small subset of tissues such as the hydathodes, vascular tissues, and leaf primordia (Williams *et al.*, 2014).

Overexpression of both kinases has led to distinct and sometimes opposite phenotypes. While flowering is delayed by KIN10 overexpression, KIN11

overexpression leads to early flowering (Williams *et al.*, 2014). Protein kinase mutants KIN10 and KIN11 both work on a wide group of genes. The expressions of more than 1000 genes are affected by KIN10 overexpression, either by transcriptional repression or activation. Consequently, enhancing catabolism and reducing the anabolism (Price *et al.*, 2004).

KIN10/11 targets a wide range of signalling and regulatory factors, together with many developmental changes associated with SnRK1 signalling (Baena-González *et al.*, 2007). They coordinate and reprogram many transcription processes. According to Chan *et al.* (2017), FUSCA3 (FUS3) is a transcription factor. Transcription factors regulate gene expressions by regulating transcription of DNA by binding to specific DNA sequences (more detailed in 1.2.4). FUS3 regulates seed maturation in Arabidopsis, and this transcription factor is phosphorylated by AKIN10/SnRK1 α . During embryogenesis, AKIN10 and FUS3 expression patterns overlap. As a result, Chan *et al.* (2017) suggest that FUS3 phosphorylation by SnRK1 is essential during early embryogenesis. SnRK1 controls the expression of these genes through phosphorylation, which contributes to metabolism, signalling pathways, transcription factors, and stress resistance in order to maintain cellular homeostasis during environmental stress conditions (Baena-González and Sheen, 2008). This kinase helps to adjust the energy balance by reprogramming metabolism, which is important for plant adaptation to environmental stress. It also affects photosynthesis through increased ATP production through the transduction of intracellular ATP signals (Baena-González and Sheen, 2008). In general, when KIN10/11 are activated, this leads to the beginning of the reprogramming processes, which save the plant energy by suppressing biosynthetic pathways such as protein synthesis and enhancing

catabolic processes such as protein degradation. This leads to an increase in the production of adenosine triphosphate ATP (Ramon *et al.*, 2008).

When SnRK1 senses the lack of energy due to the decrease in photosynthesis, which is associated with stress conditions or extended darkness, it activates specific transcription factors such as basic leucine zippers (bZIPs), which lead to transcriptional changes that aim to establish sugar homeostasis (Baena-González *et al.*, 2007). Usadel *et al.* (2008) illustrated that KIN10/11 are hypersensitive to the change in carbon levels, even small changes that are experienced during nighttime. Regarding the connection between hexokinase HXK and SnRK1, both sucrose and glucose can inhibit SnRK1 target genes which are mainly stress responsive genes. Also, the glucose metabolism products from HXK activity can prevent SnRK1 activity (Baena-González *et al.*, 2007). HXK1 of the Arabidopsis plants has a featured signalling role in addition to its metabolic functions, which can affect its allocation between the mitochondria for glycolysis and the nucleus for signalling. Regardless of the high levels of glucose phosphorylation activity that come from other HXKs, HXK1 mutants *gin2* failed to enhance growth in the presence of light under normal conditions, which increase photosynthesis. This leads to a predicted inverse relationship between the HXK1 pathway and the SnRK1 pathway (Baena-González and Sheen, 2008).

1.2.4. Transcriptional regulation of sugar signalling

Transcription factors (TFs) are proteins that regulate the transcription of different genes in cells by binding to specific sequences of DNA, which are known as activation domains, and promoting or suppressing the transcription. Transcription factors can be

found in all cells, and they are fundamental for the regulation of gene expression. They play an essential role in plant development and response to different stresses by controlling target gene transcriptions. Usually, TFs are classified into several families depending on their protein structure, which mediates the binding of DNA. The first step of gene expression is the transcription process, which produces the first copy of RNA from the DNA of a specific gene flowing by other processes such as RNA splicing and translation. This finally leads to the production of functional proteins, which have a special activity. Moreover, transcription factors play an important role in protein specificity by controlling the production of different proteins in different tissues (Joshi *et al.*, 2016).

Basic Leucine Zipper (bZIP) is one of the largest transcription factor families in the plant. It contains 72–77 bZIP members in the Arabidopsis genome sequence (Riaño-Pachón *et al.*, 2007; Corrêa *et al.*, 2008). The bZIP transcription factor family plays an important role in many vital processes. These *ATbZIP* members are classified into 13 groups or subfamilies (Jakoby *et al.*, 2002). Many bZIP transcription factors are involved in sugar and stress signalling. One of these groups, and the largest bZIP group in the Arabidopsis, is the S1-group bZIP gene, *ATbZIP1*, which is a sugar-sensitive gene. The expression of *ATbZIP1* is suppressed by sugar. The suppression is reversible and affected by hexokinase. *ATbZIP1* is known as a sugar-regulated gene; it mediates sugar signalling and affects gene expression, plant growth and the developmental process. In the absence of external sugars, *ATbZIP1* regulates early seedling growth negatively in the culture medium (Kang *et al.*, 2010). Stress such as cold and drought activates the members of the group S bZIPs. It has been reported that bZIP1 is also involved in the processes of keeping the balance between consuming and producing carbohydrates (Jakoby *et al.*, 2002). The activity of many

bZIP transcription factors such as bZIP1 is mediated by KIN10 protein kinase, which is involved in stress response and energy signalling (Baena-González *et al.*, 2007).

Another transcription factor family involved in sugar signalling is the MYB family. This is an evolutionarily conserved family in all eukaryotes. In plants, the MYB family has devolved into different groups, depending on the number and the position of the MYB domains. These groups are 1R (R1, R2or R3-MYB), 2R (R2R3-MYB), 3R (R1R2R3-MYB), and 4R, and have four repeats (Du *et al.*, 2012). The largest group is R2R3-MYB, which has many important roles in the different vital processes. It includes a repeat of the conserved MYB DNA-binding domain, and 28 sub-groups can be recognised in this group based on the amino acid sequence in the C terminal of MYB domain (Dubos *et al.*, 2010; Shelton *et al.*, 2012). MYB is composed of four different amino acid sequence repeats. Each one makes three alfa-helices. The second and third helices can make a helix-turn-helix, making a 3D HTH structure (Simon *et al.*, 2007). Many R2R3-MYB proteins are involved in different important specific processes of Arabidopsis such as metabolism, cell division, developmental process, and responses to different stress (Dubos *et al.*, 2010). MYB members are involved in the control of cell wall biosynthesis. It has been reported that some MYB genes have developed to specify and achieve a specific function (Bailey *et al.*, 2008).

1.2.5. Transcriptional regulation of SnRK1 under stress

Regulation of SnRK1 activity has been studied at the protein level through post-translational modifications that lead to the activation of the alpha subunits (Crozet *et al.*, 2014). Little is known how SnRK1 is regulated at the transcriptional level in response to environmental stress. Bechtold *et al.* (2016) have identified that KIN10 is

downregulated during drought stress and have subsequently modelled sugar-responsive genes that are also differentially expressed under drought stress. A highly resolved drought transcription time series was produced over 13 days (short dehydration experiment), combined with the analysis of metabolites and photosynthetic physiology (Bechtold *et al.*, 2016). In total, 1,800 differentially expressed genes were identified, of which 185 were responsive to glucose treatment and were involved in sugar signalling. A selection of 100 genes was subsequently modelled using VBSSM (Variational Bayesian State-Space Modelling, Figure 1.3). VBSSM is an approach that depends on an algorithm specifically designed to analyse temporal gene expression data, and it indicates key regulatory genes in a specific system (Beal *et al.*, 2005). The major disadvantage of this approach is the limited number of genes (not more than 100) that can be modelled at one time. For that, clustering the differentially expressed genes into small groups, depending on their similarities, can be useful in order to analyse these clusters. The similar expression patterns of the genes can be indicated based on simple vector distances, such as Euclidean metric and the Spearman rank correlation (Dubois *et al.*, 2017).

The resulting model provides details about gene interactions (edges), which can be either direct or indirect. Genes with a high number of connections are called "hubs." This resultant gene network model predicted that one of the most highly connected genes, DOMAIN OF UNKNOWN FUNCTION (DUF2358), negatively regulates KIN10 at the transcriptional level under drought stress conditions. The network shows all different genes that connect directly or indirectly with DUF2358 and KIN10 (Figure 1.3).

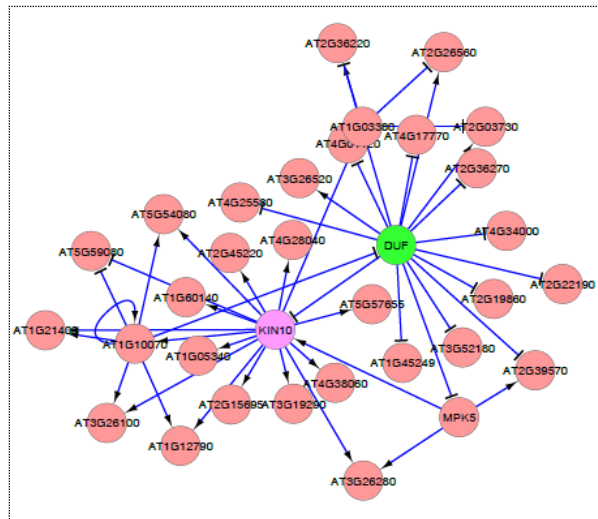


Figure 1.3. A starvation response gene networking *Arabidopsis thaliana*. The network provides details about direct and indirect gene interactions. the model predicted DUF2358 negatively regulates KIN10 at the transcriptional level under drought stress conditions. This model was based on dehydration experiment. (Bechtold *et al.*, 2016, unpublished network).

The protein DUF family indicates a wide range of proteins that have no known function. There are more than 3,000 registered DUF domains in the protein families' database (Pfam EMBL-EBI) (Luo *et al.*, 2014). One of these domains is DUF2358. This protein is predicted to be located in the chloroplast and, so far, no known role has been associated with this protein. The network inference results suggested that DUF2358 might play a role in sugar signalling pathways during drought stress conditions, potentially mediated through KIN10 (Bechtold *et al.*, 2016).

1.3. Abiotic stress

Abiotic stresses such as drought and altered light availability (darkness and high light) are likely to affect sugar homeostasis in plants through inhibiting photosynthesis. The identification of DUF2358 as part of a transcriptional sugar signalling network has led

to a review of the impact of drought and dark-induced senescence on sugar metabolism and plant growth in more detail.

1.3.1. Drought stress

Abiotic stress factors can have a negative effect on plants. In nature, many stresses can affect a plant's life, such as drought, salinity, and excess light. The continuation of plant growth under environmental stress depends on the ability of a plant to sense and respond to different stresses. Drought stress is one of the most threatening stresses plants might face and is the most common environmental factor that causes a decrease in plant productivity (Farooq *et al.*, 2009). Drought is a meteorological expression that is used to describe a period without a substantial amount of rainfall, decreasing the available soil water, while continuing the loss of water from transpiration or evaporation (Jaleel *et al.*, 2009). Drought stress can be defined as a multidimensional stress which affect plants and causes changes in the physiological, morphological, biochemical, and molecular levels in plants (Salehi-Lisar *and* Bakhshayeshan-Agdam., 2016). Drought will ultimately lead to reduced yield and, in the context of crops, will lead to a reduction in food production (Anjum *et al.*, 2011). Plants can be exposed to a short period of water shortage under field conditions lasting for days; however, many plants can respond to this condition by reducing cell damage and growth under stress conditions (Nakashima *et al.*, 2014). Consequently, adaptations to drought stress will be reviewed in more detail.

Furthermore, understanding how plants respond to drought stress is an essential task in order to understand plant resistance mechanisms that are required to adapt and survive under climate change.

1.3.1.1. Drought stress morphological effects

Drought stress represses cell expansion, cell growth, and stem expansion because of the impact of the low turgor pressure and the lack of water transferred to plant tissues through the xylem (Hussain *et al.*, 2008; Schmalenbach *et al.*, 2014). Under drought stress, the cell wall extension and osmotic adjustment modified the cells' turgor. In terms of this modification, the osmotic adjustment is more important than cell wall flexibility (Bartlett *et al.*, 2012). Usually, the osmotic adjustment can take place in small cells than larger cells, which is a very important factor when regulating turgor under drought conditions along with cell wall flexibility (Blum, 2017).

Water deficiency reduces the number of leaves on plants as a result of a reduction in photosynthesis (Borrell *et al.*, 2014). Moreover, leaf size and leaf temperature can be affected by drought stress depending on the turgor pressure. Water deficiency promotes leaf senescence and inhibits shoot and leaf expansion due to the accumulation of ethylene, which is a negative regulator of drought stress (Basu *et al.*, 2016). Water stress causes an increase in root growth in sunflower plants and *Catharanthus roseus* (Jaleel *et al.*, 2008), which increases the water uptake from plant soils. Shoots are more sensitive than roots-to-growth repression under drought stress conditions (Jaleel *et al.*, 2009). Root systems are very important as they need to obtain enough water from the soil, which is essential for plant growth and productivity. An increase in root growth under drought stress was reported in *Catharanthus roseus* (Jaleel *et al.*, 2008) and Maize (Sacks *et al.*, 1997).

When roots are exposed to drought stress, they induce signal cascades to the shoots through the xylem. These signals cause physiological changes that help plants to

adapt to drought conditions (Seo and Koshiba, 2002). Root to shoot signalling involves many factors such as abscisic acid (ABA), cytokinins, ethylene, malate, and potentially other unknown factors. The root to leaf signal is driven by transpiration leading to stomatal closure, an important adaptation to drought stress (Chaves and Oliveira, 2004; Anjum *et al.*, 2011). For example, ABA concentration increases 50 times in roots under drought stress, compared to well-watered conditions.

1.3.1.2. Abscisic acid (ABA)

One of the most important stress hormones in plants is ABA. ABA is also a stress signal that is produced in roots under drought conditions and is moved up to the shoots via the transpiration stream, leading to stomatal closure in order to minimise water loss (Seo and Koshiba, 2002; Zhang *et al.*, 2006; Munemasa *et al.*, 2015). ABA plays a fundamental role in the plant's response to drought stress, acting as a cellular signalling molecule in the translocation of water from roots to leaves (Alves and Setter, 2004). ABA acts through specific ABA-binding receptors (RCAR/PYR1/PYL), which initiate ABA-specific signalling pathways. There are 14 different RCARs in Arabidopsis genome (Tischer *et al.*, 2017) and, together with type protein phosphatase 2C (PP2C) and SNF1-related protein kinase 2 (SnRK2), play an essential role in ABA signalling (Takahashi *et al.*, 2017).

ABA induces gene expression and synthesis of proteins, which are involved in antioxidative defence responses during drought stress (Guan *et al.*, 2000; Miller *et al.*, 2010). In terms of the germination, ABA concentration affects hypocotyl growth. Increased concentrations of ABA cause a decrease in hypocotyl growth (Baguley *et al.*, 2016). Under drought stress, in response to ABA, nitric oxide (NO) is produced

through enzyme nitrate reductase (NR), which in turn mediates stomatal closure (Desikan *et al.*, 2002). Moreover, Song *et al.* (2016) clarify the role of endogenous ABA in the regulation of growth under stress conditions in order to control the initial stages of leaf senescence. This has been done by coordinating Ca^{2+} signalling through affecting the calcium concentration in the cytoplasm of guard cells.

1.3.1.3. Reactive oxygen species (ROS)

The initial biochemical responses of plant cells to abiotic stresses are the accumulation of reactive oxygen species (ROS). ROS, such as O_2 , O_2^- , H_2O_2 , and hydroxyl radical, are toxic molecules which might cause oxidative damage to proteins, DNA, and lipids (Apel and Hirt 2004; You and Chan, 2015). They also provide signalling functions in the plant response to environmental stresses, and during drought stress act as messengers to promote defence responses (Mittler *et al.*, 2004; Chan *et al.*, 2016). Under nonstress conditions, ROS production remains at a low level. Meanwhile, when plants are exposed to stress conditions, the production of ROS increases, causing a dramatic increase in ROS levels (You and Chan, 2015).

During drought stress, stomatal closure reduces CO_2 uptake, which causes photosynthetic reactions to be limited, resulting in the overproduction of the photosynthetic electron transport chain. These electrons are used to reduce molecular oxygen which, in turn, causes an increase in reactive oxygen species (ROS) levels (Mittler, 2002; Basu *et al.*, 2016). In addition, soluble sugars, such as sucrose glucose and fructose, play multiple roles in the aspect of ROS production in the plant, by the inhibition of the fatty acid transfer and peroxisomal β -oxidation (Couée *et al.*, 2006).

Plant response against the oxidative damage, which might be caused by the increase in ROS levels enzymatically system such as superoxide dismutase (SOD) and ascorbate peroxidase (APX) and non-enzymatically systems such as carotenoids, tocopherols (You and Chan, 2015). This also along with providing energy for metabolism to produce NADPH, which contributes to the antioxidative system (Couée *et al.*, 2006).

1.3.1.4. The effect of drought on photosynthesis

ROS accumulation leads to stomatal closure via ABA signalling (Kwak *et al.*, 2003), which reduces CO₂ intracellular concentration and, as a consequence, photosynthesis (Das and Roychoudhury, 2014; Bechtold *et al.*, 2016). Several explanations for a decline in photosynthesis have been proposed. For example, Cornic (2000) reported stomatal limitation decrease posthypnosis rate. Also, Bechtold *et al.* (2016) have shown that photosynthetic limitation is primarily due to stomatal limitation limiting CO₂ uptake.

Drought stress also causes changes in the chlorophyll a and b ratio and carotenoids (Farooq *et al.*, 2009). Chlorophyll levels decrease with drought due to oxidative stress, thus leading to pigment photo-oxidation and chlorophyll dissolution. The decrease in chlorophyll a and b contributes to photosynthesis suppression, limiting light-harvesting, and the production of energy (Anjum *et al.*, 2011). On the other hand, photosynthetic enzymes are also affected by drought stress. Cells shrink as a result of dehydration when the amount of water available for cells decreases, which causes an increase in the cells' viscosity, leading to protein accumulation and denaturation. The increase in the viscosity of the cytoplasm may be toxic and harmful to enzymes

(Hoekstra *et al.*, 2001). Such as PHOSPHOENOLPYRUVATE CARBOXYLASE (PEPCase), NADP-MALIC ENZYME (NADP-ME), FRUCTOSE-1,6-BISPHOSPHATASE (FBPase), and PYRUVATE ORTHOPHOSPHATE DIKINASE (PPDK) (Farooq *et al.*, 2009).

1.3.2. Dark-induced senescence

Leaf senescence is a complex integrated process involving massive reactions of different levels of hormones inducing different sets of genes. This process aims to improve plant productivity and redistribute components in response to different stresses (Maillard *et al.*, 2015; Liebsch and Keech, 2016). In many plant species, light plays a key role in regulating leaf senescence, taking into consideration the essential role of leaves in photosynthesis. Senescence process can be induced as a result of a light deficiency, especially when a part of the plant is affected by darkness, either in the shading or darkening of leaves (Keech *et al.*, 2010). During leaf senescence, massive transcription changes occur accompanied by variations of gene expressions that connect with this process, for example, chlorophyll biosynthesis genes, photosynthesis, reduced reactive oxygen species (ROS), and ethylene (Mayta *et al.*, 2018). High levels of endogenous ABA concentrations were found during leaf senescence in many plants, which is very important when controlling the beginnings of leaf senescence via Ca²⁺ signalling (Yang *et al.*, 2014).

Photosensor proteins such as Phytochromes enable plants to identify the quantity and quality of the light which help plant to produce energy. Phytochromes are red (R) and far-red (FR) light receptors in plants that mediate light-signalling retardation of senescence. Phytochrome B (phyB) plays a critical role in the delay of senescence by

R as the main photoreceptor in *Arabidopsis thaliana*. Phytochrome-Interacting Factors (PIFs) regulate light signalling negatively and promote a response to light deprivation. In *Arabidopsis*, there are seven members of the PIF family which interact with PhyA or PhyB, or both Phys. PIFs promote dark-induced senescence in *Arabidopsis* and they are degraded by PhyB or PhyA. PIFs induced by prolonged darkness, PhyB and PhyA, become inactive at both transcription and protein levels and this controls the sets of target genes during dark-induced senescence. An increase of PIF expression causes an acceleration of dark-induced senescence symptoms by enhancing 1-AMINOCYCLOPROPANE-1-CARBOXYLATE SYNTHASES (ACSs), which is a key gene in ethylene biosynthesis. Also, the expression of ETHYLENE INSENSITIVE 3 (EIN3) is activated by PIFs. EIN3 is an important transcription factor in ethylene signalling. Furthermore, PIFs directly affect ACID INSENSITIVE 5 (ABI5), ENHANCED EM LEVEL (EEL), and EIN3 expressions. ABI5 and EEL encode basic leucine zipper (bZIPs) transcription factors involved in ABA signalling. For this, PIFs affect ABA signal transduction through ABI5 and EEL genes. Integration between PIFs, ABI5, EIN3, and EEL activate senescence-associated genes (SAGs), which are chlorophyll catabolism genes such as STAY-GREEN 1 (SGR1) and NON-YELLOW COLOURING 1 (NYC1). These genes are regulated directly by PIFs, ABI5, EIN3, and EEL (Song *et al.*, 2014). The activation of SGR1 and NYC1 causes chlorophyll degradation. Also, it affects the key senescence promoter ORESARA1/ARABIDOPSIS NAC DOMAIN CONTAINING PROTEIN 92 (ORE1/ANAC092) transduction factor. On the other hand, chloroplast maintenance master regulator genes GOLDEN2-LIKE 1 and 2 (GLK1) and (GLK2) are suppressed directly by PIFs ORE1 (ATAF1).

1.4. Cross-talk between signalling pathways

Cross-talk refers to the interaction between two or more signal transduction pathways and how they may affect each other. For example, in *Arabidopsis*, a wide network of interaction takes place between sugar and ABA signalling pathways (Finkelstein and Gibson, 2002; León and Sheen, 2003). In this context, glucose activates both ABA synthesis and ABA signalling pathways (Rolland *et al.*, 2006; Cho *et al.*, 2010). Fructose-specific downstream signalling pathway FSQ6 can also interact with ABA and ethylene signalling pathways, similar to the HXK1-dependent glucose signalling pathway (Li *et al.*, 2011). The points where different signal transductions interact with each other are considered as cross-talk and, together, they make a wide signalling network. This interaction between signalling pathways can be done by activating either a common second messenger or a phosphorylation cascade, leading to the regulation of gene expression. This might directly affect the biosynthesis processes or might have an impact on other hormones such as ABA (Harrison, 2012).

1.4.1. Cross-talk between SnRK1 and TOR signalling pathways

SnRK1 is activated during low glucose levels and by diversion of nitrogen, while SnRK1 activity is decreased by phosphate starvation (Jossier *et al.*, 2009; Rodrigues *et al.*, 2013). TOR activity is downregulated under stress conditions and low sugar. TOR activity leads to S6K phosphorylation, which is inhibited by sugar starvation and can be restored by a glucose supplement (Xiong and Sheen, 2012; Li *et al.*, 2017). A decrease in SK6 activity in *Arabidopsis* has been reported in response to cold stress due to a decrease in glucose metabolism. Also, SK6 activity decreased in response to sulfate reduction as a result of suppressing glucose metabolism through the TOR

signalling pathway. . The way in which sulfate affects TOR activity was suggested to be mediated by SnRK1 (Wang *et al.*, 2017; Dong *et al.*, 2017).

TOR and SnRK1 signalling pathways play important roles in response to energy levels. Under the appropriate level of energy and different nutrients, TOR signalling is activated. On the other hand, SnRK1 became active under a shortage of energy and nutrients (Tomé *et al.*, 2014). It has been reported by Tomé *et al.* (2014) Comparing the expression of different SnRK1 and TOR target genes, from SnRK1 signalling (Baena-González *et al.*, 2007) and TOR signalling (Xiong *et al.*, 2013), there was a high number of overlapping in both signalling pathways. TOR and SnRK1 were affecting the targeted genes oppositely. For example, 294 out of 507 SnRK1 upregulated genes were downregulated by glucose in the TOR signalling pathway and 47 of them were translation-associated genes. Moreover, they have found 260 out of 515 genes which are also more than half were downregulated by SnRK1, were upregulated targeted genes of TOR. These upregulated genes contain amino acids and carbohydrate metabolism genes. This led to the suggestion of the opposite action of SnRK1 and TOR in terms of regulation carbohydrate and amino acids metabolism processes and translation processes (Tomé *et al.*, 2014). These response to energy levels is very important to initiate and regulate stress responses.

SnRK1 and TOR also contribute to stress response through autophagy mechanisms (Robaglia *et al.*, 2012; Soto-Burgos and Bassham, 2017). Autophagy includes the degradation of some unnecessary contents such as damaged cells which provide energy sources under stress. It has been reported that TOR and SnRK1 regulate the nutrient-dependent process in a different way. For example, while SnRK1 in the sugar or nitrogen depression enhance autophagy, TOR represses autophagy under

nonstress condition. TOR also contributes to nitrogen assimilation and metabolite synthesis (Robaglia *et al.*, 2012).

It has also been reported that, when TOR and SnRK1 are concurrently activated, autophagy was not induced or induced at very low levels. However, when TOR and SnRK1 were concurrently decreased, autophagy was activated. Consequently, SnRK1 was reported as upstream of TOR in autophagy regulation (Soto-Burgos and Bassham, 2017). Moreover, SnRK1 has the ability to activate autophagy through TOR signalling or independently. Under stress conditions that induce ABA signalling, TOR is inactivated in a kinase-dependent way which helps to reduce growth and maintain energy sources (Rosenberger and Chen, 2018; Wang *et al.*, 2018).

1.4.2. Cross-Talk Between ABA and glucose

The first indication for cross-talk between sugar and ABA-regulated processes came from an observation that many glucose-insensitive mutants (*gin1*, *gin5*, and *gin6*) are allelic to ABA biosynthesis mutants (*aba2* and *aba3*) with decreased internal ABA levels and seed dormancy (Roman *et al.*, 2008; Dekkers *et al.*, 2008). Also, ABA accumulation and biosynthesis are largely increased by glucose (Cheng *et al.*, 2002). It is also involved in the ABA signalling by controlling ROS homeostasis and plastocyanin PC genes in *gin1/aba2* and *gin5/aba3* background (Ramon *et al.*, 2008).

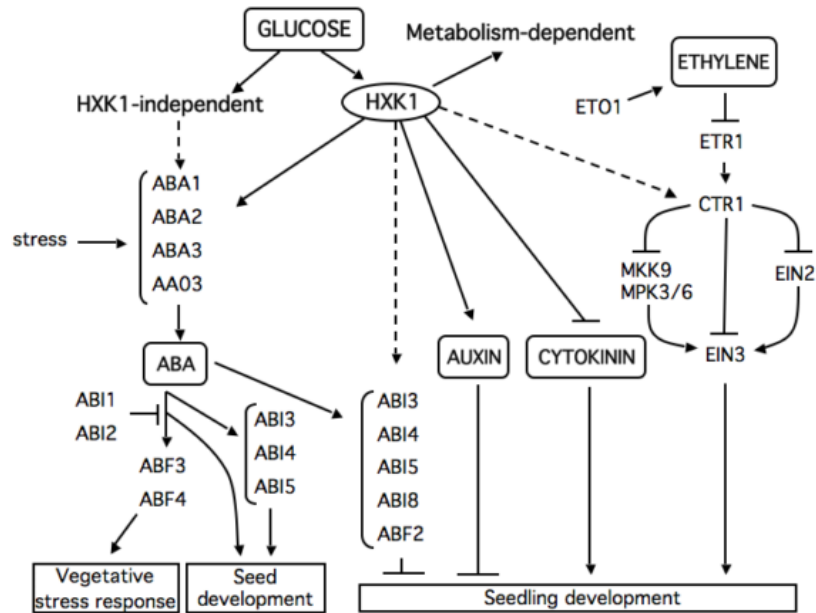


Figure 1.4. Genetic overview of interactions between Sugar and Hormone Signalling in Arabidopsis. Glucose signalling leads to the increase in ABA levels, by inducing of ABA synthesis (ABA1-3 and AAO3) which induce ABA (ABI3-5, ABI8, ABF2-mediated) signalling pathway which regulate seedling development process in the HXK-dependant pathway. ETHYLENE INSENSITIVE3 (EIN3) TF protein stability is regulated by both ethylene and glucose (mediated by HXK) signalling with the importance of CTR1 and MKK9 pathways in controlling ethylene-signalling specificity through MAPK phosphorylation sites which oppositely affect EIN3 stability. HXK-signalling also interact either positively and negatively with auxin and cytokinin signalling Scheme resource (Ramon *et al.*, 2008)

Furthermore, HXK1 mediates glucose signalling, which controls seedling development through increasing transcript levels of many ABA biosynthesis genes and, consequently, ABA concentration. This gives a mechanistic link between ABA and glucose at a molecular level (Cheng *et al.*, 2002). Therefore, both ABA synthesis (ABA1-3 and aldehyde oxidase 3 (AAO3)) genes and ABA (abscisic acid insensitive (ABI3, ABI4, ABI5 and ABI8)) signalling gene expressions are induced. ABA insensitive signalling mutants, such as *abi1-1* and *abi2-1*, do not present the glucose-insensitive (*gin*) phenotype, which means ABA signalling and glucose signalling pathways are separated during stress responses. On the other hand, ethylene

stimulates the glucose-insensitive phenotype with ethylene biosynthesis (*eto1*) and ethylene signalling (*ctr1*) mutants displaying glucose-insensitive phenotype (Ramon *et al.*, 2008). Conversely, glucose hypersensitivity (*glo*) is displayed by ethylene-insensitive mutants (*etr1-1 mein2* and *ein3*) and THE MITOGEN-ACTIVATED PROTEIN KINASE KINASE 9 *mkk9*. Glucose signalling is cross-linking with ethylene signalling ETHYLENE INSENSITIVE3 (EIN3) TF to maintain and control protein stability (Ramon *et al.*, 2008). In addition, HXK signalling also interacts positively with auxin signalling and negatively with cytokine signalling (Figure 1.4) (Ramon *et al.*, 2008).

1.5. Aims and Objective

The project aims to identify the role of a PROTEIN DOMAIN OF UNKNOWN FUNCTION (DUF2358) in sugar signalling pathways under stress conditions that alter primary metabolism. As part of this question, it aims to establish whether DUF2358, a putative chloroplast protein, specifically integrate into the well-known KIN10 signalling pathway.

There are three main objectives for this project:

1. Evaluate the effect-altered DUF2358 expression on plants subjected to starvation-inducing stress treatments.
2. Establish localisation of DUF2358 within the chloroplast.
3. Establish a signalling pathway from the chloroplast to the nucleus.

Chapter 2

Material and Methods

2.1. Molecular Biology Technique

2.1.1. Plant material, and growth conditions

Seeds of the genotypes *Arabidopsis thaliana* wild-type (Col-0), the DOMAIN OF UNKNOWN FUNCTION (DUF2358) AT2G46220 knockout mutants (*dufko3*, *dufko4*) (Table 2.1), DUF overexpression lines (*DUFOE2*, *DUFOE3*, and *DUFOE4*) (Figure 2.1), the native promoter (pNAT:DUF:GFP) and (pNAT:DUF) (Figure 2.2 A, B and C) which were used in this study were provided by Dr. Ulrike Bechtold. Also, *Arabidopsis thaliana* KOs of *kin10-2* were obtained from the Nottingham Arabidopsis stock center (NASC) (Scholl *et al.*, 2000) (Table 2.1). The seeds were sown on soil (Levington F2+S, The Scott Company, Ipswich, UK) and left for three days at 4°C. Plants were subsequently moved to the growth room under controlled conditions (eight hours of light, where the temperature was 22°C, the humidity was 60%, and light intensity was supplied by fluorescent tubes at $160 \pm 20 \mu\text{mol.m}^{-2}\text{s}^{-1}$). Seedlings were pricked out into 6 cm individual pots filled with soil two weeks post sowing and maintained under the same growth conditions and used for stress experiments. Wild-type *Nicotiana benthamiana* seeds for transient expression studies were provided by Dr. Ulrike Bechtold. *Nicotiana benthamiana* seeds were sown on soil without cooling and kept immediately in the controlled environment.

Table 2.1. List of T-DNA and Overexpression mutant lines that were screened to identify loss of function, overexpression and native promoter mutants.

Line name	Gene Locus Identified	Mutant line	NASC NO.
<i>dufko3</i>	AT2G46220	SALK_104372C	N604372
<i>dufko4</i>	AT2G46220	SALK_091794C	N591794

<i>DUFOE2</i>	AT2G46220	N/A	
<i>DUFOE3</i>	AT2G46220	N/A	
<i>DUFOE4</i>	AT2G46220	N/A	
<i>pUBQ:DUF2358:GFP</i>	AT2G46220	N/A	
pNAT:DUF2358	At2g46220	N/A	
<i>kin10-2</i>	AT3G01090	SALK_093965	N593965

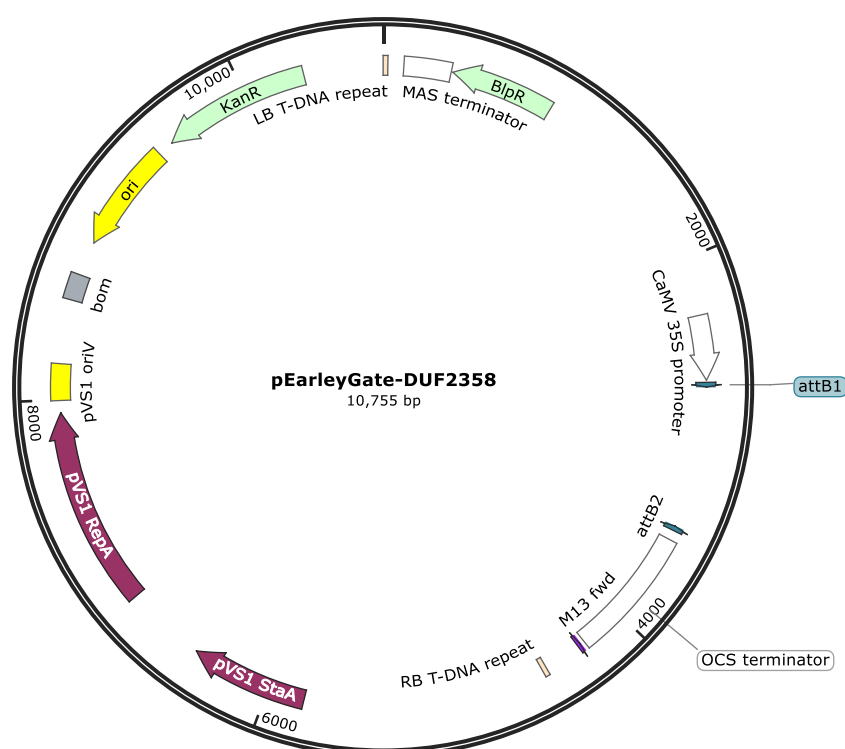


Figure 2.1. DUF2358- Overexpression construct map (*DUFOE*) (obtained from Dr. Subramaniam). cDNA used to amplify the full-length protein-coding sequence was generated from wild-type Col-0. The pEarleyGate vector contains the CaMV 35S promoter and the OCS terminator. Also, it contains the KanR gene for selection in *E. coli* using Kanamycin.

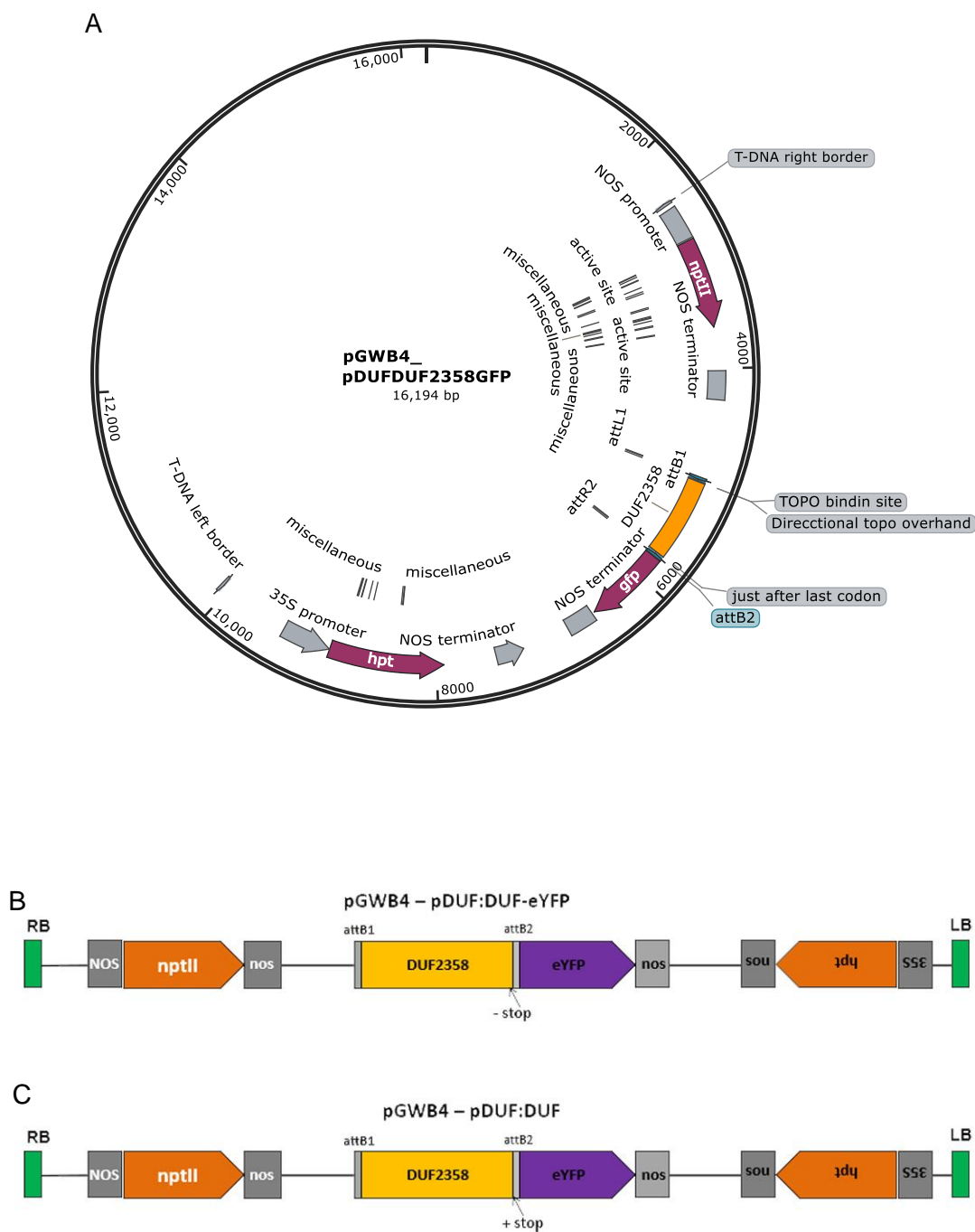


Figure 2.2. (A) pNAT:DUF2358:GFP- construct map (obtained from Dr. Exposito), (B) pNAT:DUF2358:GFP- construct map without stop codon , and (C) pNAT:DUF2358:GFP- construct map with stop codon. For all, cDNA was generated from *dufko3*. Vector pGWB4 has CaMV 35S Promoter, NOS terminator and Kanamycin and Hygromycin bacterial selection.

2.1.2. Primer design

All Primers in this thesis were designed using Primer3 online program on <http://primer3.ut.ee> (Untergasser *et al.*, 2012) or Snapgene PC software. The GC contents were 40-60%, while Melting temperatures T_m were between 58-65 °C. The full list of primers that were used to screen mutant insertions, gene expression, protein amplification for cloning, GFP amplification for sequencing, and all other primer sequences is set out in Table 2.2.

Table 2.2 List of all primers and templates which were used in this study

Line name	Gene	Forward Primer sequence 5' -3'	Reverse Primer sequence 5' -3'
<i>dufko3</i>	DUF2358 AT2G46220	ATTTTGCCGATTTTCGGAAC	CTCAAAGTAGGTCGGCTTGG
<i>dufko4</i>	DUF2358 AT2G46220	AGGTTGCTGACTATTGCCATG	TCAATCTCCGAACTCAAAGTAGG
<i>Kin10-2</i>	KIN10 AT3G01090	TGTGATCGATCGTTGAAGAAAC	ATGTTGCTCAGGCCAAAATC
<i>DUFOE2</i>	DUF2358 AT2G46220	TCATGGAATTCCTCGTGGTC	TGGAGGCGAATTAATGGCTA
<i>DUFOE3</i>	DUF2358 AT2G46220	TCATGGAATTCCTCGTGGTC	TGGAGGCGAATTAATGGCTA
<i>DUFOE4</i>	DUF2358 AT2G46220	TCATGGAATTCCTCGTGGTC	TGGAGGCGAATTAATGGCTA
pNAT:DUF2 358	DUF2358 AT2G46220	ATGGCATTCTTGTTCGTTTCGC	TCAATCTCCGAACTCAAAGTAGG
pNAT:DUF2 358:GFP	DUF2358 AT2G46220	ATGGCATTCTTGTTCGTTTCGC	TACTTGTACAGCTCGTCCATGC
DUF2358	AT2G46220	TCATGGAATTCCTCGTGGTC	TGGAGGCGAATTAATGGCTA
ABF2	AT1G45249	ACATACCAGCAATCGCAACA	CCACAAGACCACCACCTCTT
ABF3	AT4G34000	GGTGGGTTAGCTGTTGGTGT	GACTAATCGTCCGAGGCAAG

ABI5	AT2G36270	GAGACTGCGGCTAGACAACC	GGTTCGGGTTTGGATTAGGT
ACR5	AT2G03730	CCCGTTTTGTTGTCTGAGTT	TTCATCGGTCACTTGCAAAA
ACR9	AT2G39570	AAAGCGGTTCTTACCGTTGA	TCGCAGTCTTTGGAAGTCCT
ATTPS5	AT4G17770	TGTTGTAGCAGGATGCTTGG	CCCCACAGGAAGAATCTTGA
PLP2	AT2G26560	TGCCGTTATCCTTGGTTTTTC	GGTGCTTGTTCGCTATTA
ATRRP4	AT1G03360	TTGGCTGCAATGGTTTCATA	GCTTTGCTCTTTTCCTGTGG
AT2G36220	AT2G36220	ACGGATATTTGCTTCTGGA	ACCCGACTTGATTTTTGACG
TIP2	AT3G26520	TTTGTGCTGTCTCTGTTGG	CCACGGAGGAGAGTGATGT
AT4G25580	AT4G25580	TCTCATGGTGGGTTGTCAA	CCCAACCCTAACCTTCCAAT
MPK5	AT4G11330	GCCTGTTTGTCCAACCATT	CTTCACAGATTGAGCCACA
DSP4	AT3G52180	ACACTGGACAAGGGAACAGG	CTATAAACGGTTCGGCCTCA
AtHXK2	AT2G19860	ACAGAAGGCGAGGACTTTCA	AGCTGCTTAACCGGAAATGA
TPPE	AT2G22190	AGTCATGGCATGGACATCAA	TATCACCGGGAGGAATTCAG
GBF2	AT4G01120	CACCAAGCACTGGTGAAAGA	CATTGCTGTGGGCATAACAG
KIN10	AT3G01090	AGATAATATCAGGAGTGGAAT	TGCTCAGGCCAAAATCAGC
UMAMIT33	AT4G28040	GAGCCATGGCAATGACTTTT	AAGAAGCAGCCGAGTAACCA
ATPME17	AT2G45220	<i>GCAGCGTGGGAAGATTGTAT</i>	<i>TTTGAGCACTTCACGTTTGG</i>
AT5G57655	AT5G57655	<i>TCGTGGACTGAGAAATGCAG</i>	<i>ATTGCTTCCCAAGCTCAGA</i>
CYP71B4	AT3G26280	<i>ATCACGCTGGAATTGACACA</i>	<i>GTTCCGATCTCGTCTTGAGC</i>
AT1G12790	AT1G12790	<i>CCCCCTGATCTCATCTTCAA</i>	<i>ATTGCCCTTTCAGCCTCTTT</i>
DIN6	AT3G47340	GACGGGATTGATGCGATAGA	TCCGGGACATCAAGAACATC
SEN5	AT3G47340	GCGAAACTCTCTCCGACTTC	CCACAGAACAACCTTTGACG
AXP	AT2G33830	CTTCGACAAGCCTTCTCACC	TCGTCGCTGTATAGCCAATC
RAB18	AT1G43890	TGGCTTGGGAGGAATGCTTCA	CCATCGCTTGAGCTTGACCAGA
RD29B	AT5G52300	CTTGGCACCAACCGTTGGGACTA	TCAGTTCCAGAATCTTGAAC
NCED3	AT3G14440	GAGCTGCAGCCGGTATAGTC	CATCCTCCGACATAGCCAAT
GLK1	AT2G20570	AAGGGTAGTTCGGGAAAGG	TCCTTTTCCGGTCACTGTCA
ORE1	AT5G39610	GCTACTGCCATTGGTGAAGT	CCGGTCTCTCACACAGAAGA
EIN3	AT3G20770	GCTTTTGTCTGCGTTGATGC	CAAGTTGAGGCCACCAATCC

EEL	AT2G41070	GCTACTGCCATTGGTGAAGT	CCGGTCTCTCACACAGAAGA
DUF2358	AT2G46220	ATGGCATTCTTGTTCGTTT	CTCAAAGTAGGTCCGGCTTGG
mgfp5	-	ATCATGGCCGACAAGCAAAA	CCATGTGTAATCCCAGCAGC
YFP		CACCATGGTGAGCAAGGGCGAG GA	TTACTTGTACAGCTCGTCCATGC
pAD GAL4	-	GGGATGTTTAATACCACTAC	AAGAAATTGAGATGGTGCAC
		TCCTCGTCATTGTTCTCGTTCC	CATGGCCAAGATTGAAACTTAGA GG
pBD GAL4	-	TCCTCGTCATTGTTCTCGTTCC	CATGGCCAAGATTGAAACTTAGA GG
Gene	ID	Forward Primer sequence 5' -3'	Reverse Primer sequence 5' -3'
CpEF-TuB	D5LT98	ATAGAATTCGTAAACATGGTGGTT GAGCTTATCATGC	TATCTGCAGTCATTCTAAGATTT TCTGAATAACACCAGCTCC
NbGAPDH-A	A0A0A8IBT8	ATACCCGGGATGGCTTCGGCTGC TCTCTCAGTA	TATGGATCCTTATTTCCACTGGT TTGCAACAATGTCAGCAAG
E5LLE7	Phosphoglyc erate kinase	ATAGAATTCATGGCATCAGCTACA GC	TATCTGCAGCCTTGGCCTTCTCT A
NbCAS	K7ZLE1	ATAGGATCCAATGGCGCTTAGAG CTTCA	TATGTCGACTTAATCACTACCCC CTGAAAGCAA
ClpC1B	A0A088F8F4	ATAGAATTCATGGCTCGAGCTTTA GTTTCAGTCAACCAA	ATACCCGGGCTACACAGGGATA GGCTCAGGAGC
A4D0J9	-	ATAGAATTCAGCTTGTACATGGTC TTTGCCTG	TATCTGCAGTCATACGGAAAGA GAAGGAGAAAGACCG
FtsH	C9DFA3	ATAGAATTCTGATTCTGCCTTGTT GAGGCCG	TATAGATCTATCTGTCTCGCCAC TCGTGAA
DUF2358	AT2G46220	ATACCCGGGATGGCATTCTTGT TCGTTTCG	TATCTGCAGTCAATCTCCGAACT CAAAGTAGGTTCG
GAPDH	AT1G16300	ATAGAATTCCTCAAACGAACATTT TCGTGGCTCCAGAG	ATACCCGGGGTTTTACATAAAA CTTGGAGCCAAAACCGG

CLPC	AT5G50920	ATAGAATTCATGGCTATGGCCAC AAGGG	TATCTGCAGTTAAGCAACAGGG AGAGAATCTTCCTG
CAS	AT5G23060	ATAGAATTCATGGCTATGGCGGA AATGG	TATCTGCAGTCAGTCGGAGCTA GGAAGGAAC
Carbonic anhydrase	AT3G01500	ATAGAATTCATGTCGACCGCTCCT CTCTC	TATCTGCAGCTACAGCTTCCAAT GTAGTATGGTAGCCA
PGK	AT1G79550	ATAGAATTCATGGCTTCCGCTGC CG	TATGTCGACCTAACAGTGACTG GGATTGCTTCATCAAG
EF-TuB	AT4G20360	ATAGGATCCATGGCGATTTCCGC TCCAG	TATCTGCAGTCATTCGAGGATCG TCCAATAACTCC

2.1.3. Preparation of Culture Media

Different media were used in this thesis, depending on the purpose the media was used to.

2.1.3.1. preparation of 0.5 MS media for screening purposes

800 ml of Reverse Osmosis RO water was mixed with 2.15 gm Murashige and Skoog Basal Salt Mixture (MS) (#SLBN7853V, SIGMA Life Science, UK). The pH was adjusted to 5.9 with KOH, and then the volume was completed to 1 L using RO water. 9 gm of Agar was added to the 0.5 MS solution and autoclaved. Before use, a suitable antibiotic was added following the instructions from the manufacturer.

2.1.3.2. Luria-Bertani medium (LB media)

In order to prepare the LB broth media, 10 gm of Bacto-tryptone, 5 gm of yeast extract, and 10 gm NaCl were added to 800 ml H₂O and dissolved, and then the pH was adjusted to 7.5 with NaOH. The volume was completed to 1 L with RO water. For LB Agar, the same recipe was used with 14 gm Agar. Media were autoclaved to sterilise,

then all antibiotics for selections were added before use following the manufacturer's instructions.

2.1.3.3. Yeast media

2.1.3.3.1. Yeast peptone dextrose adenine (YPDA) media

In 1 L of water, Yeast extract 1% (w/v), Peptone 2% (w/v), Dextrose 2% (w/v), Adenine hemisulphate 80-100 mg/L) was added to this order. For YPDA Agar, the same recipe was used with adding Agar 2% (w/v). Both media were autoclaved to sterilise.

2.1.3.3.2. Synthetic dropout media

For 1 L of the SC media, 6.7 gm/L Yeast Nitrogen base YNB without amino acids, Glucose 20 gm/L and 20gm/L Agar (for plates only). The media were then autoclaved. To make dropout media which contains all the essential amino acids for yeast, except amino acids which are used for selection, Yeast Synthetic Dropout Media Supplements were used to make -leucine and -uracil, -leucine and -uracil and -histidine, -leucine and -uracil and adenine (#Y1771, Y2001, and Y2021 respectively; Sigmaaldrich, Germany) following the manufacturer's instruction. 200 mg/L of Tryptophan (#T2610000, Sigmaaldrich, Germany) was added to the media.

2.1.4. Screening for primary transgenics on MS plates

For screening purposes, seeds were sterilised as follows. Seeds were immersed in 95% (v/v) ethanol with 1% ml of Tween and left for five minutes. After that, the seeds

were washed with 75% (w/v) ethanol and left to dry for one hour on sterilised filter paper. The seeds were then sown in a Petri dish containing MS media supplemented with antibiotic (33 μ M hygromycin). Plants were transferred to the soil after two weeks and left to grow under the controlled conditions described above.

2.1.5. DNA Extraction PCR and Gel Analysis

Genomic DNA was extracted to screen *dufko3*, *dufko4*, *dufko5*, and *dufko6* for the DNA insertion as previously described by Edwards *et al.* (1991) and to screen plants after conducting crossing system. One leaf was ground in 200 μ l DNA extraction buffer (200mM Tris-HCl pH7.5, 250 mM NaCl, 25mM EDTA, and 0.5% SDS) until most of the leaf had dissolved into the buffer. The mixture was incubated in a water bath at 65 °C. After 30 minutes of incubation, the tube was cooled down to room temperature for 5 minutes, then 200 μ l chloroform and vortex. The tube was centrifuged for 15 minutes at 13000 rpm. The aqueous phase was transferred to a new tube, and the same volume of isopropanol was added (1:1) and mixed by inverting the tube, then incubated for 15 minutes at room temperature. The tube was spun for 15 minutes at 13000 rpm, after which the supernatant was carefully discarded. The pellet was washed using 500 μ l ice-cold 70% v/v ethanol, and the tube was centrifuged for 1 minute at 13000. After drying the tube for 30 minutes in the fume hood, the pellet was resuspended in 100 μ l RO water. The DNA was stored at -20°C for subsequent use in the PCR analysis. DNA concentration was measured using NanDrop™ ND-1000 Spectrometer (Thermo Fisher Scientific Inc.) following the manufacturer's instructions.

2.1.6. Polymerase Chain Reaction (PCR)

A Polymerase Chain Reaction (PCR) was conducted to screen mutants of the interesting genes and to verify the crossing system result, using a PCR machine (Applied Biosystems-2720 Thermal Cycler). The forward (F) primer and reverse (R) primer were added to the PCR master mix to a final concentration of 500 nM. The PCR master mix contained *Taq* DNA Polymerase (recombinant), (#EP0402, ThermoFisher Scientific™ Inc, UK), with a final concentration of 2.5 U/μL, with 10X *Taq* Buffer at a final concentration of 1X. Also, a mix of deoxyribonucleotide triphosphates dNTPs (#R0193, ThermoFisher Scientific™ Inc, UK) was added at a final concentration of 200 μM and 100-200 ng of genomic DNA. The reaction volume was filled up to 25 μl with RO water.

The PCR protocol was as follows: 94°C for 4 minutes, followed by 35 cycles of 94°C for 15 seconds, 57°C for 40 seconds, 72°C for 1.45 minutes. The final extension was performed at 72°C for 10 minutes. PCR products were mixed with 6X DNA loading dye (#SM1553, ThermoFisher Scientific™ Inc, UK). Then, the samples were separated on 1% agarose gel (w/v) with Tris-acetate EDTA (TAE) buffer (40 mM Tris, 20 mM acetic acid, 1 mM EDTA) containing 1:10,000 dilution of SafeView Nucleic Acid Stain (#NBS-SV1, NBS Biologicals Inc, UK). The samples were run along with either GeneRuler DNA Ladder mix (#SM0331, ThermoFisher Scientific™ Inc, UK) or MassRuler DNA Ladder Mix (#SM0403, ThermoFisher Scientific™ Inc, UK) for 30 minutes at 110V, and PCR products were visualised using InGenius3 gel imaging and analysis system (Syngene Gene Genius, SYNOPTICS, Ltd, Cambridge, UK) following the manufacturer's instructions.

2.1.7. RNA Extraction, cDNA, and qPCR

RNA extraction was performed to analyse the gene expression. Plant material was harvested in aluminium foil, then placed in liquid nitrogen. RNA was extracted using Tri-reagent according to the manufacturer's instructions. The RNA samples were saved in a -80 freezer. A NanoDrop™ ND-1000 spectrophotometer (ThermoFisher Scientific) was used to determine the RNA concentration and purity to calculate the number of RNA samples required for cDNA synthesis.

Copy DNA (cDNA) from the RNA samples was carried out using 1 ng of total RNA in a final volume of 11 µl H₂O and 1 µl of Random Hx primer. The mixture was heated at 65°C for 10 minutes before adding a 5X buffer, dNTPs, and Reverse Transcriptase (RT) enzyme. Samples were incubated at 42°C for one hour. The cDNA samples were diluted by 1:5 with H₂O, followed by quantitative polymerase chain reaction (qPCR) using gene-specific primers (Table 2.1) and SYBER Green mix, which was prepared by adding 40 mM Tris-HCl, pH 8.4, of 100 mM KCl, 6 mM MgCl₂, Glycerol 8%, 1X BSA, dNTPs 0.4 mM, 20 mM Fluorescein and 0.4X SyBr Green I. It was then made up to the required volume of water (Table 2.2). The qPCR was carried out to analyse the level of gene expressions compared to Col-0. The fold change of gene expressions was calculated compared to Col-0 and normalised with Actin.

2.1.8. Crossing program

A crossing program was conducted between *dufko3*, *DUFOE3*, and *kin10-2* mutants under a binocular dissecting microscope. Very fine tweezers (Type 7) were sterilised using 95% ethanol and washed with sterilised RO water and left to dry. Mother plants were chosen at the stage of 5-6 inflorescences as the buds were larger at this stage. Father plants were chosen when they started to form siliques in order to make sure of

the efficiency of the pollen. After the tweezers were dried, mature siliques were removed from the inflorescence of the mother plants and removed and cleaned all the open flowers. The flower buds on the mother plants were opened using the forceps. Immature anthers, petals and sepals were removed, and pistils with the sticky stigmas were kept to complete crossing. One open white mature flower was taken from the father plants and the pollen was tapped on the sticky stigmas until it was covered with the pollen. Then, the plant was left to grow after labelling the pollinated inflorescences, which were crossed and covered with clingfilm wrap to maintain the necessary humidity level and prevent drying. Siliques with crossed seeds were harvested when they became mature. Seeds were sown in the same conditions as described in 2.1 to obtain the first plant generation. Regarding the mutant crossing, different crossings were carried out *kin10-2* with *DUFOE3* and *kin10-2* with *dufko3*. *kin10-2* was used as a mother plant or father plant during the crossing program. The father *dufko3* vs. the mother *kin10-2* crossing grew (*duf_kin10-2*), and seeds of the first generation were harvested. Seeds were sown to screen the plants using PCR to determine the double mutants screened to obtain a positive crossed mutant plant using LB salk F and DUF R, and LB F and KIN10 R primers (Table 2.1). The homozygous plant was obtained from the third generation. Primers can be found in the supplements.

2.1.9. Protein Extraction

Total protein was extracted from plant leaves using an extraction buffer containing 50 mM HEPES (pH 8.2), 5 mM MgCl₂, 1 mM EDTA, 10% glycerol, 0.1% Triton X-100, 2 mM benzamide, 2 mM aminocaproic acid, 0.5 mM phenylmethanesulfonyl fluoride (PMSF) and 10 mM DTT. The samples were mixed with the buffer and then centrifuged to remove any impurities at 14000 rpm for 10 minutes at 4°C. Protein concentrations were determined using the Bradford assay (Bradford, 1976). Bradford

reagent (#B6916, Sigma Aldrich) was used to measure the absorbance at 595nm using the FLUOstar Omega microplate reader (BMG LABTECH, Offenburg, Germany). Along with a standard curve, which was prepared from BSA stock (2.5 µg/µl), (0, 0.2, 0.4, 0.6, 0.8, 1.0, 1.2, and 1.4), dilutions of BSA stock with protein extraction buffer were made to make the standard curve. Protein concentration was calculated by the standard curve in µg/µl using the formula: Protein concentration = (absorbance-0.6297)/0.0872.

2.1.10. Western Blot

Acrylamide gel electrophoresis was carried out with a mini-protean gel electrophoresis system using 30% Acrylamide to separate the proteins by their molecular weights. Resolving and stacking gels were made. Resolving gel was prepared (1.633 ml H₂O, 1.266 ml of 1.5 Tris-HCl, pH 8.8, 1.999 of 30% Acrylamide, 50 µl of 10% Sodium Dodecyl Sulfate (SDS), 50 µl of 10% Ammonium Persulfate (APS), and 2 µl Tetramethylethylenediamine (TEMED). After the resolving gel was set, stacking gel was prepared (1.511 ml H₂O, 0.619 ml of 0.5 Tris-HCl, pH 6.8, 0.330 ml of 30% Acrylamide, 25 µl of 10% SDS, 25 µl of 10% APS, and 2 µl TEMED). The same concentrations (10-30 µg) of proteins were loaded for each sample, as described by Mahmood and Yang (2012). The proteins were separated with running buffer (SDS, Tris Base, and glycine) with voltage 100-110 to 90-120 minutes, depending on the protein size. After that, Western blot was carried out by transferring the proteins onto a polyvinylidene difluoride membrane (PVDF membranes) using transfer buffer (Tris, Glycine), which was prepared with methanol and H₂O. The voltage was set at 66V for 66 minutes. The membranes were then incubated with different specific primary

antibodies Rubisco (1/10,000 dilution), the Calvin-Benson cycle proteins Transketolase 5 (TK) (1/5000 dilution), FBP aldolase (FBPA) (1/500 dilution), PsaA (1/1000 dilution), the photosystem I Lhca1 protein (1/2000 dilution), the electron transport cytochrome b6 Cytb6 and RieskeFeS proteins (1/10,000 dilution), green fluorescence protein GFP antibody (1/1000-1/5000 dilutions), phosphoglycerate kinase (PGK) (1/1000 dilution), and glyceraldehyde-3-phosphate dehydrogenase (GAPDH) (1/2500 dilution). Finally, the membranes were incubated in goat anti-rabbit secondary antibody (1/20,000 dilution). Protein bands were detected using Pierce™ ECL Western Blotting Substrate (#32106, ThermoFisher Scientific™, UK) following the manufacturer's instruction using chemiluminescence detection method. Coomassie blue staining was used to control the loading of protein in the Western blot analysis, and Ponceau staining was used to determine the equal protein that was transferred.

2.1.11. Protoplast isolation

Protoplast was isolated from 4-5-week-old plants following the 'tape-Arabidopsis sandwich' method described by Wu *et al.* (2009) to isolate mesophyll protoplast. Leaves were harvested, then the upper epidermal surfaces of the leaves were stuck onto an autoclave tape, and the lower epidermal surfaces were covered with magic tape. The mesophyll cells were exposed by peeling the magic tape off. The autoclave tapes containing the mesophyll cells were incubated in enzyme solution (Cellulase (0.5%, w/v), pectinase R10 (0.25%, w/v), D-mannitol (400 mM), CaCl₂ (10 mM), KCl (20 mM), Bovine Serum Albumin (0.1%, w/v) and MES (20 mM, pH 5.7)) on a platform shaker at 40 rpm for 60 minutes. The solution containing released protoplasts was centrifuged for 3 minutes at 100 rpm at 4°C. The pellet containing the protoplasts was

washed twice with W5 solution (NaCl (150 mM), CaCl₂ (125 mM), KCl (5 mM), MES (2 mM pH 5.7), and Glucose (5 mM)) then incubated on ice for 60 minutes. The protoplasts were then centrifuged for 3 minutes at 100 rpm at 4°C and resuspended in a modified MMg solution (mannitol (4 mM), MgCl₂ (15 mM), and MES (4 mM, pH 5.7)) to a final concentration of 2 to 5 × 10⁵ cells/ml.

2.1.12. Protoplast transfection

Protoplasts were transformed with Ct pUBQ:DUF:GFP by adding 2 µg/µl of reporter plasmid to the protoplast with an equal volume of a freshly prepared PEG solution (PEG4000 40% (w/v), D-mannitol (200 mM), and CaCl₂ (100 mM)). The protoplast-plasmid mixture was incubated for 15 minutes at room temperature, and then the protoplasts were washed twice using W5 solution. After that, the mixture was centrifuged for 1 minute at 100 rpm. The protoplasts were incubated in W5 solution at room temperature for 16 hours in light. Transformed protoplasts were imaged after 24 hours of incubation in darkness at room temperature using confocal microscopy (see 2.3.5).

2.1.13. Transient expression

2.1.13.1. *Agrobacterium* electro-competent cells preparation

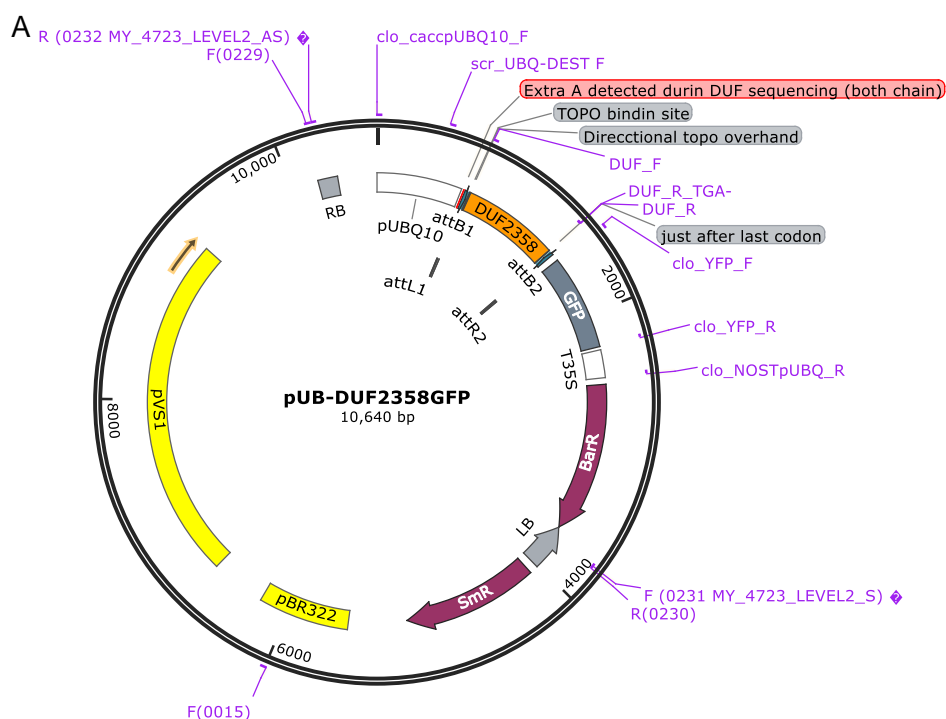
Selective LB Agar plate was supplemented with 50 µg Rifampicin (Rif) (#13292-46-1, Melford, UK) and 50 µg gentamicin (Gen) (#1405-41-0, Melford, UK). Antibiotics were spread with *Agrobacterium* GV3101 strain cells from the freezer stock and incubated for 48 hours at 28°C. 10 ml of LB broth media with Rif and Gen antibiotics were

inoculated with a colony of *Agrobacterium* then it is incubated for 48 hours at 28°C with shaking. Another 10 LB of broth media with antibiotics was incubated again with 100 µl of the starter culture, then also incubated for 48 hours at 28°C with shaking. The cells were harvested by centrifugation at 3000 g for 15 minutes at 4°C. The supernatant was discarded, then the cells were resuspended in 10 ml of ice-cold sterilised MilliQ water, and the cells gently suspended using sterile pipettes. Again, the cells were centrifuged at 3000 g for 15 minutes at 4°C. The washing step was repeated three more times, then the cells were resuspended in 200 µl of ice-cold sterile 10 % glycerol. After aliquoting *Agrobacterium* cells for 40 µl into a pre-cooled Eppendorf tube, the cells were stored at -80°C.

2.1.13.2. *Agrobacterium* transformation

Agrobacterium GV3101 cells (rifampicin and gentamicin resistance) (Koncz and Schell, 1986) were transformed with C-terminal-pUBQ:DUF2358::GFP fusion (Ct-DUF:GFP) (spectinomycin resistance) (Figure 2.3.A), N-terminal GFP::SS4 (*STARCH SYNTHASE 4*) (kanamycin resistance) which was described by Gámez-Arjona *et al.* (2014) (Figure 2.4), and pBIN61-p19 (P19) (kanamycin resistance) (Figure 2.3.B), through electroporation. 1 µl of the plasmid DNA (50-150 ng) was added to 40 µl of the *Agrobacterium* cells and gently mixed. The mix was transferred to ice-cold 2 mm electroporation cuvette (EquiBio, Boughton Manchelsea, UK) and placed into an Easyjet Prima Electroporator (EquiBio) set at 1800V pulse for about 3 seconds. After electroporation, 1 ml of LB pre-cooled medium was added into the cells and the samples were incubated on a shaker at 28°C. After 2-3 hours of incubation, 200 µl of the cells were plated on LB selective Agar plates containing Rifampicin (50 µg/ml) and

Gentamicin (25 µg/ml) along with the suitable antibiotic for each plasmid Spectinomycin (50 µg/mL # 22189-32-8, Melford, UK) for Ct-DUF::GFP or Kanamycin (50 µg/mL # 25389-94-0, Melford, UK) for GFP::SS4 and P19 plasmids. The plates were incubated for 48 hours at 28°C. Positively transformed colonies were verified by colony PCR (Table 2.2). The result positive *Agrobacterium* transferred colonies were used to carry out transient expression.



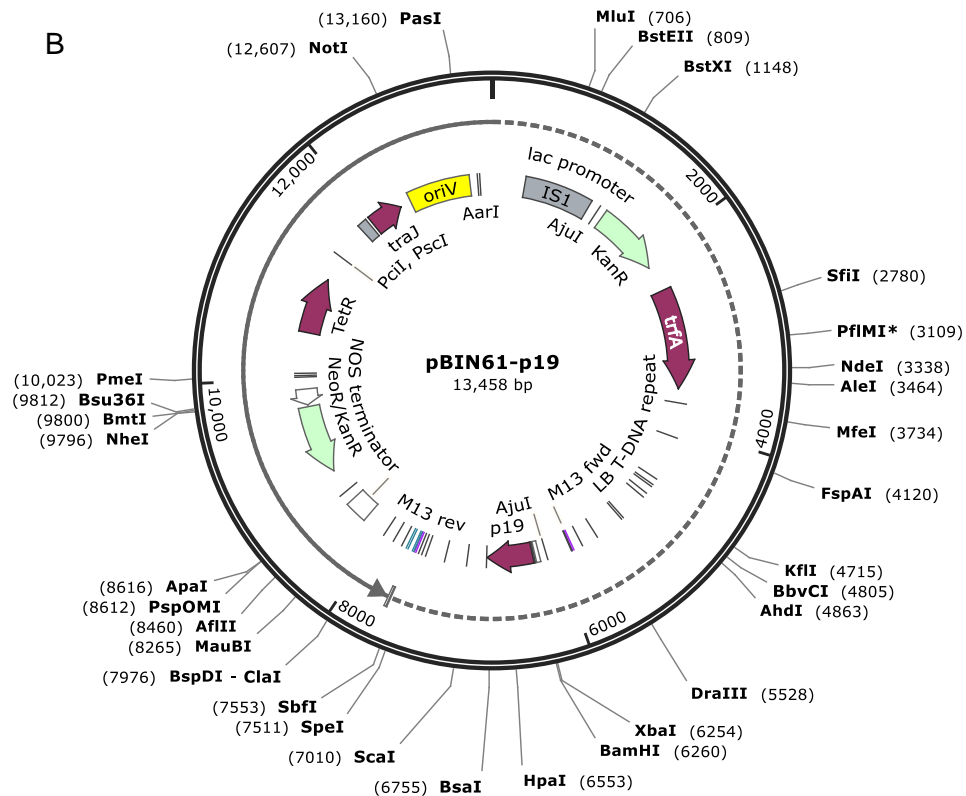


Figure 2.3. (A) Plasmid map of pUBQ:DUF2358::GFP *map was provided by Dr. Exposito. cDNA from Col-0, pUBQ10 promoter, T35S terminator, C-GFP, backbone and 35S Kan supplied in the Golden Gate Plant Parts Kit. **(B)** Plasmid map of pBIN61-p19. lac promoter, NOS terminator. Resistance to neomycin, kanamycin, and G418 (Geneticin®)



Figure 2.4. N-terminal region of starch synthase 4 SS4 fused to GFP. cDNA generated from Col-0, N-terminal region of SS4 transferred into pEarleyGate103 vector (for fusion with GFP) driven by CaMV 35S promoter. (Figure and information sources: Gámez-Arjona *et al.*, 2014).

2.1.13.3. Agro infiltration

10 ml LB medium was used to inoculate a single *Agrobacterium* colony from master plates of each plasmid Ct-DUF:GFP, GFP::SS4 and P19 with antibiotics. The cultures were grown for 24 hours at 28°C on a shaker at 180 rpm. The overnight cultures were

used again to inoculate fresh 10 ml LB mediums again until $OD_{600} = 0.4-0.8$, then the cultures were centrifuged at 1000 g for 15 minutes at room temperature. The cells were resuspended in an infiltration solution (10 mM Mes, pH 5.6, 10 mM $MgCl_2$, and 100 μ M Acetosyringone) and adjusted to a final OD_{600} of 0.5. The cultures were incubated for two hours at room temperature. Before plant infiltration, an equal volume of each culture Ct-DUF:GFP and GFP::SS4 was mixed with P19 cultured. Young *Nicotiana benthamiana* leaves were infiltrated with Ct-DUF:GFP, GFP::SS4, and P19 only as a control. After five days of infiltration, the expression of GFP proteins was determined using confocal microscopy (see 2.3.5).

2.1.14. Chloroplast isolation

Plant leaves were ground with freshly prepared ice-cold isolation buffer (0.33 M Sorbitol, 50 mM HEPES pH 7, 1% (m/v) Serum bovine albumin, 2 mM EDTA, and 1 mM $MgCl_2$) using a pre-cooled mortar and pestle. After filtering the mix through a 47 μ m nylon mesh in the dark, the homogenate was kept on ice. The filtered mix leaves were carefully placed on top of the 40% Percoll layer (4 ml Percoll + 6ml 1X chloroplast isolation buffer with BSA to make 10 ml of 40% Percoll). This was centrifuged at 1700 rpm for 6 minutes at 4°C. The remaining Percoll was removed by resuspending the pellet in isolation buffer followed by centrifugation two more times.

2.1.15. Co-immunoprecipitation and pull-down

Nicotiana benthamiana chloroplasts were isolated from the leaves after transient expression and used to carry out Co-Immunoprecipitation using the Pierce Co-Immunoprecipitation Kit (#26149 ThermoFisher Scientific, UK), following the

manufacturer's instructions with some modifications. The procedures were started by preparing the protein for the pull-down. Chloroplasts were centrifuged at 1700 g for 6 minutes at 4°C. The chloroplasts were washed with Phosphate-buffered saline PBS buffer (8 mM sodium phosphate, 2 mM potassium phosphate, 140 mM sodium chloride, and 10 mM KCl; pH 7). The protein was lysed by adding lysis/wash buffer (25 mM Tris, 150 mM NaCl, 1 mM EDTA, 1% NP-40, 5% glycerol; pH 7.4). The mixtures were incubated on ice for 5 minutes followed by centrifugation for 10 minutes at 13000 rpm. The lysates were pre-cleared using the Control Agarose Resin. The lysate was then added to 1 ml columns containing the appropriate resins, which were prepared with GFP antibody 75 µg/ml (Abcam plc. #ab6556) following the manufacturer's instruction. The mixtures were incubated overnight at 4°C with gentle rocking. The mixtures column was attached to microcentrifuge collection tubes and then centrifuged for 60 seconds at 1000 rpm. The resins were then washed with lysis/wash buffer three times and centrifuged after every wash. Elution buffer (100 mM glycine, HCl, pH 2.8) was added into the resins and incubated for 5 minutes at room temperature. After that, the columns were centrifuged for 60 seconds at 1000 g, and flow-through was collected for protein analysis.

2.1.16. Proteomics

After the proteins were pulled-down, the elution buffer was exchanged with 50 mM ammonium bicarbonate, and then the samples were sent to the Advanced Mass Spectrometry Facility in Birmingham to carry out the proteomic analysis. The raw data were filtered and analysed using Microsoft Excel, and the most interesting proteins were chosen to conduct yeast-two-hybrid.

2.1.17. Plasmid construction and cloning

Putative DUF2358 interacting proteins were selected for yeast-2-hybrid analysis. The *Arabidopsis thaliana* homologous proteins were identified by the BLAST search (The Universal Protein Resource (UniProt)) with protein sequences of the *Nicotiana benthamiana* proteins, which were obtained from proteomics. Alignments information can be found in Appendix A.

Proteins from *Nicotiana benthamiana* along with the homologous proteins from *Arabidopsis thaliana* were cloned in the pGAD-C1 (activation domain) or pGBDU-C1 (binding domain) vectors (Villar-Fernández *et al.*, 2020) (Figure 2.5 A and B) along with the *Arabidopsis* DUF2358 protein. The full-length protein-coding sequence of the different interested chosen proteins FTSH-LIKE, GLYCERALDEHYDE-3-PHOSPHATE DEHYDROGENASE (GAPDH), PHOSPHOGLYCERATE KINASE (PRK), CALCIUM-SENSING RECEPTOR (CAS), CHLOROPLAST ATP-DEPENDENT PROTEASE CHAPERONE PROTEIN (CLPC1B), CARBONIC ANHYDRASE (CA), and CHLOROPLAST ELONGATION FACTOR TUB (CpEF-TUB) and DUF2358 were amplified from wild-type *Nicotiana benthamiana* and Col-0 *Arabidopsis thaliana* cDNA by PCR with Phusion Hot StartII DNA Polymerase (#F549S, ThermoFisher Scientific, UK) following the manufacturer's instructions for 20 µl PCR reaction. Each reaction contained 100-200 ng of cDNA, and the annealing temperature was between 55-60 (see primer Table 2.2). The PCR products were cleaned up using PureLink™ PCR Micro Kit (#K310010, ThermoFisher Scientific, UK) following the manufacturer's instructions. Another method to clean up the PCR product involved adding guanidine hydrochloride and isopropanol binding buffer (pB buffer) (#19066, Qiagen, Hilden, Germany) to the sample, then spun at 13000 g for 5 minutes. The samples were then washed with 70% ethanol.

The next step was PCR product digestion using two digestion enzymes. The PCR products ligated into the two vectors, pGAD-C1 and pGBDU-c1, using the traditional cloning method starting with a restriction enzyme. A list of the full cutting enzymes used in this study is set out in Table 2.3. Restriction enzymes were used with the PCR products and the vectors. After digestion, the vectors were treated with Alkaline phosphatases Polymerase (FastAP) (# EF0652, ThermoFisher Scientific, UK) to reduce the self-ligation, which helped to reduce the background of empty clones. The next step was ligation. Ligase enzyme was used in this step to complete the ligation of the DNA with the vectors (Table 2.3). 100 ng of vectors were used in the ligation reaction using 0.5 μ l T4 DNA Ligase (1U/ μ L) (#15224017, ThermoFisher Scientific, UK) with 1 μ l of ligase buffer, and the complete reaction volume was 10 μ l. The ligation reactions were incubated overnight at 16°C (Table 2.4).

The resulting plasmids were transformed into *E. coli* Top10 competent cells using the heat-shock method to increase the plasmid. The *E. coli* cells were plated on selective LB Agar plate with 50 μ g/ml Ampicillin and incubated overnight at 37°C. Colonies PCR in PCR was performed to identify the positive transformation. Positive colonies were grown overnight at 37°C in a shaker 180 rpm and the plasmids were extracted and purified using GeneJET Plasmid Miniprep Kit (#K0503, ThermoFisher,UK). The plasmids were sent to sequencing using Eurofinsgenomics services. Finally, the resulting plasmid was used in the yeast two-hybrid system.

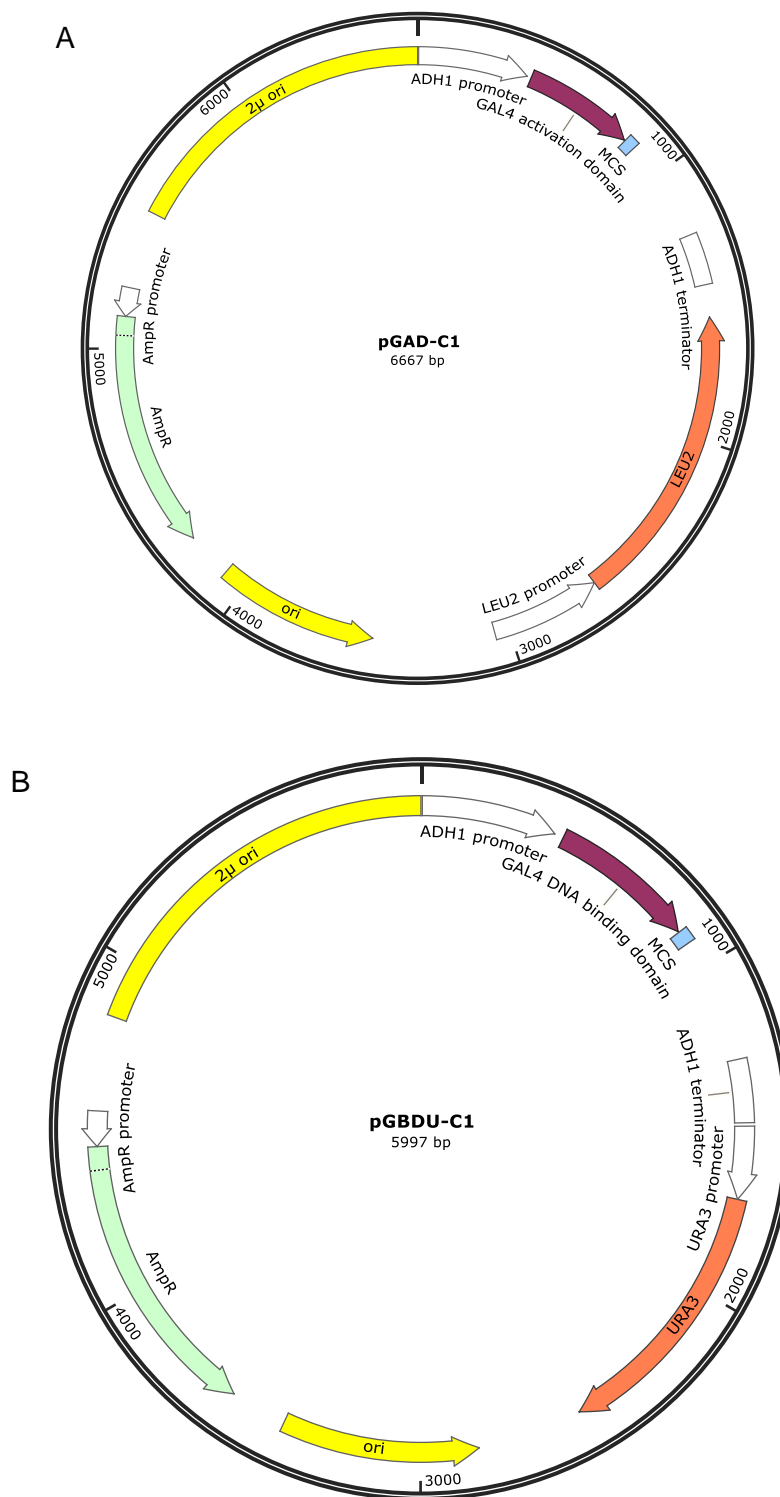


Figure 2.5. Yeast two-hybrid vectors showing restriction sites, marker, and resistance. **(A)** pGAD-C1 "prey" cloning vector for fusing a gene to the GAL4 activation domain. **(B)** pGBDU-C1 vector for fusing a gene to the GAL4 DNA binding domain.

Table 2.3. Restriction enzymes (RE) were used for cloning system in this study. Different restriction enzymes were used with the vectors depending on the restriction sites of proteins that were ligated with the vectors.

Restriction enzymes (RE) used for cloning system			
1.Yeast two-hybrid "activation" and "binding" vectors			
pGAD-C1		XmaI and BamHI, BamHI and Sall, EcoRI and XmaI, XmaI and PstI, EcoRI and PstI	
pGBDU-C1		EcoRI and PstI, XmaI and PstI, EcoRI and XmaI, EcoRI and Sall, BamHI and PstI.	
Protein	ID	Restriction enzymes	Buffer
CpEF-TuB	D5LT98	EcoRI and PstI	O buffer
NbGAPDH-A	A0A0A8IBT8	XmaI and BamHI	Cfr9I buffer
E5LLE7	E5LLE7	EcoRI and PstI	O buffer
Nb-CAS	K7ZLE1	BamHI and Sall	R buffer
ClpC1B	A0A088F8F4	EcoRI and XmaI	Cfr9I buffer
A4D0J9	A4D0J9	EcoRI and PstI	O buffer
FtsH	C9DFA3	EcoRI and PstI	O buffer
DUF2358	AT2G46220	XmaI and PstI	Cfr9I buffer
GAPDH	AT1G16300	EcoRI and XmaI	Cfr9I buffer
CLPC	AT5G50920	EcoRI and PstI	O buffer
CAS	AT5G23060	EcoRI and PstI	O buffer
Carbonic anhydrase	AT3G01500	EcoRI and PstI	O buffer
PGK	AT1G79550	EcoRI and Sall	O buffer
EF-TuB	AT4G20360	BamHI and PstI	O buffer

Table 2.4. Generated Prey and Bait constructs of *Nicotiana benthamiana* and *Arabidopsis thaliana* proteins which were used to conduct yeast-2-hybrid system.

<i>Nicotiana benthamiana</i> protein constructs		<i>Arabidopsis thaliana</i> protein constructs	
Prey Constructs	Bait Constructs	Prey Constructs	Bait Constructs
pGAD-C1:	pGBDU-C1:	pGAD-C1:	pGBDU-C1:
DUF2358	DUF2358	DUF2358	DUF2358
A4D0J9	NbGAPDH-A	GAPDH	- CAS
E5LLE7	ClpC	CLPC	-
CpEF-TuB	Nb-CAS	Carbonic anhydrase	
-	-	PGK	-
-	-	EF-TuB	-

2.1.18. Preparation of *E. coli* competent cells

A plate of LB Agar was streaked with *E. coli* competent cells from the glycerol stock, then incubated overnight at 37°C. 10 ml of LB broth media were incubated without any antibiotic with a single *E. coli* colony which was grown overnight and incubated overnight at 37°C on a shaker 180 rpm. 100 ml of LB broth media were inoculated with 1 ml of the starter culture, and then the cells were grown at 37°C for 3 hours until OD₆₀₀ reached 0.4. The culture was spun down at 4°C for 5 minutes at 3000 rpm after splitting the culture into two falcon tubes at 50 ml each. The supernatant was discarded, and the cells' pellets were resuspended in 10 ml each of ice-cold sterile CaCl₂ solution (100 mM CaCl₂, 10 mM PIPES (pH7.0 adjusted with NaOH) and 15% glycerol). The cells were centrifuged for 5 minutes at 4°C at 3000 rpm then the supernatant was discarded carefully. This step was repeated twice, and then the cells

were incubated on ice after resuspending in CaCl_2 solution for 30 minutes. After incubation, the cells were centrifuged at 4°C for 5 minutes at 2500 rpm. The cells were resuspended again and aliquoted in pre-cooled sterile tubes and stored at -80°C .

2.1.19. Yeast Two-Hybrid system

Yeast-Two-Hybrid was conducted using the proteins which were detected by Co-Immunoprecipitation CO-IP. Full-length coding sequences of DUF2358 and other chosen proteins were cloned in the pGAD-C1 (activation domain) or pGBDU-C1 (binding domain) vectors (Villar-Fernández *et al.*, 2020) (Figure. 2.6 A and B). Then, the plasmids (bait and prey) were transformed into yeast reporter strain (AH109) to conduct the Y2H screen.

Putative DUF2358 interacting patterns were selected for yeast-2-hybrid analysis. The *Arabidopsis thaliana* homologous proteins were identified by the BLAST search (The Universal Protein Resource (UniProt)) with protein sequences of the *Nicotiana benthamiana* proteins which were obtained from proteomics. Alignments data can be found in the appendix A.

In total, six proteins were tested for interaction with DUF2358 in the Y2H screen. AH109 yeast strain was used which has four independent reporter genes: mutant version of the Aureobasidin resistance AUR1 gene, Adenine requiring gene, Histidine3 requiring gene, and yeast α -galactosidase MEL1 (*AUR1-C*, *ADE2*, *HIS3*, and *MEL1*) with the GAL4 system. These reporter genes can be used to study the interaction between different proteins because these genes only express when the activation domain fused protein GAL4 DNA-AD and GAL4 DNA-BD fused protein interact with each other (Hoshijima *et al.*, 2017; Wong *et al.*, 2017) (Figure. 2.6). Adenine (-Ade)

and histidine (-His) minus medium can be used to investigate the protein-protein interaction. Reporter genes can be used to screen protein interaction in yeast because the yeast strain AH109 is unable to synthesis these amino acids. Also, it is unable to grow on the media in the absence of these amino acids. In the yeast two-hybrid, DNA-binding domain BD and activation domain AD are fused into studied putative interacted proteins resulting in bait and prey proteins. If the two proteins are interacting with each other, the reporter gene will be activated, and the yeast will grow using the amino acids from the other domain (Folter and Immink, 2011). Also, the two Y2H vectors have different markers, as pGAD-C1 has LEU2 gene and pGBDU-C1 URA3 gene which give the vector's resistance to grow in medium lacking leucine and uracil, respectively.

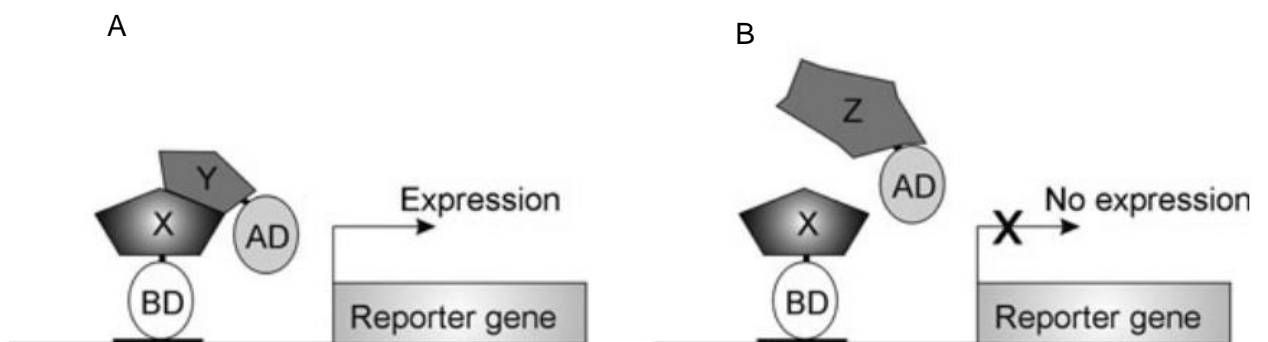


Figure 2.6 Overview of yeast two-hybrid (Y2H) GAL4 system **A**) when the two fusion (bait and prey) proteins interact, the GAL4 transcriptional activator reconstructs, activating the reporter gene. **B**) when the two proteins do not interact, then the GAL4 transcriptional activator stays inactive, repressing the expression of the reporter gene. AD, activation domain; X, protein X; Y, protein Y; Z, proteins (Folter and Immink, 2011).

2.1.19.1. Preparation of yeast AH109 cells

The yeast strain AH109 were freshly prepared every time by inoculating AH109 cells on yeast peptone dextrose adenine (YPDA) media (Yeast extract 1% (w/v), Peptone

2% (w/v), Dextrose 2% (w/v), Adenine hemisulphate 80-100 mg/lit, and Agar 2% (w/v) and incubated at 30°C for 2-3 days. One colony was picked up and inoculated in YPD broth media and left to grow at 30C until OD₆₀₀ reached 0.5. The primary culture was re-inoculated in YPD broth for 4-6 hours until OD₆₀₀ reached 1. The cells were harvested by centrifugation at 300 rpm for 5 minutes at 20°C. The cells were washed with sterilised water twice and centrifuged again at 300 rpm for 5 minutes. The cells were then resuspended in 0.1 M Lithium acetate (LiAc) and incubated on ice for 10 minutes. Then they were centrifuged at 13000 rpm for 30 seconds at room temperature. The pellets were resuspended in 0.1M LiAc with vortex and centrifuged again. Then the cells were used in yeast transformation.

2.1.19.2 Yeast transformation

The DUF2358 was initially used as a bait to screen the interaction between DUF2358 and the other putative binding partners which were cloned as prey protein. Also, the opposite was used with the proteins which did not show any interaction as a prey protein (Table 2.4). The plasmids (500 ng-1 µg) of each vectors pGAD-C1 and pGBDU-C1 (Villar-Fernández *et al.*, 2020) (Figure 2.5 A and B) were prepared and cloned then sequenced (using the Gal4 primer in Table2.2) as described in section 2.1.17 in this chapter. These were mixed with the transformation master mix (PEG 400 (40%), LiAc (1M), single-stranded carrier DNA, SS carrier DNA (2mg/ml)(# 15632011, ThermoFisher, UK) after heating ss carrier up to 95°C then cooled rapidly on ice following the manufacturer's instructions. The mixture tubes were incubated at 42°C for 30-45 minutes then centrifuged at 13000 g for 45 seconds, and then the pellet was

dissolved in sterilised water. The cells were plated on -Leucine (-Leu) and -Uracil (-Ura) dropout media and incubated for 2-3 days at 30°C.

2.1.19.3. Screening for Protein-protein interaction

Positive colonies that grew in -Leu and -Ura dropout media were inoculated again on selective dropout media -Leu and -Ura and -Histidine (-His) or selective dropout Agar media -Leu and -Ura and -Adenine (-Ade). Then, the selective plates were incubated at 30°C for 2-3 days. The colonies which appeared in the selective dropout Agar media in the screening step were considered a positive interaction. Overnight-grown cells were diluted in sterilised distilled water, OD₆₀₀ was adjusted to 0.1. These cultures were used to make a further 4 of 1:10 dilutions and 5 µl of cells were spotted on YPD selective Agar plates. The plates were incubated at 30°C for 48 hours.

2.2. Plant phenotyping and growth techniques

2.2.1. Drought stress

Two weeks after germination, plants were pricked out and placed in an individual pot (7 x 7 x 9 cm) filled with the same weight of soil. Control pots were filled with soil and fully saturated to determine the weight 100% field capacity (FC) and then left to dry out to determine 0% FC. Relative soil water content (rSWC) was calculated using the formula: $(\text{Pot with soil weights} - \text{Empty pot weights} - \text{Dry soil weights (0\% water)}) \times 100 / (\text{Water saturated soil pot weights} - \text{Dry soil weights})$.

The drought stress experiment began three weeks after the seedlings were pricked out. Half of the plants of each genotype were kept under well-watered conditions, while the watering of the remaining half was stopped. The weight of each pot (well-watered

and drought plants) was taken daily, as described in Bechtold *et al.* (2016). Leaf material was harvested at 20% rSWC and frozen in liquid nitrogen and stored at -80C for subsequent analysis (gene expression, soluble sugar, starch and H₂O₂).

2.2.2. Dark-induced senescence

Five-week-old soil-grown plants were subjected to complete darkness for 9 days, while control plants were maintained under normal light/dark conditions described above. *Fv/Fm* was measured every day at the same time using Technologica FluorImager analytical instrument (see 2.5).

2.2.3. Extended night and glucose supplementation

Rosettes of 5-week-old plants were detached from the roots and were incubated in RO water in Petri dishes for 4 hours in the middle of the day in light (L), light supplemented with 50 mM glucose (LG), dark (plants were incubated in dark for 4 hours in RO water) (D) and 4 hours incubation in dark supplemented with 50 mM glucose (DG), respectively, following the method described in (Rodrigues *et al.*, 2013). After the 4-hour incubation, *Fv/Fm* was measured using Technologica FluorImager, and plants were harvested for gene expression analysis. RNA was extracted to analyse gene expression in response to sugar and dark treatment for all genotypes. Finally, eukaryotic initiation factor 4 (EIF4), glutamine-dependent asparagine synthase 1 dark inducible 6 (DIN6), aluminium-induced protein with YGL and LRDR motifs (SEN5), SnRK1 marker genes dormancy/auxin-associated protein (AXP), Arabidopsis Rab gtpase homolog b18 (RAB18) and low-temperature-induced 65 (RD29B) protein

were studied for their expression. The sequence data can be found in Table 2.2. Finally, soluble sugar and starch were determined using carbohydrate assay.

2.2.4. Growth analysis

Growth analysis was conducted to determine the morphological and developmental phenotypes of all the mutant genotypes and Col-0. Seed germination after sowing the seeds was recorded every day to calculate the average germination time for each genotype, and growth stages (Table 2.5) were determined by counting leaf numbers and recording progression to flowering daily. Average days were calculated from the date of sowing, including the 3-day stratification at 4°C to synchronise seed germinations. Also, daily pictures were taken to determine all other growth stages as described by Boyes *et al.* (2001). Leaf was counted using a ruler to measure leaves <1 mm. For measuring visible rosette areas, daily pictures were taken of the rosette. The pictures were analysed using the ImageJ program (<https://imagej.nih.gov/ij/index.html>). Growth stages for *Arabidopsis thaliana* were defined as per Boyes *et al.*'s (2001) study (Table 2.5). Finally, seed weight for each genotype was analysed.

Table 2.5. Arabidopsis Growth Stages for the Soil-Based Phenotypic Analysis Platform. Table based on Boyes *et al.*, 2001.

Stage	Description
Principal growth stage 0	Seed germination
0.10	Seed imbibition
0.50	Radicle emergence
0.7	Hypocotyl and cotyledon emergence
Principal growth stage 1	Leaf development
1.0	Cotyledons fully opened
1.02	2 rosette leaves >1 mm in length

1.03	3 rosette leaves >1 mm in length
1.04	4 rosette leaves >1 mm in length
1.05	5 rosette leaves >1 mm in length
1.06	6 rosette leaves >1 mm in length
1.07	7 rosette leaves >1 mm in length
1.08	8 rosette leaves >1 mm in length
1.09	9 rosette leaves >1 mm in length
1.10	10 rosette leaves >1 mm in length
1.11	11 rosette leaves >1 mm in length
1.12	12 rosette leaves >1 mm in length
1.13	13 rosette leaves >1 mm in length
1.14	14 rosette leaves >1 mm in length
Principal growth stage 3	Rosette growth
3.20	Rosette is 20% of final size
3.50	Rosette is 50% of final size
3.70	Rosette is 70% of final size
3.90	Rosette growth complete
Principal growth stage 5	Inflorescence emergence
5.10	First flower buds visible

2.3. Bioinformatics techniques

2.3.1. Chlorophyll fluorescence measurements

Chlorophyll fluorescence was measured using Technologica FluorImager (chlorophyll fluorescence imaging analytical instrument) (CF Imager) (Technologica Ltd, UK) which was described by Barbagallo *et al.* (2003). The images were analysed using V2.305 FluorImager software. Different fluorescence parameters were measured. At the weak measuring pulses, minimal fluorescence from dark-adapted leaves (F_0) was measured, while maximal fluorescence from dark-adapted leaves (F_m) was measured after the plants were exposed to 800-ms pulses of high intensity about $2900 \mu\text{mol m}^{-2}$

s⁻¹. The camera also took a series of sequential photos during the last 650 ms at 20 Hz. The image with the highest mean value was used to generate the PSII Maximum efficiency (F_v/F_m) image by the program (Barbargallo *et al.*, 2003).

The Technologica FluorImager was used following the manufacturer's instructions. The sample stage rack was adjusted to 140 mm as instructed by the manufacturer, and then the plants were placed under the camera and the LED imaging light. The connection with the camera and light system was established. The protocol was carried out following the manufacturer's instruction. The fluorescence parameter data were copied to Excel to calculate the means and further analysis.

2.3.2. H₂O₂ measurement

100 mg of leaf material were harvested then ground on dry ice, then 0.5 ml ice-cold phosphate buffer PB (100 mM) was added (at a ratio of 1:5) and vortexed for 10 seconds. The samples were incubated at room temperature for 30 minutes on a shaker and centrifuged at room temperature for 5 minutes at 12000 rpm. The supernatants were transferred into a clean Eppendorf tube and centrifuged for an additional 2 minutes at 12000 rpm, and the clear supernatant was used to conduct the H₂O₂ analysis. 30% H₂O₂ was mixed with PB to make 100 mM fresh stock of H₂O₂. The H₂O₂ stock was used to create a standard curve of (0,2,20,50 and 100 μ M) dilutions in pB buffer. In a microtitre plate, 5 μ l of each sample or standard solution was mixed with 45 μ l of Amplex red mix (100 mM PB, 10 mM Amplex red stock (#A12222, ThermoFisher, UK), and horseradish peroxidase HRP enzyme). The plate was covered with aluminium foil and shaken for 1 minute at 450 nm and incubated at 30°C for 30 minutes. A FLUOstar Omega microplate reader (BMG LABTECH,

Offenburg, Germany) was used to measure fluorescence (Excitation at 530-560 nm at 590 nm Emission).

2.3.3. Carbohydrate assay

2.3.3.1. Carbohydrate extraction

Soluble sugar and starch were extracted from about 20 mg of frozen plant material. 80% ethanol was added to frozen samples and mixed well. The samples were heated to 20 minutes at 80°C and were centrifuged at room temperature at 3000 rpm for 5 minutes. The ethanol supernatant was collected, and the pellet was re-extracted in 80% ethanol for a total of three times. Supernatants of all three extractions were combined and contained the soluble sugars, while the pellet contained the insoluble starch. Both supernatant and pellets were freeze-dried overnight.

2.3.3.2. Hexose sample preparations

The dried ethanol extracts were resuspended into HEPES buffer (100 mM, pH 7.5 using HCl) and vortexed. The samples were centrifuged twice at 3000 rpm for 5 minutes to eliminate all debris. The clean hexose extracts were stored on ice until the carbohydrate assay was used

2.3.3.3. Starch sample preparations

To solubilise the starch, sodium acetate (100 mM, pH5) was added to the dried pellet and mixed well. The samples were incubated at 100°C for 10 minutes and were mixed by pipetting for 30 seconds to break up the pellet. The samples were re-heated for a further 2 minutes before allowing to cool to room temperature. A master mix containing

sodium acetate (50 mM, pH5), alpha-amylase (1.2 U/ μ l), and amyloglucosidase (1.2 U/ μ l)) was added to the samples and mixed well. The samples were incubated at 37°C overnight. After incubation, the samples were centrifuged at 13000 rpm for 5 minutes and the clear supernatants were used in hexose assays.

2.3.3.4. Hexose assay

A 170 μ l of master mix containing 100 mM HEPES buffer (pH 7.5), 40 mM NADP, 100mM ATP and Glucose-6-phosphate dehydrogenase G6PDH (0.05 U/ μ l)) was added to each well of a 96-well plate. Then, 20 μ l of each sample was added and the final reaction volume was 190 μ l. Each sample was analysed in triplicate. The plate was transferred to the FLUOstar Omega microplate reader (BMG LABTECH, Offenburg, Germany) and the temperature was set to 23°C. Absorbance was measured every 2 minutes at 340 nm for approximately 15 minutes until the reaction had stabilised. 10 μ l of Hexokinase (0.05 U/ μ l) was subsequently added into each well and mix, then the absorbance at 340nm was measured every 2 minutes for approximately 25 minutes until the reaction had stabilised. After that, 10 μ l Phosphoglucose isomerase (PGIsomerase) (0.06 U/ μ l) was added and absorbance was measured every 2 minutes at 340 nm for approximately 35 minutes until the reaction had stabilised. Finally, 10 μ l of invertase (0.06 U/ μ l) was added and the plate measured every 2 minutes at 340 nm for about 50 minutes until the reaction had stabilised. Standards containing 20 mg ml⁻¹ glucose, 20 mg ml⁻¹ sucrose, and 20 mg ml⁻¹ fructose were run parallel. Each standard was diluted 5 times (20, 15, 10, 5, 2.5 and 1.25 mg ml⁻¹) to create the standard curve. The carbohydrate concentrations were calculated using the formula which was generated from the curves of standard

concentration vs. absorbance using the known standard concentration. The drought stress carbohydrate measurement was calculated with the following formulas:

Glucose concentration = $(\text{absorbance} - 0.0689) / 0.6787$, Fructose concentration = $(\text{absorbance} / 0.6932)$, and sucrose concentration = $(\text{absorbance} - 0.1007) / 0.6932$. The starch samples were measured in a similar set-up, but reactions only contained G6PDH and Hexokinase enzymes. The starch calculation formula was starch concentration = $(\text{absorbance} - 0.0689) / 0.6787$. Then, carbohydrate contents were calculated for each sample under different conditions.

2.3.4. Confocal Laser Scanning Microscopy

Nikon confocal laser microscope A1 Plus (Nikon Instruments Europe BV, Amsterdam, Netherlands). The expression of GFP, and chlorophyll autofluorescence, were imaged by a confocal microscope with a setting of 488.0 nm excitation wavelength for all constructs. Emission wavelength was set at 525 nm and 700 nm for transformed protoplast and transient expression constructs, respectively

2.3.5. RNA Sequencing (RNA-Seq)

RNA-Seq analysis was performed after continuous dark treatments were carried out with *dufko3* mutants, and raw data was provided by Dr. Bechtold. The raw data was analysed, as described below.

2.3.5.1. RNA-Seq data analysis

Quality control of the raw reads and adapter trimming was carried out as described previously (Wingett and Andrews., 2018). Read counts and transcript per million reads (TPMs) were generated using tximport R package version 1.10.0 and length Scaled TPM method (Soneson *et al.*, 2016) with transcript quantification files generated from Kallisto (Bray *et al.*, 2016). Low-expressed transcripts and genes were filtered based on analysing the data mean-variance trend. The expected decreasing trend between data mean and variance was observed when expressed transcripts were determined as to which had 1 of the 12 samples with count per million reads (CPM) 1, which provided an optimal filter of low expression. The TMM method was used to normalise the gene and transcript read counts to -CPM (Bullard *et al.*, 2010). The genomic FASTA sequence, GTF annotation files of *Arabidopsis thaliana* Col-0, were downloaded from EnsemblPlants (<https://plants.ensembl.org/index>) (Howe *et al.*, 2020). Raw reads were aligned to the Arabidopsis genome. The principal component analysis (PCA) plot showed that the RNA-seq data did not have distinct batch effects. Downstream analysis can be directly proceeded.

2.3.5.2. Gene anthology analysis

Gene enrichment and functional annotation were carried out on all differentially expressed genes (DEGs) containing upregulated and downregulated genes separately. The analysis was carried out using AgriGo v2 (Analysis tool kit and database for the agricultural community) (<http://bioinfo.cau.edu.cn/agriGO/>) (Du *et al.*, 2010). The reference was the Arabidopsis gene model (TAIR9) background reference. Also, DAVID (Bioinformatics Resources 6.8) use used. Singular enrichment analysis (SEA) tool was used on the upregulated and downregulated genes separately. The GO annotation and gene enrichment analysis was performed after the hypergeometric statistical test Benjamini-Hochberg procedure false discovery rate (FDR), $P < 0.01$ from the background which was determined using AgriGo database. Genes that did not belong to any GO terms were not included in GO analysis.

2.3.6. Metabolite analysis

Continuous dark treatment was repeated. The samples were harvested for metabolite profiling on the fourth day of darkness at a time point just before the differences became significant between Col-0 and *dufko3*. This time point was chosen depending on the results in Chapter3. The plant material was freeze-dried and provided to a metabolomics service (University of Exeter) for extraction and downstream analysis using mass spectrometry (LC-MS/MS). Data was preprocessed and analysed using MetaboAnalyst 4.0 (Chong *et al.*, 2018) and Venny online tools.

2.3.6.1. Metabolite Statistical analysis

A One-way Analysis of Variance (ANOVA) was carried out. Tukey Honestly Significant Difference (Tukey's HSD) was subsequently carried out to determine which genotype and treatment groups showed a significant difference. The full statistical output is presented in Appendix H and I.

2.3.7. Statistical analysis

R-studio and XLSTAT were used to analyse the differences between the collected data for the different experiments in this study. Analysis of variance one way (ANOVA) was performed to determine the statistical differences between genotype groups. Statistical significance was determined when P-value <0.05 . For normally distributed data, post hoc Tukey's test was conducted for comparison of different mutants and Col-0 with each other to determine the differences between the groups, under the same and different treatments. The significance of P-values of Bonferroni correction was used in these comparisons. For two groups of variances, comparison of students' t-test was used and the significance was confirmed at $P < 0.05$. Finally, Microsoft Office Excel 2007 and SigmaPlot V14 were used to analyse the data and to create graphs. Graphs will show the statistical significance between Col-0 and mutant under the same treatment, and between Col-0 under different treatment.

Chapter 3

The impact of altered *DUF2358* expression on plant growth and abiotic stress responses

3.1. Introduction

The phenotype is defined as all characteristics of an organism that can be observed and measured. This set of observable characteristics is the result of the interactions between the genotype of the plant with the surrounding environment (Walter *et al.*, 2015).

Plants in nature can be affected by different environmental conditions along with other factors such as climate and soil changes. Sometimes, some of these conditions can cause stress in plants. The plant's ability to co-exist, adapt, or exceed these stresses is a determinant factor of the plant's ability to grow, sustain and produce in its environment (Duan *et al.*, 2007; Baena-González *et al.*, 2007).

Abiotic stresses lead to imbalances between carbon fixation and utilisation, which usually leads to altered sugar concentration. Under stress conditions, plants tend to regulate and suppress sugar catabolism to save vital resources. This can be achieved by suppressing plant growth and promoting respiration based on the catabolism of proteins and lipids instead of glucose. (Bläsing *et al.*, 2005; Ishizaki *et al.*, 2005; Rolland *et al.*, 2006; Lastdrager *et al.*, 2014).

Plants are able to sense changes in levels of carbohydrates through sugar sensors and respond through complex signalling cascades that modify gene expression and protein modification in order to cope with the environmental challenge (Koch *et al.*, 1992; Winkler *et al.*, 2000; and Baena-González, 2010).

One of the signalling networks involves the *SUCROSE NON-FERMENTING RELATED PROTEIN KINASE 1* (*SnRK1*), also known as KIN10 and KIN11. KIN10 plays an important role in regulating sugar signalling, responding to low-carbon

availability and initiating the transcriptional networks that lower sugar consumption, which helps plants to adapt and survive under stress (Ramon *et al.*, 2008). Consequently, *SnRK1* is essential in maintaining the energy balance between plant growth and stress responses, depending on the extracellular conditions (Crozet *et al.*, 2016). It has also been reported that, the activity of the *SnRK1* is regulated at the transcriptional level (Lu *et al.*, 2010).

The effect of sugar on gene expression indicates the importance of sugar signalling in plants to control vital processes and regulate responses to environmental conditions. In general, sugars have hormone-like regulatory activities such as controlling important life processes during plant life cycles, starting with germination to senescence, including almost all fundamental processes in between, such as growth or even response to the environment. These include other important roles in plants, such as a metabolic resource and structural component of cells and energy sources (Lu *et al.*, 2007).

A highly resolved drought transcription time series was produced by Bechtold *et al.* (2016), the dataset of which was used to infer sugar-responsive gene regulatory networks. One of the most highly connected genes, DUF2358, was predicted to negatively regulate KIN10 expression at the transcriptional level under drought stress conditions (Figure 3.1). DUF2358 expression was downregulated in Col-0 under drought stress, while KIN10 was upregulated under drought stress (Bechtold *et al.*, 2016) (Figure 3.2 A and B).

Bioinformatics analysis (Protein Prowler Subcellular Localisation Predictor version 1.2) predicts DUF2358 to be localised in the chloroplast. The protein has no known

functional domains that would allow us to infer its role or how it may be involved in the *SnRK1* signalling cascade.

This chapter aims to interrogate the gene regulatory network involving DUF2358 and *SnRK1* identified in drought stress responses in *Arabidopsis thaliana*. To do this, we will evaluate the effect of altered DUF2358 expression (overexpression and knockout) on plants subjected to starvation-inducing stress treatments that initiate the *SnRK1* signalling cascades. We chose drought stress and dark-induced senescence as the main treatments to alter the sugar status of plants. Phenotypic characterisation, expression of genes in the gene regulatory and photosynthesis-related proteins were subsequently analysed in plants with elevated and reduced levels of DUF2358 (Figure 1.3).

3.2. Results

3.2.1. DUF2358 and KIN10 expression under drought conditions

To verify the expression of the two hub genes KIN10 and DUF2358 under drought conditions, we repeated the drought experiment and performed qPCR with gene-specific primers. The results confirmed that the data obtained in the original microarray study (Bechtold *et al.*, 2016) DUF2358 was downregulated during drought (Figure. 3.1A), while KIN10 was indeed upregulated under drought conditions (Figure. 3.1B).

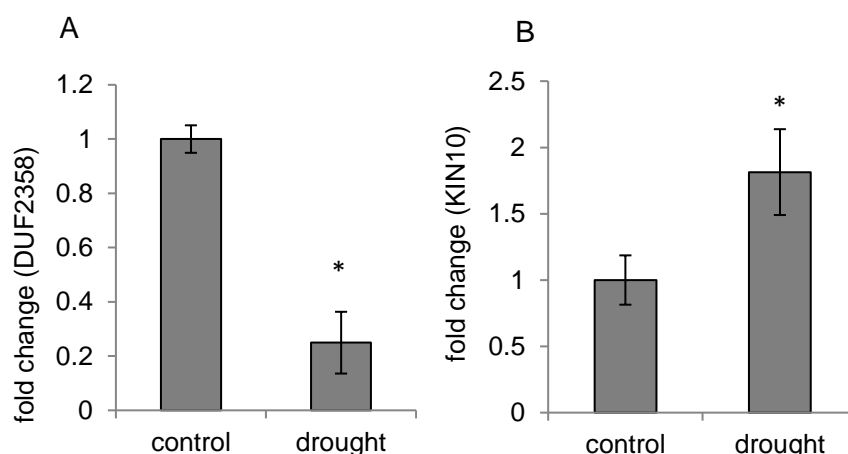


Figure 3.1. (A) DUF expression downregulated in Col-0 under drought stress, (B) KIN10 upregulated under drought stress, * indicates significant differences relative to Col-0 P-value < 0.05 (n=6).

3.2.2. Screening *dufko4*, *dufko5*, and *dufko6*

One existing homozygous T-DNA insertion line, *dufko3*, was provided by Dr. Bechtold. Additional T-DNA insertion lines were ordered from the Nottingham Arabidopsis stock centre and were screened by PCR to identify the putative T-DNA insertion. The DNA extraction was carried out, followed by PCR using gene-specific and T-DNA-specific primers. The result showed a positive PCR reaction for some of the *dufko4* plants

using the T-DNA specific primer (Figure 3.2 A). However, it also amplified a Col-0 band (Figure 3.2 B), indicating that *dufko4* plants were heterozygous. Seeds were harvested from the positive heterozygous *dufko4* plants and sown to obtain homozygous mutants in the next generation. Unfortunately, we couldn't obtain any seeds due to growth difficulties (Figure 3.2 A and B). *dufko5* and *dufko6* did not give any positive results for the T-DNA insertion (Figure 3.2 A and B).

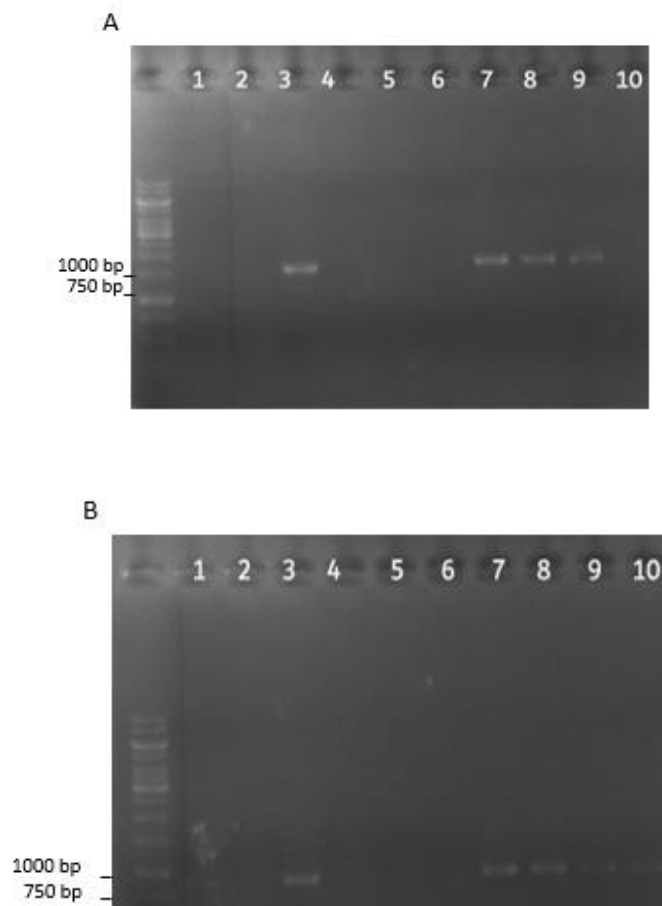


Figure 3.2. PCR confirmation of T-DNA in *dufko4* plants. **(A)** Using DUF2358 forward and DUF2358 reverse primers. **(B)** Using LB (SALK_104372C) and DUF2358 reverse primers.

3.2.3. Screening 35S:DUF2358

The 35S:DUF2358 (*DUFOE*) lines were generated by Dr. Bechtold and Dr. Subramaniam (Figure 2.1). The T2 seeds were homozygous and, to confirm that seeds from three independent lines (*DUFOE1-4*) were sown on soil and selected by watering with 0.62 mM of BASTA glufosinate-ammonium (Kaspar; Bayer CropScience, Cambridge, UK) in order to obtain the homozygous plants. All the screened seeds of all mutants were grown when they selected by BASTA, which confirmed that the seeds were homozygous for the transgene and that no segregation remained in any line of them.

RNA was extracted from homozygous plants and DUF2358 expression was analysed by qPCR using DUF2358 specific primers. The fold change DUF2358 expression was calculated and compared to expression in Col-0. Only *DUFOE2* and *DUFOE3* showed a significant increase in DUF2358 expression. In *DUFOE4*, only two plants were analysed, with a high variation in gene expression between both plants, while *DUFOE1* did not show levels of DUF2358 expression above wild type (Figure 3.3).

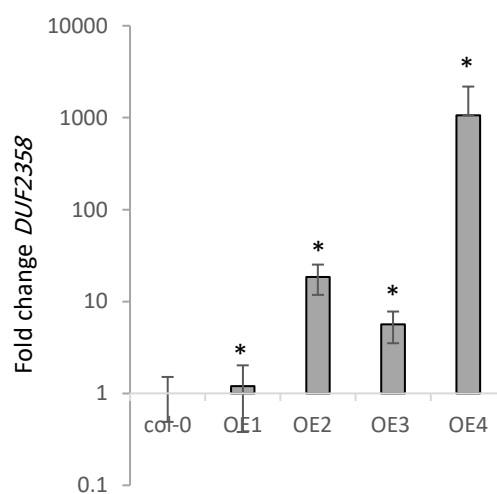


Figure 3.3. Fold change of relative gene expression of *DUFOE1*, *DUFOE2*, *DUFOE3*, and *DUFOE4* shows a significant difference compared to Col-0.

3.2.4. Screening of native promoter: DUF:GFP (pNAT:DUF:GFP) and native promoter: DUF (pNAT:DUF) plants in a *dufko3* background

Seeds of *dufko3* plants complemented with a native promoter constructs (pNAT:DUF:GFP and pNAT:DUF) were obtained from Dr. Exposito and were sown on MS media supplemented with 33ug/ml hygromycin to screen for transgenic plants, along with Col-0 as a control. To detect the restor of DUF2358 gene expression which is expected in the native promoter lines. After two weeks, seedlings with the first pair of true leaves were transferred to soil. RNA extraction was conducted to analyse gene expression alongside wild-type and *dufko3* plants using DUF2358 specific primers (Figure 3.4). Both transgenic lines restored DUF2358 gene expression compared to *dufko3*. Expression levels were significantly higher compared to Col-0, suggesting that the native promoter constructs led to DUF2358 overexpression. Seeds from the positive plants were harvested and sown again in MS media with hygromycin to obtain homozygous plants in the third generation.

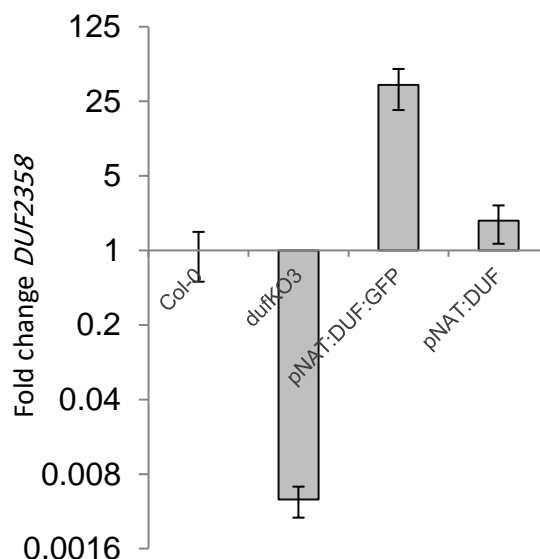


Figure 3.4. Fold change of relative gene expression of *dufko3*, pNAT:DUF:GFP and pNAT:DUF compared with Col-0 showing the expression of DUF2358 was restored in the native promoter lines.

For *in vivo* subcellular localisation studies, we generated a GFP translational fusion (pNAT:DUF:GFP). DUF2358 was expressed in the *dufko3* background (Figure 3.6), and we subsequently checked for GFP expression by RT PCR. We did not observe any GFP expression, which was confirmed by Western blot using Anti-GFP (Abcam (ab6556) 1/1000 dilution) with Ct-DUF2358:GFP protein as a positive control. There was no GFP band in the pNAT:DUF:GFP samples (Figure 3.5 A). pNAT:DUF:GFP PCR product was therefore sequenced, and the results indicated that there was a stop codon (TGA) prior to the GFP sequence, terminating translation ahead for the GFP (Figure 3.5 B; full sequence in Appendix B).



Figure 3.5. (A) Detection of GFP expression by Western blot analyses 1- positive control Ct DUF:GFP protein sample, 2 and 3 pNAT:DUF:GFP protein samples. Rabbit Anti-GFP antibody Abcam (ab6556) was used. (B) Stop codon (TGA) were detected in pNAT:DUF:GFP. The full output sequencing is attached to Appendix B.

3.2.5. Screening *kin10-2* mutant

Seeds of *kin10-2* knockout mutant which was described in Simon *et al.* (2018) were obtained from the Nottingham Stock Centre. The seeds were screened for T-DNA

insertion using KIN10 and T-DNA specific primers SALK_093965 (Simon *et al.*, 2018) with Col-0 as a negative control. The wild-type KIN10 gene was amplified using KIN10 specific primers only, and Col-0 as a positive control. The *kin10-2* mutants were shown to homozygous for the T-DNA insertion (Figure 3.6)

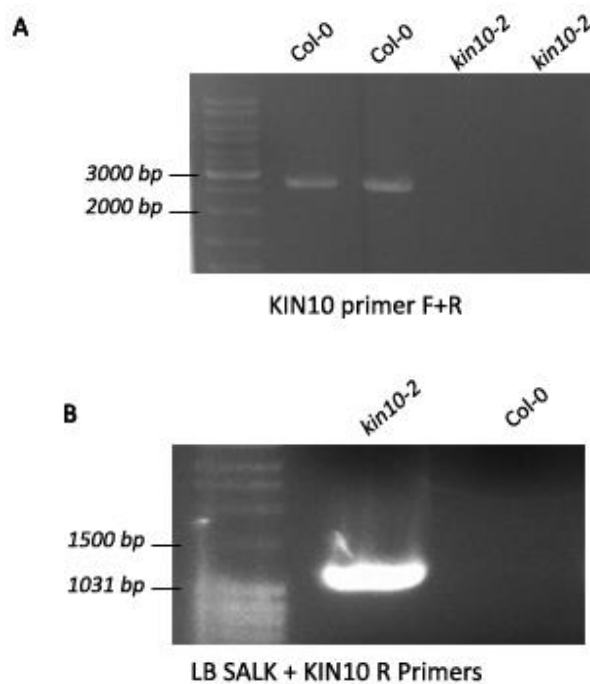


Figure 3.6. PCR confirmation of T-DNA in *kin10* plants. **(A)** Using KIN10 F and KIN10 R primers. **(B)** Using LB + KIN10 R primers.

3.2.6. Screening crosses plant *dufko3* with *kin10-2* (*dufko_kin10-2*)

We crossed *dufko3* into the *kin10-2* background in order to obtain genetic evidence of a link between DUF2358 and KIN10, as observed in the gene regulatory network model (Figure 1.3). The crossed plants were screened for the presence of both T-DNA insertions with the aim to obtain homozygous plants from T2 seed. Plants were screened using (DUF2358 F+R, LB + DUF2358 R, KIN10 F+R, and LB+KIN10 R).

Seeds were collected from the positive plant (#12) and used for subsequent analysis (Figure 3.7).

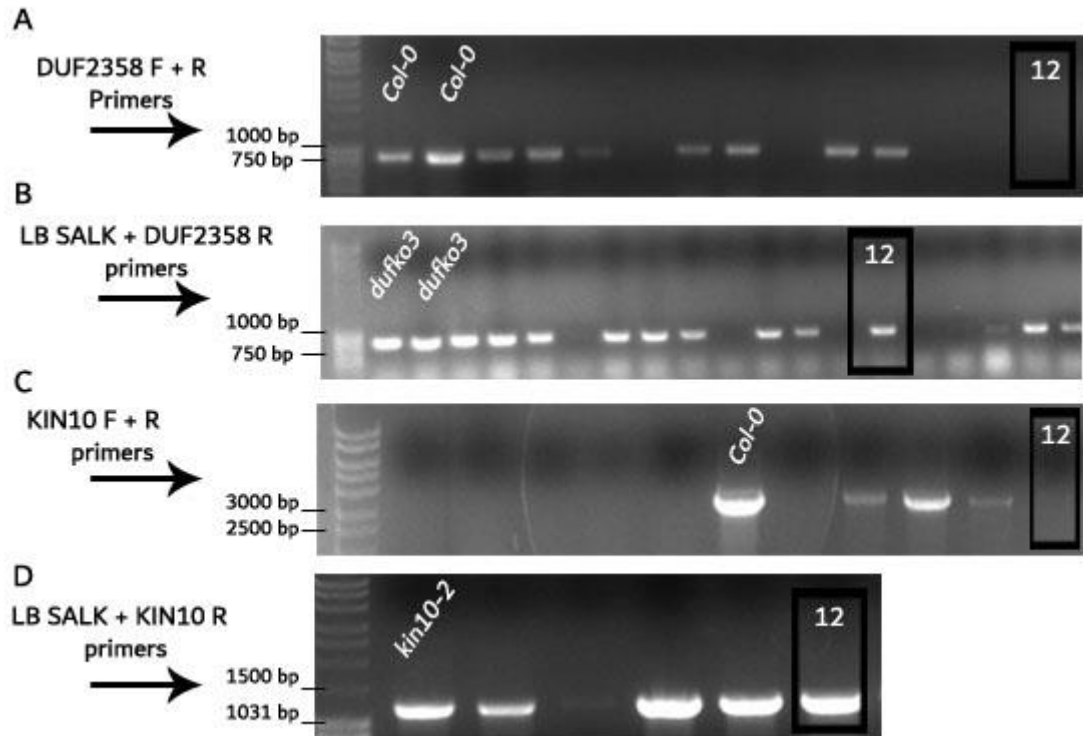
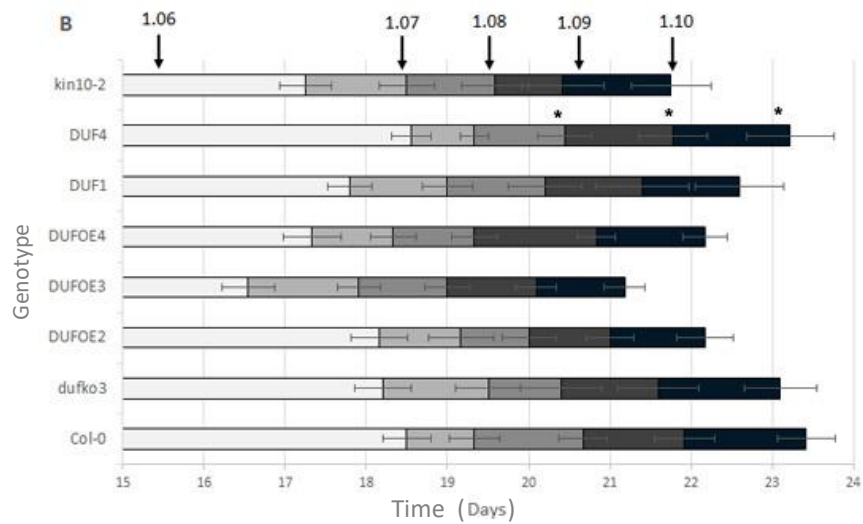
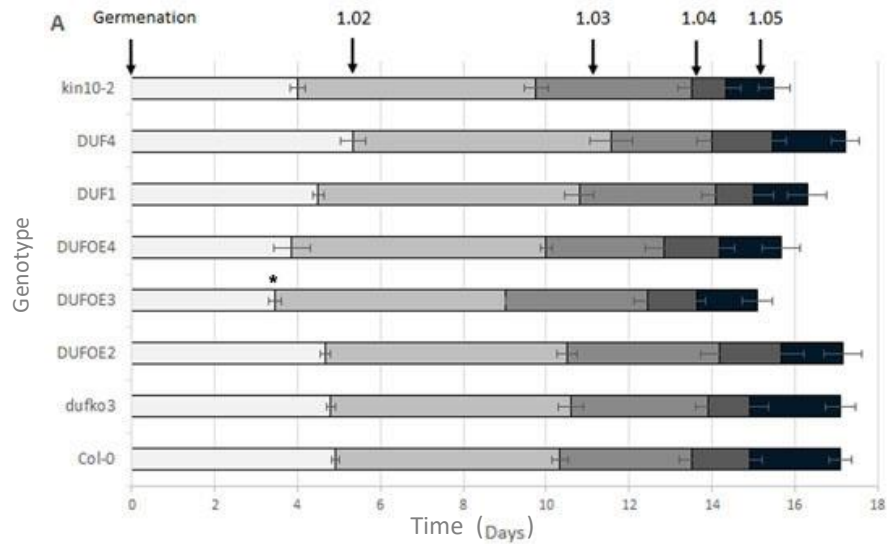


Figure 3.7. PCR screening of crossed plant (*duf_kin10-2*) (A) DUF2358 F + R primers, (B) LB Salk + DUF2358 R primers, (C) LB salk + KIN10 R primers and (D) KIN10 F + R primers.

3.3. Growth Analysis

Growth analysis was conducted on all the genotypes (*Col-0*, *dufko3*, *DUFOE2*, *DUFOE3*, *DUFOE4*, pNAT:DUF1 (*DUF1*), pNAT:DUF4 (*DUF4*), and *kin10-2*) with 7 replicates for each genotype. The result shows that *DUFOE3* mutant germinated the earliest at an average of 3.45 days and there was a significant difference between *DUFOE3* and *Col-0* in the time to germination. Subsequent growth and developmental stages recorded the significant difference between *Col-0* and *DUF4* in the 1.08, 1.09, and 1.10 stages (Figure 3.8 A, B, and C). The remaining genotypes recorded

developmental rates similar to each other and there was no significant difference in development across all genotypes. A table showing the Arabidopsis growth stages for different genotypes can be found in Appendix C.



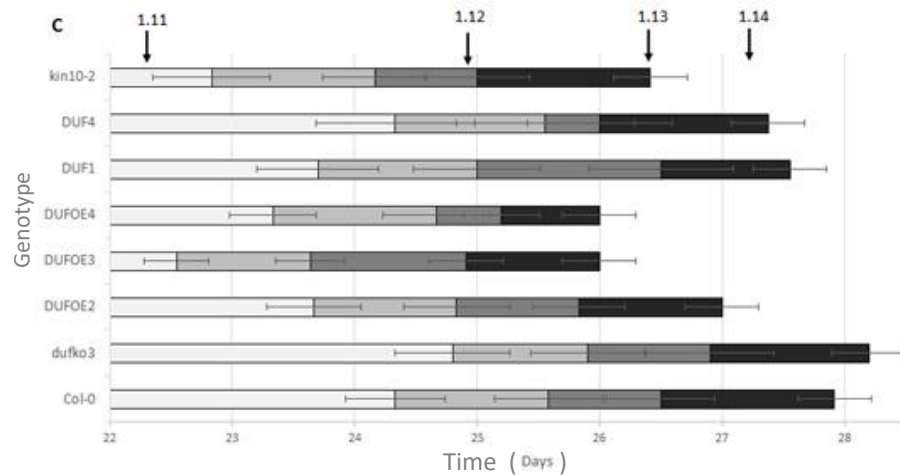


Figure 3.8. All germination and growth stages for all the genotypes compared with Col-0 under normal conditions. Principal growth stage <1 (Seed germination), Principal growth stage 1 (Leaf development), Principal growth stage 3 (Rosette growth) and Principal growth stage 5 (Inflorescence emergence). Each colour indicates one growth stage which is written upper the bars. The details of each stage explained in Table 2.5 Error bars signify SEM (standard error of the mean). *denotes significant differences compare with Col-0 at $P < 0.05$. $n = 18$. Minimum replication was 7 plants.

The total exposed leaf area shows differences between genotypes in the rosette area, *DUFOE*, and *kin10-2*, and showed significant differences compared to Col-0. The significant differences were started from day 30 (for *kin10-2*) until day 38 (for *DUFOE*, and *kin10-2*) (Figure 3.9).

Also, plant flowering was determined by measuring the flower stem lengths and comparing these with those of the Col-0 plants. At the end of the flowering period, *DUFOE*, with *kin10-2*, were significantly larger than Col-0 (Figure 3.10).

After complete growth, the principal growth stage 3 (Stage 3.20 Rosette is 20% of the final size. Stage 3.50 Rosette is 50% of the final size. Stage 3.70 Rosette is 70% of the final size. Stage 3.90 Rosette growth complete) was determined based on Boyes *et al.* (2001) by calculating 20, 50, and 70% of the final size of each plant. All the genotypes were close to each other in all growth stages and no statistical differences

were recorded (Figure 3.11). The principal growth stage 5 (First flower buds visible) was determined when the first flower buds became visible for each plant and a comparison was made with the genotype with Col-0 after calculating the averages. No significant differences were recorded between all genotypes (Figure 3.12). Finally, there were no significant differences between all genotypes in their seed weight (Figure 3.13). The image in Figure 3.14 shows the plant phenotype in the 25th day from sowing for Col-0, *dufko3*, and *kin10-2*.

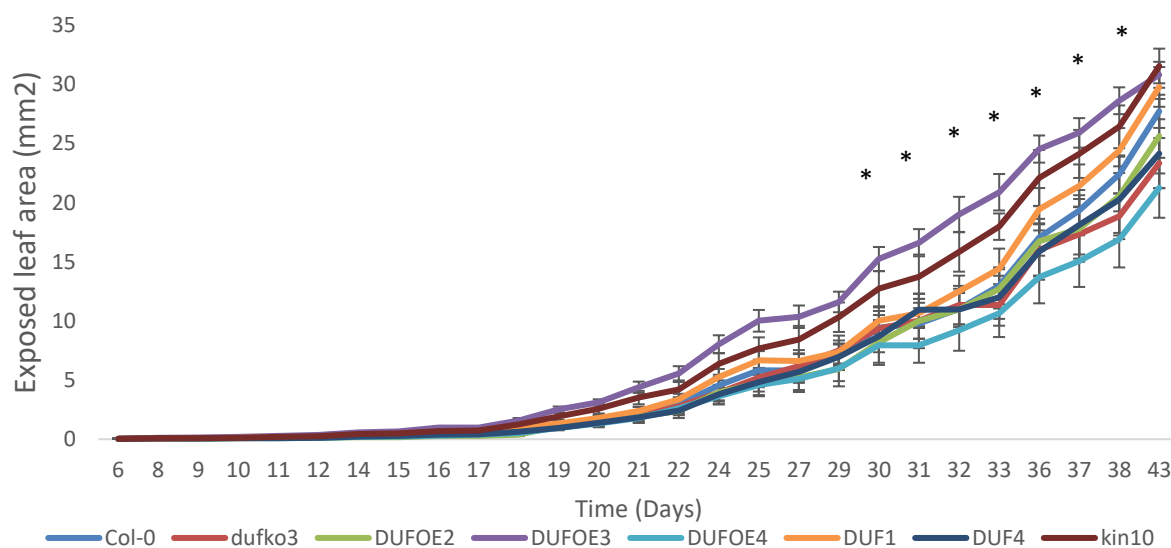


Figure 3.9. Total averages of exposed leaf area measured in mm². Error bars signify SEM (standard error of the mean). *denotes significant differences compare with Col-0 at P < 0.05. n=7.

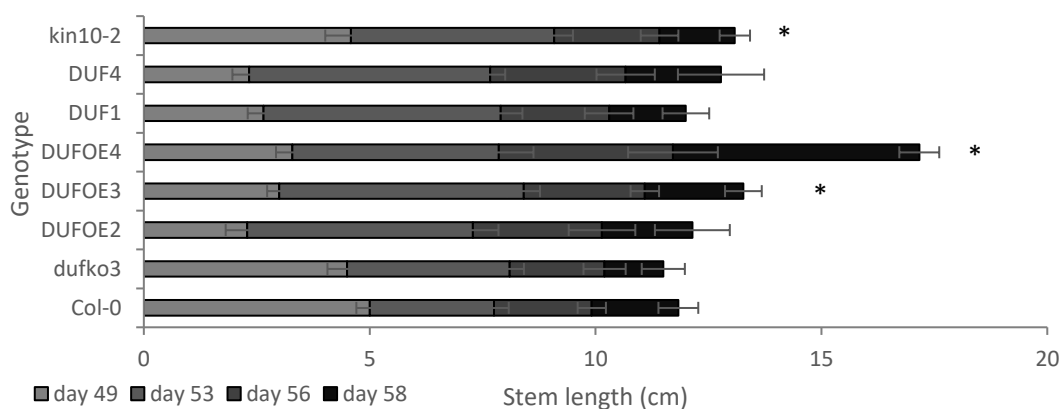


Figure 3.10. Flower stem length is measured in cm. Error bars signify SEM (standard error of the mean). *denotes significant differences compare with Col-0 at $P < 0.05$. $n = 18$, Minimum replication was seven plants.

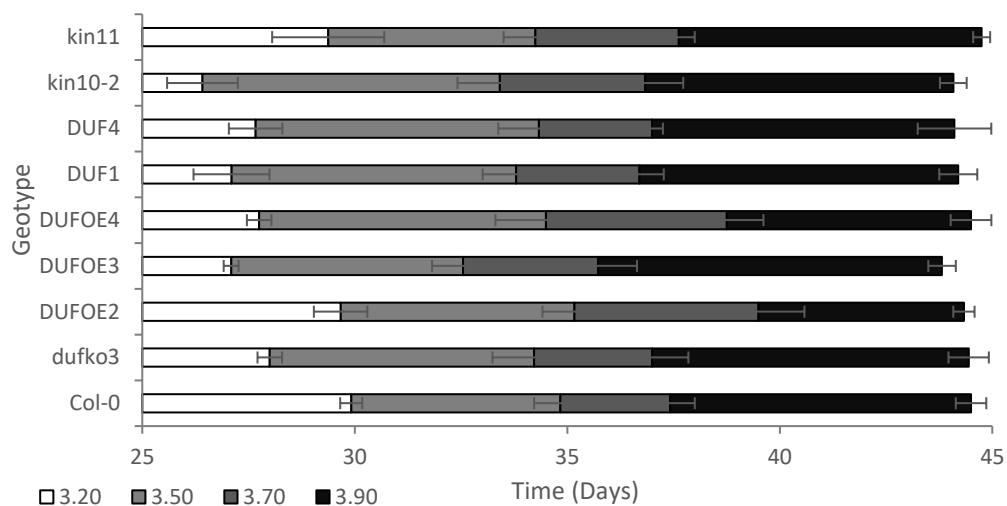


Figure 3.11. Principal growth stage 3 (Stage 3.20 Rosette is 20% of the final size. Stage 3.50 Rosette is 50% of the final size. Stage 3.70 Rosette is 70% of the final size. Stage 3.90 Rosette growth complete). Error bars signify SEM (standard error of the mean). $n = 18$, Minimum replication was seven plants.

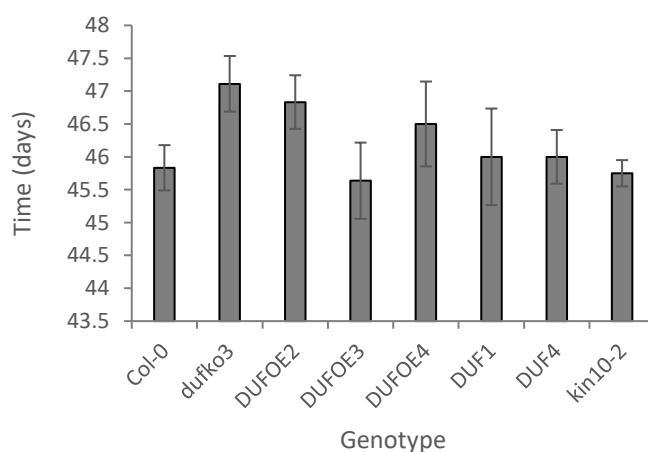


Figure 3.12. Principal growth stage 5 (First flower buds visible). Error bars signify SEM (standard error of the mean). $n = 18$, Minimum replication was seven plants.

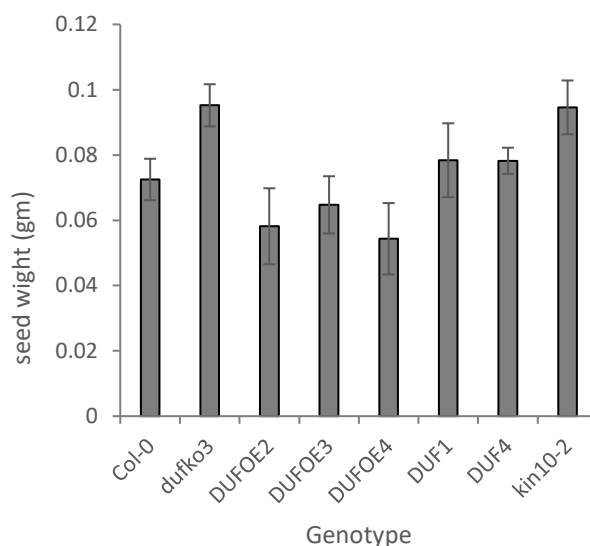


Figure 3.13. Seed weight in gm for each genotype. Error bars signify SEM (standard error of the mean). n=12, Minimum replication was 7 plants.



Figure 3.14. Plants on the 25th day from sowing the plants.

3.4. Localisation of DUF2358

The protein is predicted to be localised in the chloroplast and, so far, no known role has been associated with this protein. The localisation of DUF2358 was confirmed using transient gene expression in *Nicotiana benthamiana* plants. After five days of infiltration with transformed *Agrobacterium* with C-terminal end of DUF:GFP (Figure 3.15 A), leaves were screened using a Nikon confocal microscope A1 HD25/A1R HD25 at Essex University (School of Life Sciences). The result confirmed the localisation of DUF2358 in the chloroplast (Figure 3.15 B). Moreover, to verify the localisation of DUF2358 protoplasts were isolated from *Arabidopsis thaliana* plants,

followed by protoplast transfected with Ct pUBQ:DUF:GFP. Transformed protoplasts imaging verify the localisation of DUF2358 in the chloroplast (Figure 3.15 C and D).

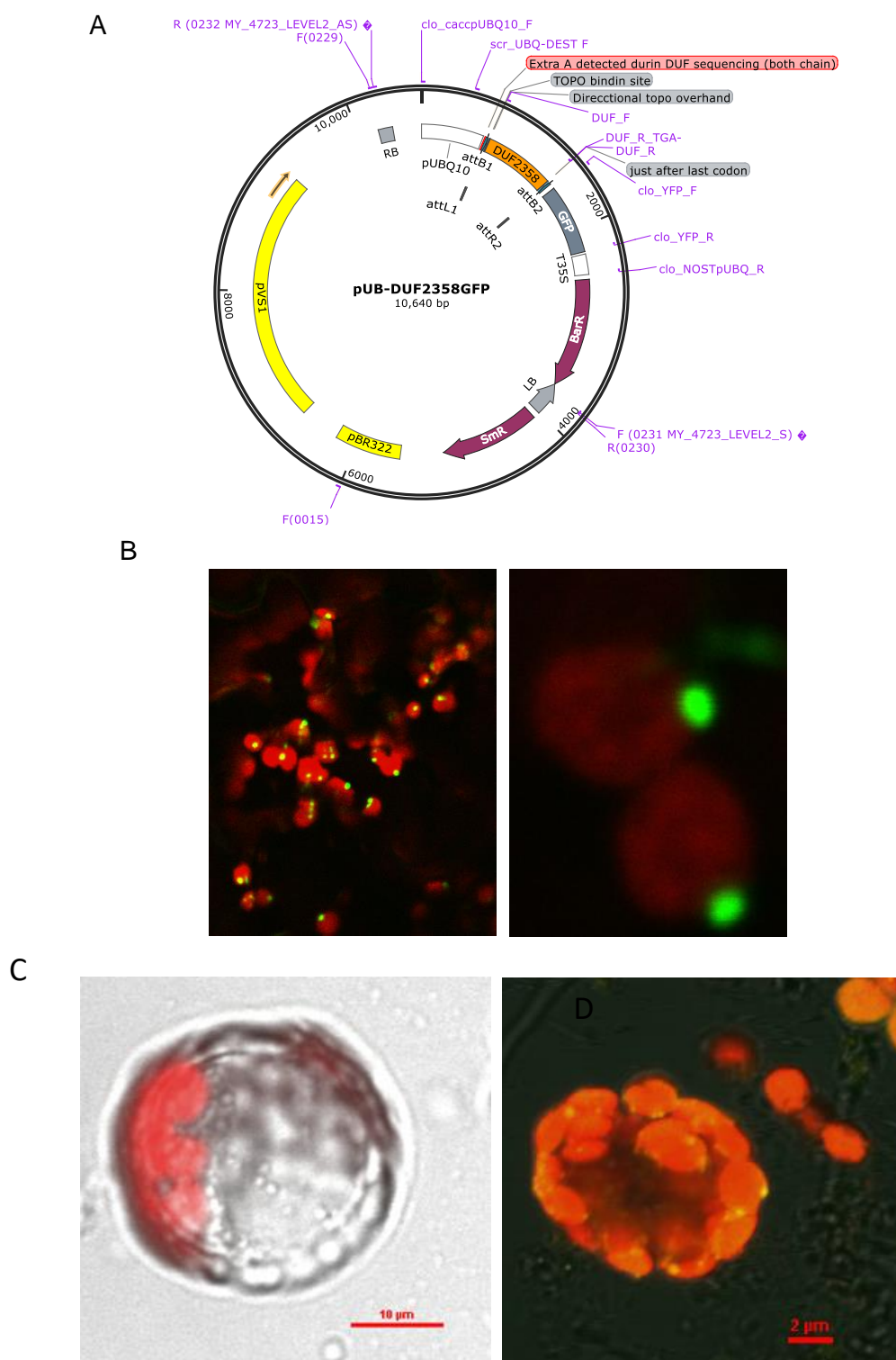


Figure 3.15. (A) Plasmid map of pUBQ:DUF2358::GFP *map was provided by Dr. Exposito. **(B)** Microscopy images displaying subcellular localisation of transiently expressed Ct DUF2358-GFP from

agroinfiltrated transgenic *Nicotiana benthamiana* leaves after five days of infiltration. **(C)** confocal microscopy images for isolated protoplast from *Arabidopsis thaliana* plants. **(D)** protoplast transfection with Ct pUBQ:DUF:GFP. The images show a yellow signal (GFP fluorescence).

The network inference results suggested that DUF2358 might be a part of the transcriptional signalling cascade.

3.5. Drought stress

3.5.1. Drying rate

Bechtold *et al.* (2016) initially identified and modelled drought-responsive transcription factor genes. The same dataset was used to generate gene regulatory network models associated with primary metabolism and sugar responses. From this network, it was predicted that the DUF2358 protein negatively regulates KIN10 in *Arabidopsis* under drought conditions (Figure 1.3).

Drought stress was conducted on soil-grown Col-0, and mutant (*dufko3*, *DUFOE2*, *DUFOE3*, *kin10-2*, and pNATDUF) plants through a progressive drying experiment, by withdrawing water until the relative soil water content (rSWC) had reached 20% (Ferguson *et al.*, 2018). The pot weights were taken every day during the experiment, and the slope of the soil drying was calculated for each genotype as linear regression to determine the difference between genotypes in response to drought stress. The comparison between Col-0 and *dufko3* was repeated twice. This experiment was repeated once more with the plant after crossing between *kin10-2* and *dufko3* mutants (*dufko3_kin10-2*). Overall, there were no significant differences between all genotypes in the drying rate (Figure 3.16). This suggests that the drying responses and vegetative water use were unchanged in all genotypes.

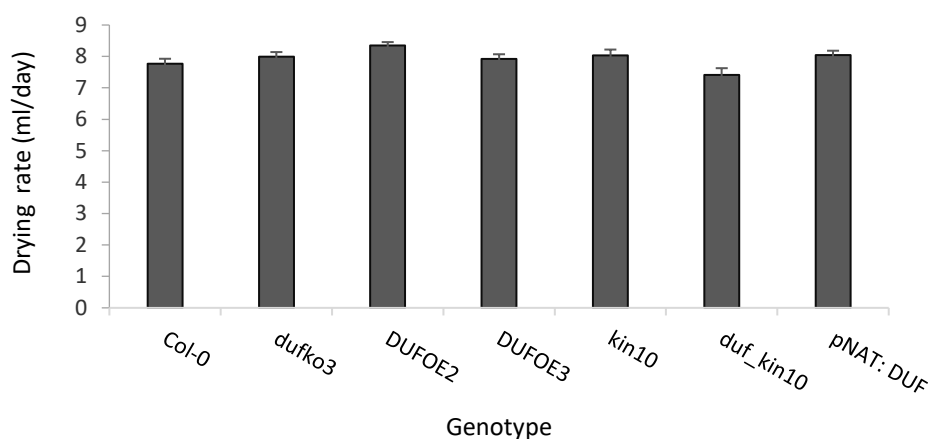


Figure 3.16. Drying rates were determined as the slope of the decrease in soil water. Bars show the averages of 15 replicated per genotype. No significant differences between all mutants compared to Col-0 plants. Error bars signify SEM (standard error of the mean). $P < 0.05$ $n = 15$

3.5.2. Gene Expression

A total of 23 genes were selected from the drought response gene regulatory network (Figure 1.3), of which 17 genes were direct targets of DUF2358 and five genes were indirect targets (Figure 1.3, Table 3.1).

Table 3.1. Direct and indirect targets genes of DUF2358 main information; genes were selected from the drought response gene regulatory network Bechtold *et al.* (2016).

Direct target genes of DUF2358		
Abbreviation	Locus ID	Gene Full name
ABF2	AT1G45249	<i>ABSCISIC ACID-RESPONSIVE ELEMENTS-BINDING FACTOR 2</i> (ABA related gene)
ABF3	AT4G34000	<i>ABSCISIC ACID-RESPONSIVE ELEMENTS-BINDING FACTOR 3</i> (ABA related gene)
ABI5	AT2G36270	<i>ABA INSENSITIVE 5</i> (ABA related gene)
ACR5	AT2G03730	<i>ACT DOMAIN REPEAT 5</i>

ACR9	AT2G39570	<i>ACT DOMAIN REPEAT 9</i>
ATTPS5	AT4G17770	<i>TREHALOSE PHOSPHATE SYNTHASE 5</i> (sugar-related gene)
PLP2	AT2G26560	<i>PHOSPHOLIPASE A2</i>
ATRRP4	AT1G03360	<i>RIBOSOMAL RNA-PROCESSING PROTEIN 4</i>
AT2G36220	AT2G36220	<i>HYPOTHETICAL PROTEIN</i> (sugar-related gene)
TIP2	AT3G26520	<i>TONOPLAST INTRINSIC PROTEIN 2</i>
AT4G25580	AT4G25580	(ABA related gene)
MPK5	AT4G11330	<i>MITOGEN-ACTIVATED PROTEIN KINASE 5</i>
DSP4	AT3G52180	<i>DUAL SPECIFICITY PROTEIN PHOSPHATASE</i> (sugar-related gene)
AtHXK2	AT2G19860	<i>HEXOKINASE 2</i> (sugar-related gene)
TPPE	AT2G22190	<i>TREHALOSE-6-PHOSPHATE PHOSPHATASE</i> (sugar-related gene)
GBF2	AT4G01120	<i>G-BOX BINDING FACTOR 2</i>
KIN10	AT3G01090	<i>SNF1-RELATED PROTEIN KINASE (KIN10)</i>
UMAMIT33	AT4G28040	<i>USUALLY, MULTIPLE AMINO ACIDS MOVE IN AND OUT TRANSPORTER 33</i>
ATPME17	AT2G45220	<i>PECTIN METHYLESTERASE 17</i>
AT5G57655	AT5G57655	<i>XYLOSE ISOMERASE PROTEIN</i>
CYP71B4	AT3G26280	<i>CYTOCHROME P450 MONOOXYGENASE</i>
AT1G12790	AT1G12790	<i>DNA LIGASE-LIKE PROTEIN</i>

As shown previously, DUF2358 expression was downregulated in Col-0 under drought stress, while KIN10 was upregulated under drought stress (Figure 3.1 A and B).

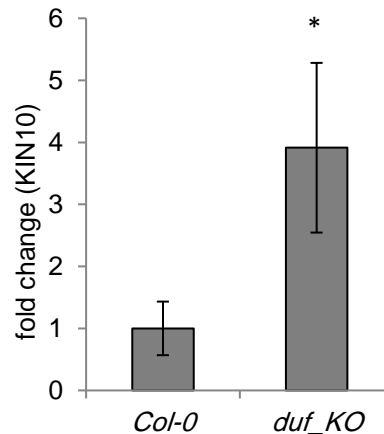


Figure 3.17. KIN10 expression in *dufko* upregulated under control condition. * indicates significant differences relative to Col-0 P-value < 0.05 (n=6).

The gene network model generated based on the data in Bechtold *et al.* (2016) suggested that DUF2358 either directly or indirectly regulated *KIN10* gene expression (Figure 1.3). Also, *KIN10* expression in *dufko3* was upregulated under non-stress conditions, which supports the notion that there is a connection between DUF2358 and *KIN10* expression (Figure 3.17).

In our drought experiment, we confirmed the initial results that DUF2358 was downregulated in Col-0 under drought conditions (Figure 3.18 A). Regarding *KIN10* expression under normal and drought conditions, while *KIN10* was upregulated under drought stress, *KIN10* expression was also elevated in *dufko3* mutant under well-watered conditions compared to Col-0 but did not show a further increase under drought stress conditions (Figure 3.18 B). The *duf_kin10* plants showed a significant difference under drought stress compared to Col-0 under the same condition. *KIN10* was significantly increasing in *DUFOE* mutant plants under drought conditions compared with Col-0 (Figure 3.18 A, B).

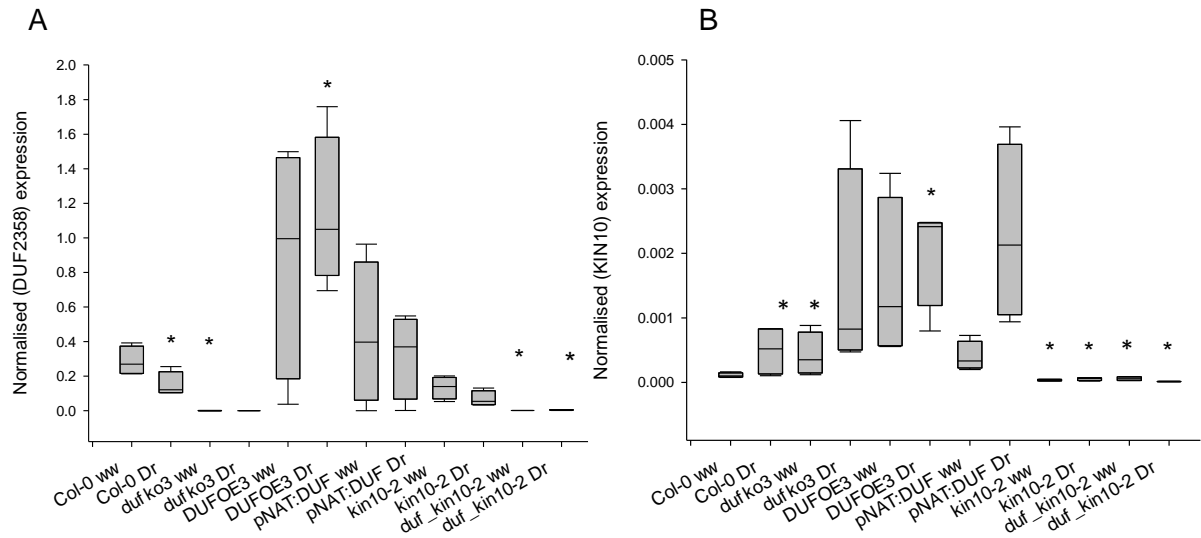


Figure 3.18. Normalised gene expression to actin, under well-watered and drought conditions for Col-0 plants and mutants. **(A-B)** DUF2358 and KIN10, respectively. The graphs indicate the comparison between Col-0 and other genotypes for well-watered and drought conditions. (ww) refers to well-watered condition and (Dr) refers to drought conditions. * indicates a significant difference from control conditions. Col-0 Dr was compared with Col-0 ww, while all other mutants were compared to Col-0 under the same conditions (n=4).

3.5.2.1. ABA-regulated gene expression during progressive drought

Genetic analysis showed that sugar signalling in plants is closely associated with ABA biosynthesis and signalling (León and Sheen, 2003; Finkelstein and Gibson, 2002). Many sugar response mutants were identified as ABA deficient mutants (Arenas-Huertero *et al.*, 2000; Huijser *et al.*, 2000), and the link between sugar and ABA signalling is reflected in a large number of ABA-responsive genes within the gene regulatory network (Figure 1.3, Table 3.1). ABA is an important phytohormone in response to drought stress, regulating many physiological and molecular changes, including stomatal closure, induction of stress-responsive gene expression and accumulation of stress proteins (Takahashi *et al.*, 2018). This is done through the action of three important bZIP transcription factors (ABF2, ABF3, and ABF4), which are members of the ABF gene family (Yoshida *et al.*, 2015).

We, therefore, tested some of the ABA-responsive genes to evaluate the change in their expression when the expression of DUF2358 and KIN10 was altered.

There was no significant change in ABA-responsive genes in *dufko3*, and *DUFOE3*, suggesting that altering *DUF2358* expression did not broadly impact on ABA signalling pathways (Figure 3.19 A-D). However, *dufko_kin10-2* cross showed a significantly high level of *ABF3* expression under well-watered conditions compared to Col-0 plants. Similarly, *ABI5* and *AT4G25580* were significantly increased in *kin10-2* under drought condition, and *dufko_kin10-2* mutants under both well-watered and drought conditions. This suggests that removing the KIN10 catalytic subunit (*kin10-2*) impacts ABA-responsive genes. *CYP71B4*, which is an ABA-inducible gene (Hoth *et al.*, 2002) suggested to be an indirect target of DUF2358, also showed a significant decrease under drought stress in Col-0, while it showed a significant increase under drought stress for *dufko3* mutant plants. Also, there was a significant increase in *DUFOE* compared to Col-0 under normal and drought conditions (Figure 3.19 E).

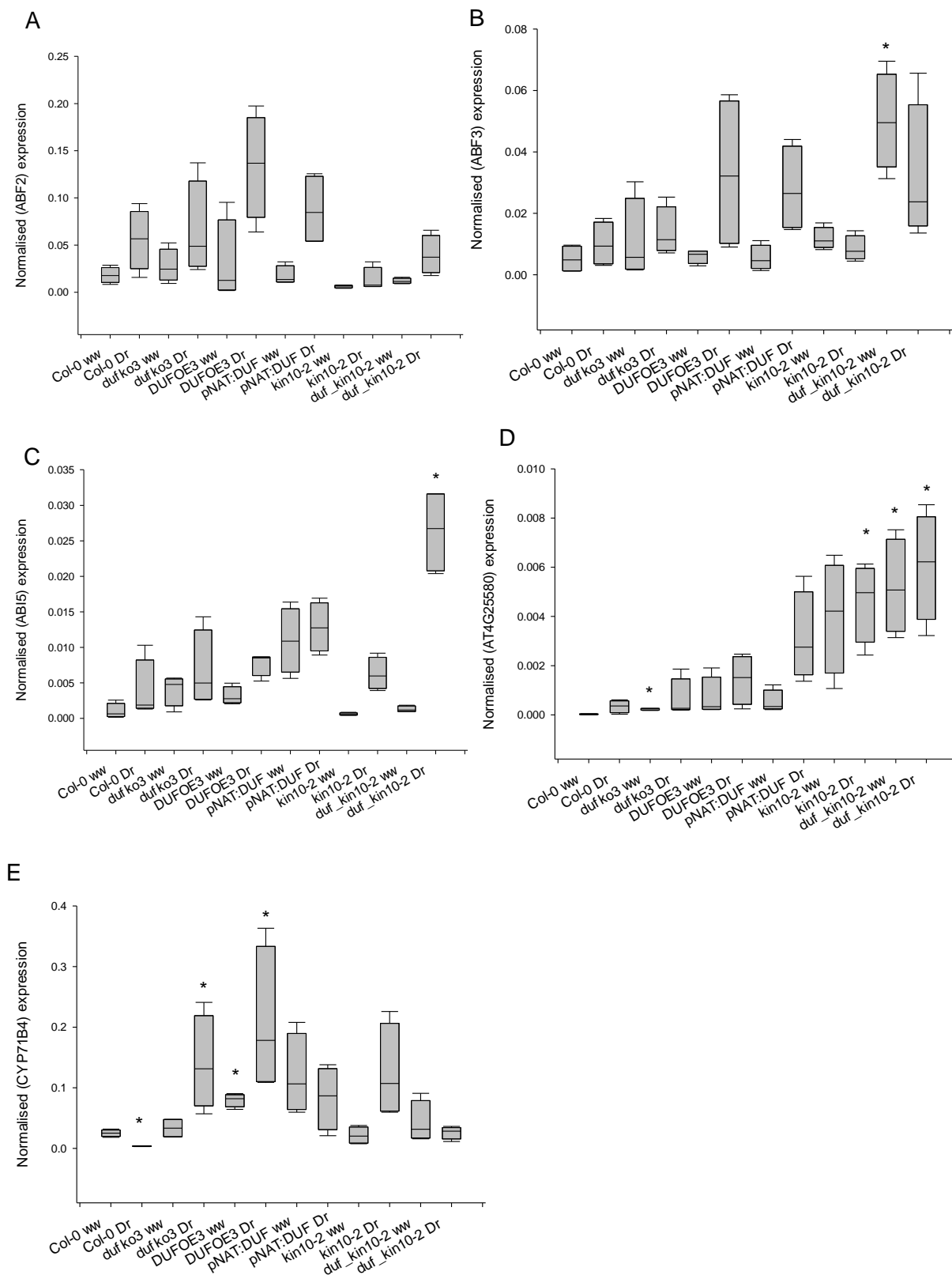


Figure 3.19. Normalised gene expressions to actin for ABA-related genes under well-watered and drought conditions for Col-0 plants and mutants. **(A- E)** ABF2, ABF3, ABI5, AT4G25580 and CYP71B4, respectively. All other differences between other genotypes are reported in Appendix E. (ww) refers to

well-watered conditions while (Dr) refers to drought conditions. * indicates a significant difference from control conditions. Col-0 Dr was compared with Col-0 ww, while all other mutants were compared with Col-0 under the same conditions (n=4).

3.5.2.2. Sugar-responsive gene-expression during progressive drought

Sugar signalling-related genes, AtHXK2, ATPME17, DSP4, TPS5, and AT2G36220 gene expressions increased in Col-0 under drought conditions compared to well-watered plants (Figure 3.20 A-D). TPS5 was the only gene to be significantly altered in the *dufko3* mutant, showing a significant increase in expression under both conditions (Figure 3.20 D). This suggests that *dufko3* does not respond to the altered sugar status.

duf_kin10-2 plants showed differences in drought plants compared with Col-0 plants for ATPME17 and the differences were significant. DSP4 significantly decreased in the well-watered condition in *duf_kin10-2* plants, while ATPME17 was increased. Also, AT2G36220 significantly increased in *duf_kin10-2* under drought compared with Col-0 plants under the same condition. Remarkably, sugar-related genes, in *duf_kin10-2* plants, responded to the drought condition in the same way as *dufko3* plants, suggesting this response was affected by the altered DUF2358 expression (Figure 3.20 A-E). The sugar-responsive gene ATTPS5 was significantly increased in the *dufko3* mutant under drought conditions. ATPME17, which is also a sugar-responsive gene, showed a significant increase in *DUFOE3* mutant plants under well-watered conditions compared to Col-0. This suggests that sugar signalling is affected by *DUFOE* plants (Figure 3.20 A-E).

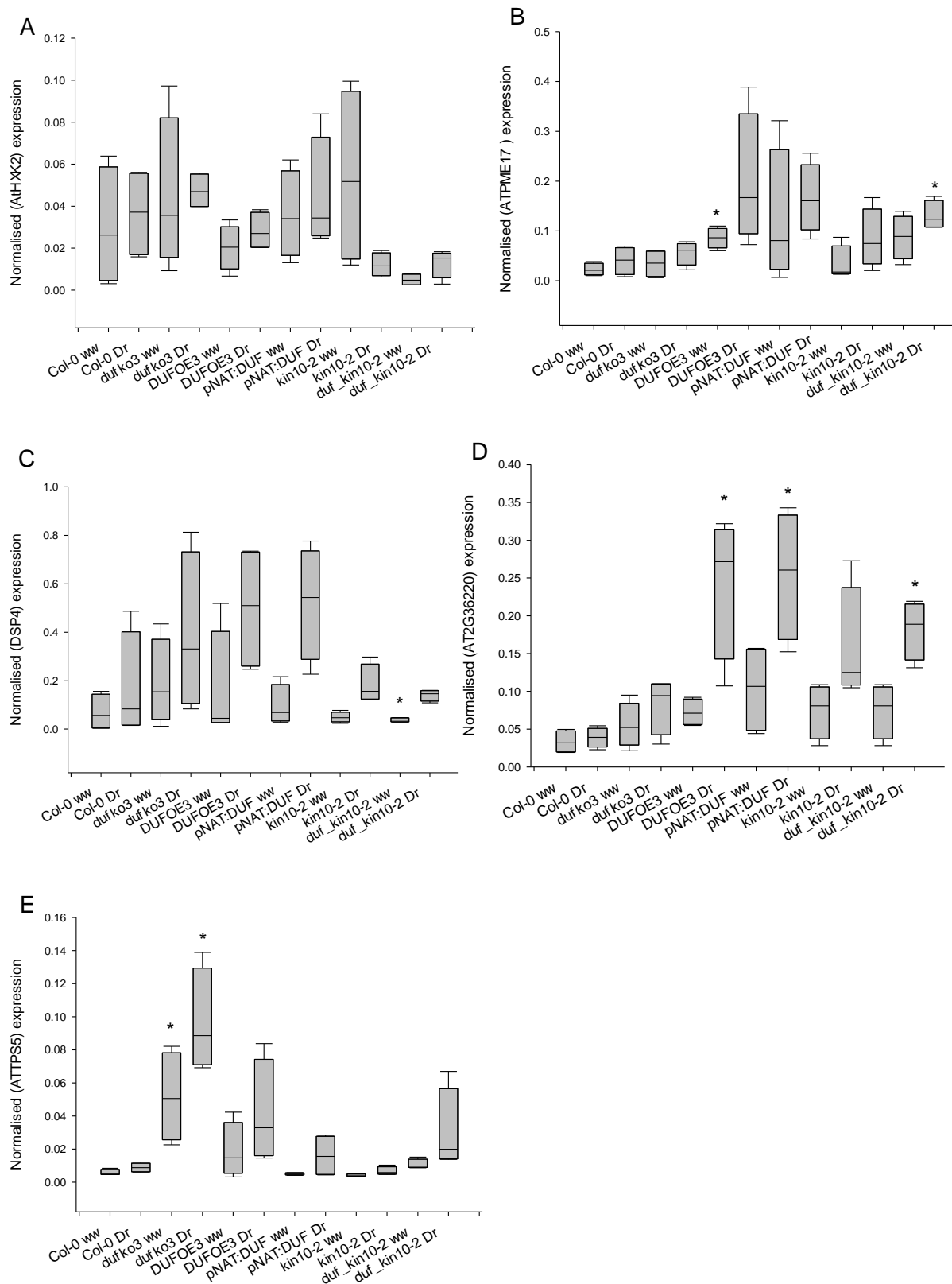
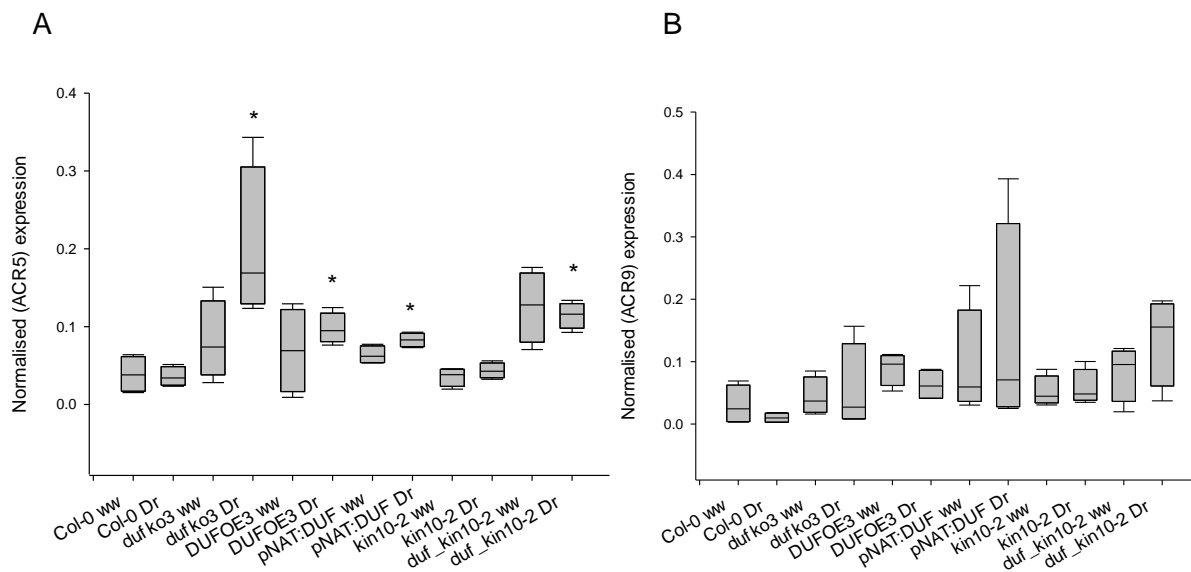


Figure 3.20. Normalised gene expressions to actin for sugar-responsive genes under well-watered and drought conditions for Col-0 plants and mutants. **(A-E)** AtHXK2, ATPME17, DSP4, AT2G36220 and AtTPS5, respectively. Col-0 Dr was compared with Col-0 ww, while all other mutants were compared with Col-0 under the same conditions (n=4).

ACR5 gene showed a high level of expression under drought stress in the *DUFOE* drought compared to Col-0 plants. ACR5 showed a significant increase in the *pNAT:DUF*, *dufko3* mutant, and *DUFOE3* plants under drought conditions. Also, *duf_kin10-2* showed a high level of ACR5 expression under normal and drought conditions. This increase was also significant under drought conditions, while ACR9 did not show any significant change in all mutants (Figure 3.21 A and B). Also, PLP2 and AtRRP4, which were reported to be involved in stress response, showed upregulation in *kin10-2*, *duf_kin10-2*, and *DUFOE3*, while AtRRP4 showed significant differences compared to Col-0 only in *DUFOE3* plants (Figure 3.21 C and D). The remaining gene expression data is in (Appendix D).



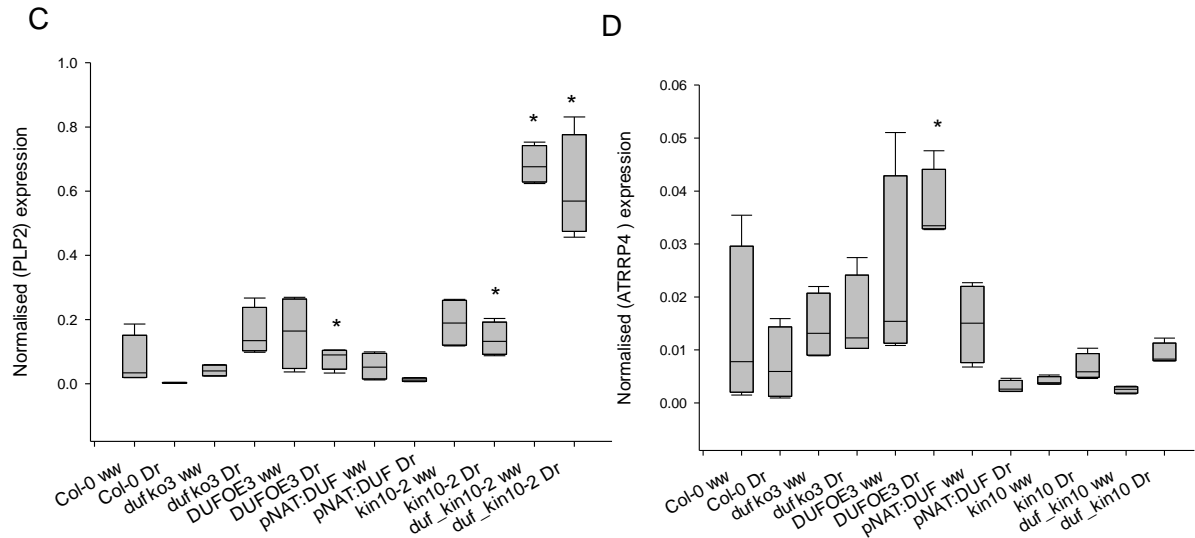


Figure 3.21. Normalised gene expression of different investigated genes in Col-0 and all mutant genotypes subjected to drought stress (**A**) ACR5 and (**B-D**) ACR9, PLP2, and ATRRP4, respectively. * indicates a significant difference from control conditions at $P < 0.05$ ($n=4$).

3.5.3. Carbohydrate measurement

Soluble sugars (glucose, fructose, and sucrose) and starch levels were determined under well-watered and drought stress conditions to investigate whether DUF2358 is involved in regulating sugar levels. Glucose, fructose, and sucrose were significantly higher under drought stress in all genotypes *dufko3*, *DUFOE3*, *pNAT:DUF*, and Col-0 compared with well-watered plants (Figure 3.22 A-C). Glucose levels were significantly lower in *dufko3* after drought stress compared to Col-0, *DUFOE3*, and *pNAT:DUF*. Also, in the *duf_kin10-2* crosses, glucose levels were significantly lower than in the other genotypes. Fructose, sucrose, and starch showed no significant differences between genotypes under well-watered and drought stress conditions (Figure 3.22 A, B, and D).

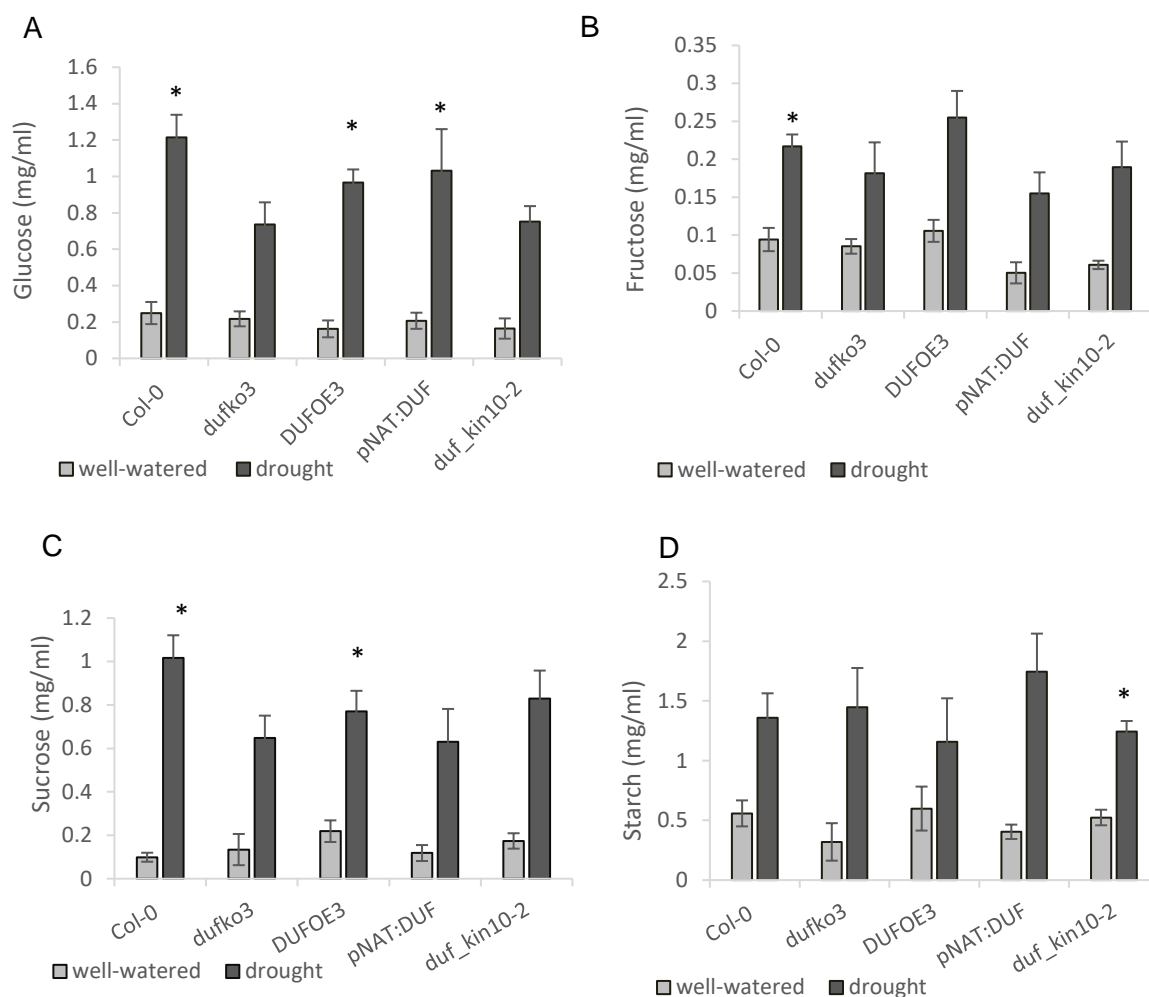


Figure 3.22. Analysis of soluble sugar levels in Col-0 and mutant genotypes subjected to drought stress. **(A)** Glucose levels **(B)** Fructose **(C)** Sucrose **(D)** Starch. * indicates significant differences from control conditions for the same genotype at $P < 0.05$ ($n=8$). Error bars signify SEM (standard error of the mean).

3.5.4. H₂O₂ Content

Hydrogen peroxide H₂O₂ content was determined under normal and stress conditions. Drought stress did not induce H₂O₂ production in all genotypes, and there were no significant differences between genotypes under both well-watered and drought conditions, suggesting that altered DUF2358 expression does not lead to oxidative stress due to increased H₂O₂ production (Figure 3.23).

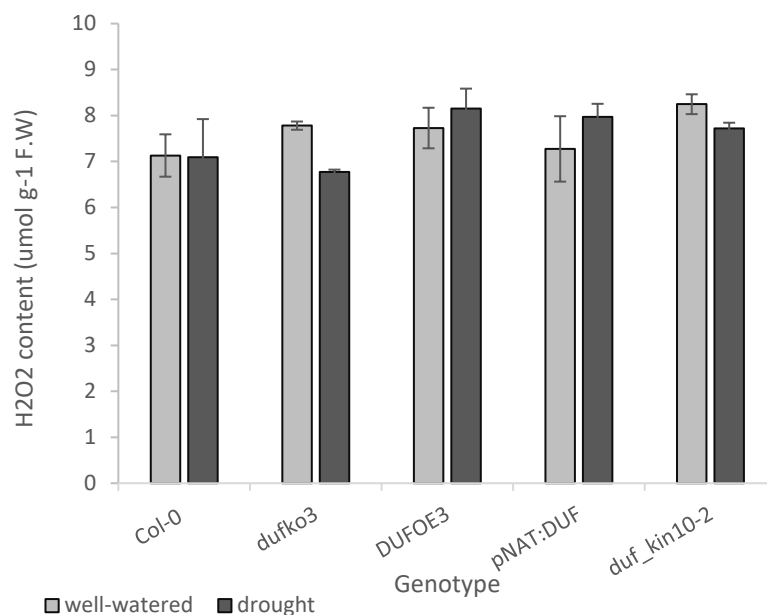


Figure 3.23. Analysis of hydrogen peroxide levels in Col-0 and mutant genotypes subjected to drought stress. No significant differences were recorded. Error bars signify SEM (standard error of the mean) (n=4).

3.6. Prolonged dark treatment

3.6.1. The maximum efficiency of photosystem II measurement

Prolonged dark treatment was conducted on 4-week-old *Arabidopsis* plants to study the effect of darkness and sugar starvation in the different genotypes. Eight plants of each genotype (Col-0, *dufko3*, and pNAT:DUF) were exposed to darkness for nine days, along with the same number of plants under normal dark/light conditions. The maximum efficiency of photosystem II (Fv/Fm) was measured daily. In the dark-treated plants, there were significant differences between Col-0 and *dufko3* in Fv/Fm after nine days. Fv/Fm gradually decreased from the third day to the ninth day in all genotypes, but this decrease was more pronounced in the *dufko3* mutant. The results showed that pNAT:DUF plants behaved like Col-0 in response to darkness, while *dufko3* plants failed to maintain Fv/Fm in response to darkness (Figure 3.24 A and B).

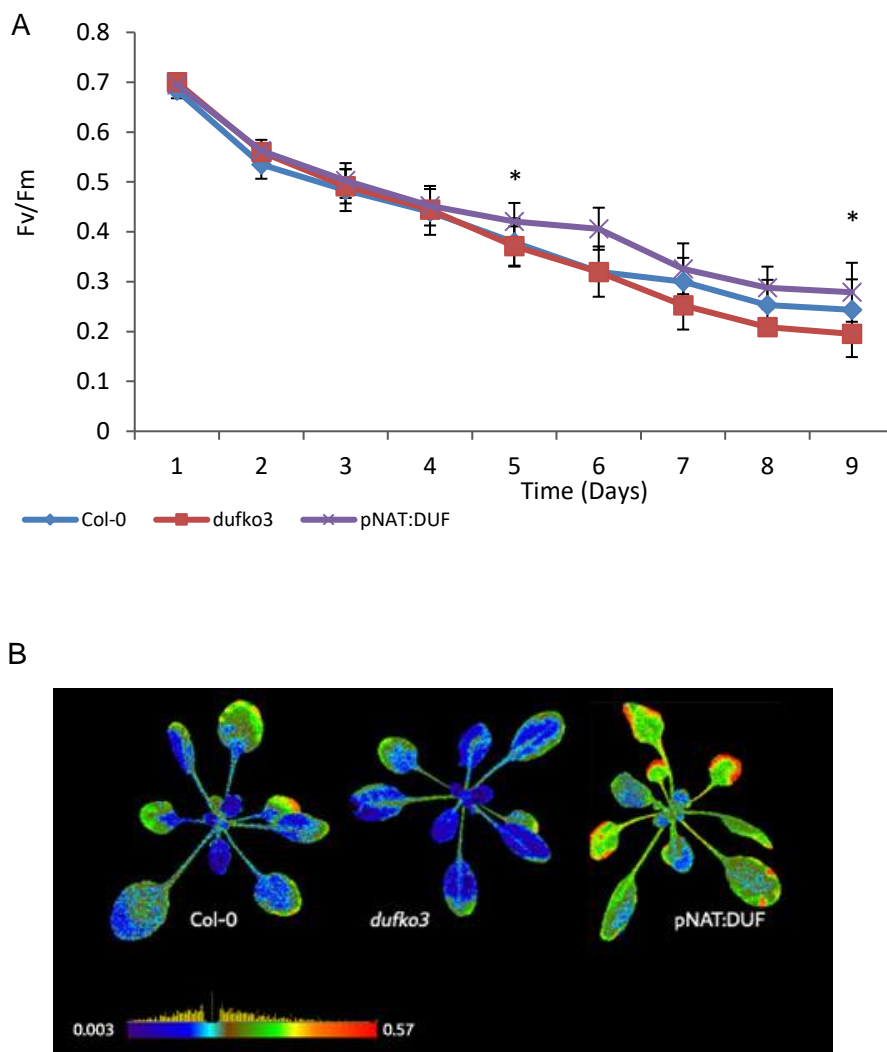


Figure 3.24. (A) Time course of Fv/Fm averages of Col-0, *dufko3*, and pNAT:DUF kept in darkness for nine days. Error bars signify SEM (standard error of the mean). *indicates significant differences from control conditions at $P < 0.05$. $n = 12$. (B) False colour image of Fv/Fm values after 9 days of darkness. Dark blue represents a lower value.

3.6.2. Gene Expression

The same 23 genes which were selected from the drought response gene regulatory network were studied (Table 3.1), along with known dark responsive genes such as ASPARAGINE SYNTHASE 1 DARK INDUCIBLE 6 (DIN6) and SENESCENCE-ASSOCIATED PROTEIN 5 (SEN5), to examine the effect of dark-induced starvation

observed in the *dufko3* genotype compared to pNAT:DUF and Col-0 (Table 3.2). Only genes with significant changes in gene expression compared to Col-0 under darkness will be shown here, the remaining figures will be in (Appendix F). Col-0 DUF2358 and KIN10 showed a higher level of expression under darkness compared to the usual light/dark cycle grown in Col-0 (Figure 3.25 A and B).

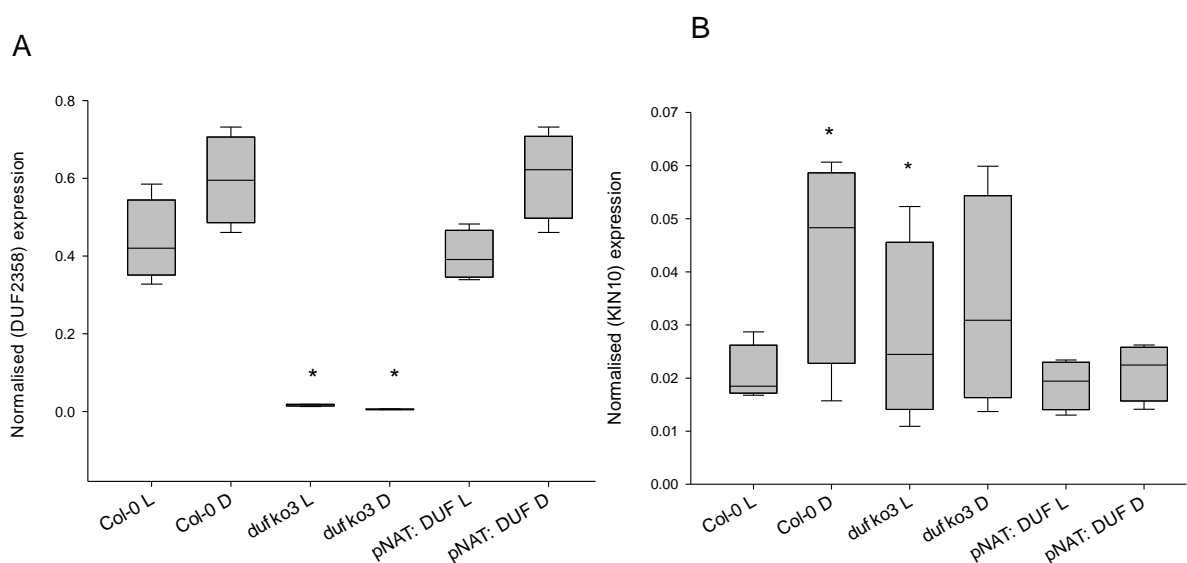
Table 3.2. investigated genes under 9 days of darkness. genes were selected from the drought response gene regulatory network Bechtold *et al.* (2016). Also, other dark responsive genes and dark-induced senescence genes.

Abbreviation	Locus ID	Gene Full name
ABF2	AT1G45249	<i>ABSCISIC ACID-RESPONSIVE ELEMENTS-BINDING FACTOR 2</i> (ABA related gene)
ABF3	AT4G34000	<i>ABSCISIC ACID-RESPONSIVE ELEMENTS-BINDING FACTOR 3</i> (ABA related gene)
ABI5	AT2G36270	<i>ABA INSENSITIVE 5</i> (ABA related gene)
ACR5	AT2G03730	<i>ACT DOMAIN REPEAT 5</i>
ACR9	AT2G39570	<i>ACT DOMAIN REPEAT 9</i>
ATTPS5	AT4G17770	<i>TREHALOSE PHOSPHATE SYNTHASE 5</i> (sugar-related gene)
PLP2	AT2G26560	<i>PHOSPHOLIPASE A2</i>
ATTRP4	AT1G03360	<i>RIBOSOMAL RNA-PROCESSING PROTEIN 4</i>
AT2G36220	AT2G36220	<i>HYPOTHETICAL PROTEIN</i> (sugar-related gene)
TIP2	AT3G26520	<i>TONOPLAST INTRINSIC PROTEIN 2</i>
AT4G25580	AT4G25580	(ABA related gene)
MPK5	AT4G11330	<i>MITOGEN-ACTIVATED PROTEIN KINASE 5</i>
DSP4	AT3G52180	<i>DUAL SPECIFICITY PROTEIN PHOSPHATASE</i> (sugar-related gene)

AtHXK2	AT2G19860	<i>HEXOKINASE 2</i> (sugar-related gene)
KIN10	AT3G01090	<i>SNF1-RELATED PROTEIN KINASE (KIN10)</i>
AT1G12790	AT1G12790	<i>DNA LIGASE-LIKE PROTEIN</i>
CYP71B4	AT3G26280	<i>CYTOCHROME P450 MONOOXYGENASE</i>
ATPME17	AT2G45220	<i>PECTIN METHYLESTERASE 17</i>
UMAMIT33	AT4G28040	<i>USUALLY, MULTIPLE AMINO ACIDS MOVE IN AND OUT TRANSPORTER 33</i>
ATTPE	AT2G22190	<i>TREHALOSE-6-PHOSPHATE PHOSPHATASE</i> (sugar-related gene)
SEN5	AT3G15450	<i>SENESCENCE-ASSOCIATED PROTEIN 5</i> (SnRK1.1 activated marker gene)
DIN6	AT3G47340	<i>ASPARAGINE SYNTHASE 1 DARK INDUCIBLE 6</i> (SnRK1.1 activated marker gene)
RD29B	AT5G52300	<i>RESPONSIVE TO DESICCATION 29B</i> (ABA activated marker gene)
RAB18	AT5G66400	<i>RESPONSIVE TO ABA 18</i> (ABA activated marker gene)
EIF4	AT3G13920	<i>EUKARYOTIC TRANSLATION INITIATION FACTOR 4A1</i>
AXP	AT2G33830	(SnRK1.1 activated marker gene)
GLK2	AT2G20570	<i>GOLDEN2-LIKE</i>
ORE1	AT5G39610	<i>ARABIDOPSIS NAC DOMAIN CONTAINING PROTEIN 92</i>
EIN3	AT3G20770	<i>ETHYLENE-INSENSITIVE3</i>
EEL	AT2G41070	<i>ENHANCED EM LEVEL</i>

3.6.2.1. Sugar responsive genes

PECTIN METHYLESTERASE 17 (ATPME17) expression significantly decreased in response to darkness in Col-0 and it shows a lower level of expressions under darkness in other mutant genotypes (Figure 3.25 C). ATPME17 was significantly decreasing in *dufko3* under normal light conditions compared with Col-0. *DSP4* significantly decreased in Col-0 under dark stress. However, *DSP4* expression was significantly increased in *dufko3* mutant under darkness compared to Col-0 under the same conditions. In normal light conditions, *DSP4* was significantly lower in *dufko3* plants compared with Col-0 (Figure 3.25 D). Finally, AT2G36220 was significantly decreased in the *dufko3* mutant under normal and dark conditions (Figure 3.25 E). *AtHXK2* increased in *dufko3* mutants in response to darkness, but this increase was not significant. Also, *ATTPS5* significantly decreased under darkness in Col-0, but it did not show any crucial change in gene expression mutants under darkness compared to Col-0 under the same conditions (Figure 3.25 F and G). The remaining gene expression and differences data are in (Appendix F and G).



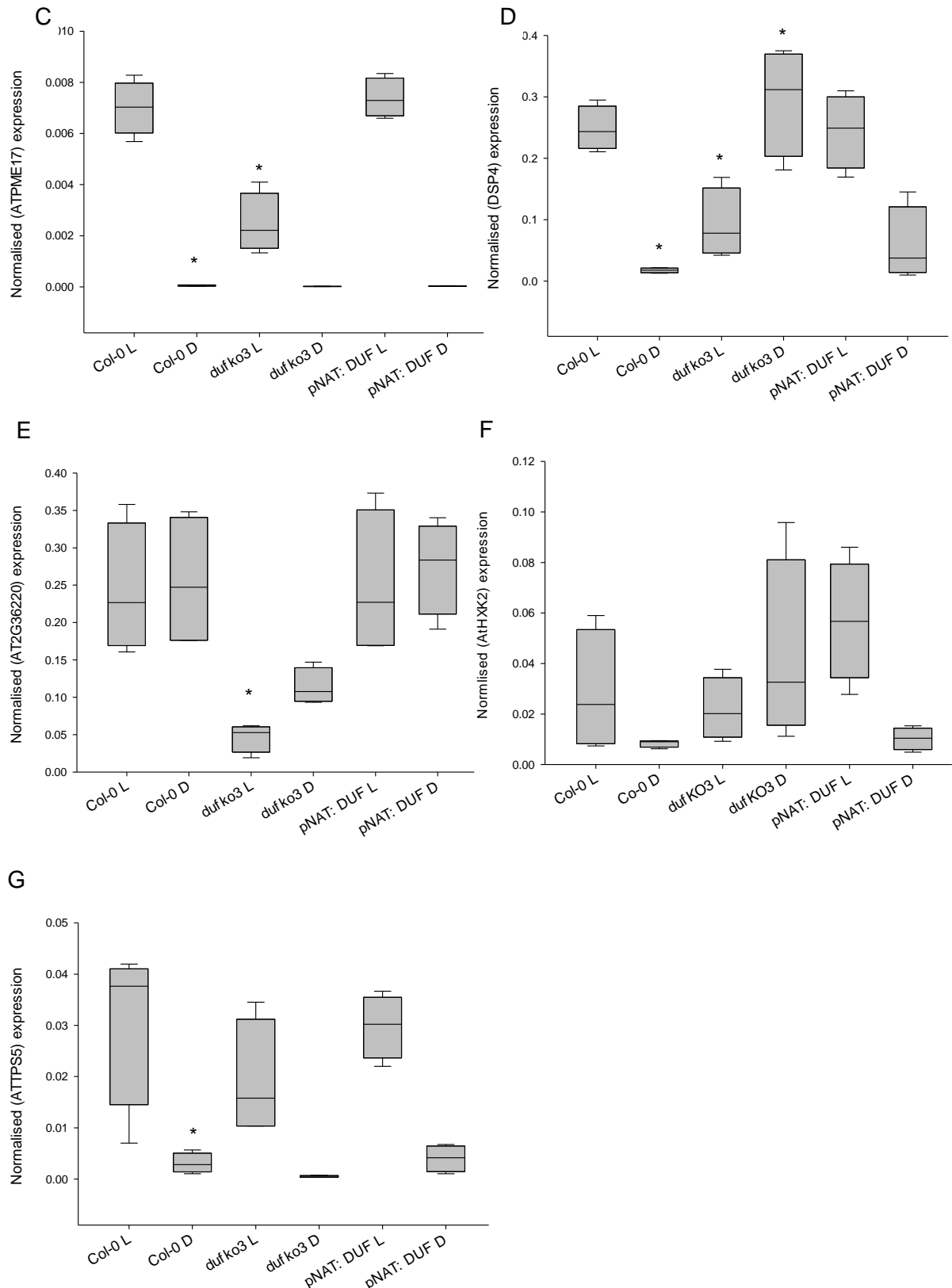


Figure 3.25. Normalised gene expression in Col-0 and all mutant genotypes subjected to 9 days of darkness. **(A)** DUF2358. **(B)** KIN10 **(C-G)** (ATPME17, DSP4, At2g36220, AtHXK2 and ATTPS5 respectively). * indicates a significant difference from control conditions at $P < 0.05$ ($n = 4$). Significant

difference relative to the respective Col-0 (Col-0 D was compared with Col-0 L, all other mutants were compared with Col-0 under the same conditions). L indicates normal light/dark cycle and D indicate dark treatment.

3.6.2.2. ABA signalling genes

ABF2 showed a significant decrease in gene expression under darkness in Col-0 (Figure 3.26 A). Also, ABF2 and ABI5 gene expressions significantly decreased in the *dufko3* plants under normal conditions compared to Col-0 under the same conditions (Figure 3.26 A and B). The decrease in ABA-responsive genes in *dufko3* under control conditions suggests that removing DUF2358 affects the ability of plants to sense ABA low levels, but this decrease was not observed in the drought control comparison. None of the other ABA-related genes showed significant changes in their expression compared to Col-0. The remaining gene expression data is in (Appendix F).

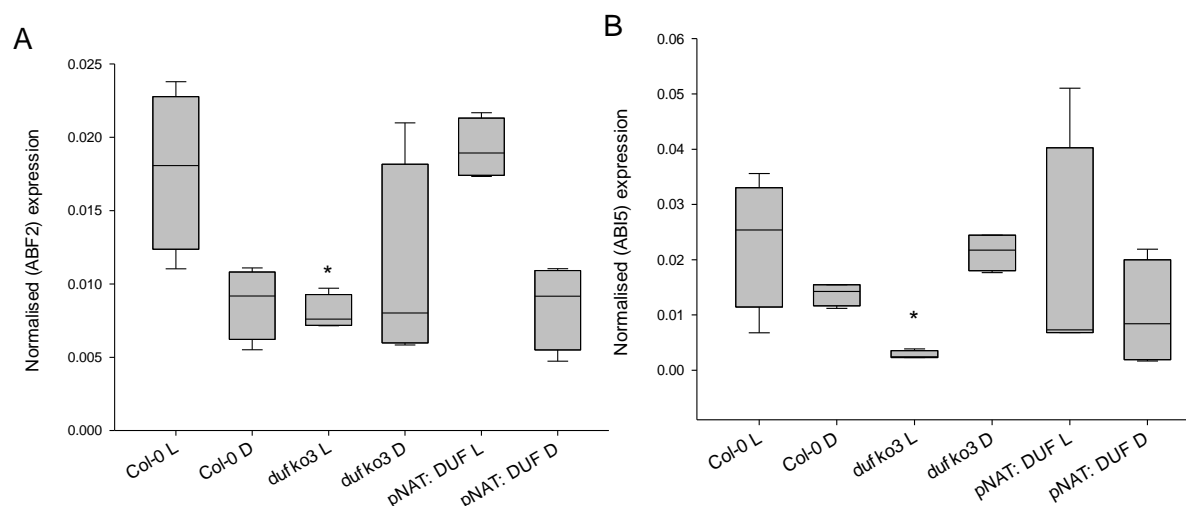


Figure 3.26. Normalised ABA signalling gene expression after nine days of darkness **(A)** *ABF2* **(B)** *ABI5* gene expressions of Col-0 and mutant plants under normal and nine days of dark conditions. * indicates a significant difference from control conditions at $P < 0.05$ ($n=4$). Significant difference is relative to the respective Col-0 (Col-0 D was compared with Col-0 L, all other mutants were compared with Col-0 under the same conditions). L indicates normal light/dark cycle and D indicates dark treatment.

3.6.2.3. Dark inducible genes

Apart from all-dark inducible tested genes, only DIN6 showed significant differences under darkness between Col-0 under the normal light conditions and Col-0 under dark conditions. DIN6 was upregulated under the dark condition and shows a significant increase compared with Col-0 under normal condition. This increase didn't show under the dark condition in *dufko3* mutant plants (Figure 3.27).

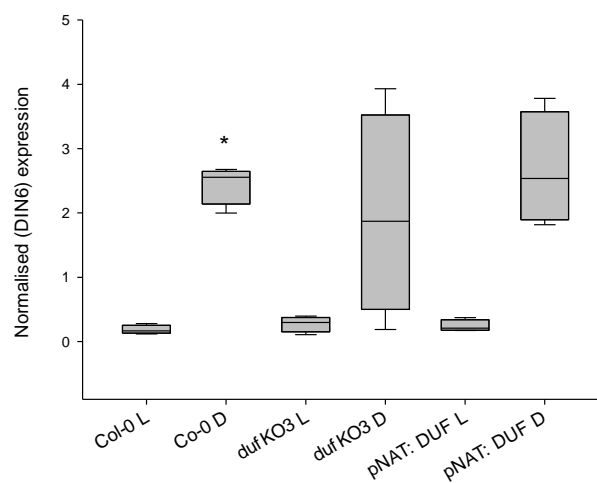
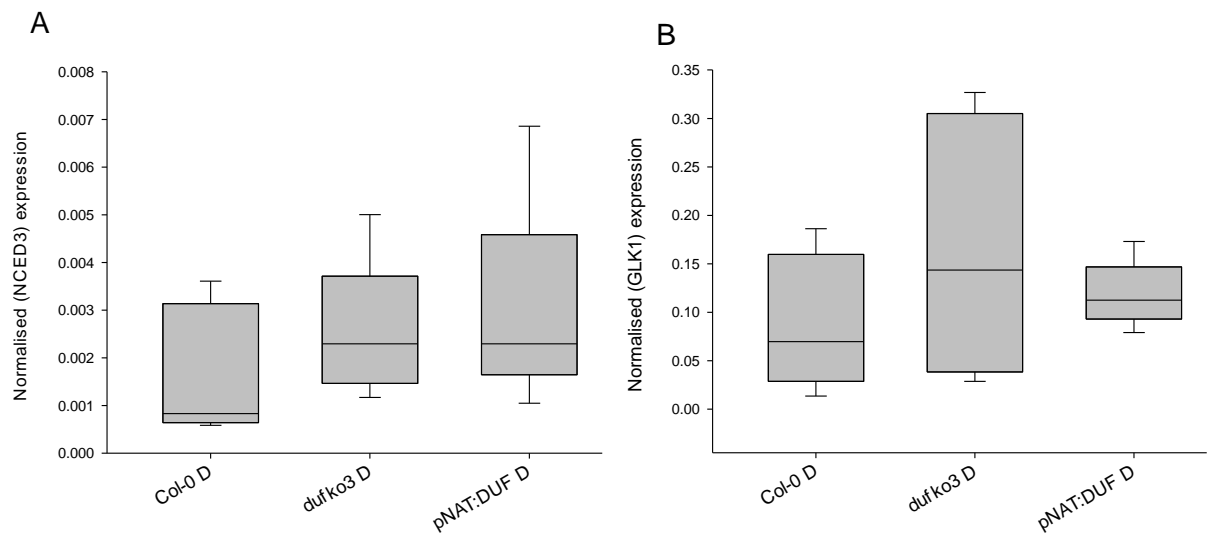


Figure 3.27. Normalised DIN6 gene expression after nine days of darkness * indicates a significant difference from control conditions at $P < 0.05$. Significant difference relative to the respective Col-0. L indicates normal light/ dark cycle and D indicates dark treatment (n=4).

3.6.2.4. Dark-induced leaf senescence genes

Due to the more severe decline in Fv/Fm during prolonged darkness in the *dufko3* mutant (Figure 3.24), we also investigated the expression of five genes known to be involved in the dark-induced leaf senescence. These genes are 9-CIS-EPOXYCAROTENOID DIOXYGENASE 3 (NCED3), which is the rate-limiting enzyme in ABA biosynthesis (Susmilch *et al.*, 2017; Huang *et al.*, 2018); the chloroplast maintenance master regulator GOLDEN2-LIKE 1 (GLK1); the senescence master

regulator *ORESARA1* (*ORE1*); ETHYLENE-INSENSITIVE3 (*EIN3*); and ENHANCED EM LEVELS (*EEL*) (Liebsch and Keech, 2016). Gene expression for *NCED3*, *GLK1*, *ORE1*, *EIN3* and *EEL* expression under darkness showed no significant change in *dufko3* compared to Col-0. This result indicated that the altered *DUF2358* expression does not affect dark-induced leaf senescence genes (Figure 3.28 A-E).



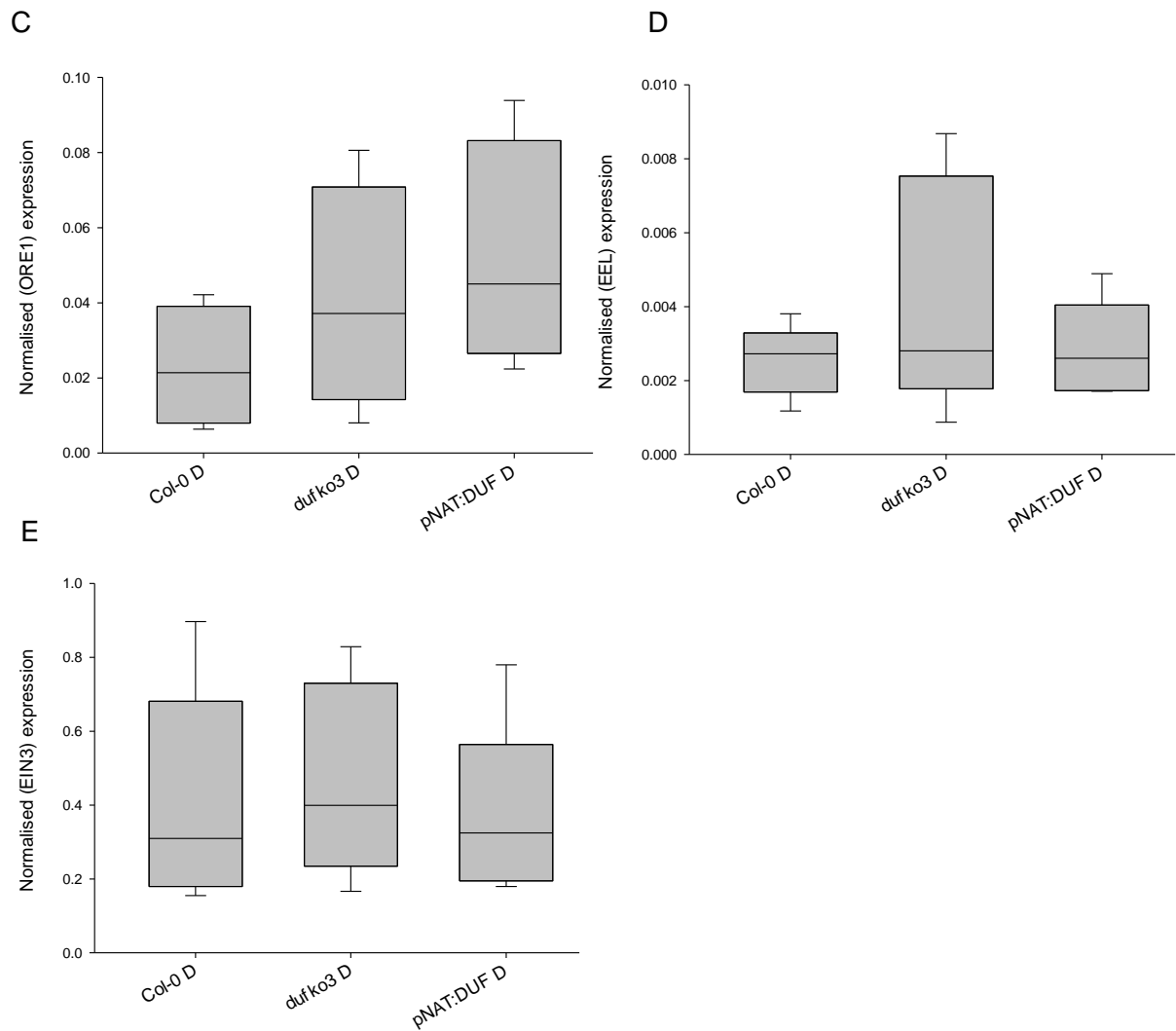


Figure 3.28. Normalised genes expression which involved in dark-induced leaf senescence after 9 days of darkness (**A-E**) NCED3, GLK1, ORE1, EEL, and EIN3, respectively. Mutants were compared with Col-0 under dark conditions. D indicates the dark condition. $P < 0.05$ $n = 4$.

3.6.2.5. Other investigated genes

Among direct and indirect target genes of DUF2358 which were investigated ACR5, MPK5, UMAMIT33, and AT1G12790 showed significant differences in their expression compared to Col-0. ACR5, MPK5, UMAMIT33, and AT1G12790 expressions in *dufko3* mutants were significantly lower than their expression in Col-0 under normal conditions (Figure 3.29 A-D). The remaining gene expression data is in (Appendix F).

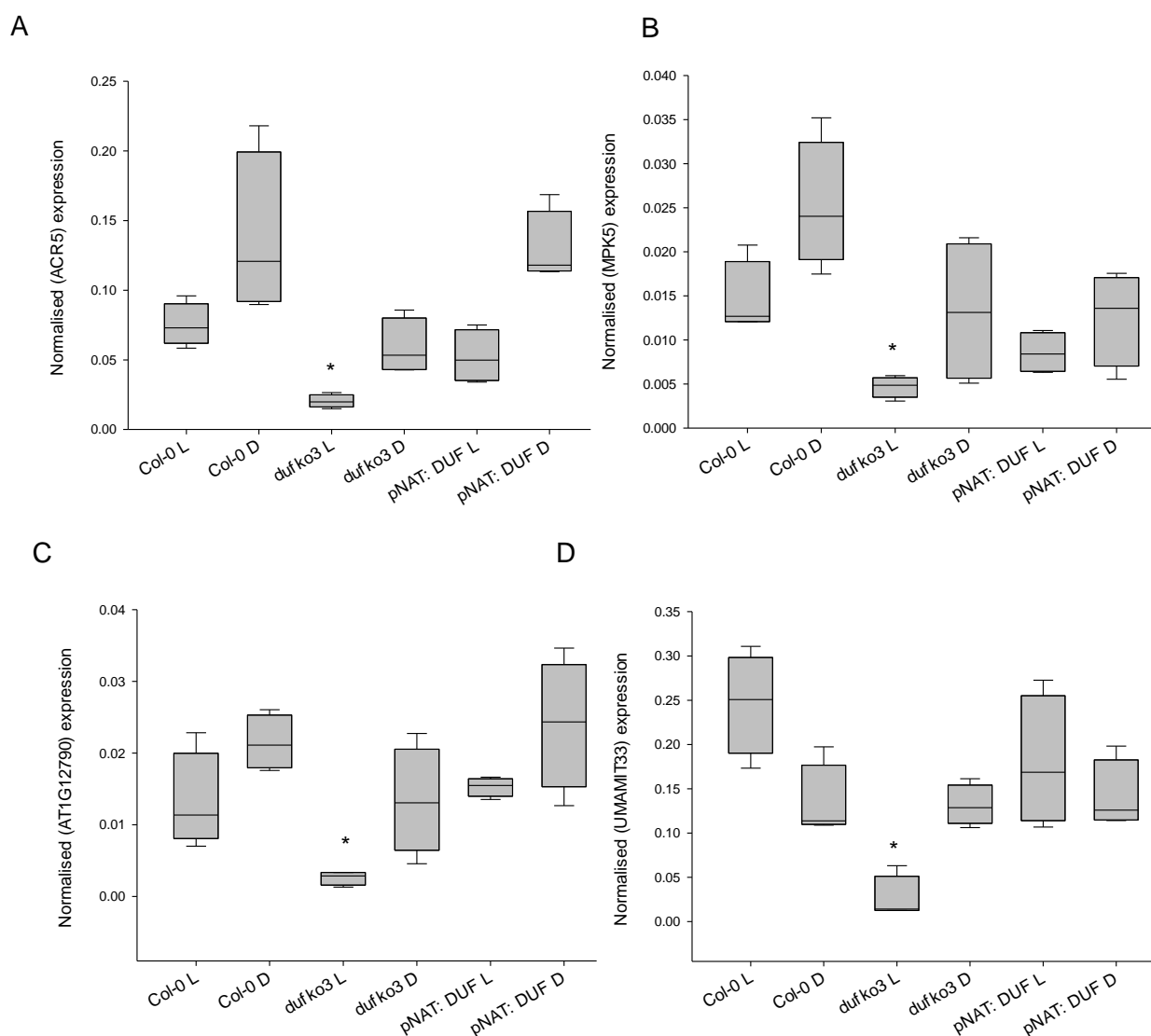


Figure 3.29. Normalised gene expression after 9 days of darkness **(A-D)** ACR5, MPK5, AT1G12790, and UMAMIT33, respectively. * indicates a significant difference from control conditions at $P < 0.05$ ($n=4$). Significant difference relative to the respective Col-0 (Col-0 D was compared with Col-0 L. All other mutants were compared with Col-0 under the same conditions). L indicates a normal light/ dark cycle and D indicates dark treatment.

3.7. Sugar dark treatment

Sugar dark treatment was conducted in order to examine whether DUF affects responses to changes in the altered sugar status. Also, effect altered DUF2358

expression on plants' response to unexpected darkness, which was sensed as stress and activated KIN10 protein kinase.

3.7.1. The maximum efficiency of photosystem II Fv/Fm measurement

Short-term dark treatment with or without glucose treatment did not have an effect on PSII maximum efficiency Fv/Fm (Figure 3.30)

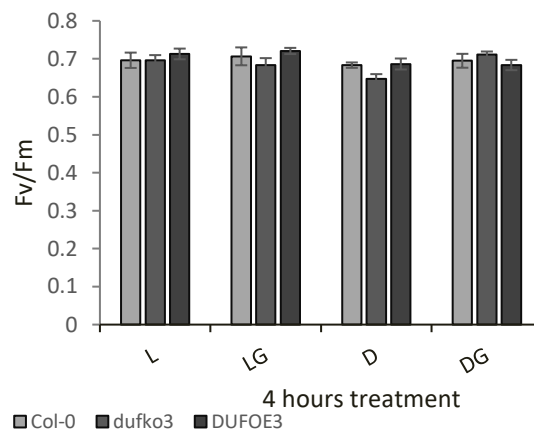


Figure 3.30. Fv/Fm for *dufko3* mutant, *DUFOE* mutant, and Col-0 after four hours of different treatments. Error bars signify SEM (standard error of the mean). L indicates normal light treatment, LG indicates light and glucose treatment, D indicates Dark treatment, and DG indicates dark with glucose treatment n=6.

3.7.2. Gene Expression

Known KIN10-upregulated and sugar-repressed genes were measured (ASPARAGINE SYNTHASE 1 DARK INDUCIBLE 6 (DIN6), PUTATIVE AUXIN-REGULATED PROTEIN (AXP) and SENESCENCE-ASSOCIATED PROTEIN 5 (SEN5)) (Rodrigues *et al.*, 2013) in the DUF2358 mutant backgrounds. Darkness promoted the significant increase of DIN6 and SEN5 expression in Col-0, while

glucose significantly repressed gene expression (Figure 3.31), as has been previously shown by (Rodrigues *et al.*, 2013).

The *dufko3* and *DUFOE3* genotypes showed altered patterns in the expression of all three genes. DIN6 expression in the *dufko3* mutant followed the same pattern as Col-0, while *DUFOE3* failed to decrease expression in the presence of glucose (Figure 3.31 A).

Similarly, SEN5 expression pattern was similar in the *dufko3* mutant in response to D and DG treatments, while overall expression levels were significantly lower than Col-0. *DUFOE3*, on the other hand, showed significantly higher expression levels than Col-0 under light, which did not change in response to darkness, but reduced significantly when supplemented with glucose (Figure 3.31 B). AXP expression was higher than Col-0 under the light in *dufko3* plants (Figure 3.31 C). AXP gene expression patterns under the different treatments were altered compared to Col-0. In the *dufko3*, expression levels did not increase during darkness compared to the light treatment but showed responsiveness to glucose supplementation. In *DUFOE3*, AXP expression was high during the light, significantly reducing in darkness, and darkness plus glucose treatment (Figure 3.31 C). These results suggest that altering DUF2358 expression impacts on KIN10 and sugar-regulated genes.

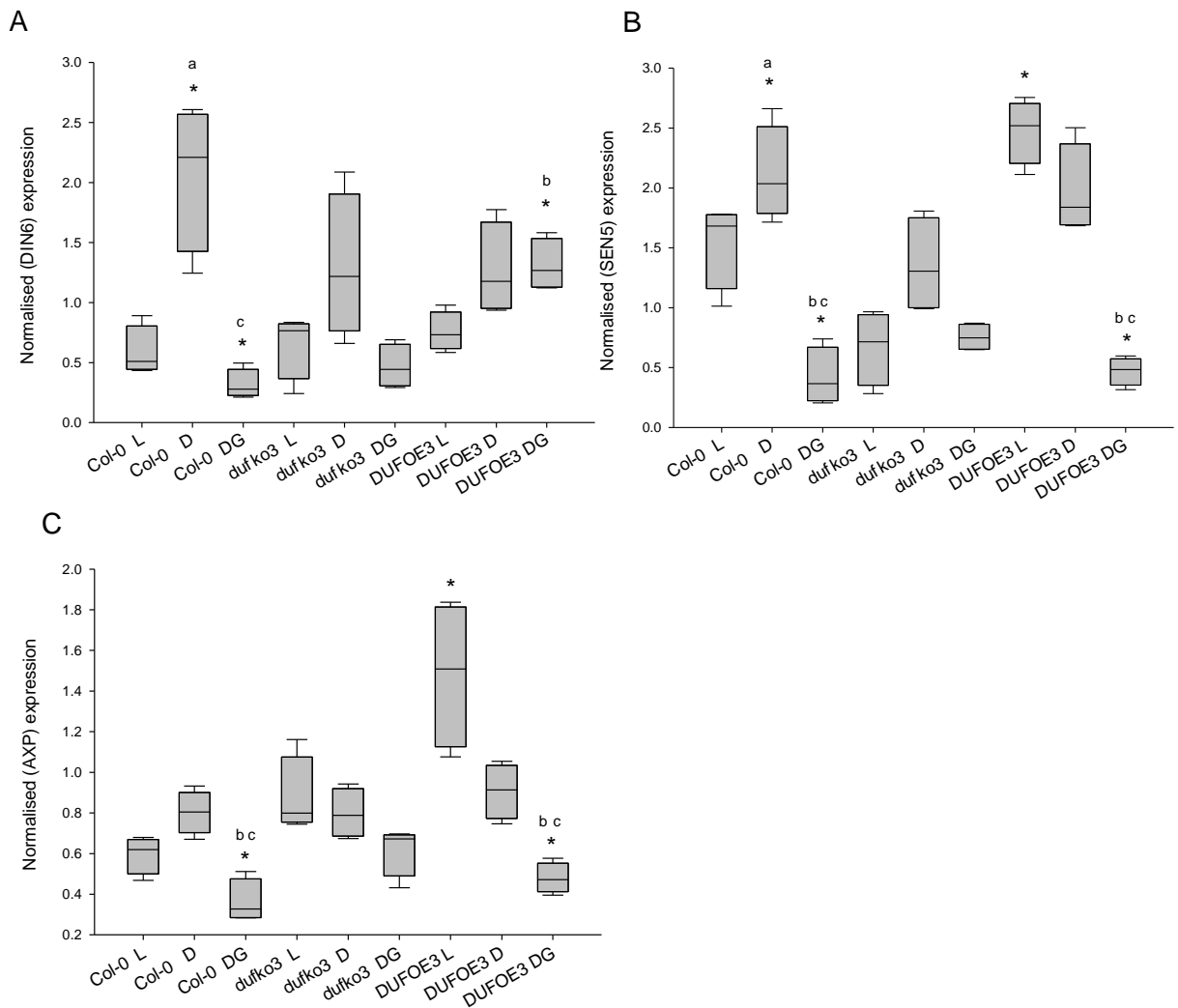


Figure 3.31. Normalised gene expression in Col-0 and all mutant genotypes subjected to 4 hours of darkness (D) and 4-hour darkness supplemented with glucose (DG), (L) indicates the normal light condition. **(A)** DIN6. **(B)** SEN5 and **(C)** AXP. * indicates a significant difference from control conditions between the same genotypes *a – D vs. L and *b – DG/L and *c – DG/D. at $P < 0.05$ ($n=4$). * only indicates significant difference relative to the respective Col-0 under the same condition (post hoc Tukey's test).

We extended the analysis to selected drought-responsive genes from the gene regulatory network (Table 3.1) to see whether they follow the same pattern as the KIN10 dark upregulated and sugar-repressed expression genes in Col-0. In total, seven drought-responsive genes were analysed, of which only AT4G25580 showed the typical expression pattern observed for KIN10-upregulated and sugar-repressed genes in Col-0. Also, ATTPS5 significantly increases in the dark supplemented with glucose

(Figure 3.32 A and B). This suggests that the majority of drought-responsive genes in our gene regulatory network model are not KIN10-regulated under extended night conditions, and that drought stress and extended night conditions are very different stresses that lead to different responses.

This was also confirmed when the drought time series dataset (Bechtold *et al.*, 2016) was compared to a publicly available microarray data set of KIN10 overexpressors (Baena-González *et al.*, 2007, Table 3.3). While there was significant overlap, none of the genes were part of the drought gene regulatory network and/or direct targets of DUF2358 (Table 3.1).

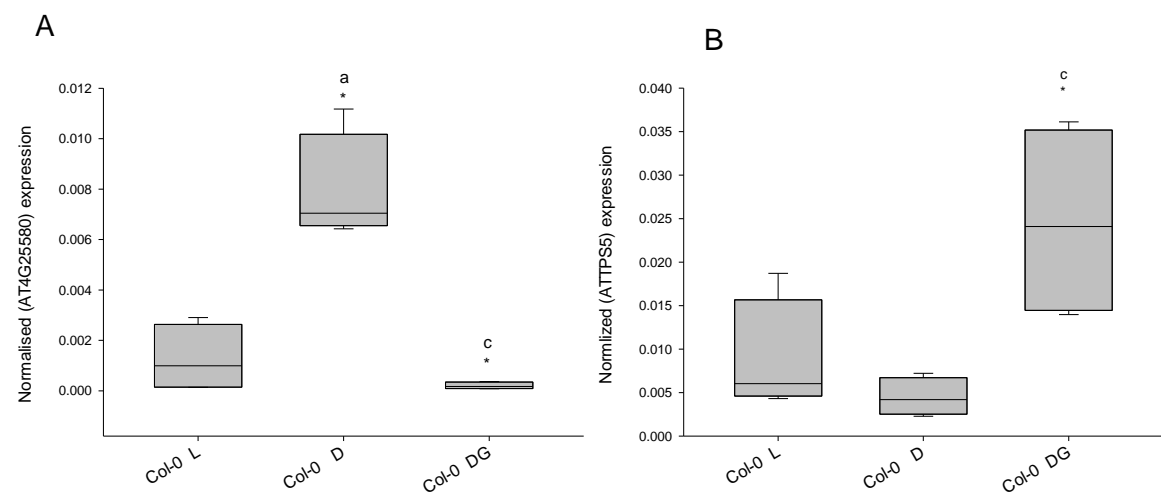


Figure 3.32. Normalised gene expression in Col-0 subjected to 4 hours of darkness (D) and 4-hour darkness supplemented with glucose (DG), (L) indicates the normal light condition. **(A)** AT4G25580 and **(B)** ATTPS5. * indicates a significant difference from control conditions *a – D vs L and *b – DG/L and *c – DG/D. at $P < 0.05$ ($n=4$). * significant difference relative to the respective Col-0.

Table 3.3. Overlap between the drought time series dataset (Bechtold *et al.*, 2016) and KIN10 regulated genes (KIN10 over-expressing plants; Baena González *et al.*, 2007).

AGI number	KIN10 average	Gene Model Description	Primary Gene Symbol
AT1G04440	-1.77	Member of CKL gene family (CKL-C group).	CASEIN KINASE LIKE 13 (CKL13)
AT1G12790	-1.29	DNA ligase-like protein	
AT1G15010	-1.47	mediator of RNA polymerase II transcription subunit	
AT1G15930	-2.56	Ribosomal protein L7Ae/L30e/S12e/Gadd45 family protein	
AT1G19610	-1.26	Predicted to encode a PR (pathogenesis-related) protein.	(PDF1.4)
AT1G21400	-2.05	Thiamin diphosphate-binding fold (THDP-binding) superfamily protein	
AT1G22890	-2.15	Secreted peptide which functions in plant growth and pathogen defense.	(STMP2)
AT1G26770	-1.59	Encodes an expansin.	EXPANSIN A10 (EXPA10)
AT1G27400	-3.27	Ribosomal protein L22p/L17e family protein	
AT1G35580	-2.03	CINV1 / A/N-InvG is an alkaline/neutral invertase that breaks sucrose down into fructose and glucose (GH100).	CYTOSOLIC INVERTASE 1 (CINV1)
AT1G64660	-1.56	Encodes a functional methionine gamma-lyase	METHIONINE GAMMA-LYASE (MGL)
AT1G69295	-1.41	Encodes a member of the X8-GPI family of proteins.	PLASMODESMATA CALLOSE-BINDING PROTEIN 4 (PDCB4)
AT1G69530	-1.44	Member of Alpha-Expansin Gene Family.	EXPANSIN A1 (EXPA1)

AT1G70290	-1.58	Encodes an enzyme putatively involved in trehalose biosynthesis.	TREHALOSE-6-PHOSPHATASE SYNTHASE S8 (TPS8)
AT1G72370	-2.19	Acidic protein associated to 40S ribosomal subunit of ribosomes.	40S RIBOSOMAL PROTEIN SA (P40)
AT1G80190	-2.25	Similar to the PSF1 component of GINS complex.	PARTNER OF SLD FIVE 1 (PSF1)
AT1G80530	-1.76	Major facilitator superfamily protein	
AT2G13360	-2.33	Encodes a peroxisomal photorespiratory enzyme.	ALANINE: GLYOXYLATE AMINOTRANSFERASE (AGT)
AT2G15695	-2.74	peptide methionine sulfoxide reductase.	
AT2G18700	-2.48	Encodes an enzyme putatively involved in trehalose biosynthesis.	TREHALOSE PHOSPHATASE/SYNTHASE 11 (TPS11)
AT2G19670	-1.91	protein arginine methyltransferase 1A.	PROTEIN ARGININE METHYLTRANSFERASE 1A (PRMT1A)
AT2G19810	-2.37	Encodes Oxidation-related Zinc Finger 1 (OZF1).	OXIDATION-RELATED ZINC FINGER 1 (OZF1)
AT2G20670	-1.99	sugar phosphate exchanger, putative (DUF506).	
AT2G25200	-2.11	hypothetical protein (DUF868).	
AT2G26560	-2.50	Encodes a lipid acyl hydrolase.	PHOSPHOLIPASE A 2A (PLA2A)
AT2G33370	-2.41	Ribosomal protein L14p/L23e family protein.	
AT2G36220	-2.51	hypothetical protein.	
AT2G36620	-1.66	RPL24A encodes ribosomal protein L24, homolog of cytosolic RPL24.	RIBOSOMAL PROTEIN L24 (RPL24A)
AT2G37400	-1.61	Tetratricopeptide repeat (TPR)-like superfamily protein.	
AT2G39570	-1.45	Encodes a ACT domain-containing protein.	ACT DOMAIN REPEATS 9 (ACR9)

AT2G44120	-1.53	Ribosomal protein L30/L7 family protein	
AT2G45170	-2.21	Involved in autophagy.	AUTOPHAGY 8E (ATG8E)
AT2G47610	-1.86	Ribosomal protein L7Ae/L30e/S12e/Gadd45 family protein	
AT3G05560	-1.84	Ribosomal L22e protein family	
AT3G07110	-1.60	Ribosomal protein L13 family protein	
AT3G10740	-1.88	Encodes a bifunctional alpha-l-arabinofuranosidase/beta-d-xylosidase	ALPHA-L-ARABINOFURANOSIDASE 1 (ASD1)
AT3G13450	-1.74	branched chain alpha-keto acid dehydrogenase E1 beta	DARK INDUCIBLE 4 (DIN4)
AT3G13750	-1.70	beta-galactosidase, glycosyl hydrolase family 35	BETA GALACTOSIDASE 1 (BGAL1)
AT3G15450	-1.98	aluminum induced protein with YGL and LRDR motifs	
AT3G15630	-1.83	plant/protein	
AT3G16780	-1.93	Ribosomal protein L19e family protein	RIBSOMAL PROTEIN LIKE 19B (RPL19B)
AT3G19290	-1.95	bZIP transcription factor	ABRE BINDING FACTOR 4 (ABF4)
AT3G23000	-1.84	Encodes a serine/threonine protein kinase	CBL-INTERACTING PROTEIN KINASE 7 (CIPK7)
AT3G25520	-2.42	Encodes ribosomal protein L5	RIBOSOMAL PROTEIN L5 (ATL5)
AT3G26280	-1.89	cytochrome P450 monooxygenase	CYTOCHROME P450, FAMILY 71, SUBFAMILY B, POLYPEPTIDE 4 (CYP71B4)
AT3G26520	-2.17	gamma tonoplast intrinsic protein 2 (TIP2).	TONOPLAST INTRINSIC PROTEIN 2 (TIP2)
AT3G28900	-1.58	Ribosomal protein L34e superfamily protein	
AT3G46540	-1.28	ENTH/VHS family protein	

AT3G47340	-2.63	encodes a glutamine-dependent asparagine synthetase,	GLUTAMINE-DEPENDENT ASPARAGINE SYNTHASE 1 (ASN1)
AT3G47370	-1.59	Ribosomal protein S10p/S20e family protein	
AT3G49010	-2.32	Encodes 60S ribosomal protein L13.	BREAST BASIC CONSERVED 1 (BBC1)
AT3G52340	-1.47	sucrose-phosphatase (SPP2)	SUCROSE-6F-PHOSPHATE PHOSPHOHYDROLASE 2 (SPP2)
AT3G56340	-1.83	Small ribosomal subunit protein.	RIBOSOMAL PROTEIN S26E (RPS26E)
AT4G01026	-1.59	Encodes a member of the PYR	PYR1-LIKE 7 (PYL7)
AT4G01120	-1.63	bZIP (basic leucine zipper) transcription factor	G-BOX BINDING FACTOR 2 (GBF2)
AT4G17390	-1.71	Ribosomal protein L23/L15e family protein	
AT4G31700	-2.15	Encodes a putative ribosomal protein S6 (rps6a)	RIBOSOMAL PROTEIN S6 (RPS6)
AT4G36660	-1.56	polyol transporter, putative (DUF1195)	
AT4G38060	-1.59	hypothetical protein	CLAVATA COMPLEX INTERACTOR 2 (CCI2)
AT4G38470	-1.84	Serine/threonine kinase t	SERINE/THREONINE/TYROSINE KINASE 46 (STY46)
AT5G02160	-1.37	Zinc-finger domain containing protein	FTSH5 INTERACTING PROTEIN (FIP)
AT5G07090	-2.08	Ribosomal protein S4 (RPS4A) family protein	
AT5G10360	-2.23	RPS6A and RPS6B	EMBRYO DEFECTIVE 3010 (EMB3010)
AT5G16130	-1.58	Ribosomal protein S7e family protein	
AT5G19120	-1.65	Eukaryotic aspartyl protease family protein	

AT5G20250	-2.73	encodes a member of glycosyl hydrolase family 36.	DARK INDUCIBLE 10 (DIN10)
AT5G21170	-1.39	Encodes AKINbeta1, a subunit of the SnRK1 kinase (Sucrose non-fermenting-1-related protein kinase).	(AKINBETA1)
AT5G22920	-1.56	Encodes a protein with sequence similarity to RING, zinc finger proteins.	RING ZINC-FINGER PROTEIN 34 (RZPF34)
AT5G24490	-1.53	30S ribosomal protein.	
AT5G39740	-1.32	Encodes a ribosomal protein RPL5B	RIBOSOMAL PROTEIN L5 B (RPL5B)
AT5G54080	-1.50	Encodes a homogentisate 1,2-dioxygenase	HOMOGENTISATE 1,2-DIOXYGENASE (HGO)
AT5G57660	-1.84	CONSTANS-like 5	CONSTANS-LIKE 5 (COL5)
AT5G59080	-2.24	hypothetical protein	
AT5G59480	-1.53	Haloacid dehalogenase-like hydrolase (HAD) superfamily protein	
AT5G59850	-1.33	Ribosomal protein S8 family protein	
AT5G60670	-1.61	Ribosomal protein L11 family protein	RIBOSOMAL PROTEIN LIKE 12C (RPL12C)
AT5G63400	-1.63	encodes a protein similar to adenylate kinase.	ADENYLATE KINASE 1 (ADK1)

Table (3.1) shows the overlap between the drought time series dataset (Bechtold et al., 2016) and data set of KIN10 overexpresses (Baena-González et al., 2007). Comparing this two data sets with each other shows none of the overlap genes between the two data sets were part of the direct or indirect DUF2358 target genes.

3.7.3. Carbohydrate measurement

Soluble sugar and starch were measured for each genotype. The significant difference in glucose in the glucose supplemented samples is to be expected and will not be

discussed further. Overall, there were no significant differences in soluble sugar and starch levels between the genotypes for each treatment (Figure 3.33).

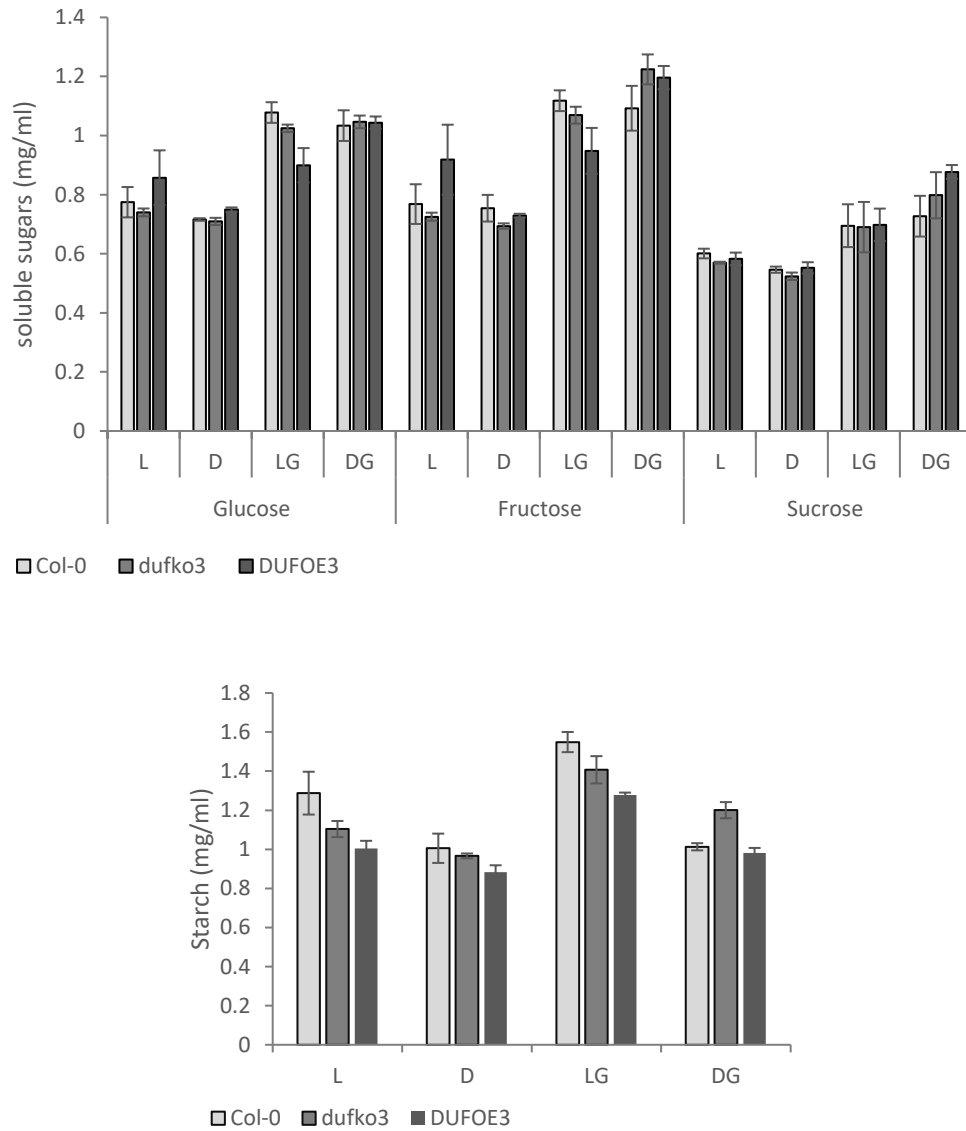


Figure 3.33. The content of soluble sugars and starch in Col-0, *dufko3*, *DUFOE3* under the treatments. L: light, D: Darkness, DG: Dark with glucose treatment, LG: light with glucose treatment.

3.8. Western Blot

Due to the putative location of DUF inside the chloroplast and the proposed involvement in sugar signalling/sensing, we investigated whether there were differences in photosynthetic components. We used specific antibodies to a range of proteins associated with electron transport and Calvin Cycle (chapter 2 section 1.10). Leaf protein samples were loaded in three concentrations, namely 3X, 5X and 10X $\mu\text{g}/\mu\text{l}$. There were no differences between all genotypes compared with Col-0 using TK, FBPa, PsaALhca1, cytb6, RiskeFeS, and Rubisco antibodies. This indicates that *dufko3* has no obvious phenotype photosynthetic electron transport under control conditions (Figure 3.34).

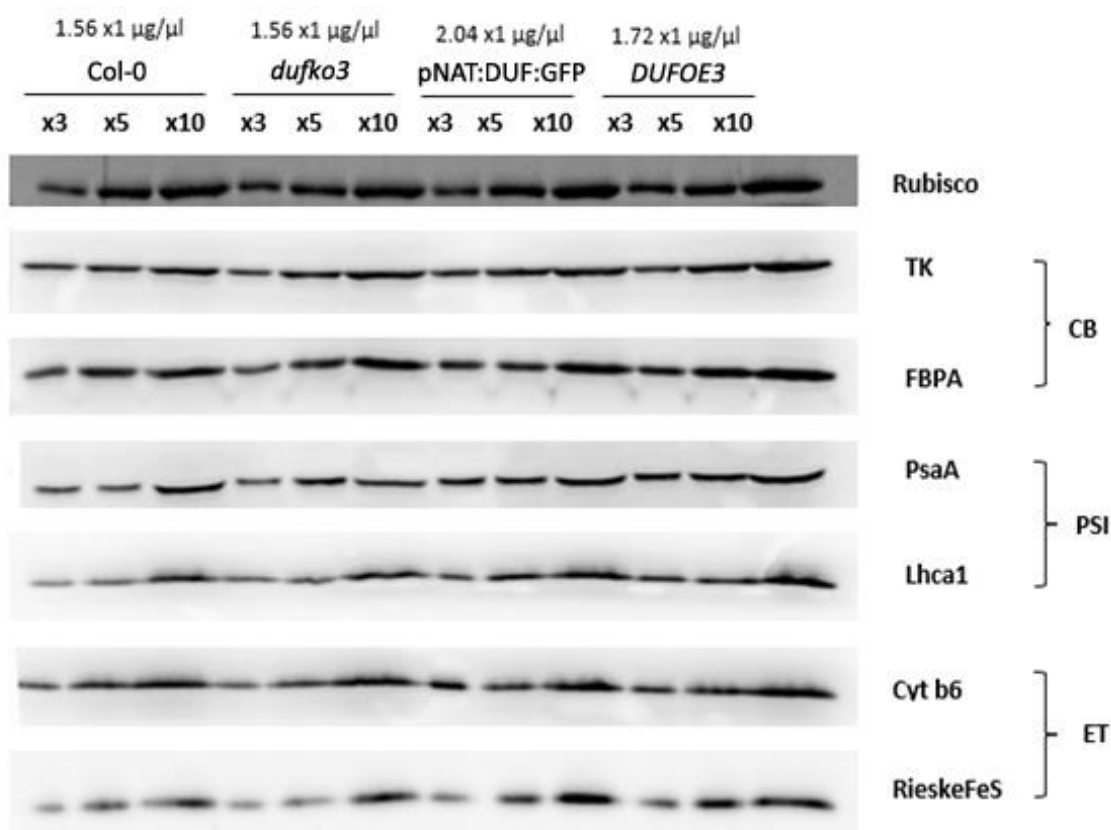


Figure 3.34. Western blot analysis of the protein samples were extracted from different genotypes with different antibodies: Rubisco, the Calvin-Benson cycle proteins (CB) Transketolase 5 (TK), FBPA

aldolase (FBPA), the photosystem I(PS1) PsaA, Lhca1 proteins, and the electron transport (ET) cytochrome b6 Cytb6 and RieskeFeS proteins.

3.9. Conclusion

Based on the drought gene regulatory network (Figure 1.3), genes that are direct and indirect targets of DUF2358 were examined. These included known sugar and ABA-responsive genes (Table 3.1). To do this, we opted for stress conditions that would alter the sugar status of plants in different ways. Under drought stress, DUF2358 was confirmed to be downregulated and showed a low level of expression in contrast to KIN10, which showed a high level of expression under drought stress for all genotypes. Mostly, Col-0 and mutants respond to altered sugar status differently (Table 3.4 and 3.5). The biggest effect of altering DUF2358 expression was observed under drought stress conditions (Table 3.4), the stress treatment during which DUF2358 was initially identified (Bechtold *et al.*, 2016). A proportion of the genes within the network were affected in the *dufko3*, *kin10-2* and the double mutant, suggesting that some of the predicted transcriptional regulations may indeed be affected by DUF2358 mostly under drought stress. Continuous and short-term dark treatments had less of an observable difference at the transcript level of selected genes (Table 3.4). This may primarily be due to the fact that genes chosen were mostly part of the drought gene regulatory network, suggesting that, in dark treatments, the same network is not functional. Nevertheless, *dufko3* showed a distinct chlorophyll fluorescence phenotype (Figure 3.24).

There is considerable inconsistency among control experiments, and the overall picture suggests that knocking out DUF23258 has little impact on the gene regulatory network under control conditions. This is corroborated by the lack of growth phenotype

under control conditions. The inconsistency may be due to differences in plant ages used in the experiments and problems in replicating qPCR results.

From these early results, it appears that *dufko3* may have altered sugar-signalling responses, but not ABA-related responses under drought stress conditions. KIN10 activity is reported to increase under stress and by a decrease in energy levels to restore and maintain the energy balance (Baena-González and Sheen, 2008). Here, we show that KIN10 was upregulated at the transcript level by drought stress and darkness in Col-0 plants. Whether this transcriptional regulation led to an increase in kinase activity, that subsequently triggered the transcriptional changes of the direct KIN10 targets, remains to be seen. However, due to inconsistencies in replicating key results, firm conclusions as to the role of DUF2358 in sugar signalling or sensing pathways cannot be drawn. If and how DUF2358 connects with this response, by regulating KIN10 at the transcriptional level, therefore, remains to be seen.

Table 3.4. Overview of all of qRT-PCR stress treatments. NA = not applicable, ns – not significant. Green cell colour indicates significant down-regulation compared to Col-0 and red cell colour indicates up-regulation compared to Col-0 in the stress treatment.

	Drought stress				Continuous darkness		Short-term darkness/glucose supplement			
	<i>dufko3</i> /Col-0	<i>Kin10 -2</i> /Col-0	<i>duf_kin10-2</i> /Col-0	<i>DUF2358</i> /Col-0	<i>dufko3</i> /Col-0	<i>duf_kin10-2</i> /Col-0	<i>dufko3</i> dark/Col-0	<i>dufko3</i> dark + glucose/Col-0	<i>DUF2358</i> dark/Col-0	<i>DUF2358</i> dark + glucose/Col-0
DUF2358	down	ns	down	up	down	NA	down	down	ns	up
KIN10	ns	down	down	up	ns	NA	ns	ns	ns	ns
ABF2	ns	ns	ns	ns	ns	NA	ns	ns	ns	ns
ABF3	ns	ns	ns	ns	ns	NA	ns	ns	ns	ns

ABI5	<i>ns</i>	<i>ns</i>	up	<i>ns</i>	<i>ns</i>	NA	<i>ns</i>	<i>ns</i>	<i>ns</i>	<i>ns</i>
ACR5	up	<i>ns</i>	up	up	<i>ns</i>	NA	<i>ns</i>	<i>ns</i>	<i>ns</i>	<i>ns</i>
ACR9	<i>ns</i>	<i>ns</i>	<i>ns</i>	<i>ns</i>	<i>ns</i>	NA	<i>ns</i>	<i>ns</i>	<i>ns</i>	<i>ns</i>
ATTPS5	up	<i>ns</i>	<i>ns</i>	<i>ns</i>	<i>ns</i>	NA	<i>ns</i>	<i>ns</i>	<i>ns</i>	<i>ns</i>
AT2G36220	<i>ns</i>	<i>ns</i>	up	up	<i>ns</i>	NA	<i>ns</i>	<i>ns</i>	<i>ns</i>	<i>ns</i>
CYP71B4	up	<i>ns</i>	<i>ns</i>	up	<i>ns</i>	NA	<i>ns</i>	<i>ns</i>	<i>ns</i>	<i>ns</i>
AT1G12790	<i>ns</i>	<i>ns</i>	up	<i>ns</i>	<i>ns</i>	NA	<i>ns</i>	<i>ns</i>	<i>ns</i>	<i>ns</i>
AT4G25580	<i>ns</i>	up	up	<i>ns</i>	<i>ns</i>	NA	down	<i>ns</i>	down	<i>ns</i>
MPK5	<i>ns</i>	<i>ns</i>	<i>ns</i>	<i>ns</i>	<i>ns</i>	NA	<i>ns</i>	<i>ns</i>	<i>ns</i>	<i>ns</i>
DSP4	<i>ns</i>	<i>ns</i>	<i>ns</i>	<i>ns</i>	up	NA	<i>ns</i>	<i>ns</i>	<i>ns</i>	<i>ns</i>
AtHXK2	<i>ns</i>	<i>ns</i>	<i>ns</i>	<i>ns</i>	<i>ns</i>	NA	<i>ns</i>	<i>ns</i>	<i>ns</i>	<i>ns</i>
ATPME17	<i>ns</i>	<i>ns</i>	up	<i>ns</i>	<i>ns</i>	NA	<i>ns</i>	<i>ns</i>	<i>ns</i>	<i>ns</i>
GBF2	<i>ns</i>	<i>ns</i>	<i>ns</i>	<i>ns</i>	<i>ns</i>	NA	<i>ns</i>	<i>ns</i>	<i>ns</i>	<i>ns</i>
UMAMIT33	<i>ns</i>	<i>ns</i>	<i>ns</i>	<i>ns</i>	<i>ns</i>	NA	<i>ns</i>	<i>ns</i>	<i>ns</i>	<i>ns</i>
AT5G57655	<i>ns</i>	<i>ns</i>	<i>ns</i>	<i>ns</i>	NA	NA	<i>ns</i>	<i>ns</i>	<i>ns</i>	<i>ns</i>
TPPE	<i>ns</i>	<i>ns</i>	<i>ns</i>	<i>ns</i>	NA	NA	<i>ns</i>	<i>ns</i>	<i>ns</i>	<i>ns</i>
TIP2	<i>ns</i>	<i>ns</i>	<i>ns</i>	<i>ns</i>	<i>ns</i>	NA	<i>ns</i>	<i>ns</i>	<i>ns</i>	<i>ns</i>
PLP2	<i>ns</i>	up	up	up	<i>ns</i>	NA	<i>ns</i>	<i>ns</i>	<i>ns</i>	<i>ns</i>
ATRRP4	<i>ns</i>	<i>ns</i>	<i>ns</i>	up	<i>ns</i>	NA	<i>ns</i>	<i>ns</i>	<i>ns</i>	<i>ns</i>
DIN6	NA	NA	NA	NA	<i>ns</i>	NA	<i>ns</i>	<i>ns</i>	<i>ns</i>	<i>ns</i>
SEN5	NA	NA	NA	NA	<i>ns</i>	NA	<i>ns</i>	<i>ns</i>	<i>ns</i>	<i>ns</i>
AXP	NA	NA	NA	NA	<i>ns</i>	NA	<i>ns</i>	<i>ns</i>	<i>ns</i>	<i>ns</i>
RAB18	NA	NA	NA	NA	<i>ns</i>	NA	<i>ns</i>	<i>ns</i>	<i>ns</i>	<i>ns</i>
RD	NA	NA	NA	NA	<i>ns</i>	NA	<i>ns</i>	<i>ns</i>	<i>ns</i>	<i>ns</i>
EIF	NA	NA	NA	NA	<i>ns</i>	NA	<i>ns</i>	<i>ns</i>	<i>ns</i>	<i>ns</i>

Table 3.5. Overview of all of qRT-PCR control experiments. NA = not applicable, ns = not significant. Green cell colour indicates significant down-regulation compared to Col-0 and red cell colour indicates up-regulation compared to Col-0 in the control samples

	Drought experiment (controls)				Continuous darkness experiment (controls)		Short-term Darkness/Glucose supplement experiment		
	<i>dufko3</i> / Col-0	<i>Kin10-2</i> / Col-0	<i>duf_kin10-2</i> / Col-0	<i>DUFQE3</i> / Col-0	<i>dufko3</i> / Col-0	<i>duf_kin10</i> / Col-0	<i>dufko3</i> / Col-0	<i>DUFQE3</i> / Col-0	<i>duf_kin10-2</i> / Col-0
DUF2358	down	ns	down	up	down	NA	down	up	NA
KIN10	up	down	down	up	up	NA	ns	ns	NA
<i>ABF2</i>	ns	ns	ns	ns	down	NA	ns	ns	NA
<i>ABF3</i>	ns	ns	up	ns	ns	NA	ns	ns	NA
<i>ABI5</i>	ns	ns	ns	ns	down	NA	ns	ns	NA
<i>ACR5</i>	ns	ns	ns	ns	down	NA	ns	ns	NA
<i>ACR9</i>	ns	ns	ns	ns	ns	NA	ns	ns	NA
<i>ATPS5</i>	up	ns	ns	ns	ns	NA	ns	ns	NA
<i>AT2G36220</i>	ns	ns	ns	ns	down	NA	ns	ns	NA
<i>CYP71B4</i>	ns	ns	ns	up	NA	NA	ns	ns	NA
<i>AT1G12790</i>	ns	ns	up	up	down	NA	ns	ns	NA
<i>AT4G25580</i>	up	ns	up	ns	ns	NA	ns	ns	NA
<i>MPK5</i>	ns	ns	ns	ns	down	NA	ns	ns	NA
<i>DSP4</i>	ns	ns	down	ns	down	NA	ns	ns	NA
<i>AtHXK2</i>	ns	ns	ns	ns	ns	NA	ns	ns	NA
<i>ATPME17</i>	ns	ns	ns	up	down	NA	ns	ns	NA
<i>GBF2</i>	ns	ns	ns	ns	NA	NA	ns	ns	NA
<i>UMAMIT33</i>	ns	ns	ns	ns	down	NA	ns	ns	NA
<i>AT5G57655</i>	ns	ns	ns	ns	NA	NA	ns	ns	NA
<i>TPPE</i>	ns	ns	ns	ns	ns	NA	ns	ns	NA
<i>TIP2</i>	ns	ns	ns	ns	ns	NA	ns	ns	NA
<i>PLP2</i>	ns	ns	up	ns	ns	NA	ns	ns	NA
<i>ATRRP4</i>	ns	ns	ns	ns	ns	NA	ns	ns	NA
<i>DIN6</i>	NA	NA	NA	NA	ns	NA	ns	ns	NA
<i>SIN5</i>	NA	NA	NA	NA	ns	NA	ns	ns	NA

<i>AXP</i>	NA	NA	NA	NA	ns	NA	ns	up	NA
<i>RAB18</i>	NA	NA	NA	NA	ns	NA	ns	ns	NA

Under control conditions, most ABA and sugar-related genes did not show any differences in the *dufko3* and *kin10-2* mutants, while they showed significant changes in the double mutants (Table 3.5). Among the dark-induced senesce genes, *ABI5* was downregulated in *dufko3* under control conditions. While under darkness in *dufko3* all the dark-induced senesce, genes were slightly higher compared to Col-0, but no significant increase was recorded. From a general view, removing DUF2358 affects the ability of plants to recognise altered sugar levels, which could suggest DUF2358 linking to a sugar-signalling pathway.

Chapter 4

The effect of altered DUF2358 expression on Metabolite components using Metabolomics technology

4.1 Introduction

Plants produce many different metabolites, which can be classified into two main groups, namely primary metabolites and secondary metabolites. Primary metabolites have conserved structures and play key roles in plant growth and development (Zaynab *et al.*, 2019), whereas secondary metabolites are important for responding to environmental stress which enables plants to survive under difficult conditions (Shulaev *et al.*, 2008). However, secondary metabolite structures differ among plant species (Scossa *et al.*, 2016).

Many metabolites play a fundamental role in plant response to stress (Shulaev *et al.*, 2008; Gauthier *et al.*, 2015; Pott *et al.*, 2019). For example, sugars such as sucrose, trehalose, and fructose, and amino acids, such as proline, are involved in the abiotic stress responses acting as osmolytes and osmoprotectants (Shulaev *et al.*, 2008). Measuring changes in metabolites is, therefore, an important tool to understand how different metabolic and catabolic pathways respond to environmental changes (Gauthier *et al.*, 2015; Nakabayashi and Saito., 2015) because metabolic adaptation is an important feature in abiotic stress response (Hildebrandt, 2018).

Under dark treatment, leaves show a "metabolically suppressed state" aiming to maintain the capacity of photosynthesis, which demonstrates the need to have alternative sources for energy production (Law *et al.*, 2018). The lysis of proteins has been reported to be increased as a source of amino acids to produce ATP. Also to prepare reduced nitrogen and sulphur under stress conditions. That leads to sugar starvation such as darkness (Araújo *et al.*, 2011; Hildebrandt, 2018). While the synthesis of some amino acids such as proline and glutamine are continued during external stress, these amino acids play an important role in survival under osmotic

stress or as storage of organic nitrogen (Hildebrandt, 2018). An important adjustment of metabolic processes accrues during the long period of darkness, which causes sugar starvation in which ATP can be produced from amino acids and, potentially, monosaccharides. At the same time, accumulated amino acids with a high level of nitrogen and carbon provide a mechanism to store the cytotoxic ammonium safely, which can be used in recovery and normal growth after returning to normal light conditions (Law *et al.*, 2018).

In Chapter 3, it has been shown that *dufko3* mutant plants were unable to maintain maximum efficiency of photosystem II (Fv/Fm) in response to darkness and showed a greater decline compared to Col-0 after the fourth day of darkness (Figure 3.25), which is likely to affect primary metabolites. In addition, we observed differences in glucose levels in *dufko3* mutants during drought stress (Figure 3.23), and the initial gene regulatory network suggests involvement in sugar signalling (Figure 3.1).

This chapter will produce a metabolite profile of the *dufko3* mutants subjected to long-term darkness compared to Col-0 in order to discern whether *DUF2358* may affect primary metabolites under starvation conditions.

4.2. Results

4.2.1. The maximum efficiency of photosystem II measurement

We repeated the long-term dark treatment as described in Chapter 3, and verified that the *dufko3* failed to cope with the darkness as Fv/Fm values were reduced compared to Col-0 and pNAT:DUF. The samples were harvested for metabolite profiling on the fourth day of darkness at a time point just before significant differences between Col-

0 and *dufko3* were observed. This time point was chosen based on the result presented in Chapter3 (Figure. 4.1 and Figure. 3.25 A).

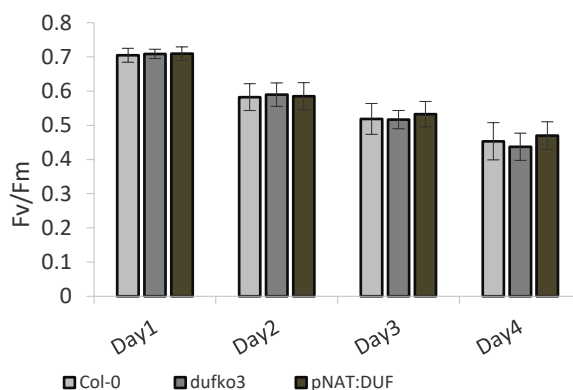


Figure 4.1. Bars compare Fv/Fm averages between the three genotypes for four days. Error bars signify SEM (standard error of the mean). Time point just before the differences became significant was chosen n=6.

After metabolites were measured in total, 274 peaks out of more than 12,000 peaks were selected from the individual chromatograms; and, from those, 137 features with obvious differences between experimental conditions were selected using the Agilent mass hunter quantitative data analysis software. The 137 features were subjected to downstream analysis to normalise samples and identify abundant differential metabolites between treatments and genotypes.

4.2.2. Data filtering

The peak intensities of the 137 features were initially filtered to identify and remove variables that are unlikely to be of use when modelling the data, for example, if the datasets contain much noise. In addition, missing values will cause difficulties in the downstream analysis. Missing values were, therefore, removed or replaced by values estimation using the K means Nearest Neighbour (KNN) methodology. Further feature filtering based on the interquartile range was carried out, and 10 variables in total were

removed at a threshold of more than 50% missing values, recovering 127 features after data processing (Appendix H; Table 4.1).

Table 4.1. Summary of the initial data processing results

	Features (positive)	Missing/Zero	Features (processed)
Col-0L2	131	6	135
Col-0L4	127	10	135
Col-0L5	128	9	135
Col-0L6	128	9	135
dufKO3L2	129	8	135
dufKO3L3	127	10	135
dufKO3L4	131	6	135
dufKO3L5	127	10	135
pNATDUFL2	130	7	135
pNATDUFL3	128	9	135
pNATDUFL5	130	7	135
pNATDUFL6	129	8	135
Col-0D1	129	8	135
Col-0D3	128	9	135
Col-0D4	131	6	135
Col-0D6	129	8	135
dufKO3D1	134	3	135
dufKO3D2	131	6	135
dufKO3D3	130	7	135
dufKO3D6	132	5	135
pNATDUFD2	129	8	135
pNATDUFD4	132	5	135
pNATDUFD5	135	2	135
pNATDUFD6	135	2	135

4.2.3. Data normalisation

Peak intensities were adjusted for weight and subsequently normalised using the internal standard Adonitol which was added to each sample prior to extraction. In addition, the data were log-transformed and autoscaled (mean-centred and divided by the standard deviation of each variable) to make features more comparable (Figure 4.2).

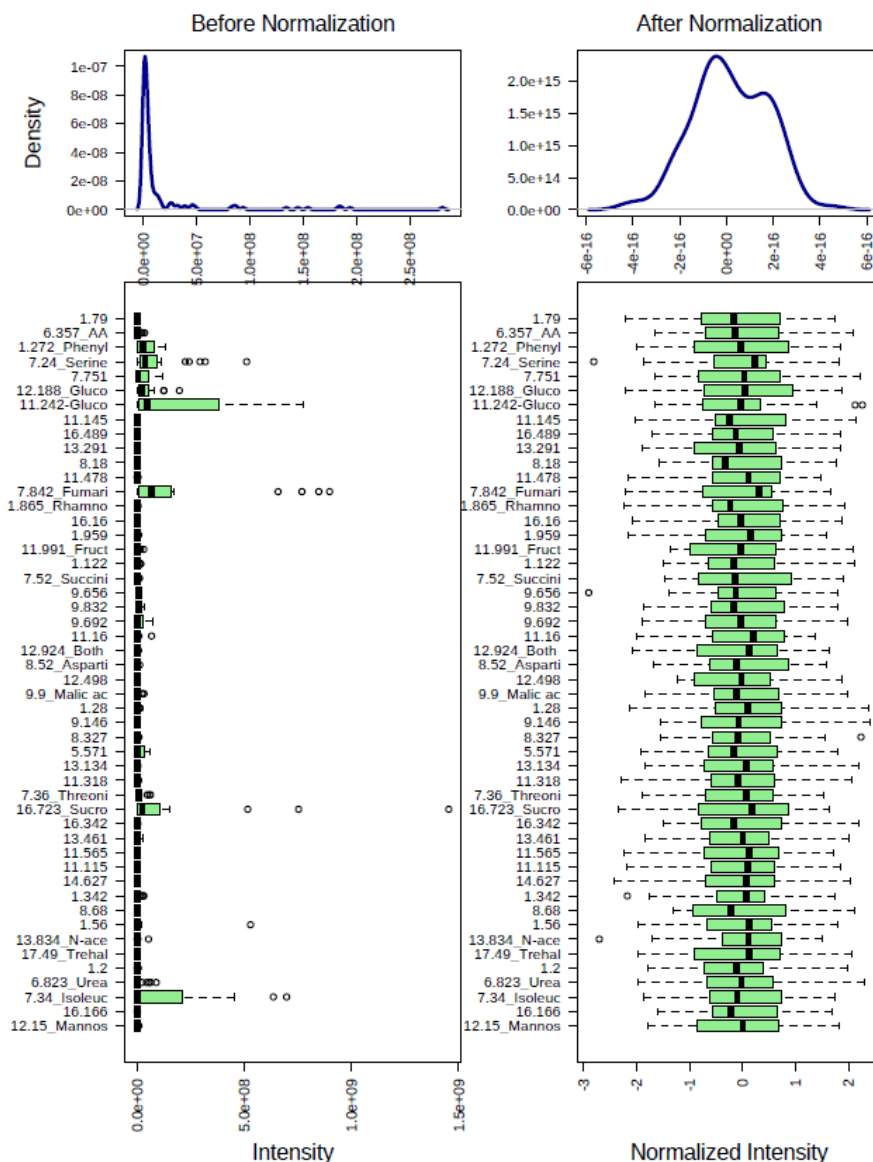


Figure 4.2. Box plot and kernel density plots of the top 50 features before and after normalisation.

4.2.4. Exploratory data analysis

4.2.4.1. Statistical analysis

50 significant features below a p-value threshold of 0.01, and 80 at a threshold of $p < 0.025$ were identified. The full statistical output is presented in Appendix H and I) (Figure 4.3).

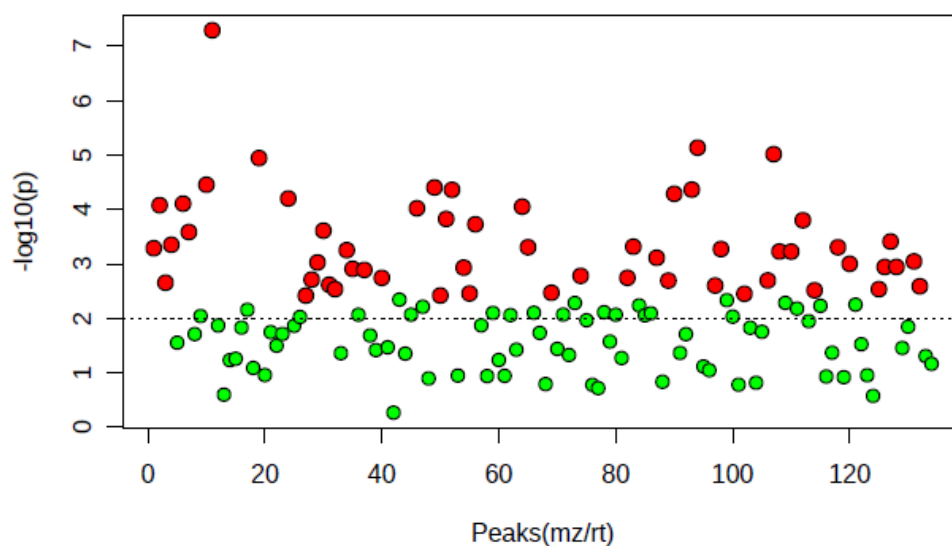


Figure 4.3. Significant features (red circles) across the 3 genotypes and 2 treatments above a threshold of $p < 0.01$ ($n=4$).

4.2.4.2. Principal component analysis (PCA)

We performed multivariate principal component analysis (PCA) on the 127 metabolite features to reduce the number of variables and to detect structure in the relationship between metabolites. PCA reduced the trait space to five statistically significant trait principal components (PCs), with the first two PCs explaining 56.7% of the overall variation (Figure 4.4).

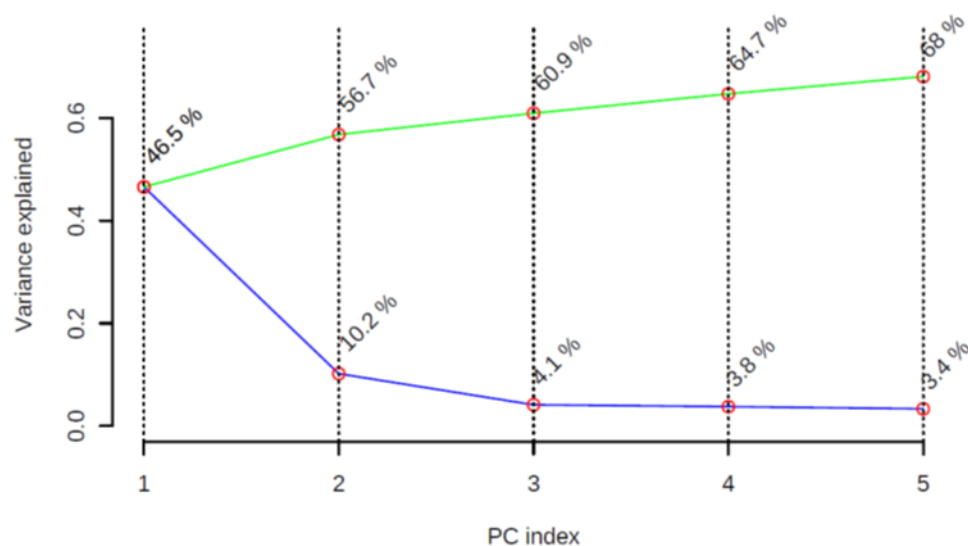


Figure 4.4. Scree plot showing the 5 significant principal components with total accumulative variance (green line) and individual variance (blue line) explained.

The first principal component (PC1), accounting for 46.5% of the total variance, resolved the samples according to genotypes. The second principal component (PC2), accounting for 10.2% of the total variance, resolved the genotypes into distinct treatment groups (light vs. continuous darkness) (Figure. 4.5). This difference is shown in the loadings of all metabolites onto PC2, which demonstrated a trade-off between amino acids (serine, valine, isoleucine) and compounds involved in primary metabolic pathways and sugars (Appendix J).

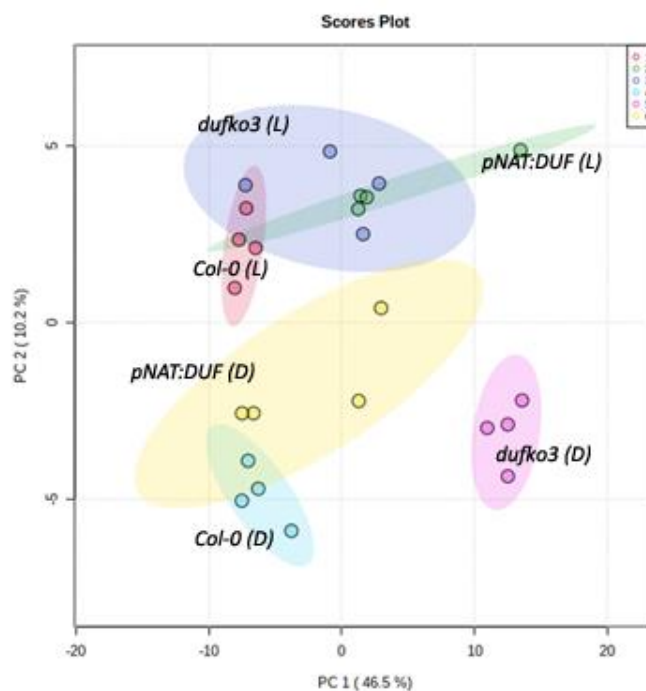


Figure 4.5. PCA plot of significant metabolites in Col-0 *dufko3* and pNAT:DUF under light and dark conditions. Variances are shown in brackets. 1- Col-0 light, 2- *dufko3* light, 3- pNAT:DUF light, 4- Col-0 dark, 5- *dufko3* dark, and 6- pNAT:DUF dark.

In the light, there was little distinction between genotypes (groups 1-3), especially between *dufko3* and the pNAT:DUF complemented plants, suggesting that metabolically the complementation was not successful.

4.2.4.3. Clustering

Hierarchical clustering (hclust) was used to visualise overall patterns in response to dark treatment within and between genotypes. The majority of significant differences is observed in the continuous dark treatment, where *dufko3* samples show predominantly increased metabolite levels compared to Col-0 across a range of

primary metabolites (Figure 4.6). This pattern is also observed in dark/light-grown plants, although to a much lesser extent.

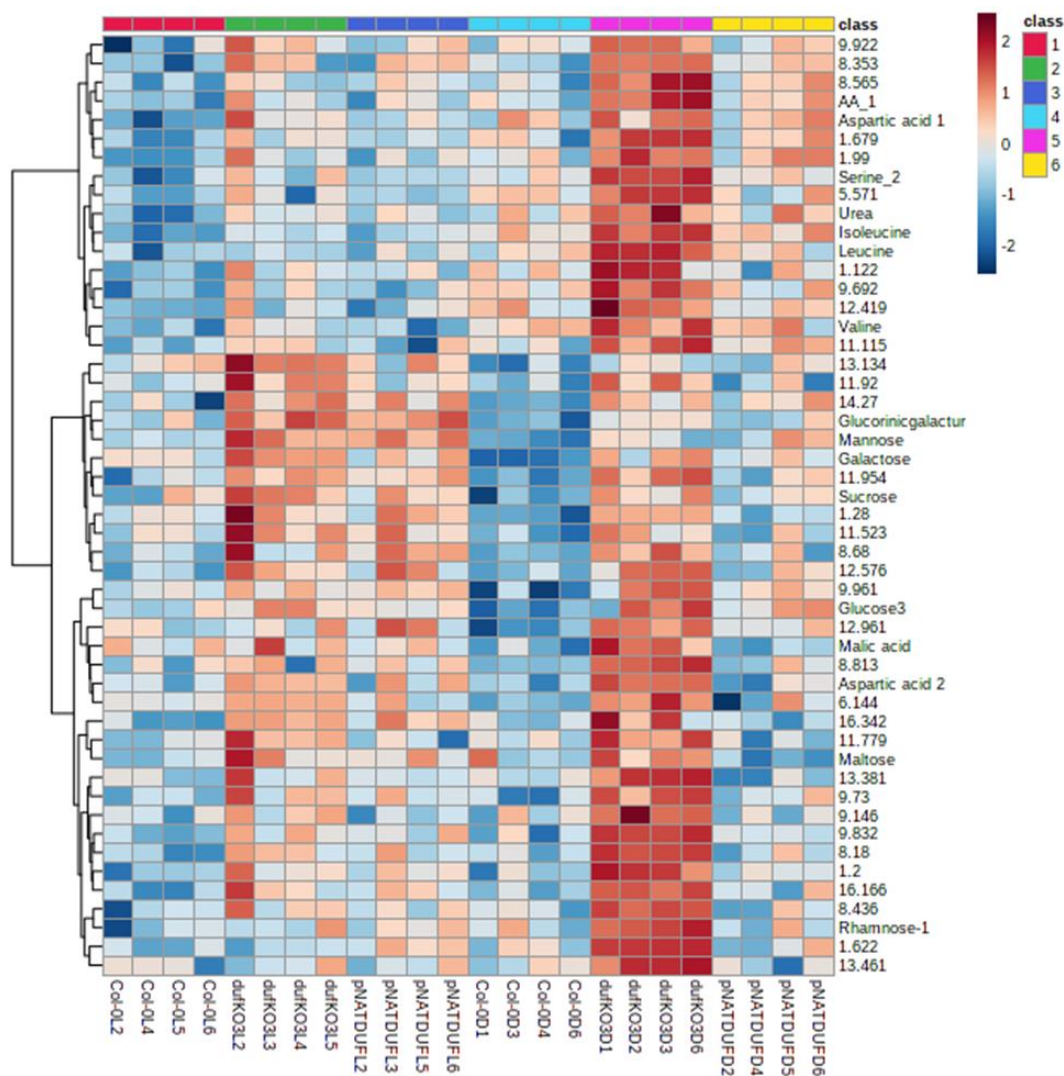
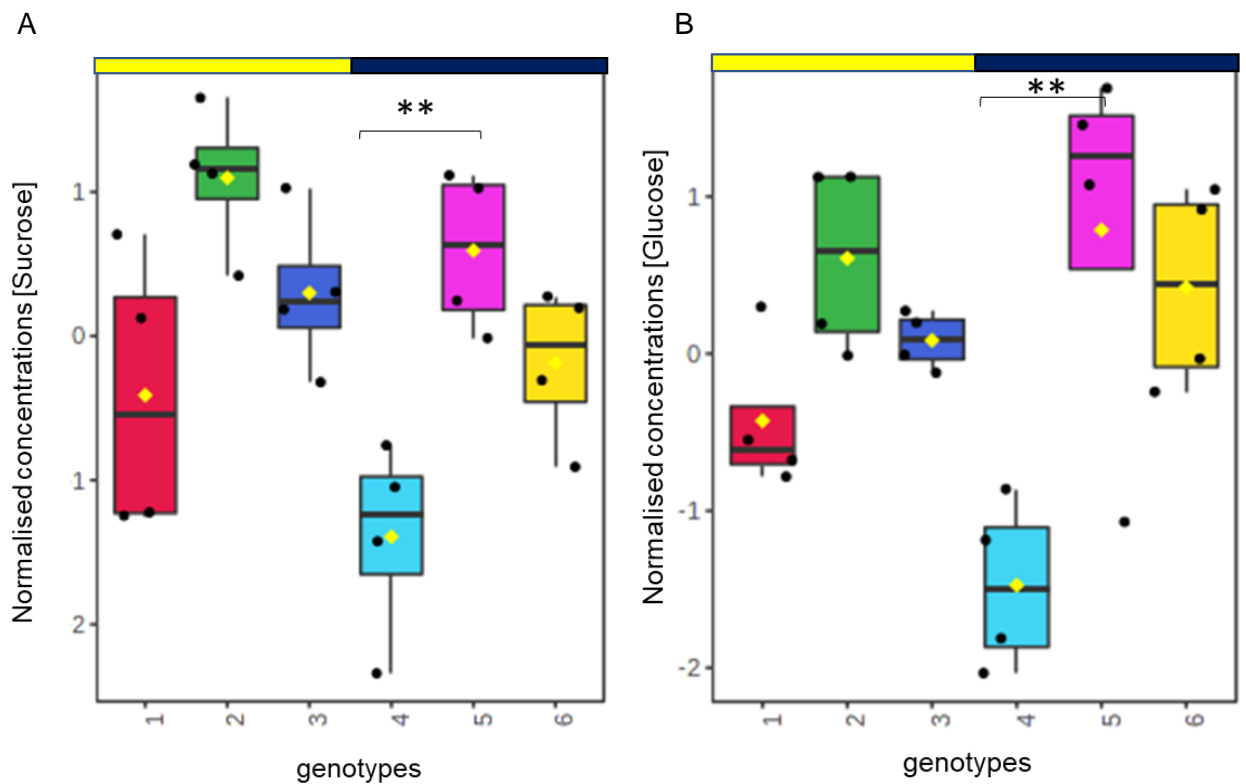


Figure 4.6. Heatmap generated hierarchical clustering using Euclidean distance measure and the Ward clustering algorithm. Each sample initial considered as a separate cluster and the algorithm proceeds to combine the samples until all samples belong to one cluster. This heatmap was generated using MetaboAnalyst 4.0 online tool. 1- Col-0 light (L, red), 2- *dufko3* light (L, green), 3- pNAT:DUF light (L, dark blue), 4- Col-0 dark (D, light blue), 5- *dufko3* dark (D, pink) and 6- pNAT:DUF dark (D, orange). Each row represents a significant feature with colour indicating normalised peak intensities.

Importantly, sucrose and glucose levels are significantly elevated after 4d of dark treatment in the *dufko3* plants compared to Col-0 (Figure 4.7. A, B). Sugar levels showed an expected decline under darkness in Col-0, which was mostly not observed in the *dufko3* mutant. The complemented *dufko3* often exhibited an intermediate phenotype, not completely following the pattern observed for Col-0 (Figure 4.7).



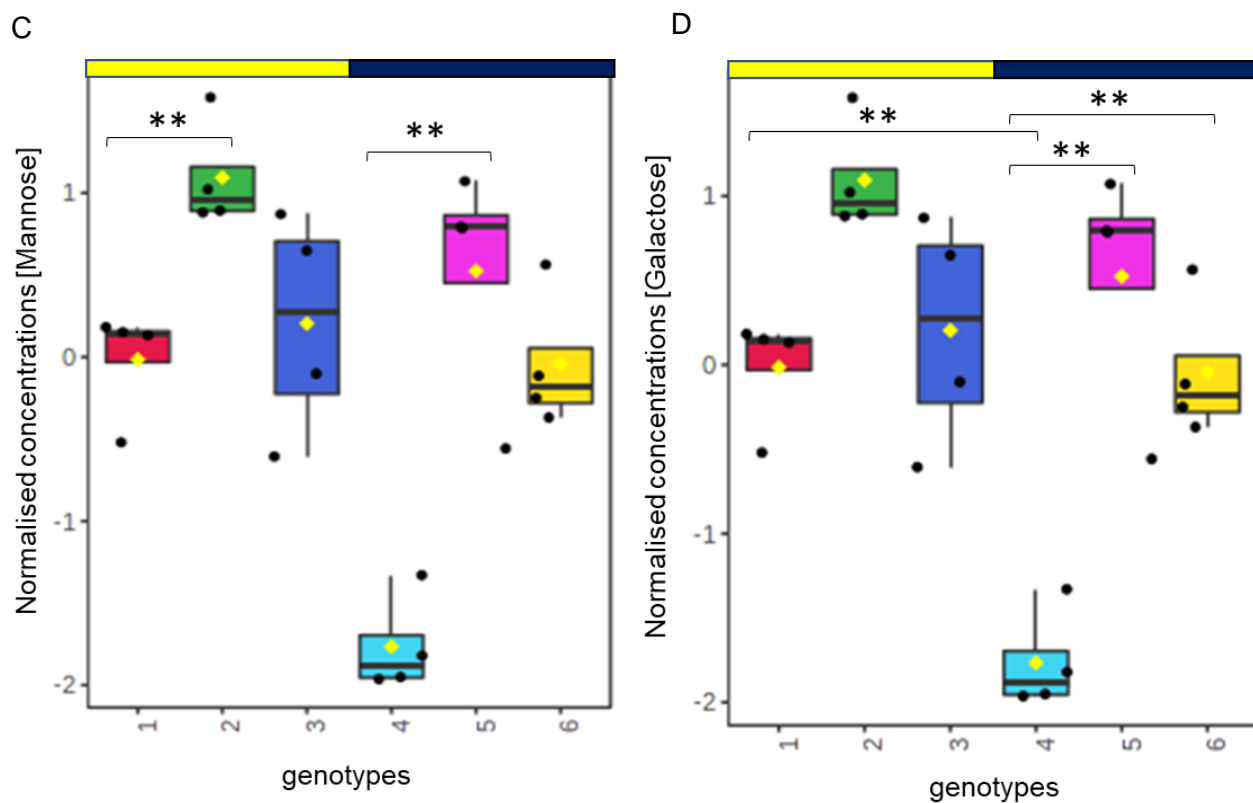


Figure 4.7. Box plots summarising the normalised sugar concentrations of (A) sucrose, (B) glucose, (C) mannose, and (D) galactose. 1- Col-0 light, 2- *dufko3* light, 3- pNAT:DUF light, 4- Col-0 dark, 5- *dufko3* dark and 6-pNAT:DUF dark. The yellow bar: light/dark-grown plants, black bar: continuous dark-grown plants. The yellow diamond represents the 95% confidence interval around the median of the group (black line). The black dots represent the concentration for the metabolite in individual samples. ** indicates significant difference at $p < 0.01$, * $p < 0.025$ ($n=4$).

Amino acid levels also showed significant increases in the *dufko3* mutant under darkness compared to Col-0. Importantly, the complemented pNAT:DUF genotype follows the pattern of Col-0 (Figure 4.8).

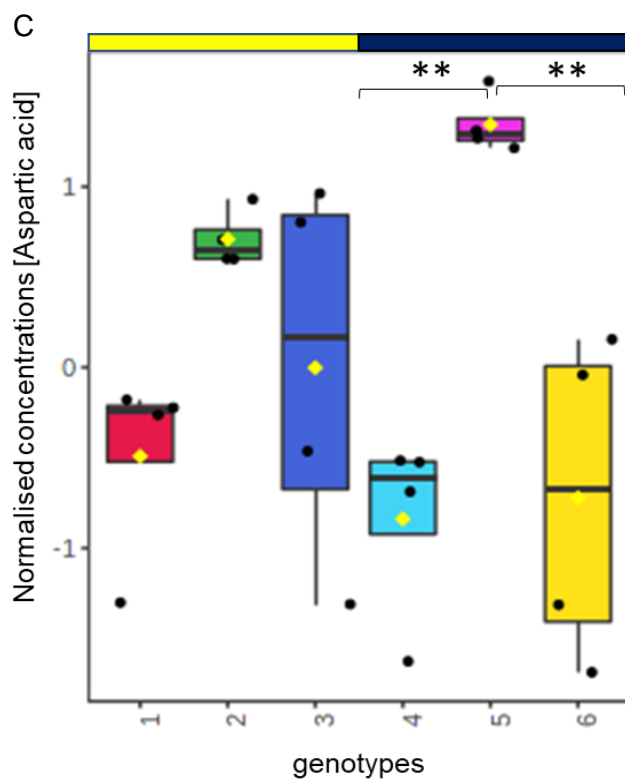
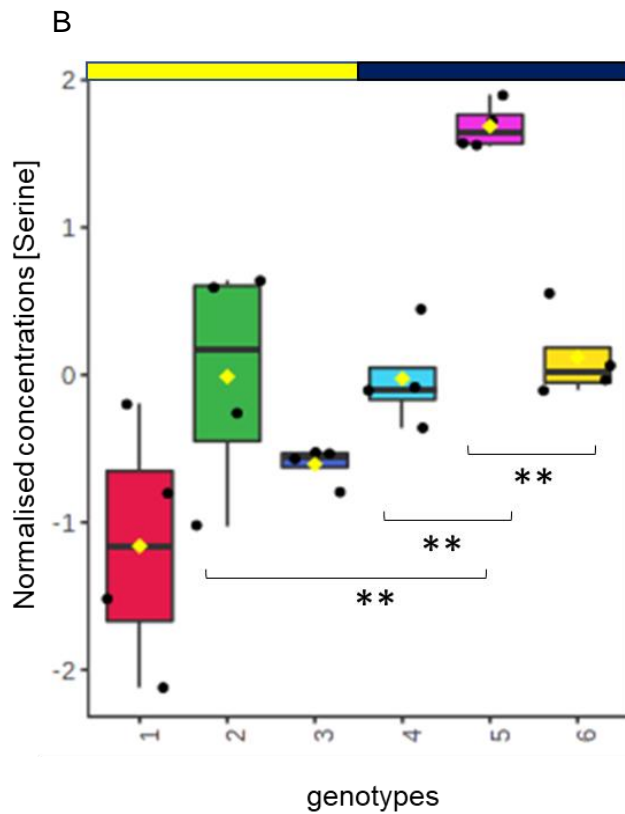
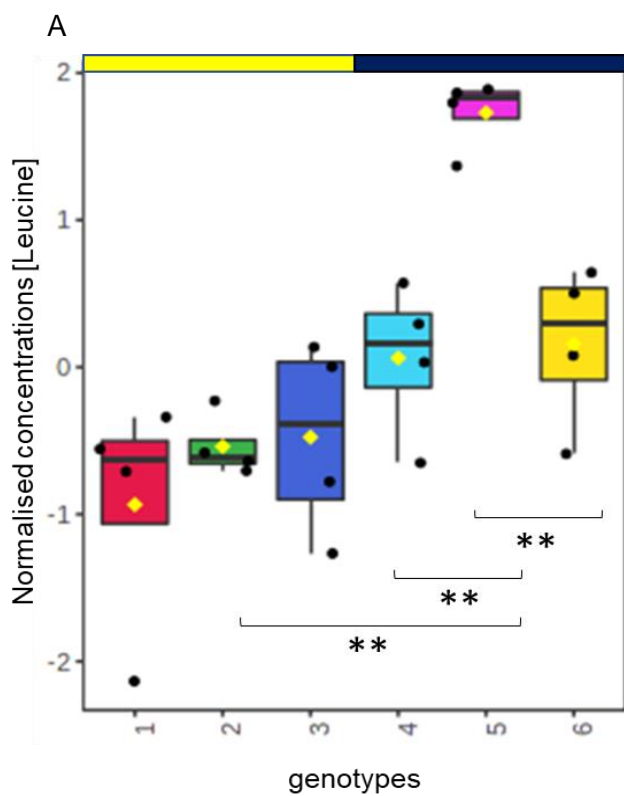


Figure 4.8. Box plots summarising the normalised amino acid concentrations of **(A)** leucine, **(B)** serine, and **(C)** aspartic acid. 1- Col-0 light, 2- *dufko3* light, 3- pNAT:DUF light, 4- Col-0 dark, 5- *dufko3* dark and 6- pNAT:DUF dark. The orange bar: light/dark-grown plants, black bar: continuous dark-grown plants. The yellow diamond represents the 95% confidence interval around the median of the group (black line). The black dots represent the concentration for the metabolite in individual samples. ** indicates significant difference at $p < 0.01$, * $p < 0.025$ (n=4).

4.2.4.4. Correlation analysis

To evaluate any relationships between significant metabolites, a correlation analysis was conducted under both dark/light and continuous dark conditions (Figure 4.9). There was a moderate and strong positive correlation >0.6 (Pearson correlation) between sugars (myo-inositols, galactose, fmannose, trehalose, and sucrose). Similarly, amino acids also showed a significant degree of correlation.

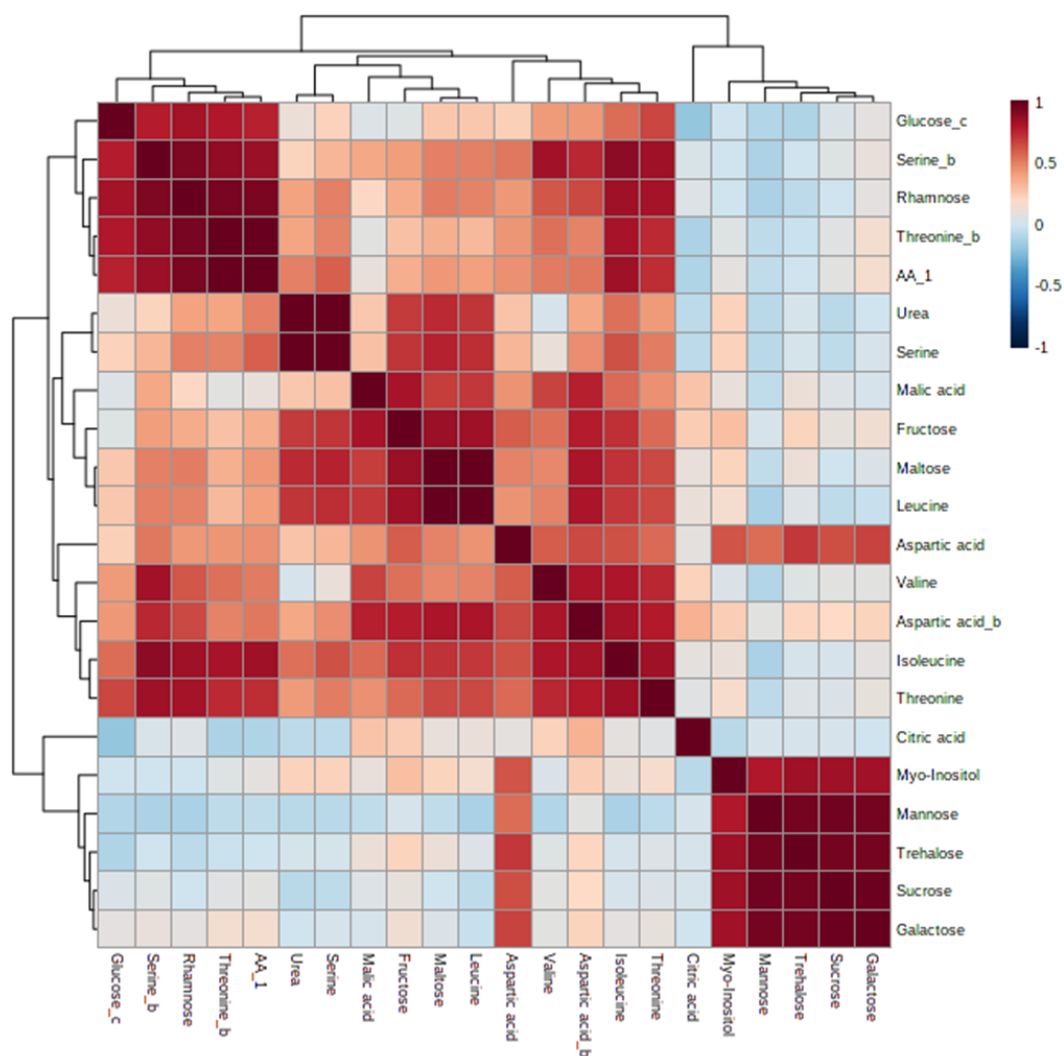


Figure 4.9. Heat map generated using the Pearson correlation matrix of significant metabolites under both light and continuous dark treatments in Col-0 *dufko3* and pNAT:DUF. Each metabolite component is represented on a column and a row. The colour scale is set for correlation values between -1 (dark blue) and 1 (dark red). -1 indicates the negative correlation, while +1 indicates the complete positive correlation. Hierarchical clustering is also represented in both dimensions (n =4 per genotype and treatment). $p \leq 0.05$ for each comparison.

4.3. Conclusion

This chapter aimed to identify the most relevant differences of metabolic reaction for both *dufko3* and Col-0 under dark conditions.

dufko3 shows different levels of response to darkness compared with Col-0. Firstly, increasing the metabolite levels under prolonged darkness in *dufko3* plant compared with Col-0 may indicate *dufko3* could fail to percept and respond to darkness. Sugar levels have been reported to be decreased under extended darkness, which causes sugar starvation by abstracting photosynthesis in WT plants (Law et al., 2018; Hildebrandt, 2018). In contrast, in this study, the *dufko3* mutant shows a high level of sugars compared to Col-0, which perhaps indicates that sugar signalling affected by the absence of DUF2358 and plant failed to see the darkness, which causes sugar accumulation as a result of falling in breakdown the sugar to provide an additional source of ATP production.

Amino acids also showed an increase in their level in both *dufko3* and Col-0. The increase in the amino acids has been reported by Hildebrandt et al. (2018). Also, Law et al. (2018) demonstrate the increase of amino acid biosynthesis in WT plants under dark conditions. In this study, *dufko3* showed more high levels of amino acids compared with Col-0, which seems to be an increase in protein degradation caused by darkness. Also, Izumi and Ishida. (2019) demonstrate an increase in amino acids under dark-induced sugar starvation originating from chloroplast degradation, produces free amino acids and which can be used as an energy source. In the RNA-seq chapter, we found an increase in genes associated with dark-induced senescence in *dufko3* compared with Col-0. Also, photosynthetic electron transport and light-harvesting were significantly down-regulated in *dufko3* compared to Col-0, which compared with Col-0. All these differences between *dufko3* and Col-0 indicate *dufko3* was more affected by darkness and failed to respond to darkness compared to Col-0.

Chapter 5

**The effect of prolonged dark treatment on the
global gene expression in Col-0 and *dufko3***

5.1. Introduction

Gene expression quantification is crucial to connect genome sequences with phenotypic and physiological data. Here, we use RNA sequencing (RNA-Seq) to analyse the changes in the cellular transcriptome in response to continuous dark treatment. *dufko3* mutant during prolonged darkness (Figure 3.25) showed a more rapid decline of Chlorophyll fluorescence parameter Fv/Fm compared to Col-0, accompanied by changes in the metabolite profile (Chapter 4). Gene expression analysis using qPCR of the network-related and some dark inducible genes were inconclusive (Chapter 3), and we therefore opted for global gene expression analysis using RNASeq.

5.2. Results

A continuous dark experiment was carried out by Dr. Bechtold, as described in Chapters 2 and 4, and the raw sequencing data was provided by Dr. Bechtold. Data were analysed and grouped in order to understand the global changes between *dufko3* and Col-0 under normal dark/light conditions as well as extended darkness.

5.2.1. Data pre-processing

Quality control of the raw reads and adapter trimming was carried out as described previously (Wingett and Andrews., 2018). Read counts and transcript per million reads (TPMs) were generated using tximport R package version 1.10.0 and the length scaled TPM method (Soneson *et al.*, 2016), with transcript quantification files generated through Kallisto (Bray *et al.*, 2016). Low expressed transcripts and genes

were filtered based on analysing the data mean-variance trend. The expected decreasing trend between data mean and variance was observed when expressed transcripts were determined and which had ≥ 1 of the 12 samples with count per million reads (CPM) ≥ 1 , which provided an optimal filter of low expression (Figure 5.1). The TMM method was used to normalise the gene and transcript read counts to \log_2 -CPM (Bullard *et al.*, 2010).

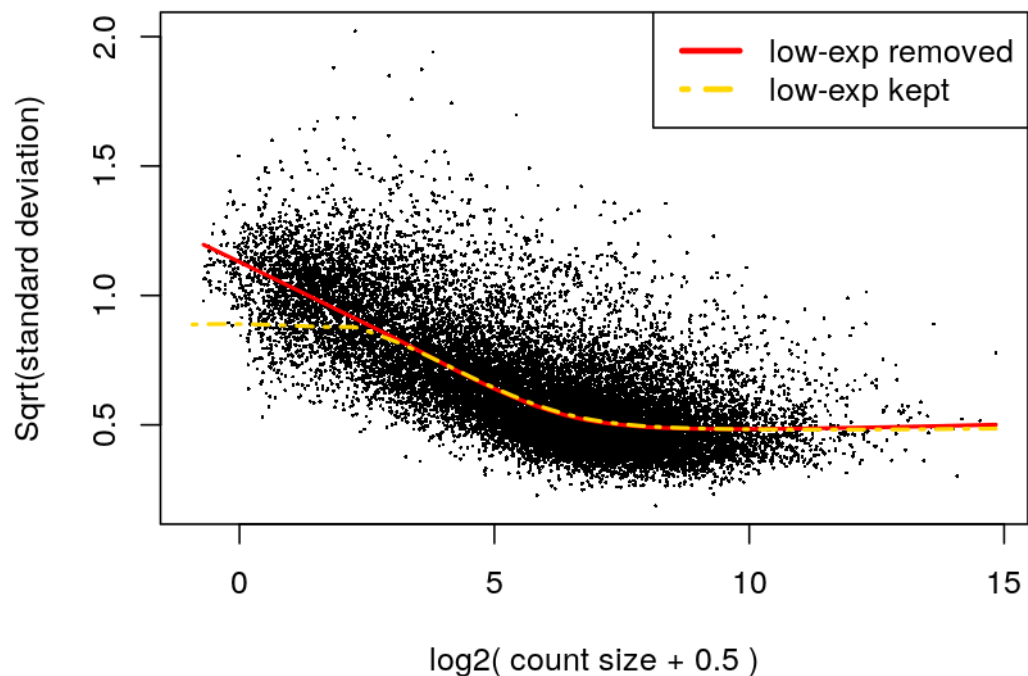


Figure 5.1. Mean-variance trend of filtered counts with a cutoff: cpm = 1 in at least 1 sample

The genome and annotation files of *Arabidopsis thaliana* Col-0 were downloaded from EnsemblPlants (<https://plants.ensembl.org/index>) (Howe *et al.*, 2020).

After pre-processing, the resulting dataset contained 24 samples with a sequencing data size ranging from about 21 to 33×10^6 reads (Table 5.1). Pre-processed raw data were filtered for a minimum read length of 51 base pairs and Illumina adapters were removed.

Table 5.1. summary of alignments for each sample in this chapter compared to *Arabidopsis thaliana* Col-0.

Sample ID Left reads	Number of Reads Raw Data	Number of Mapped Reads	Sample ID Right reads	Number of Reads Raw Data	Number of Mapped Reads
KO D2	16938693	683009	KO D2	16938693	16277864
KO3	16792299	16359898	KO3	16792299	16131883
KO4	20148045	672433	KO4	20148045	19220045
KOL2	14975407	14751452	KOL2	14975407	14553506
KOL3	18425858	17977093	KOL3	18425858	17773190
KOL4	16484802	779945	KOL4	16484802	16014306
WT D2	18498171	993507	WT D2	18498171	17859122
WT D3	16520691	16302646	WT D3	16520691	16117956
WT D4	15211561	14960779	WT D4	15211561	14766097
WT L3	19788566	933794	WT L3	19788566	19289697
WT L4	18876808	804737	WT L4	18876808	18316432
WT L5	9732163	9582374	WT L5	9732163	407257

5.2.2. Overview of the significantly expressed group of genes

Raw reads were aligned to the *Arabidopsis* genome and significantly differentially expressed genes (DEGs) ($P < 0.01$) underwears determined for light/dark and darkness

treatment. Table 5.2 summaries the differences in the number of DEGs under both conditions, including the overlapping between light and dark conditions.

Table 5.2. All significant genes which were expressed under non-stress and dark conditions. Significant calculated as $P < 0.01$. L indicates normal light/dark conditions while D indicates dark condition; the overlapping was determined using Venny V2.1.

	Total DEGs	Upregulated genes	Downregulated genes	Overlapping between L and D
<i>dufko3</i> vs Col-0 (L)	247	141	106	60
<i>dufko3</i> vs Col-0 (D)	344	120	224	

To determine the split between up- and downregulated genes under both conditions, a Venn diagram was generated. The diagram shows no large overlap was observed between upregulated genes under light/dark and dark conditions. Different potential overlapping in the diagram (Figure 5.2).

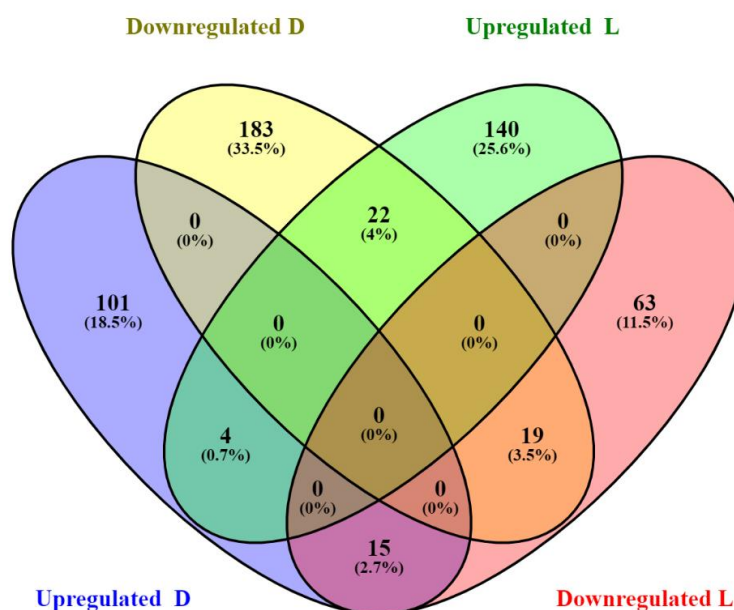


Figure 5.2. Venn diagram illustrates overlapping between upregulated and downregulated genes under dark and no stress conditions. Significant calculated as $P < 0.01$. Total numbers of upregulated, overlapping, and unique genes in each treatment with the percentage regarding the total number of gene lists. D – darkness, L- light/dark.

5.2.3. Gene Ontology (GO) analysis of all DEGs

GO analysis was carried out using AgriGo online databases (Du *et al.*, 2010) and DAVID bioinformatics online resources 6.8 (Huang *et al.*, 2009) to investigate the gene enrichment and functional annotation. Up- and downregulated genes were analysed.

5.2.3.1. Functional analysis of upregulated genes in *dufko3* under darkness

A Venn diagram was generated to identify unique upregulated genes under both conditions (Figure 5.3). Results indicate a little overlap between upregulated genes under prolonged dark and normal dark/light conditions. There were only five

upregulated genes in common between dark and light/dark conditions. The remaining 115 dark and 136 dark/light upregulated genes are unique (Figure 5.3). A full list of unique genes can be found in Appendix K.

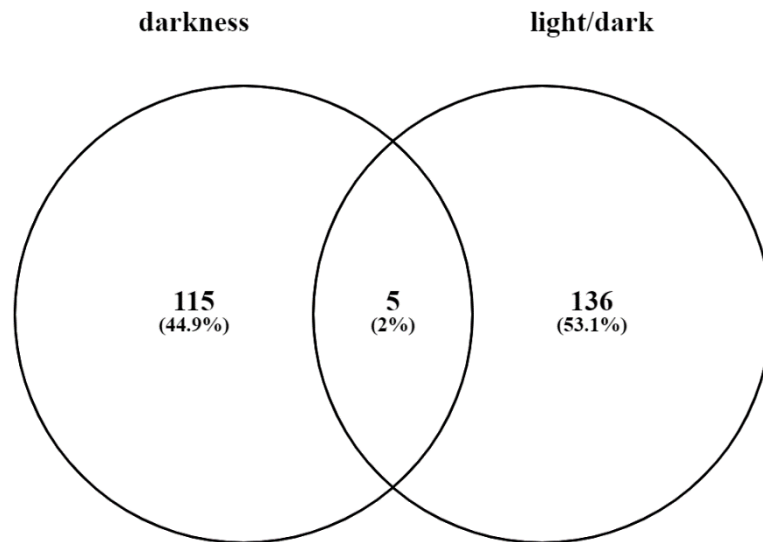


Figure 5.3. Venn diagram illustrates unique and common upregulated genes under dark and light/dark conditions. Total numbers of upregulated, overlapping, and unique genes in each treatment with the percentage regarding the total number of gene lists (adjusted $P < 0.01$).

Under dark conditions, genes upregulated in the *dufko3* compared to Col-0 were associated with responses to stress, stimulus, and senescence-related processes, such as response to the stimulus, chemical, stress, and abiotic stress. Also, aging, leaf senescence processes (Figure 5.4) and different gene expressions associated with stress were upregulated in *dufko3* under darkness (Figure 5.5), as well as senescence-associated genes (Figure 5.6).

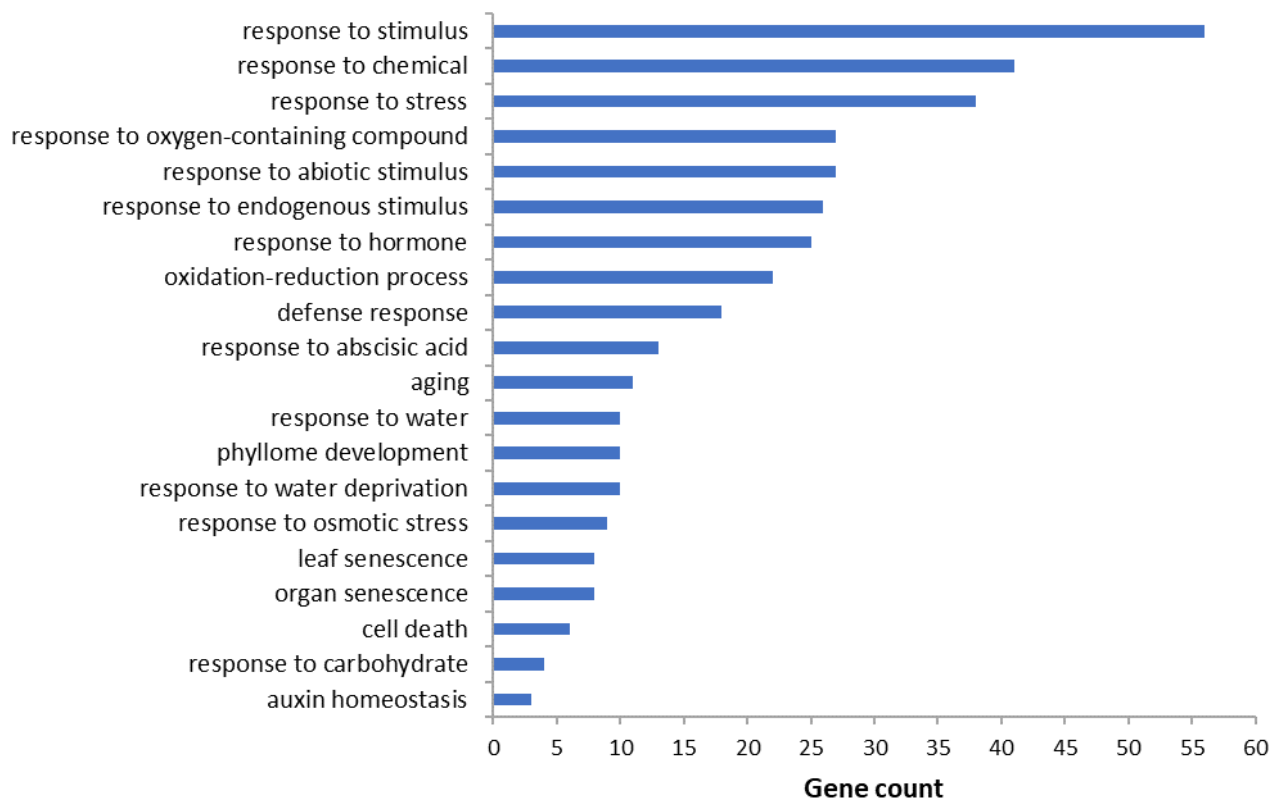


Figure 5.4. The most significant gene ontology enrichment of biological processes for upregulated genes in *dufko3* under dark conditions compared to Col-0. The significant term (adjusted $P < 0.01$).

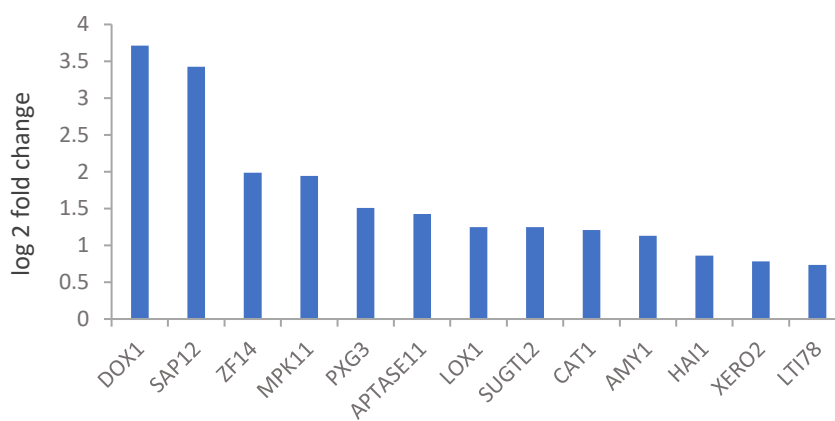


Figure 5.5. Log₂ fold change (*dufko3*/Col-0) unique genes under dark conditions, response to ABA-associated genes.

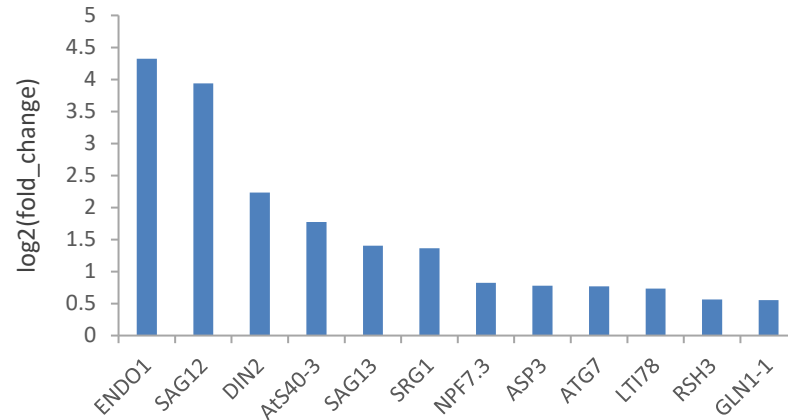


Figure 5.6. Log₂ fold change (*dufko3/Col-0*) genes under dark conditions, senescence-associated genes

Go terms in the molecular function category of *dufko3* upregulated group of genes under dark conditions highlight GO:0003824 catalytic activity as a significantly enriched term (Figure 5.7).

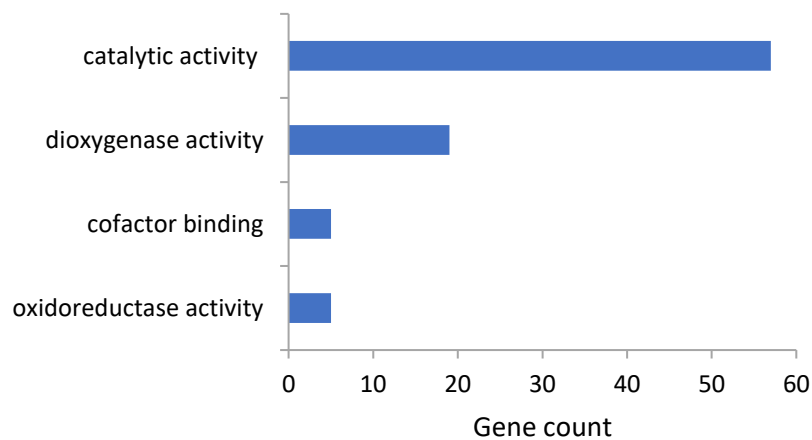


Figure 5.7. Gene ontology enrichment map of the molecular function of upregulated genes under dark conditions. The significant term (adjusted $P < 0.01$).

5.2.3.2. Functional analysis of genes downregulated in *dufko3* under continuous darkness

The number of downregulated genes in the *dufko3* mutant was increased 2.5 fold from 106 genes under dark/light cycle conditions to 224 genes under continuous dark conditions (Table 5.2, Appendix L).

Under prolonged dark treatment, chloroplast-associated genes are significantly enriched in the *dufko3* mutants, especially processes associated with light-harvesting and photosynthetic electron transport (Table 5.3). Genes located in the thylakoid membrane are also enriched in the downregulated group of genes, suggesting that, under prolonged darkness, thylakoid-associated processes are significantly more downregulated compared to Col-0. Importantly, this matches the predicted location for DUF2358 and suggests that DUF2358 may be essential for the adjustment of chloroplast processes under starvation conditions (Table 5.3, Figure 5.8).

Table 5.3. Summary of the cellular compartment significantly enriched in the downregulated group of genes in the *dufko3* under prolonged dark treatment.

GO term	Description	Gene count	Fold enrichment	adj p-value
GO:0030076	Light-harvesting complex	4	19.6	0.006721
GO:0009522	Photosystem I	6	16.7	0.000325
GO:0009521	Photosystem	8	10.1	0.000219
GO:0009523	Photosystem II	6	9.8	0.002757
GO:0010287	Plastoglobuli	6	9.8	0.002757
GO:0009505	Plant-type cell wall	18	6.2	2.55E-07

GO:0030312	External encapsulating structure	31	4.7	3.43E-10
GO:0005618	Cell wall	31	4.7	3.43E-10
GO:0048046	Apoplast	17	4.2	6.07E-05
GO:0009535	Chloroplast thylakoid membrane	13	3.9	0.001463

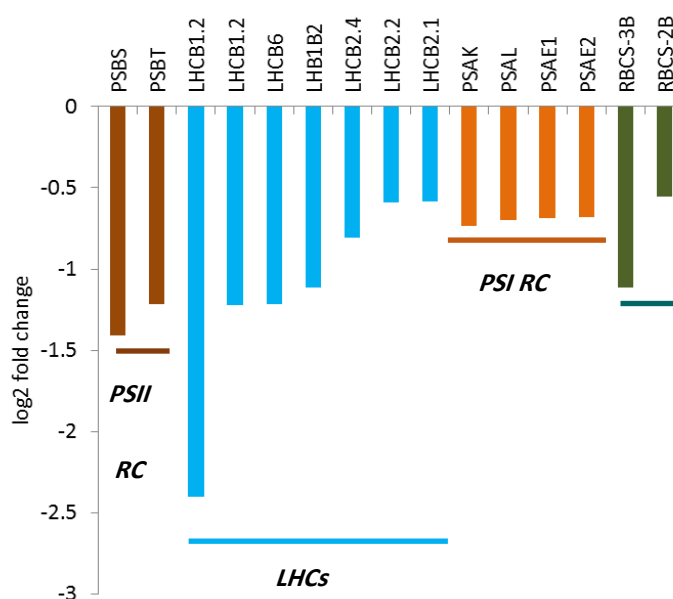


Figure 5.8. Log₂ fold change (*dufko3/Col-0*) of chloroplast and thylakoid membrane-associated genes. (PSII – photosystem II reaction centre, PSI-RC – photosystem I reaction centre, LHCs – light harvesting complex).

For biological processes, the most enriched terms included response to stress, response to chemical, and response to external stimulus, which was also enriched under dark conditions in *dufko3* compared to Col-0 (Figure 5.9).

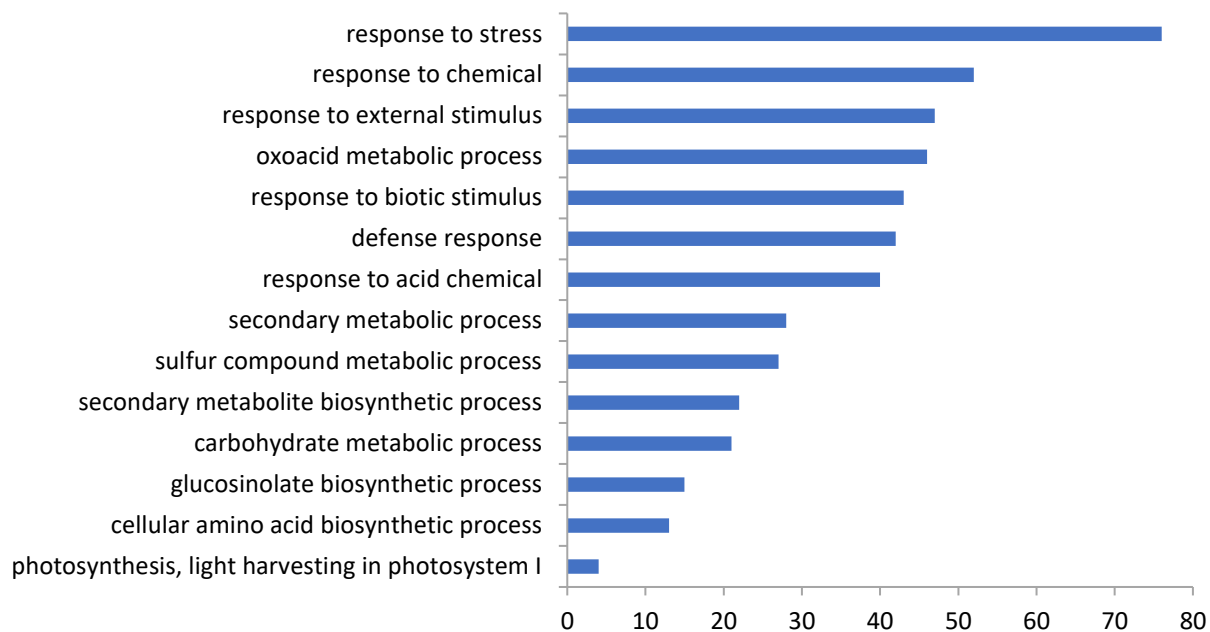


Figure 5.9. Summary of biological processes significantly enriched in the downregulated group of genes in the *dufko3* under prolonged dark treatment. The significant term (adjusted $P < 0.01$).

Gene ontology analysis of downregulated genes under darkness reveals the most significant GO terms group was GO:0016787 hydrolase activity and GO:0016491 oxidoreductase activity (Figure 5.10).

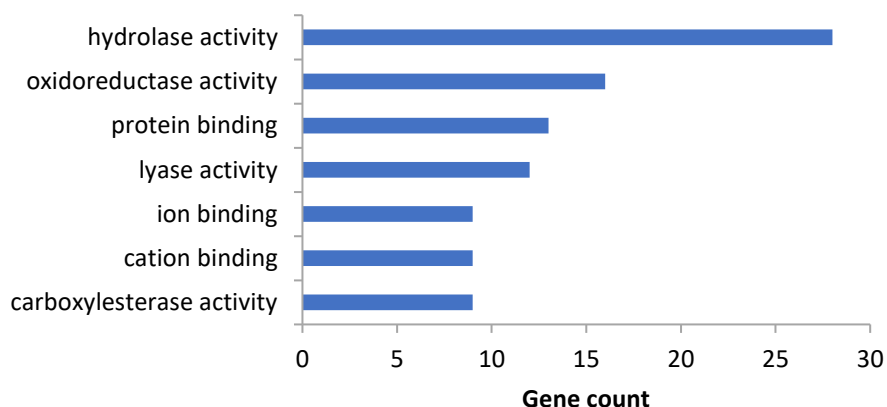


Figure 5.10. Summary of molecular function significantly enriched in the downregulated group of genes in the *dufko3* under dark conditions. The significant term adjusted $P < 0.01$.

5.2.3.3. Functional analysis of genes downregulated in *dufko3* under light/dark conditions

The 106 downregulated genes in the *dufko3* under light/dark conditions did not substantially overlap with the downregulated groups of genes under darkness. There were little enrichments in gene ontology, the most notable being a GO term associated with aging/senescence-related processes (Figure 5.11, Table 5.4).

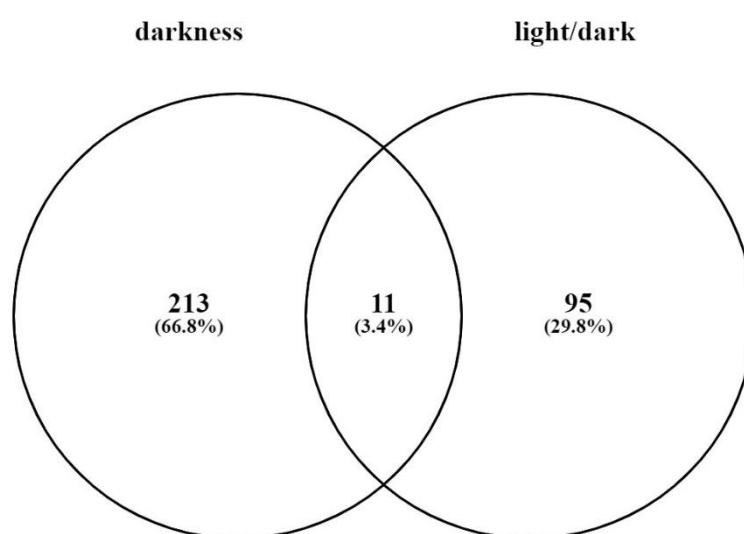


Figure 5.11. Venn diagram illustrates unique and common downregulated genes under dark and light/dark conditions. Total numbers of downregulated overlapping and unique genes in each treatment including the percentage of the total number of genes in the list.

Table 5.4. GO term associated with aging and senescence-related processes for a downregulated group of genes in *dufko3* under light/dark conditions.

Term	Description	Gene count	Fold Enrichment	adj p-value
GO:0007568	Aging	7	9.3	0.0359442
GO:0019748	Secondary metabolic process	11	4.4	0.045061
GO:0044699	Single-organism process	70	1.4	0.001765

This suggests that, under normal growth conditions, the absence of DUF2358 has little impact on the growth and physiology of the plant, which changes under starvation conditions.

Under dark/light cycle conditions, the highly significant biological function terms were GO:0003824 catalytic activity and GO:0016491 oxidoreductase activity (5.12).

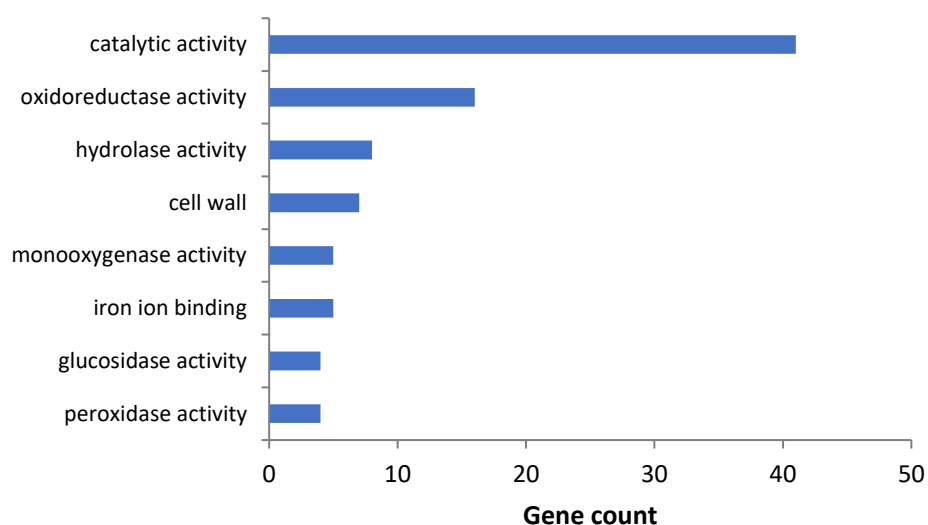


Figure 5.12. Summary of molecular function significantly enriched in the downregulated group of genes in the *dufko3* under light/dark conditions. The significant term (adjusted $P < 0.01$).

5.2.4. Dark-induced leaf senescence

Prolonged dark treatment will induce a process called dark-induced senescence triggering pathways linked to ABA and ethylene signalling leading to changes in primary metabolism (Figure 5.15).

Under darkness, *dufko3* mutants show higher levels of gene expressions for some senescence-associated genes such as NYC1, ANAC029, SGR1, ANAC002, NCED3, and ORE1. ACs, which a key biosynthetic enzyme of ethylene, shows less

expression. The differences between Col-0 and mutant in ORE1, NCED3, SGR1 and NYC1 were significant (Figure 5.13). NYC1 and ORE1 showed slightly lower expression under light/dark conditions. Importantly, under light conditions, Col-0 vs. *dufko3* mutants showed differences in expression of genes associated with senescence but none of them were significant, suggesting that a lack of DUF2358 does not induce senescence-related or other developmental processes (Figure 5.13 and 5.14, Table 5.5).

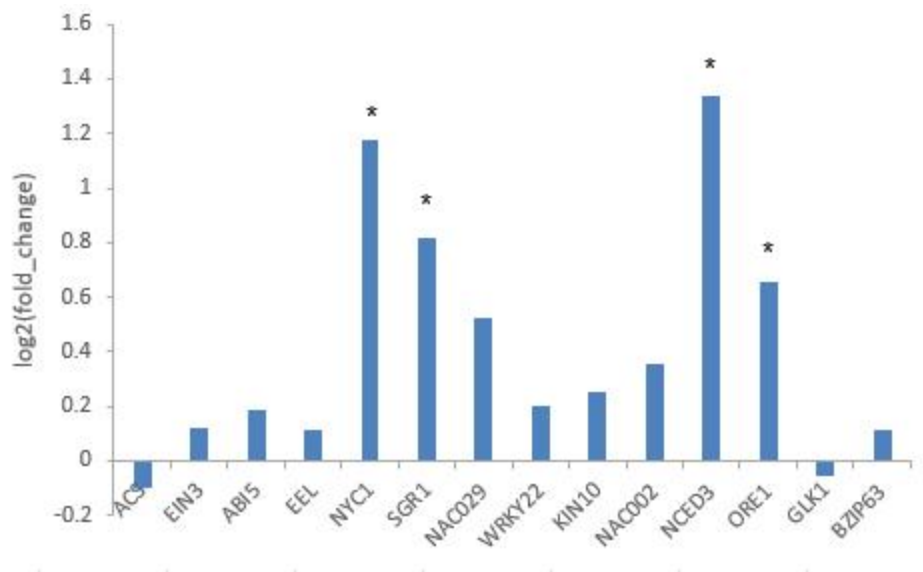


Figure 5.13. Dark-induced leaf senescence-associated genes expression for *dufko3* vs. Col-0 under dark conditions. Significant differences were highlighted with * P<0.01.

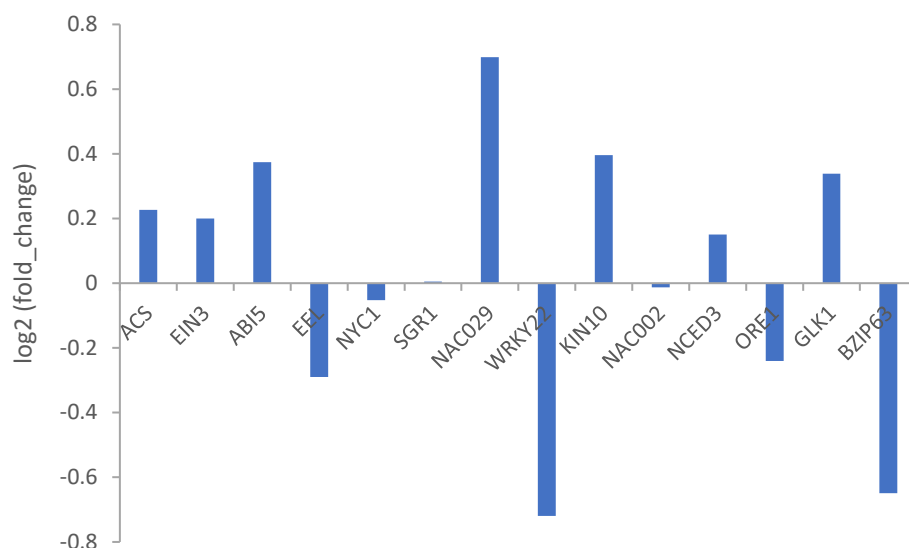


Figure 5.14. Dark-induced leaf senescence-associated genes expression for *dufko3* vs Col-0 under light/dark conditions. No significant differences were founded $P < 0.01$.

Table 5.5. Dark-induced leaf senescence-associated gene expressions for *dufko3* vs Col-0 under dark and light/dark conditions. Significant calculated at $P < 0.01$

Gene locus identified	Gene	Dark		light/dark	
		Log2 fold change (<i>dufko3</i> /WT)	adjusted p-value	Log2 fold change (<i>dufko3</i> /WT)	adjusted p-value
AT5G36880	ACS	-0.09819	0.999251	0.22711	0.888539
AT3G20770	EIN3	0.124078	0.999251	0.199493	0.917201
AT2G36270	ABI5	0.188513	0.999251	0.373713	0.924408
AT2G41070	EEL	0.110485	0.999251	-0.29027	0.944
AT4G13250	NYC1	1.1785	0.003356	-0.05213	0.994422
AT4G22920	SGR1	0.816484	0.00335562	0.280474	0.811386
AT1G69490	NAC029	0.526088	0.114904	0.699048	0.099107
AT4G01250	WRKY22	0.201895	0.999251	-0.71942	0.433942
AT3G01090	KIN10	0.253571	0.992165	0.396148	0.598209

AT1G01720	NAC002	0.355829	0.999251	-0.01325	0.996511
AT3G14440	NCED3	1.33571	0.003356	0.150602	0.96666
AT5G39610	ORE1	0.655917	0.022263	-0.24053	0.933561
AT2G20570	GLK1	-0.05322	0.999251	0.338896	0.780193
AT5G28770	BZIP63	0.1162	0.999251	-0.64972	0.389853

Also, the differences in some leaf senescence-associated gene expressions are demonstrated (Figure 5.15), which also demonstrates the regulatory network of energy deprivation-induced leaf senescence. Under light/dark conditions, some associated dark-induced senescence genes were of a higher expression than Col-0 under the same conditions.

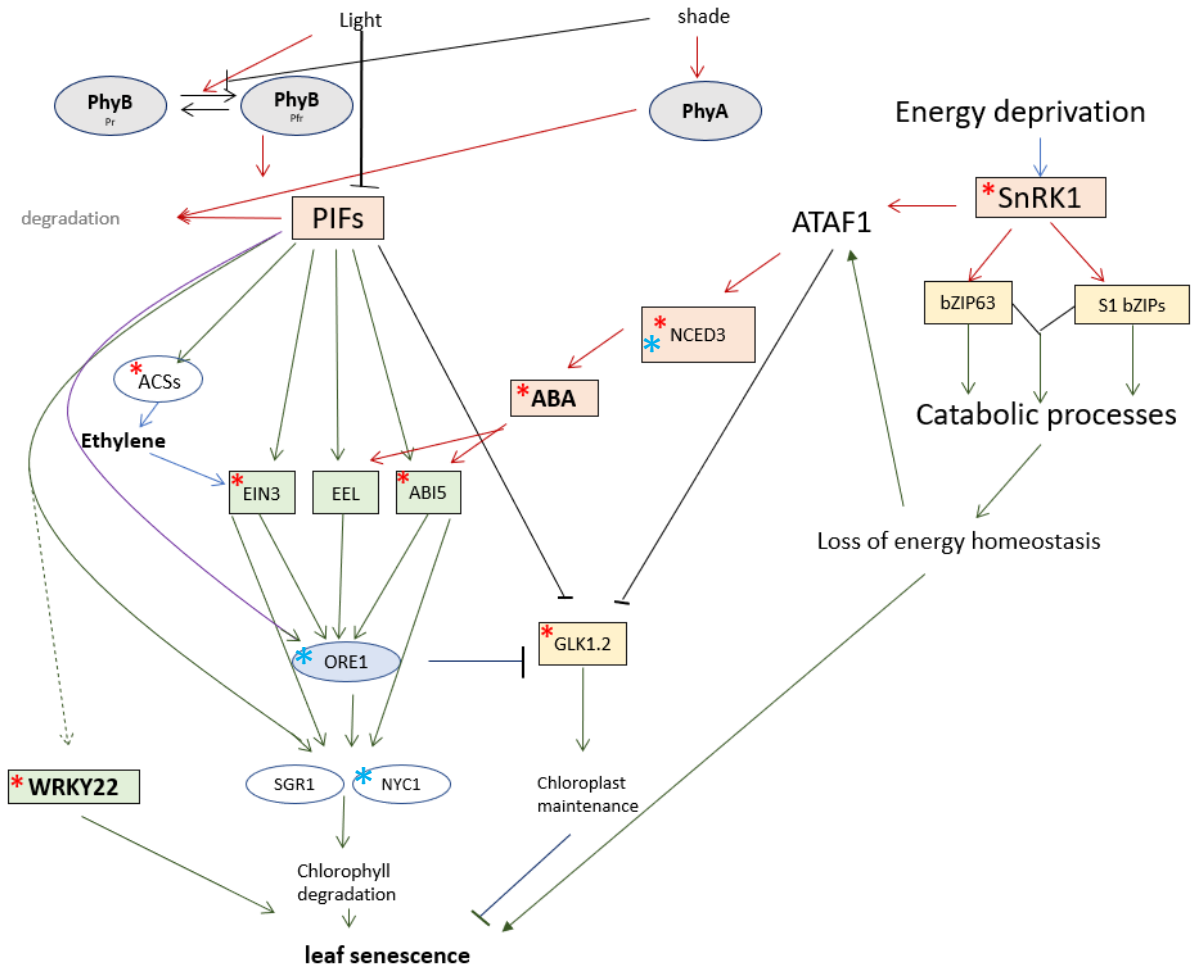


Figure 5.15. The molecular regulatory network under light and energy deprivation-induced leaf senescence. *indicate those genes which show higher expression in *dufko3* compared with Col-0. * indicates the genes which show significant differences in their expression under darkness. The graph was generated using the information from Liebsch and Keech (2016).

A comparison between the fold expression of RNA-seq and the targeted qPCR results in Chapter 3 (see 3.6) showed that both dark treatments were not fully comparable in their transcriptional response. 77% of genes showed a similar response, while others showed the opposite behaviour or responded only in the RNASeq dataset taking in consideration the timing different between samples which will be discussed later (Table 5.6).

Table 5.6. Comparison of the fold expression results from RNA-seq and fold expression from prolonged dark treatment gene expression using qPCR, showing it is very close.

Locus ID	Gene	qPCR data	RNA-seq data
AT2G46220	DUF2358	0	0.088598
AT3G15450	SEN5	0.724434	1.130429
AT2G33380	RD29	0.099545	2.840589
AT5G66400	RAB18	0.367174	0.962964
AT1G13020	EIF	0.670924	0.973364
AT3G47340	DIN6	0.811299	0.999451
at2g33830	AXP	0.946303	0.920057
AT4G17770	ATTPS5	0.673634	1.02566
AT2G36270	ABI5	0.747477	1.139589
AT1G45249	ABF2	1.055464	1.296433
AT3G01090	KIN10	1.278332	1.192154
AT2G03730	ACR5	1.336389	1.077571
AT4G34000	ABF3	1.461597	1.14001
AT4G11330	MPK5	2.249501	1.12702
AT1G44980	ATPME7	2.108111	1
AT2G19860	ATHXK	0.760398	1.167881
AT3G52180	DSP4	0.944433	0.772233
AT2G20570	GLK	2.101258	0.963783
AT5G39610	ORE	1.784986	1.575617
AT3G20770	EIN3	1.496201	1.089811
AT2G41070	EEL	1.43425	1.079591
AT3G14440	NECD3	0.952899	1.336

5.3. Conclusion

RNA-seq data for *dufko3* vs. Col-0 show differential gene expressions under both dark/light and continuous dark conditions, with substantial differences in responses for both conditions. Under darkness, chloroplast-associated and senescence-related processes showed altered expression in the *dufko3* mutant compared with Col-0. The downregulation of photosynthetic processes and upregulation of stress and senescence-related processes are closely linked to the energy status of plants. Under starvation conditions, these processes are downregulated in Col-0. However, they appear to be responding more strongly in the *dufko3* mutant, suggesting that DUF2358 may integrate energy status with downstream metabolic adjustments. ACSs play the main role in ethylene synthesis, but this does not affect the activation of EIN3, which shows an increase in the expression in mutants. Under light/dark conditions also, the key genes involved in the dark-induced senescence illustrate slightly higher expressions in *dufko3* than Col-0, such as ABI5, KIN10, but other genes were slightly suppressed than Col-0 such as bZIP63, which is a key transcription factor in the low-energy response. Differences in gene expressions might indicate a connection of DUF2358 with dark-induced senescence by affecting some of the key genes in the dark-induced senescence network. Although these genes did not show a significant increase in their expression using qPCR in Chapter 3 after nine days of darkness (Table 3.4) under continuous dark treatment, this may be dependent on how many days the plants were exposed to darkness before analysing gene expression. This is because RNA-seq was performed over four days of darkness, before significant changes occurred to Fv/Fm, while qPCR samples under prolonged dark treatment were performed over nine days of darkness (see Chapter 3, section 3.6 in this study).

Chapter 6

Identification of putative DUF2358 interacting proteins

6.1. Introduction

We have previously shown that DUF2358 protein is localised to the chloroplast residing in the thylakoid membrane (Figure 3.16 B and C). The transcriptional network modelling (Bechtold *et al.*, 2016) and subsequent gene expression and metabolomic studies under dark-induced senescence have shown that DUF2358 was found to be involved in the transcriptional regulation of a known sugar signalling pathway involving SnRK1 KIN10). Furthermore, the phenotype under continuous darkness suggests that DUF2358 may not sense or signal sugar status correctly. In order to find out how DUF2358 could integrate a sugar signal derived in chloroplasts with downstream signalling pathways, Co-Immunoprecipitation (Co-IP) was conducted. In general, investigating all possible interactions with DUF2358 can provide an overall idea about the potential role of DUF2358 in sugar signalling or other functions.

This chapter aims to identify and analyse potential interacting proteins with DUF2358 using transient expression of a GFP tagged DUF2358 protein in *Nicotiana benthamiana*, followed by Co-Immunoprecipitation to pull down interacting proteins. Candidates identified via Co-IP are subsequently investigated through a Yeast-2-Hybrid (Y2H) approach to verify the interaction between DUF2358 and these proteins.

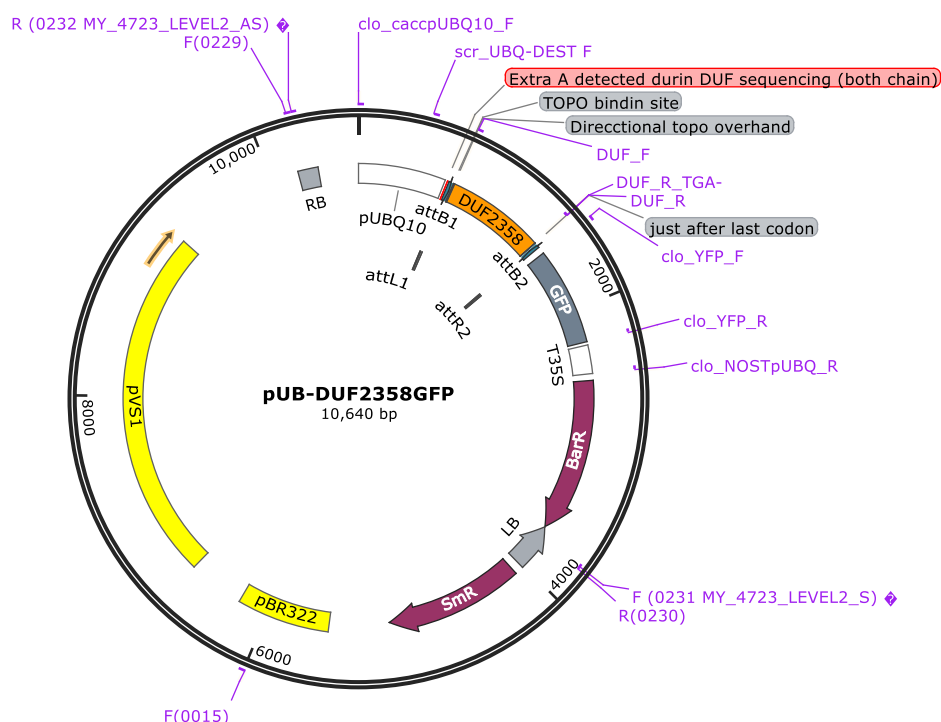
6.2. Result

6.2.1. DUF2358 localisation and Co-Immunoprecipitation

Transient expression was conducted to express DUF2358 tagged with GFP in *Nicotiana benthamiana* plants. Agrobacterium (GV3101) was transformed with a plasmid containing the C terminal-pUBQ:DUF2358::GFP fusion (Ct-DUF:GFP)

(Figure 6.1 A) and was infiltrated into 5-week-old *Nicotiana benthamiana* plant leaves. As a control, the N-terminal part of starch synthase, 4 (SS4) (Gómez-Arjona *et al.*, 2014) fused to GFP was also infiltrated in 5-week-old *Nicotiana benthamiana* plant leaves as a positive control. It was previously shown that the N-terminal GFP::SS4 fusion protein localised the chloroplast thylakoid membrane (Gómez-Arjona *et al.*, 2014), which is the same putative location of the DUF2358 protein. We also infiltrated plants with pBIN61-p19 containing p19, a viral suppressor of gene silencing (P19) (Figure 6.1 B) as a negative control. On day 5 post infiltration, plant leaves were monitored using confocal laser scanning microscopy to detect the localisation and the DUF::GFP and GFP::SS4 fusion proteins.

A



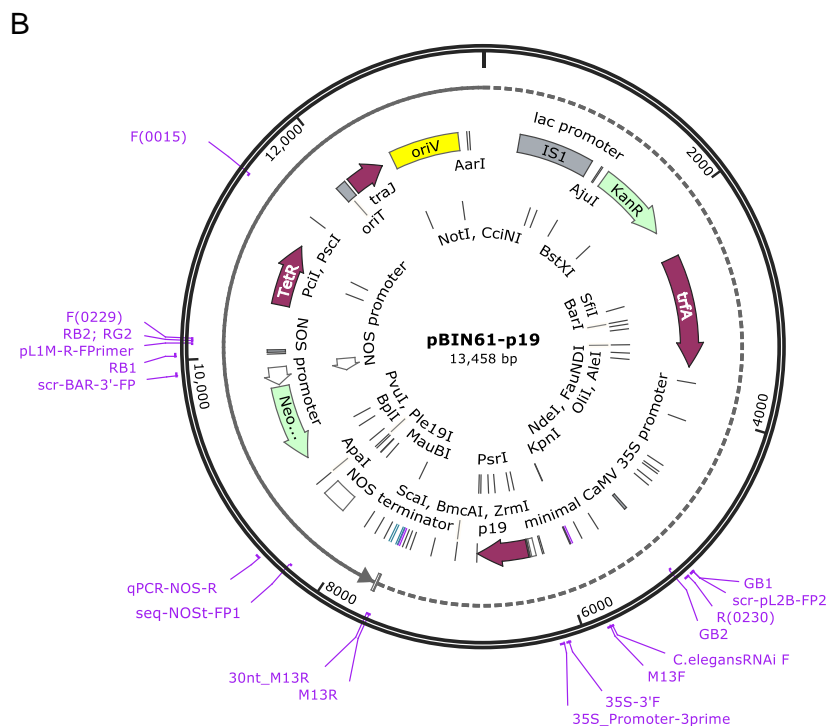
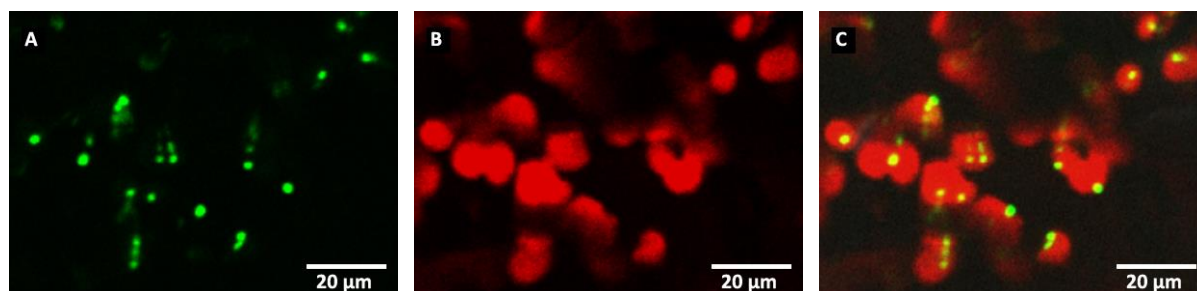


Figure 6.1. (A) Plasmid map of pUBQ:DUF2358::GFP *the plasmid and map was provided by Dr. Exposito. **(B)** Plasmid map of pBIN61-p19.

Screening *Nicotiana benthamiana* infiltrated leaves showed that Ct-DUF::GFP was localised in the chloroplast, which confirmed the potential location of DUF in Chapter 3 (Figure 6.2 A-C; G-I). The positive GFP control, Nt-GFP::SS4, also showed GFP expression in the chloroplast thylakoid membrane similar to Ct-DUF::GFP (Figure 6.2 D-F). There was no GFP expression from p19 plants (Figure 6.2 J).



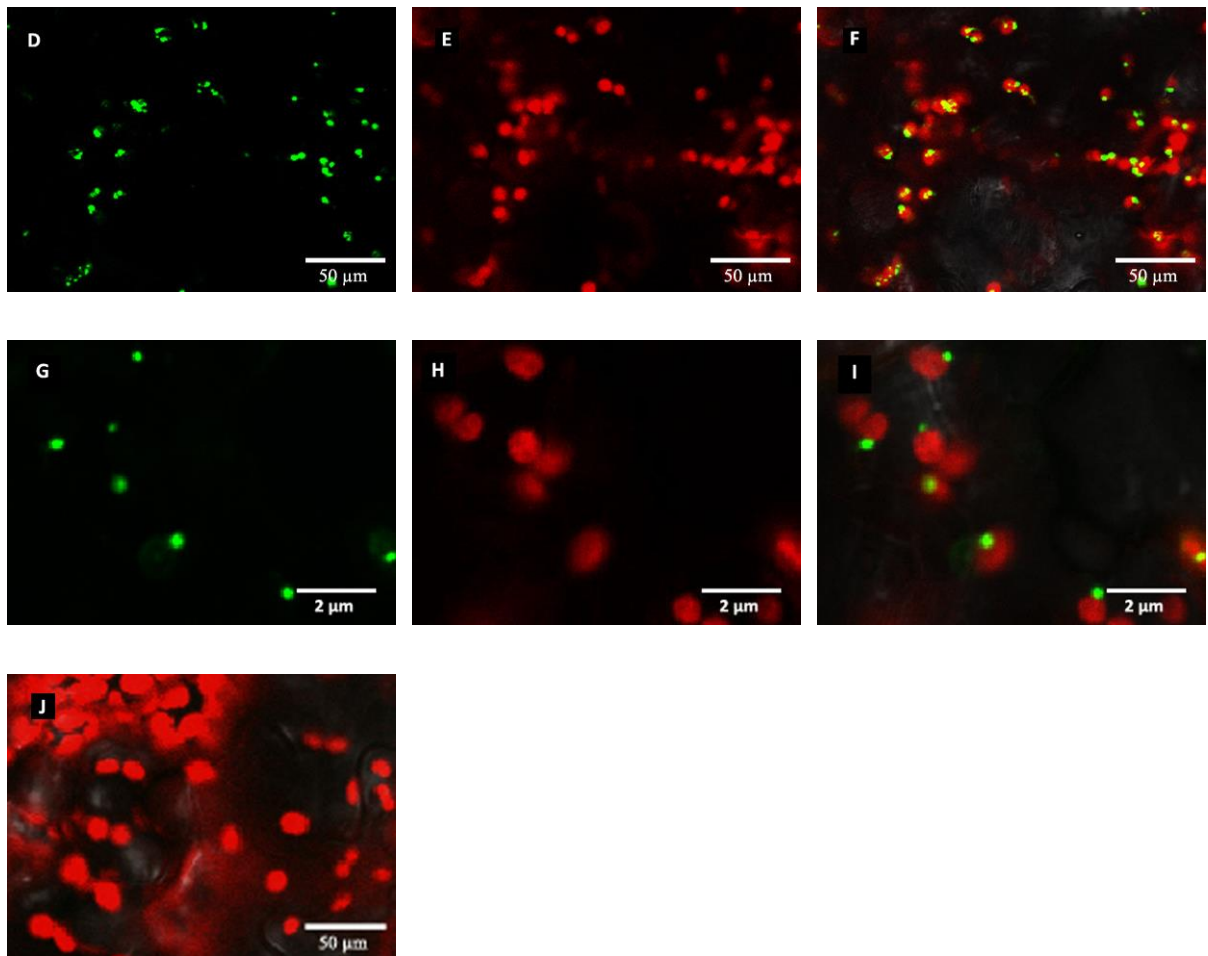


Figure 6.2. Transient expression of Ct-DUF::GFP (**A-C, G-I**), Nt-GFP::SS4 (**D-F**), and P19 (**J**) in *Nicotiana benthamiana* chloroplasts. Expression and localisation of all the constructs were monitored by confocal microscopy. Yellow signal (GFP fluorescence, A, D and G), red signal (Chlorophyll) autofluorescence (B, C, and H), and merged both images (C, F, I and g), respectively.

After GFP expression was confirmed in the chloroplast thylakoid membrane, chloroplasts were isolated from infiltrated plants, and Co-immunoprecipitation using a GFP antibody was carried out to pull down interacting proteins. Also, chloroplasts from non-infiltrated plants, p19 infiltrated plants, and the positive Nt-GFP::SS4 plants were isolated as controls (Figure 6.3).

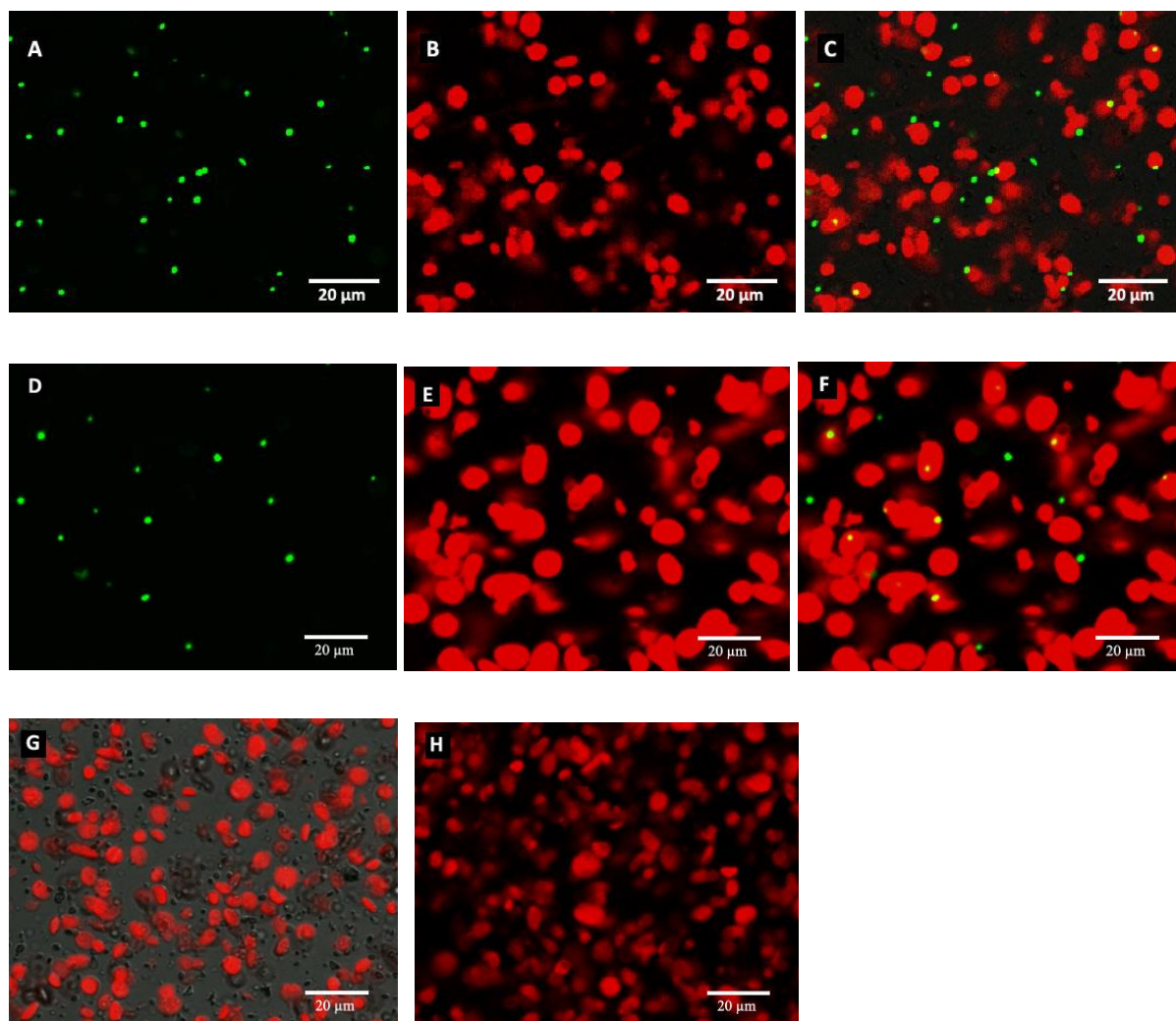


Figure 6.3. GFP expression after chloroplast isolation. Chloroplasts were isolated after transient expression of Ct-DUF::GFP (**A-C**), Nt-GFP::SS4 (**D-F**), and P19 (**G-H**) in *Nicotiana benthamiana* Yellow signal (GFP fluorescence - A and D), red signal (Chlorophyll autofluorescence -B, C, and G), and merged both images (C, F and H), respectively.

After precipitation, samples as described in Chapter 2 (2.1.15), were sent to the Advanced Mass Spectrometry facility (University of Birmingham) to carry out quantitative proteomics analysis.

The protein analysis revealed the number of proteins in the DUF and respective control samples. Control samples were pulled down from Nt-SS4::GFP to provide information

about the proteins which were potentially binding to GFP and not DUF2358. If the same proteins occur in both the GFP::SS4 and DUF:GFP samples, this indicates interaction with GFP and not a specific binding to DUF2358. P19-only samples and WT samples were used as a negative control for GFP expression and to identify common pulled-down proteins. Identification of the common proteins between samples containing GFP and the controls reduces the assumptions about putative proteins, which are putative binding to DUF:GFP. We identified the common and unique proteins between all the samples, which are listed in Table 6.1. The full list of most detected proteins can be found in Appendix M.

Table: 6.1. Proteins were detected after co-immunoprecipitation with GFP antibody. Yes indicates the presence in the sample, No indicates absence in the sample. Protein information was collected from The Universal Protein Resource (UniProt) n=3.

Protein	Ct-DUF	Nt-SS4	P19	WT	Protein name
A0A0A8IBT8	Yes	Yes	Yes	No	GLYCERALDEHYDE-3-PHOSPHATE DEHYDROGENASE
E5LLE7	Yes	No	Yes	No	PHOSPHOGLYCERATE KINASE
K7ZLE1	Yes	No	Yes	Yes	CALCIUM-SENSING RECEPTOR
A0A088F8F4	Yes	No	No	No	CHLOROPLAST ATP-DEPENDENT CLP PROTEASE CHAPERONE PROTEIN
A4D0J9	Yes	No	No	No	CARBONIC ANHYDRASE
I0B7J5	Yes	No	Yes	No	CHLOROPLAST PSBP1
C9DFA3	Yes	No	Yes	No	FTSH-LIKE PROTEIN
D5LT98	Yes	No	No	No	CHLOROPLAST ELONGATION FACTOR TUB

Q6XX19	Yes	No	Yes	Yes	TRANSLATION ELONGATION FACTOR 1 ALPHA
D2DMF5	No	No	Yes	Yes	PLASTOCYANIN

There were three proteins uniquely present in the Ct-DUF:GFP sample. Many were detected in the P19 sample which may indicate connecting these proteins to P19 as they would not be pulled with WT. Testing these proteins in the downstream experiment (Yeast-two-hybrid) is important to verify the possible association of these proteins with DUF2358.

6.2.2. Yest-2-Hybrid (Y2H) screening of putative interaction

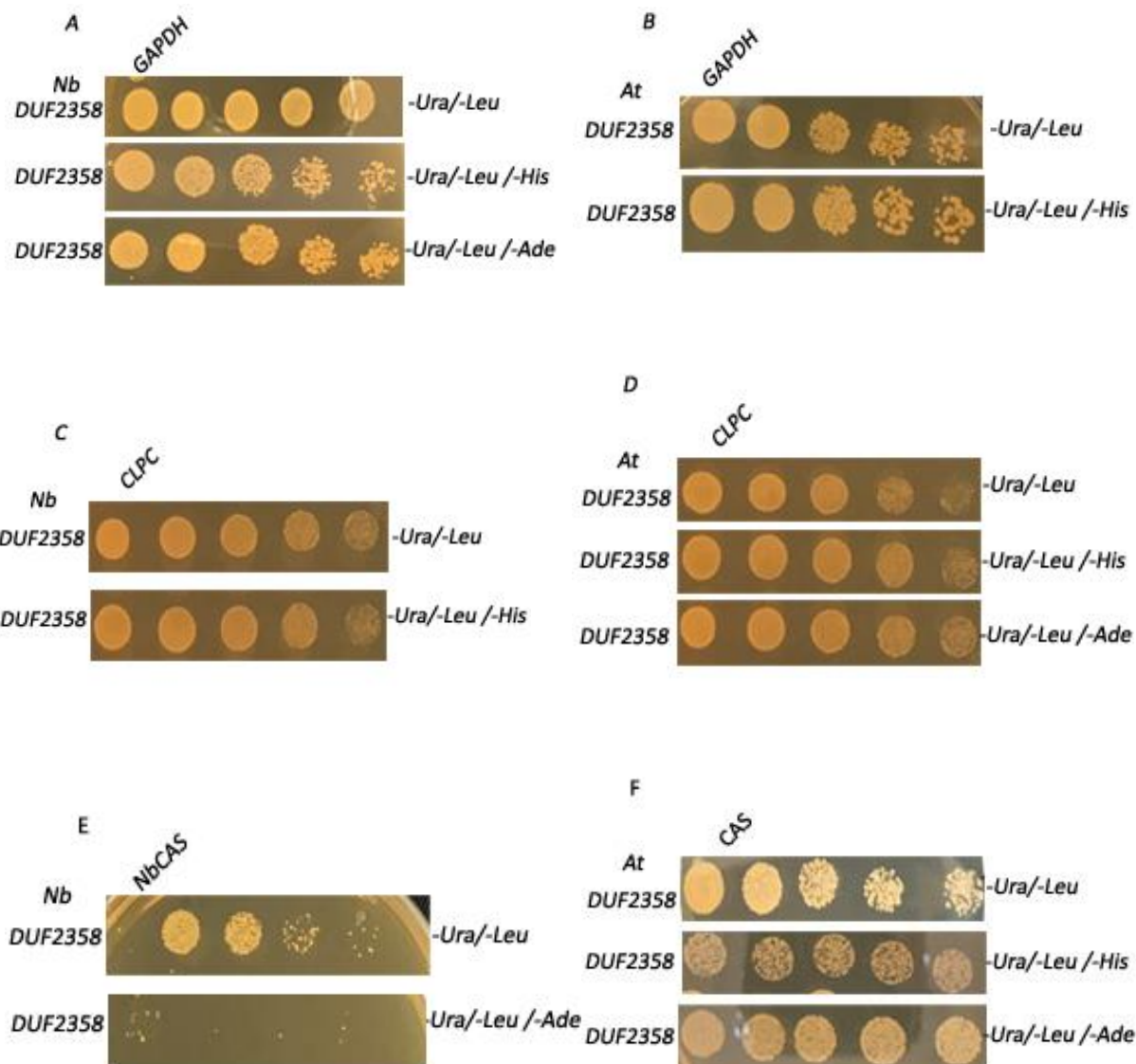
To verify these putative interactions, we carried out a Y2H screen using these proteins from *Nicotiana benthamiana* along with the homologous proteins from *Arabidopsis thaliana*. We selected a range of proteins showing highly specific interactions with Ct-DUF::GFP, as well as proteins with interactions in some of the control samples. Proteins were chosen to test by Y2H based on the presence in Co-IP and the protein function in the cells. Proteins were used both as bait and prey to detect the putative interaction. Unfortunately, the cloning FTSH-LIKE protein was not successful. GLYCERALDEHYDE-3-PHOSPHATE DEHYDROGENASE (GAPDH), PHOSPHOGLYCERATE KINASE (PRK), CALCIUM-SENSING RECEPTOR (CAS), CHLOROPLAST ATP-DEPENDENT PROTEASE CHAPERONE PROTEIN (CLPC1B), CARBONIC ANHYDRASE (CA), and CHLOROPLAST ELONGATION FACTOR TUB (CpEF-TUB) were selected to test their putative interaction with DUF2358. The Y2H screen was carried out as described in (2.1.19).

CpEF-TUB, and PRK did not grow in SD selective medium -Ura -Leu -His/ -Ade, which indicates no or very weak interaction between DUF2358 and both *Nicotiana* and *Arabidopsis* proteins. On the other hand, strong to medium-strong interactions between DUF2358 and GAPDH, CLPC1B, and CAS for both *Nicotiana* and *Arabidopsis* proteins were observed. CA, on the other hand, showed a positive interaction for only the *Nicotiana benthamiana* protein (Table 6.2; Figure 6.4).

Table 6.2. Yeast-two-hybrid results in putative DUF2358 interacting proteins. Results depending on the growth of yeast colonies in a selective medium. -Leu - Ura refers to the selective medium lacking leucine and uracil, Leu -Ura -His refers to selective medium lacking leucine, uracil, and histidine, -Leu -Ura -Ade refers to selective medium lacking leucine, uracil, and adenine. + indicates interaction, - indicates no interaction between DUF2358 and the target protein.

Protein	<i>Nicotiana benthamiana</i>			<i>Arabidopsis thaliana</i>				
	ID	-Leu -Ura	-Leu -Ura -His	Leu -Ura -Ade	ID	-Leu -Ura	-Leu -Ura -His	Leu -Ura -Ade
Glyceraldehyde-3-phosphate dehydrogenase (NbGAPDH-A)	A0A0A8IBT8	+	+	+	AT1G16300	+	+	-
Chloroplast ATP-dependent Clp protease protein (NbClpC1B)	A0A088F8F4	+	+	-	AT5G50920	+	+	+
Calcium-sensing receptor (NbCAS)	K7ZLE1	+	-	+	AT5G23060	+	+	+
Carbonic anhydrase	A4D0J9	+	+	-	AT3G01500	+	-	-
Phosphoglycerate kinase (PRK)	E5LLE7	+	-	-	AT1G79550	+	-	-

Chloroplast elongation factor TuB	D5LT98	+	-	-	AT4G20360	+	-	-
-----------------------------------	--------	---	---	---	-----------	---	---	---



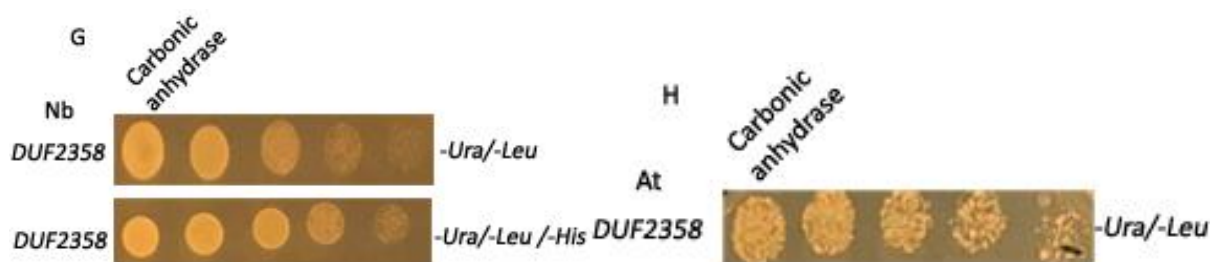


Figure 6.4. Yeast-two-hybrid plate screening results for different putative DUF2358 interacting proteins. Yeast cells were grown overnight in yeast extract peptone dextrose (YEPD) medium lacking different amino acid supplements (Uracil -Ura, Leucine – Leu, Histidine – His). The OD600 was adjusted to 0.1, and fivefold dilutions with 0.9% saline were made. 5 μ l of cells from each dilution were spotted on YEPD agar plates and incubated for 24-48 hours at 30°C.

6.3. Discussion

Three proteins show significant moderate to strong interactions with DUF2358 in the Y2H screen in both *Arabidopsis thaliana* and *Nicotiana benthamiana*, while one protein unique to the DUF2358 pulldown only exhibited weak interactions in *Nicotiana benthamiana*.

6.3.1. DUF2358 interacts with GAPDH

The Co-IP of transiently expressed constructs suggested that NbGAPDH_A interacted with the GFP portion of the construct, as both Ct-DUF::GFP and Nt-GFP::SS4 showed positive identification of NbGAPDH_A (Table 6.1). However, the Y2H screen suggested that DUF2358 protein moderate to strongly interacted with NbGAPDH-A and AtGAPDH-A2 Arabidopsis homologues (Table 6.2). Besides its important role in primary metabolic processes such as glycolysis and photosynthesis, GAPDH has been shown to be directly involved in the stress response and immunity (Henry *et al.*, 2015; Wang and Liu 2013).

Furthermore, cytosolic GAPDH interacts with FERONIA (FER), a CrRLK1L subfamily member, physically interacts with cytosolic GAPDHs to interact with energy metabolism and contributes to energy production (Yang *et al.*, 2015). It has been shown that in *fer* mutants, the activity of GAPDH is suppressed, leading to starch accumulation in Arabidopsis and rice leaves (Yang *et al.*, 2015; Li *et al.*, 2016), allowing FER to integrate stress signals with energy metabolism, allowing plants to balance growth and defence.

Plastid GAPCP also plays a fundamental role in starch metabolism during dark periods through PHOSPHO-GLYCERATE KINASE (PRK) to supply starch metabolism with essential ATP (Backhausen *et al.*, 1998). Interestingly, PRK was also initially identified as a putative interacting partner in the Co-IP (Table 6.1), but no interaction resulted in the Y2H screen (Table 6.2). Whether DUF2358 contributes to these signalling pathways by conveying energy status remains to be investigated.

6.3.2. DUF2358 interacts with CLPC1B

The Co-IP of the transiently expressed construct in *Nicotiana benthamiana* and Y2H suggested a strong interaction with CLPC1B, which is located in the chloroplast stroma (Nishimura *et al.*, 2016). ClpC1B is a molecular chaperone of the HSP100 family (Nishimura and van Wijk, 2015), which is essential for normal plant development and metabolism maintaining photosynthetic performance (Sjögren *et al.*, 2006). As such, it regulates plastid protein biosynthesis and maintains protein function especially during stress conditions, when protein degradation rates increase (Sjögren *et al.*, 2006). This role is very important because the accumulation of damaged polypeptides causes damage to all related bioprocesses during periods of stress

allowing for the recycling of amino acids and regulating the activity of key enzymes (Baker and Sauer, 2006).

CLPC1B and other chloroplast proteases are regulated by high light and temperature stress, during which these proteases modify the chloroplast proteome (Nishimura *et al.*, 2017). Consequently, ClpC1B interaction with DUF2358 may be essential to maintain DUF2358 stability and function under normal and stress conditions.

6.3.3. DUF2358 interacts with CAS

The Co-IP of the transiently expressed construct in *Nicotiana benthamiana* and Y2H only suggested a strong interaction with CAS, which is a known chloroplast thylakoid membrane protein (Nomura *et al.*, 2008). It is a crucial regulator of extracellular calcium-induced stomatal closure in response to stresses that induce H₂O₂ and Nitric Oxide (NO).

Studies demonstrated the involvement of Ca²⁺ transients in the stroma in basal resistance of PAMP-induced activation of defence gene expression (Zhang *et al.*, 2018). Furthermore, stromal Ca²⁺ transients were reported under abiotic stress and during the light-to-dark transition. CAS plays an important role in external Ca²⁺ induced stomatal closure (Nomura *et al.*, 2008) and is, therefore, important in guard cell signalling. When the extracellular calcium (Ca^{2+o}) levels increase, free cytosolic (Ca²⁺ⁱ) increases through the CAS signalling pathway leading to stomatal closure (Wang *et al.*, 2012; Han *et al.*, 2003). This allows CAS to regulate transpiration and improve photosynthesis effectivity, electron transport in photosynthesis, and control stomatal closure to optimise water use efficiency (Wang *et al.*, 2014). In this context,

CAS has also been shown to play an important role in response to stresses, such as drought (Zhang *et al.*, 2018).

6.3.4. DUF2358 interacts with CA

The Y2H essay only suggested a weak interaction between DUF2358 and CA for be *Nicotiana benthamiana* protein, although the transformation in *Arabidopsis thaliana* was positive (Table 6.2), while in the Co-IP this was one of three proteins that were unique to Ct-DUF::GFP pulldown (Table 6.1). *Arabidopsis thaliana* has 19 carbonic anhydrase genes, CAs catalyse the production of bicarbonate HCO_3^- from CO_2 and play a role in the CO_2 stomatal signalling pathway (Lazova *et al.*, 2004; Bhat *et al.*, 2017). CAs are located in the chloroplast, cytosol, and mitochondria (DiMario *et al.*, 2017; Kolbe *et al.*, 2019). It has been reported that CAs in *Nicotiana benthamiana* and *Arabidopsis* are salicylic-acid binding proteins that play an antioxidant role during biotic stress (Slaymaker *et al.*, 2002). Moreover, CA is important to maintain photosynthesis rate. In chloroplasts, CA controls the pH during fast changes in light conditions and protects enzymes in the chloroplast stroma from denaturation. It has been found that CAs increase with CO_2 concentration and help to increase plants' ability to respond to stress (Bhat *et al.*, 2017). Under drought conditions, CA increased in the first period of drought in plant leaves and decreased in the last stage (Rudenko *et al.*, 2020). Under drought stress, the CA protein content increases while the activity of CA was lower than the plant leaves under control conditions due to amino acids phosphorylation (Wang *et al.*, 2016). CA is proposed to be involved in the cascades of mitogen-activated protein kinases (MAPKs), by changing the state of their cysteine redox (Kim *et al.*, 2000).

6.4. Conclusion

Investigating putative binding partners of DUF2358 has identified several chloroplast proteins with potential signalling roles under normal and stress conditions. All these putative interactors share some functional role in chloroplasts with regard to their contribution to stress responses and tolerances including darkness, salinity, and drought. The interaction between DUF2358 and these proteins aids in explaining how DUF2358 may sense and/or signal sugar status under different stress conditions.

Chapter 7

Final discussion

7.1. Overview of the outcomes of this study

This study highlights some promising aspects of the potential roles of DUF2358 in regulating chloroplast processes associated with sugar signalling. Based on the study by Bechtold *et al.* (2016), the DOMAIN OF UNKNOWN FUNCTION PROTEIN (DUF2358) was suggested to be involved in sugar signalling, potentially mediated through KIN10 (Figure 3.1). This study performed experiments to establish the link between a chloroplast localised protein and sugar-signalling pathways.

Firstly, we established the putative localisation of DUF2358 within the chloroplast most likely attached to the thylakoid membrane using transient expression in *Nicotiana benthamiana* (Figure 3.16 B), and protoplast transfection in *Arabidopsis thaliana* (Figure 3.16 C and D). Subcellular localisation in the complemented *dufko3* mutants using a 35S:DUF:GFP construct was unsuccessful due to the presence of a stop codon in the DUF coding region, preventing the translation of the DUF:GFP fusion protein in the complemented mutant (Figure 3.6).

The putative subcellular localisation determined by transient expression was underpinned by some of the phenotypes observed for the *dufko3*, *DUF0E*, and complemented *dufko3* mutants (pNAT-DUF2358), particularly under stress conditions. However, altering the level of DUF2358 had no significant effect on the plant phenotype under control conditions, nor did it affect chloroplast processes associated with electron transport (Figure 3.25) and Western blot using specific antibodies against a range of proteins associated with photosynthetic processes proteins (Figure 3.35).

Different stresses causing sugar starvation, such as drought stress and prolonged or intermittent darkness, resulting in mild to severe growth and photosynthetic phenotypes and changes to sugar and ABA signalling pathways in *dufko3*.

At the transcriptional level, most of the differences were observed under drought stress in *dufko3* (Table 3.4), suggesting that sugar-signalling response was altered in *dufko3* under drought stress. This might indicate a role for DUF2358 in these sugar-signalling or sensing pathways.

Under continuous darkness, the metabolite profile suggests that *dufko3* was either unable to perceive or respond to darkness. Moreover, the increase in the sugar level in *dufko3* (Figure 4.7) suggests that sugar signalling may have been affected in *dufko3*. Furthermore, an increase was recorded in amino acids in *dufko3*, which indicates an increase in protein degradation in *dufko3* compared to Col-0. RNA-Seq supported these outcomes, as genes associated with senescence, and especially chloroplast-associated processes, were enriched in *dufko3* (Figure 5.14 and 5.15). Genes associated with photosynthetic electron transport and light harvesting were significantly downregulated in *dufko3* (Figure 5.9), which might indicate high levels of chloroplast degradation, giving another source of amino acids. The differences between the up and downregulation processes under darkness in *dufko3* were primarily associated with energy status and senescence genes and suggests a connection between DUF2358 with dark-induced senescence. In order to find out how DUF2358 could integrate sugar status from chloroplasts with downstream signalling pathways, Co-IP of transiently expressed GFP fusion protein, coupled with proteomics analysis, was performed followed by Yeast-Two-Hybrid to confirm the DUF2358 interacting proteins. The outcome indicated a moderate to strong interaction between DUF2358 and three proteins (CLPC1B, CAS, and AtGAPDH-A2) in *Arabidopsis thaliana*, while CA showed a weak interaction with DUF2358 in *Nicotiana benthamiana* plants only.

7.2. Putative involvement of DUF2358 in plant light signal transduction

The strong interaction between CAS, a thylakoid membrane protein (Zhang *et al.*, 2018; Vainonen *et al.*, 2008; Nomura *et al.*, 2008) and DUF2358 in Arabidopsis plants, links DUF2358 to calcium-signalling responses under stress such as drought, salt stress or even response to biotic stress (Zhang *et al.*, 2018). Importantly, the thylakoid CAS protein has been reported to be involved in a retrograde signalling pathway from plastid to the nucleus (Guo *et al.*, 2016), through the generation of cytosolic calcium transients Ca^{2+} and activating the MPK3/MPK6 signalling pathway, which phosphorylates ABI4 in the nucleus leading to the suppression of LHCB (Guo *et al.*, 2016). Light-harvesting gene LHCB expression was significantly downregulated in *dufko3* (Figure 5.7), which suggests that DUF2358 may be essential for the adjustment of chloroplast processes under starvation conditions, potentially regulated via CAS. DUF2358 may be regulating CAS negatively through direct interaction, and, in the absence of DUF2358 in *dufko3* mutant, this negative regulation is not occurring, which suppressed the expression of LHCB. The RNA-seq data under light/dark control conditions showed that MPK3 was significantly upregulated in *dufko3*, which supports our hypothesis that DUF2358 might negatively regulate the function of CAS, which indicates the involvement of DUF2358 in CAS signalling in an indirect way. DUF2358 may, therefore, play a role in the regulation of, or contribute to, the generation of cytosolic calcium transients Ca^{2+} through the interaction at the thylakoid membrane. As a calcium-sensing receptor in the thylakoid membrane, CAS has a direct connection with cytosolic Ca^{2+} which has been reported to regulate many physiological processes along with its role in response to abiotic stresses such as drought (Cooke, 1986, cited in Zhang *et al.*, 2018).

CAS also contributes in response to drought stress and other environmental stress which important to stress resistance by activating MPK3/MPK6, through generating cytosolic Ca^{+2} (Wang *et al.*, 2014; Zhang *et al.*, 2018). Furthermore, ABI4 is involved in sugar and ABA signalling by regulating the expression of ABI5 and starch branching enzyme SBE2.2, in a glucose-dependent manner (Bossi *et al.*, 2009). Also, ABI4 plays a role in repressing sugar-related genes at the transcriptional level, which places ABI4 downstream of ABA-mediated sugar signalling (Bossi *et al.*, 2009). We have reported in this study that DUF2358 responds to drought and prolonged darkness, which indicates that DUF2358 may respond to the overall sugar status. We also found that sugar accumulated under stress conditions in *dufko3* compared to Col-0, which indicates that *dufko3* may have altered sugar-signalling responses, which might be regulated through CAS and ABI4 signalling pathways. The way in which DUF2358 might involve CAS in the signalling needs to be further investigated.

7.3. Involvement of DUF2358 in sugar-signalling and dark-induced senescence pathways

One of the detected proteins to strongly interact with DUF2358 is CLPC1. CLPC1 subunit is a plastid protease that plays an important role in maintaining the balance between protein synthesis and protein degradation of chlorophyllide a oxygenase (Nakagawara *et al.*, 2007). Clp protease subunits such as ClpS1, ClpC1, and ClpD contribute to Phytoene synthase (PSY) homeostasis. PSY plays a critical role in carotene biosynthesis by directing isoprenoid carbon to the carotene biosynthesis pathway (Welsch *et al.*, 2018). CLPC1 has been reported to interact with TRANSLOCON AT THE INNER ENVELOPE MEMBRANE OF CHLOROPLASTS 40

(TIC40; AT5G16620) (Kovacheva *et al.*, 2005) and interact with CALCIUM-DEPENDENT PROTEIN KINASE 4 (CPK4; AT4G09570) (Uno *et al.*, 2009). TIC40 is one of Translocon at the inner membrane of chloroplast proteins, which are important as a chloroplast protein importer (Chou *et al.*, 2018). In our result, no significant change was observed in *dufko3* in TIC40 expression. On the other hand, another member of the TIC complex (TIC55) was found to form a protein complex with TIC40 and CLPC (Jouhet and Gray, 2009; Chou *et al.*, 2018). In this complex, TIC55 was found to be involved in dark-induced aging by positively regulating the expression of seven senescence-associated downstream genes (SAGs) (Chou *et al.*, 2018). These genes are ASPARTATE AMINOTRANSFERASE 3 (ASP3), AUTOPHAGY-RELATED 7, UBIQUITIN-LIKE MODIFIER-ACTIVATING ENZYME ATG7 (ATG7), DARK INDUCIBLE 2, BETA-GLUCOSIDASE 30 (DIN2), DARK INDUCIBLE 11, 2-OXOACID-DEPENDENT DIOXYGENASE-LIKE PROTEIN(DIN11), SENESCENCE-ASSOCIATED GENE 12, CYSTEINE PROTEASE (SAG12), SENESCENCE-ASSOCIATED GENE 13, SENESCENCE-ASSOCIATED PROTEIN (SAG13), and YELLOW-LEAF-SPECIFIC GENE 9, PROTEIN NDR1/HIN1-LIKE 10 (YLS9). All these genes were upregulated under dark conditions in *dufko3*. ASP3, ATG7, DIN2, SAG12, and SAG13 showed a significant increase in expression in *dufko3*, while the YLS9 and DIN11 showed a higher level of expression, but this increase was not significant (Figure 5.6).

We suggest that DUF2358 negatively regulates the interaction between TIC55 in a CLPC complex. DUF2358 is also upregulated under darkness, which enforces this negative regulation under dark conditions. In the knockout mutant, this regulation is absent, causing a significant increase in the associated-senescent genes. This might

indicate the connection between removing DUF2358 with the significant increase of these gene expressions.

Also, our RNA-seq result showed that senescence-associated genes such as BIFUNCTIONAL NUCLEASE I (ENDO1), AtS40-3, SENESCENCE-RELATED GENE 1 (SRG1), NITRATE TRANSPORTER 1.5 (NPF7.3), LOW-TEMPERATURE-INDUCED 78 (LTI78), ROOT HAIR SPECIFIC 3 (RSH3), GLUTAMINE SYNTHASE 1;1 (GLN1;1) were significantly upregulated in *dufko3* under darkness. Increasing the expression of dark-associated senescence genes was accompanied by significant downregulation of photosynthetic electron transport and light-harvesting genes (Table 5.3; Figure 5.9) in *dufko3* under dark condition. This result supported the outcome in Chapter 3 (section 3.6.1), where we found the maximum efficiency of photosystem II Fv/Fm was lower in *dufko3* plants after four days of darkness and showed severe dark senescence phenotype compared to Col-0 plants (3.25). This indicates that *dufko3* failed to maintain Fv/Fm in response to darkness and was affected more than Col-0 by darkness (Figure 3.25).

Moreover, Liebsch and Keech (2016) demonstrated the molecular regulatory network under light and energy deprivation-induced leaf senescence (Figure 5.15). We found that some key regulatory genes in the dark-induced senescence network were affected significantly by the absence of DUF2358 under dark conditions. AtNAC TFs, ABA and Ethylene biosynthesis genes were significantly upregulated in *dufko3* compared to Col-0 under darkness (Figure 3.29, Figure 5.14 and Table 5.5). Increasing the expression of these key elements in dark-induced senescence contributes to the increase in chloroplast degradation compared to Col-0. This is also supported by metabolomics analysis in this study, which revealed a significant increase in amino acid in the *dufko3* mutant under darkness (Figure 4.8). The plant

response to darkness in the absence of DUF2358 might indicate the involvement of DUF2358 in the dark-induced senescence pathway as an indirect regulator (Figure 7.1).

7.4. Involvement of DUF2358 in ABA signalling pathways

As previously mentioned, CLPC1 was also reported to interact with CALCIUM-DEPENDENT PROTEIN KINASE 4 (CPK4) (Uno *et al.*, 2009), which is important in response to osmotic stress (Shinozaki *et al.*, 2003). The CPK4 kinases are located in the cytoplasm and nucleus (Milla *et al.*, 2006), and has been reported to be a positive regulator of ABA signal transduction in Arabidopsis through the phosphorylation of ABF1 and ABF4 (Zhu *et al.*, 2007). Both ABF1 and ABF4 are essential transcription factors that play an important role under drought conditions in the ABA signalling pathway (Yoshida *et al.*, 2015). After ABFs are activated through phosphorylation, a downstream transcriptional signalling cascade is initiated that leads to response and tolerance to drought stress and other stress (Kang *et al.*, 2002, cited in Yoon, 2020; Yoshida *et al.*, 2015). ABF4 binds to the STAY-GREEN 1 (SGR1) promoter which plays a key role in ABA-dependent regulating chlorophyll degradation and leaf senescence (Gao *et al.*, 2016). Our RNA-seq result shows a significant increase in SGR1 expression in *dufko3* under dark conditions (5.14; Table 5.5). Also, we found different ABA-associated stress response and senescence genes were upregulated in *dufko3* after four days of darkness (Figure 5.5), which suggests that DUF2358 modulates the function of CLPC1 interacting proteins to regulate the phosphorylation of ABF4 and ABF1.

7.5. Conclusion

We suggest that DUF2358 is involved in dark-induced senescence through regulating some key-signalling components of the pathway either directly or indirectly. We also propose that DUF2358 responds to the sugar status and suggest a possibility for DUF2358 to contribute to the sugar-signalling pathways. This may also involve ABA signalling pathways through modulating the function of CLPC1 interacting protein, and CPK4 to regulate the phosphorylation of ABF4 and ABF1.

Also, we demonstrated a possible involvement of DUF2358 in a retrograde signalling pathway between plastid and nucleus, possibly by regulating MPK3. How DUF2358 might be involved or how it regulates this signalling pathway remains to be investigated. To summarise our findings, we suggest model for DUF2358, involved in dark-induced senescence (Figure7.1). The suggested model is highlighting some of the key dark-associated genes which were significantly upregulated under the dark condition in *dufko3* compared to Col-0.

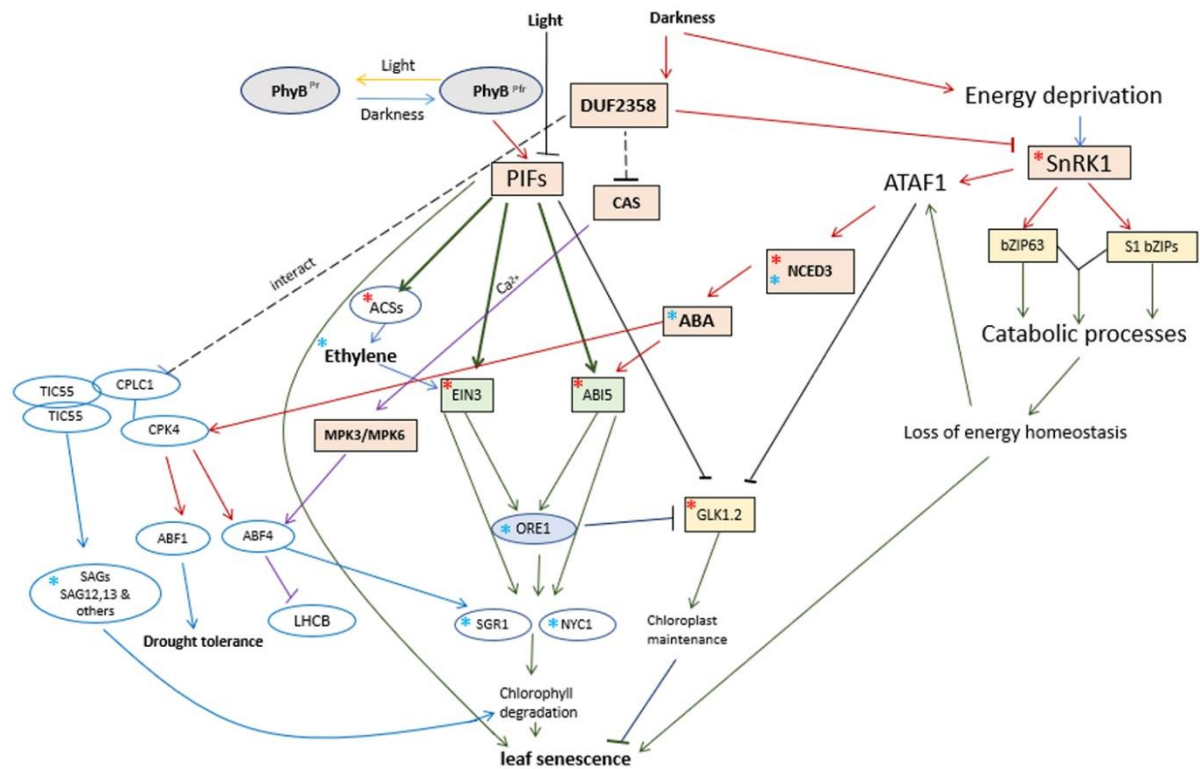


Figure 7.1. The molecular regulatory network under light and energy deprivation-induced leaf senescence, including our suggestion of the involvement of DUF2358 in the dark-induced senescence and regulating KIN10 activity. *Indicates those genes which show higher expression in *dufko3* compared with Col-0. *Indicates the genes which show significant differences in their expression under darkness. The graph was generated based on the information from Liebsch and Keech (2016).

The model suggests that DUF2358 sits upstream of some of the key-signalling components of dark-induced senescence, impacting hormone biosynthesis (Ethylene and ABA) and signalling processes. In WT, may be involved in timing these responses via the activity of different kinases (SnRK1, CPK4), leading to the degradation of chlorophyll in an ABA-dependent and/or sugar-dependent manner. None of the TFs showed changes at the gene expression levels. Therefore, downstream responses, such as the phosphorylation of key TFs in both pathways, need to be investigated further to verify the role of DUF2358 in the energy response pathways. Using more mutants of CAS knockout plants and apply crossing system between *dufko* and CAS knockout and overexpression to study the effect of alter their expression on plant.

References

- Aguilera-Alvarado, G. P. and Sánchez-Nieto, S. (2017). Plant hexokinases are multifaceted proteins. *Plant and Cell Physiology*, 58(7), 1151-1160.
- Akpinar, B. A., Avsar, B., Lucas, S. J., and Budak, H. (2012). Plant abiotic stress signaling. *Plant signaling & behavior*, 7(11), 1450-1455.
- Almodares, A., Hadi, M. R., and Dosti, B. (2008). The effects of salt stress on growth parameters and carbohydrates contents in sweet sorghum. *Research Journal of Environmental and Earth Sciences*, 2(4), 298-304.
- Alves, A. A., and Setter, T. L. (2004). Abscisic acid accumulation and osmotic adjustment in cassava under water deficit. *Environmental and experimental botany*, 51(3), 259-271.
- Anjum, S. A., Xie, X. Y., Wang, L. C., Saleem, M. F., Man, C., and Lei, W. (2011). Morphological, physiological and biochemical responses of plants to drought stress. *African journal of agricultural research*, 6(9), 2026-2032.
- Apel, K., and Hirt, H. (2004). Reactive oxygen species: metabolism, oxidative stress, and signal transduction. *Annual Review of Plant Biology*, 55, 373-399.
- Arabzadeh, N. (2012). The effect of drought stress on soluble carbohydrates (sugars) in two species of *Haloxylon persicum* and *Haloxylon aphyllum*. *Asian Journal of Plant Sciences*, 11(1), 44-51.
- Araújo, W. L., Nunes-Nesi, A., and Fernie, A. R. (2011). Fumarate: Multiple functions of a simple metabolite. *Phytochemistry*, 72(9), 838-843.
- Arenas-Huertero, F., Arroyo, A., Zhou, L., Sheen, J., and León, P. (2000). Analysis of Arabidopsis glucose insensitive mutants, gin5 and gin6, reveals a central role of the plant hormone ABA in the regulation of plant vegetative development by sugar. *Genes & development*, 14(16), 2085-2096.
- Backhausen, J. E., Emmerlich, A., Holtgreffe, S., Horton, P., Nast, G., Rogers, J. J., Müller-Röber, B., and Scheibe, R. (1998). Transgenic potato plants with altered

expression levels of chloroplast NADP-malate dehydrogenase: interactions between photosynthetic electron transport and malate metabolism in leaves and in isolated intact chloroplasts. *Planta*, 207(1), 105-114.

Baena-González, E. (2010). Energy signaling in the regulation of gene expression during stress. *Molecular plant*, 3(2), 300-313.

Baena-González, E., and Hanson, J. (2017). Shaping plant development through the SnRK1–TOR metabolic regulators. *Current Opinion in Plant Biology*, 35, 152-157.

Baena-González, E., and Sheen, J. (2008). Convergent energy and stress signaling. *Trends in plant science*, 13(9), 474-482.

Baena-González, E., Rolland, F., Thevelein, J. M., and Sheen, J. (2007). A central integrator of transcription networks in plant stress and energy signalling. *Nature*, 448 (7156), 938-942.

Baguley, B., Chen, C., Fernandez, A., and Hara, K. (2016). Effect of abscisic acid on the germination of wild-type and cer10 mutant *Arabidopsis thaliana* seeds. *The Expedition*, 6.

Bailey, P. C., Dicks, J., Wang, T. L., and Martin, C. (2008). IT3F: a web-based tool for functional analysis of transcription factors in plants. *Phytochemistry*, 69(13), 2417-2425.

Baker, T. A., and Sauer, R. T. (2006). ATP-dependent proteases of bacteria: recognition logic and operating principles. *Trends in biochemical sciences*, 31(12), 647-653.

Barbagallo, R. P., Oxborough, K., Pallett, K. E., and Baker, N. R. (2003). Rapid, noninvasive screening for perturbations of metabolism and plant growth using chlorophyll fluorescence imaging. *Plant Physiology*, 132(2), 485-493.

Bartlett, M. K., Scoffoni, C., and Sack, L. (2012). The determinants of leaf turgor loss point and prediction of drought tolerance of species and biomes: a global meta-analysis. *Ecology letters*, 15(5), 393-405.

Basu, S., Ramegowda, V., Kumar, A., and Pereira, A. (2016). Plant adaptation to drought stress. *F1000Research*, 5.

- Beal, M. J., Falciani, F., Ghahramani, Z., Rangel, C., and Wild, D. L. (2005). A Bayesian approach to reconstructing genetic regulatory networks with hidden factors. *Bioinformatics*, 21(3), 349-356.
- Bechtold, U., Penfold, C. A., Jenkins, D. J., Legaie, R., Moore, J. D., Lawson, T., Matthews, J. S. A., Vialet-chabrand, S. R. M., Baxter, L., Subramaniam, S., Hickman, R., Florance, H., Sambles, C., Salmon, D. L., Feil, R., Bowden, L., Hill, C., Baker, N. R., Lunn, J. E., *et al* and Smirnoff, N. (2016). Time-series transcriptomics reveals that AGAMOUS-LIKE22 affects primary metabolism and developmental processes in drought-stressed Arabidopsis. *The Plant Cell*, 28(2), 345-366.
- Bhat, F. A., Ganai, B. A., and Uqab, B. (2017). Carbonic anhydrase: mechanism, structure and importance in higher plants. *Asian Journal of Plant Science*, 7, 17-23.
- Bläsing, O. E., Gibon, Y., Günther, M., Höhne, M., Morcuende, R., Osuna, D., Osuna, D., Thimm, O., Usadel, B., Scheible, W., and Stitt, M. (2005). Sugars and circadian regulation make major contributions to the global regulation of diurnal gene expression in Arabidopsis. *The Plant Cell*, 17(12), 3257-3281.
- Blum, A. (2017). Osmotic adjustment is a prime drought stress adaptive engine in support of plant production. *Plant, cell & environment*, 40(1), 4-10.
- Borrell, A. K., Mullet, J. E., George-Jaeggli, B., van Oosterom, E. J., Hammer, G. L., Klein, P. E., and Jordan, D. R. (2014). Drought adaptation of stay-green sorghum is associated with canopy development, leaf anatomy, root growth, and water uptake. *Journal of experimental botany*, 65(21), 6251-6263.
- Bossi, F., Cordoba, E., Dupré, P., Mendoza, M. S., Román, C. S., and León, P. (2009). The Arabidopsis ABA-INSENSITIVE (ABI) 4 factor acts as a central transcription activator of the expression of its own gene, and for the induction of ABI5 and SBE2. 2 genes during sugar signaling. *The Plant Journal*, 59(3), 359-374.
- Boyes, D. C., Zayed, A. M., Ascenzi, R., McCaskill, A. J., Hoffman, N. E., Davis, K. R., and Görlach, J. (2001). Growth stage-based phenotypic analysis of Arabidopsis: a model for high throughput functional genomics in plants. *The Plant Cell*, 13(7), 1499-1510.

- Bradford, M. M. (1976). A rapid and sensitive method for the quantitation of microgram quantities of protein utilizing the principle of protein-dye binding. *Analytical biochemistry*, 72(1-2), 248-254.
- Bray, N. L., Pimentel, H., Melsted, P., and Pachter, L. (2016). Near-optimal probabilistic RNA-seq quantification. *Nature biotechnology*, 34(5), 525-527.
- Broeckx, T., Hulsmans, S., and Rolland, F. (2016). The plant energy sensor: evolutionary conservation and divergence of SnRK1 structure, regulation, and function. *Journal of Experimental Botany*, 67(22), 6215-6252.
- Bullard, J. H., Purdom, E., Hansen, K. D., and Dudoit, S. (2010). Evaluation of statistical methods for normalization and differential expression in mRNA-Seq experiments. *BMC bioinformatics*, 11(1), 1-13.
- Chan, A., Carianopol, C., Tsai, A. Y. L., Varatharajah, K., Chiu, R. S., and Gazzarrini, S. (2017). SnRK1 phosphorylation of FUSCA3 positively regulates embryogenesis, seed yield, and plant growth at high temperature in Arabidopsis. *Journal of Experimental Botany*, 68(15), 4219-4231.
- Chan, K. X., Phua, S. Y., Crisp, P., McQuinn, R., and Pogson, B. J. (2016). Learning the languages of the chloroplast: retrograde signaling and beyond. *Annual review of plant biology*, 67, 25-53.
- Chaves, M. M., and Oliveira, M. M. (2004). Mechanisms underlying plant resilience to water deficits: prospects for water-saving agriculture. *Journal of experimental botany*, 55(407), 2365-2384.
- Cheng, S. H., Willmann, M. R., Chen, H. C., and Sheen, J. (2002). Calcium signaling through protein kinases. The Arabidopsis calcium-dependent protein kinase gene family. *Plant physiology*, 129(2), 469-485.
- Cheng, W., Zhang, H., Zhou, X., Liu, H., Liu, Y., Li, J., Han, S., and Wang, Y. (2011). Subcellular localization of rice hexokinase (OsHXK) family members in the mesophyll protoplasts of tobacco. *Biologia Plantarum*, 55(1), 173-177.
- Cho, Y. H., and Yoo, S. D. (2007). ETHYLENE RESPONSE 1 histidine kinase activity of Arabidopsis promotes plant growth. *Plant Physiology*, 143(2), 612-616.

- Cho, Y. H., Sheen, J., and Yoo, S. D. (2010). Low glucose uncouples hexokinase1-dependent sugar signaling from stress and defense hormone abscisic acid and C2H4 responses in Arabidopsis. *Plant physiology*, 152(3), 1180-1182.
- Cho, Y. H., Yoo, S. D., and Sheen, J. (2006). Regulatory functions of nuclear hexokinase1 complex in glucose signaling. *Cell*, 127(3), 579-589.
- Cho, Y. H., Yoo, S. D., and Sheen, J. (2007). Glucose signaling through nuclear hexokinase1 complex in Arabidopsis. *Plant signaling & behavior*, 2(2), 123-124.
- Chong, J., Soufan, O., Li, C., Caraus, I., Li, S., Bourque, G., Wishart, D., and Xia, J. (2018). MetaboAnalyst 4.0: towards more transparent and integrative metabolomics analysis. *Nucleic acids research*, 46(W1), W486-W494.
- Chou, M. L., Liao, W. Y., Wei, W. C., Li, A. Y. S., Chu, C. Y., Wu, C. L., et al. and Lin, L. F. (2018). The direct involvement of dark-induced Tic55 protein in chlorophyll catabolism and its indirect role in the MYB108-NAC signaling pathway during leaf senescence in Arabidopsis thaliana. *International journal of molecular sciences*, 19(7), 1854.
- Cordoba, E., Aceves-Zamudio, D. L., Hernández-Bernal, A. F., Ramos-Vega, M., and León, P. (2015). Sugar regulation of SUGAR TRANSPORTER PROTEIN 1 (STP1) expression in Arabidopsis thaliana. *Journal of experimental botany*, 66(1), 147-159.
- Cornic, G. (2000). Drought stress inhibits photosynthesis by decreasing stomatal aperture - not affecting ATP synthesis. *Trend in Plant Sciences*. 5:187-188.
- Corrêa, L. G. G., Riaño-Pachón, D. M., Schrago, C. G., dos Santos, R. V., Mueller-Roeber, B., and Vincentz, M. (2008). The role of bZIP transcription factors in green plant evolution: adaptive features emerging from four founder genes. *PloS one*, 3(8), e2944.
- Couée, I., Sulmon, C., Gouesbet, G., and El Amrani, A. (2006). Involvement of soluble sugars in reactive oxygen species balance and responses to oxidative stress in plants. *Journal of experimental botany*, 57(3), 449-459.
- Crozet, P., Margalha, L., Butowt, R., Fernandes, N., Elias, C. A., Orosa, B., Tomanov, K., Teige, M. Bachmair, A., Sadanandom, A., and Baena-González, E. (2016).

SUMOylation represses SnRK1 signaling in Arabidopsis. *The Plant Journal*, 85(1), 120-133.

Crozet, P., Margalha, L., Confraria, A., Rodrigues, A., Martinho, C., Adamo, M., Elias, C., and Baena-González, E. (2014). Mechanisms of regulation of SNF1/AMPK/SnRK1 protein kinases. *Frontiers in plant science*, 5, 190.

Das, K., and Roychoudhury, A. (2014). Reactive oxygen species (ROS) and response of antioxidants as ROS-scavengers during environmental stress in plants. *Frontiers in environmental science*, 2, 53.

de Folter S., Immink R.G. (2011) Yeast Protein–Protein Interaction Assays and Screens. In: Yuan L., Perry S. (eds) *Plant Transcription Factors*. Methods in Molecular Biology (Methods and Protocols), vol 754. Humana Press

De Vleeschauwer, D., Filipe, O., Hoffman, G., Seifi, H. S., Haeck, A., Canlas, P., Van Bockhaven, J., De Waele, E., Demeestere, K., Ronald, P., and Hofte, M. (2018). Target of rapamycin signaling orchestrates growth–defense trade-offs in plants. *New Phytologist*, 217(1), 305-319.

Dekkers, B. J., Schuurmans, J. A., and Smeekens, S. C. (2008). Interaction between sugar and abscisic acid signalling during early seedling development in Arabidopsis. *Plant molecular biology*, 67(1-2), 151-167.

Deng, K., Yu, L., Zheng, X., Zhang, K., Wang, W., Dong, P., Zhang, J., and Ren, M. (2016). Target of rapamycin is a key player for auxin signaling transduction in Arabidopsis. *Frontiers in plant science*, 7, 291.

Deprost, D., Yao, L., Sormani, R., Moreau, M., Leterreux, G., Nicolai, M., ... & Meyer, C. (2007). The Arabidopsis TOR kinase links plant growth, yield, stress resistance and mRNA translation. *EMBO reports*, 8(9), 864-870.

Desikan, R., Griffiths, R., Hancock, J., and Neill, S. (2002). A new role for an old enzyme: nitrate reductase-mediated nitric oxide generation is required for abscisic acid-induced stomatal closure in Arabidopsis thaliana. *Proceedings of the National Academy of Sciences*, 99(25), 16314-16318.

- DiMario, R. J., Clayton, H., Mukherjee, A., Ludwig, M., and Moroney, J. V. (2017). Plant carbonic anhydrases: structures, locations, evolution, and physiological roles. *Molecular plant*, 10(1), 30-46.
- Dobrenel, T., Marchive, C., Sormani, R., Moreau, M., Mozzo, M., Montané, M. H., Robaglia, C., and Meyer, C. (2011). Regulation of plant growth and metabolism by the TOR kinase. *Biochemical Society Transactions*, 39(2), 477-481.
- Dong, Y., Silbermann, M., Speiser, A., Forieri, I., Linster, E., Poschet, G., Samami, A., Wanatabe, M., Sticht, C., Teleman, A., Deragon, J., Saito, K., Hell, R., and Wirtz, M. (2017). Sulfur availability regulates plant growth via glucose-TOR signaling. *Nature communications*, 8(1), 1-10.
- Du, H., Feng, B. R., Yang, S. S., Huang, Y. B., and Tang, Y. X. (2012). The R2R3-MYB transcription factor gene family in maize. *PloS one*, 7(6), e37463.
- Du, Z., Zhou, X., Ling, Y., Zhang, Z., and Su, Z. (2010). agriGO: a GO analysis toolkit for the agricultural community. *Nucleic acids research*, 38(suppl_2), W64-W70.
- Duan, B., Yang, Y., Lu, Y., Korpelainen, H., Berninger, F., and Li, C. (2007). Interactions between water deficit, ABA, and provenances in *Picea asperata*. *Journal of experimental botany*, 58(11), 3025-3036.
- Dubois, M., Claeys, H., Van den Broeck, L., and Inzé, D. (2017). Time of day determines *Arabidopsis* transcriptome and growth dynamics under mild drought. *Plant, cell & environment*, 40(2), 180-189.
- Dubos, C., Stracke, R., Grotewold, E., Weisshaar, B., Martin, C., and Lepiniec, L. (2010). MYB transcription factors in *Arabidopsis*. *Trends in plant science*, 15(10), 573-581.
- Edwards, K., Johnstone, C., and Thompson, C. (1991). A simple and rapid method for the preparation of plant genomic DNA for PCR analysis. *Nucleic acids research*, 19(6), 1349.
- Farooq, M., Wahid, A., Kobayashi, N., Fujita, D. B. S. M. A., and Basra, S. M. A. (2009). Plant drought stress: effects, mechanisms and management. In *Sustainable agriculture* (pp. 153-188). Springer, Dordrecht.

- Feng, J., Zhao, S., Chen, X., Wang, W., Dong, W., Chen, J., Shen, J., Liu, L., Kuang, T. (2015). Biochemical and structural study of Arabidopsis hexokinase 1. *Acta Crystallographica Section D: Biological Crystallography*, 71(2), 367-375.
- Ferguson, J. N., Humphry, M., Lawson, T., Brendel, O., and Bechtold, U. (2018). Natural variation of life-history traits, water use, and drought responses in Arabidopsis. *Plant Direct*, 2(1), e00035.
- Finkelstein, R. R., and Gibson, S. I. (2002). ABA and sugar interactions regulating development: cross-talk or voices in a crowd?. *Current opinion in plant biology*, 5(1), 26-32.
- Fu, L., Wang, P., and Xiong, Y. (2020). Target of Rapamycin signaling in plant stress responses. *Plant Physiology*, 182(4), 1613-1623.
- Gómez-Arjona, F. M., Raynaud, S., Ragel, P., and Mérida, Á. (2014). Starch synthase 4 is located in the thylakoid membrane and interacts with plastoglobule-associated proteins in Arabidopsis. *The Plant Journal*, 80(2), 305-316.
- Gao, S., Gao, J., Zhu, X., Song, Y., Li, Z., Ren, G., Zhou, x., and Kuai, B. (2016). ABF2, ABF3, and ABF4 promote ABA-mediated chlorophyll degradation and leaf senescence by transcriptional activation of chlorophyll catabolic genes and senescence-associated genes in Arabidopsis. *Molecular Plant*, 9(9), 1272-1285.
- Gauthier, L., Atanasova-Penichon, V., Chéreau, S., and Richard-Forget, F. (2015). Metabolomics to decipher the chemical defense of cereals against *Fusarium graminearum* and deoxynivalenol accumulation. *International journal of molecular sciences*, 16(10), 24839-24872.
- Ghillebert, R., Swinnen, E., Wen, J., Vandesteene, L., Ramon, M., Norga, K., Rolland, F., and Winderickx, J. (2011). The AMPK/SNF1/SnRK1 fuel gauge and energy regulator: structure, function and regulation. *The FEBS journal*, 278(21), 3978-3990.
- Gibson, S. I. (2005). Control of plant development and gene expression by sugar signaling. *Current opinion in plant biology*, 8(1), 93-102.

- Gill, P. K., Sharma, A. D., Singh, P., & Bhullar, S. S. (2001). Effect of various abiotic stresses on the growth, soluble sugars and water relations of sorghum seedlings grown in light and darkness. *Bulgarian Journal of Plant Physiology*, 27(1-2), 72-84.
- Granot, D. (2007). Role of tomato hexose kinases. *Functional Plant Biology* 34: 564-570
- Granot, D., David-Schwartz, R., and Kelly, G. (2013). Hexose kinases and their role in sugar-sensing and plant development. *Frontiers in Plant Science*, 4, 44.
- Guan, L. M., Zhao, J., and Scandalios, J. G. (2000). Cis-elements and trans-factors that regulate expression of the maize Cat1 antioxidant gene in response to ABA and osmotic stress: H₂O₂ is the likely intermediary signaling molecule for the response. *The Plant Journal*, 22(2), 87-95.
- Guo, J., Zeng, W., Chen, Q., Lee, C., Chen, L., Yang, Y., Cang, C., Ren, D., and Jiang, Y. (2016). Structure of the voltage-gated two-pore channel TPC1 from *Arabidopsis thaliana*. *Nature*, 531(7593), 196-201.
- Gupta, A. K., and Kaur, N. (2005). Sugar signalling and gene expression in relation to carbohydrate metabolism under abiotic stresses in plants. *Journal of biosciences*, 30(5), 761-776.
- Halford, N. G., and Hey, S. J. (2009). Snf1-related protein kinases (SnRKs) act within an intricate network that links metabolic and stress signalling in plants. *Biochemical Journal*, 419(2), 247-259.
- Halford, N. G., Hey, S., Jhurreea, D., Laurie, S., McKibbin, R. S., Paul, M., and Zhang, Y. (2003). Metabolic signalling and carbon partitioning: role of Snf1-related (SnRK1) protein kinase. *Journal of experimental botany*, 54(382), 467-475.
- Hamasaki, H., Kurihara, Y., Kuromori, T., Kusano, H., Nagata, N., Yamamoto, Y. Y., Shimada, H., and Matsui, M. (2019). SnRK1 kinase and the NAC transcription factor SOG1 are components of a novel signaling pathway mediating the low energy response triggered by ATP depletion. *Frontiers in plant science*, 10, 503.

- Han, S., Tang, R., Anderson, L. K., Woerner, T. E., and Pei, Z. M. (2003). A cell surface receptor mediates extracellular Ca²⁺ sensing in guard cells. *Nature*, 425(6954), 196-200.
- Harrison, M. A. (2012). Cross-talk between phytohormone signaling pathways under both optimal and stressful environmental conditions. In *Phytohormones and abiotic stress tolerance in plants*. (eds) pp. 49-76. Springer, Berlin, Heidelberg.
- Henriques, R., Bögre, L., Horváth, B., and Magyar, Z. (2014). Balancing act: matching growth with environment by the TOR signalling pathway. *Journal of experimental botany*, 65(10), 2691-2701.
- Henry, C., Bledsoe, S. W., Griffiths, C. A., Kollman, A., Paul, M. J., Sakr, S., and Lagrimini, L. M. (2015). Differential role for trehalose metabolism in salt-stressed maize. *Plant Physiology*, 169(2), 1072-1089.
- Henry, E., Fung, N., Liu, J., Drakakaki, G., and Coaker, G. (2015). Beyond glycolysis: GAPDHs are multi-functional enzymes involved in regulation of ROS, autophagy, and plant immune responses. *PLoS Genet*, 11(4), e1005199.
- Hildebrandt, T. M. (2018). Synthesis versus degradation: directions of amino acid metabolism during Arabidopsis abiotic stress response. *Plant molecular biology*, 98(1-2), 121-135.
- Hoekstra, F. A., Golovina, E. A., and Buitink, J. (2001). Mechanisms of plant desiccation tolerance. *Trends in plant science*, 6(9), 431-438.
- Hoshijima, M., Hattori, T., and Takigawa, M. (2017). Yeast two-hybrid system. In: *Protocols for screening for binding partners of CCN proteins*. pp.145-154. Humana Press, New York, NY.
- Hoth, S., Morgante, M., Sanchez, J. P., Hanafey, M. K., Tingey, S. V., and Chua, N. H. (2002). Genome-wide gene expression profiling in Arabidopsis thaliana reveals new targets of abscisic acid and largely impaired gene regulation in the *abi1-1* mutant. *Journal of cell science*, 115(24), 4891-4900.

Howe, K. L., Contreras-Moreira, B., De Silva, N., Maslen, G., Akanni, W., Allen, J., et al. (2020). Ensembl genomes 2020—enabling non-vertebrate genomic research. *Nucleic acids research*, 48(D1), D689-D695.

Huang, D. W., Sherman, B. T., Zheng, X., Yang, J., Imamichi, T., Stephens, R., and Lempicki, R. A. (2009). Extracting biological meaning from large gene lists with DAVID. *Current protocols in bioinformatics*, 27(1), 13-11.

Huang, Y., Guo, Y., Liu, Y., Zhang, F., Wang, Z., Wang, H., Wang, F., Li, D., Mao, D., Luan, S., Liang, M. and Chen, L. (2018). 9-cis-Epoxycarotenoid dioxygenase 3 regulates plant growth and enhances multi-abiotic stress tolerance in rice. *Frontiers in plant science*, 9, 162.

Huijser, C., Kortstee, A., Pego, J., Weisbeek, P., Wisman, E., and Smeekens, S. (2000). The Arabidopsis SUCROSE UNCOUPLED-6 gene is identical to ABSCISIC ACID INSENSITIVE-4: involvement of abscisic acid in sugar responses. *The Plant Journal*, 23(5), 577-585.

Hussain, M., Malik, M. A., Farooq, M., Ashraf, M. Y., and Cheema, M. A. (2008). Improving drought tolerance by exogenous application of glycinebetaine and salicylic acid in sunflower. *Journal of Agronomy and Crop Science*, 194(3), 193-199.

Ishizaki, K., Larson, T. R., Schauer, N., Fernie, A. R., Graham, I. A., and Leaver, C. J. (2005). The critical role of Arabidopsis electron-transfer flavoprotein: ubiquinone oxidoreductase during dark-induced starvation. *The Plant Cell*, 17(9), 2587-2600.

Izumi, M., and Ishida, H. (2019). An additional role for chloroplast proteins—an amino acid reservoir for energy production during sugar starvation. *Plant signaling & behavior*, 14(1), 1552057.

Jakoby, M., Weisshaar, B., Dröge-Laser, W., Vicente-Carbajosa, J., Tiedemann, J., Kroj, T., and Parcy, F. (2002). bZIP transcription factors in Arabidopsis. *Trends in plant science*, 7(3), 106-111.

Jaleel, C. A., Gopi, R., Sankar, B., Gomathinayagam, M., and Panneerselvam, R. (2008). Differential responses in water use efficiency in two varieties of *Catharanthus roseus* under drought stress. *Comptes Rendus Biologies*, 331(1), 42-47.

- Jaleel, C. A., Manivannan, P. A. R. A. M. A. S. I. V. A. M., Wahid, A., Farooq, M., Al-Juburi, H. J., Somasundaram, R. A. M. A. M. U. R. T. H. Y., and Panneerselvam, R. (2009). Drought stress in plants: a review on morphological characteristics and pigments composition. *International Journal of Agriculture and Biology*, 11(1), 100-105.
- Joshi, R., Wani, S. H., Singh, B., Bohra, A., Dar, Z. A., Lone, A. A., Pareek, A., and Singla-Pareek, S. L. (2016). Transcription factors and plants response to drought stress: current understanding and future directions. *Frontiers in Plant Science*, 7, 1029.
- Jossier, M., Bouly, J. P., Meimoun, P., Arjmand, A., Lessard, P., Hawley, S., Hardie, D.G. Thomas, M. (2009). SnRK1 (SNF1-related kinase 1) has a central role in sugar and ABA signalling in *Arabidopsis thaliana*. *The Plant Journal*, 59(2), 316-328.
- Jouhet, J., and Gray, J. C. (2009). Interaction of actin and the chloroplast protein import apparatus. *Journal of Biological Chemistry*, 284(28), 19132-19141.
- Kang, S. G., Price, J., Lin, P. C., Hong, J. C., and Jang, J. C. (2010). The *Arabidopsis* bZIP1 transcription factor is involved in sugar signaling, protein networking, and DNA binding. *Molecular plant*, 3(2), 361-373.
- Karve, A., Rauh, B. L., Xia, X., Kandasamy, M., Meagher, R. B., Sheen, J., and d. Moore, B. (2008). Expression and evolutionary features of the hexokinase gene family in *Arabidopsis*. *Planta*, 228(3), 411.
- Karve, A., Xia, X., and d. Moore, B. (2012). *Arabidopsis* Hexokinase-Like1 and Hexokinase1 form a critical node in mediating plant glucose and ethylene responses. *Plant Physiology*, 158(4), 1965-1975.
- Karve, R., Lauria, M., Virnig, A., Xia, X., Rauh, B. L., and d. Moore, B. (2010). Evolutionary lineages and functional diversification of plant hexokinases. *Molecular plant*, 3(2), 334-346.
- Keech, O., Pesquet, E., Gutierrez, L., Ahad, A., Bellini, C., Smith, S. M., and Gardeström, P. (2010). Leaf senescence is accompanied by an early disruption of the microtubule network in *Arabidopsis*. *Plant Physiology*, 154(4), 1710-1720.

Kelly, A. A., van Erp, H., Quettier, A. L., Shaw, E., Menard, G., Kurup, S., and Eastmond, P. J. (2013). The sugar-dependent1 lipase limits triacylglycerol accumulation in vegetative tissues of Arabidopsis. *Plant Physiology*, 162(3), 1282-1289.

Kelly, G., David-Schwartz, R., Sade, N., Moshelion, M., Levi, A., Alchanatis, V., and Granot, D. (2012). The pitfalls of transgenic selection and new roles of AtHXK1: a high level of AtHXK1 expression uncouples hexokinase1-dependent sugar signaling from exogenous sugar. *Plant Physiology*, 159(1), 47-51.

Kim, J. R., Yoon, H. W., Kwon, K. S., Lee, S. R., and Rhee, S. G. (2000). Identification of proteins containing cysteine residues that are sensitive to oxidation by hydrogen peroxide at neutral pH. *Analytical biochemistry*, 283(2), 214-221.

Kim, Y. M., Heinzl, N., GIESE, J. O., Koeber, J., Melzer, M., Rutten, T., Wirén, N., Sonnewald, U., and Hajirezaei, M. R. (2013). A dual role of tobacco hexokinase 1 in primary metabolism and sugar sensing. *Plant, cell & environment*, 36(7), 1311-1327.

Koch, J. L., Boulanger, S. C., Dib-Hajj, S. D., Hebbar, S. K., and Perlman, P. S. (1992). Group II introns deleted for multiple substructures retain self-splicing activity. *Molecular and Cellular Biology*, 12(5), 1950-1958.

Kolbe, A. R., Studer, A. J., Cornejo, O. E., and Cousins, A. B. (2019). Insights from transcriptome profiling on the non-photosynthetic and stomatal signaling response of maize carbonic anhydrase mutants to low CO₂. *BMC genomics*, 20(1), 1-13.

Kovacheva, S., Bédard, J., Patel, R., Dudley, P., Twell, D., Ríos, G., Koncz, C. and Jarvis, P. (2005). *In vivo* studies on the roles of Tic110, Tic40 and Hsp93 during chloroplast protein import. *The Plant Journal*, 41(3), 412-428.

Kunz, S., Gardeström, P., Pesquet, E., and Kleczkowski, L. A. (2015). Hexokinase 1 is required for glucose-induced repression of bZIP63, At5g22920, and BT2 in Arabidopsis. *Frontiers in plant science*, 6, 525.

Kwak, J. M., Mori, I. C., Pei, Z. M., Leonhardt, N., Torres, M. A., Dangl, J. L., Bloom, R. E., Bodde, S. Jones, J. and Schroeder, J. I. (2003). NADPH oxidase AtrbohD and AtrbohF genes function in ROS-dependent ABA signaling in Arabidopsis. *The EMBO journal*, 22(11), 2623-2633.

Lastdrager, J., Hanson, J., and Smeekens, S. (2014). Sugar signals and the control of plant growth and development. *Journal of experimental botany*, 65(3), 799-807.

Law, S. R., Chrobok, D., Juvany, M., Delhomme, N., Lindén, P., Brouwer, B., Ahad, A., Moritz, T., Jansson, S., Gardestrom, P., and Keech, O. (2018). Darkened leaves use different metabolic strategies for senescence and survival. *Plant Physiology*, 177(1), 132-150.

Lazova, G. N., Naidenova, T., and Velinova, K. (2004). Carbonic anhydrase activity and photosynthetic rate in the tree species *Paulownia tomentosa* Steud. Effect of dimethylsulfoxide treatment and zinc accumulation in leaves. *Journal of plant physiology*, 161(3), 295-301.

León, P., and Sheen, J. (2003). Sugar and hormone connections. *Trends in plant science*, 8(3), 110-116.

Li, C., Wu, H. M., and Cheung, A. Y. (2016). FERONIA and her pals: functions and mechanisms. *Plant physiology*, 171(4), 2379-2392.

Li, L., and Sheen, J. (2016). Dynamic and diverse sugar signaling. *Current opinion in plant biology*, 33, 116-125.

Li, P., Wind, J. J., Shi, X., Zhang, H., Hanson, J., Smeekens, S. C., and Teng, S. (2011). Fructose sensitivity is suppressed in *Arabidopsis* by the transcription factor ANAC089 lacking the membrane-bound domain. *Proceedings of the National Academy of Sciences*, 108(8), 3436-3441.

Li, X., Cai, W., Liu, Y., Li, H., Fu, L., Liu, Z., Xu, L., Liu, H., Xu, T., and Xiong, Y. (2017). Differential TOR activation and cell proliferation in *Arabidopsis* root and shoot apices. *Proceedings of the National Academy of Sciences*, 114(10), 2765-2770.

Liebsch D, and Keech O (2016). Dark-induced leaf senescence: new insights into a complex light-dependent regulatory pathway. *New Phytol*, 212: 563–570

Lu, C. A., Lin, C. C., Lee, K. W., Chen, J. L., Huang, L. F., Ho, S. L., Liu, H., Hsing, Y., and Yu, S. M. (2007). The SnRK1A protein kinase plays a key role in sugar signaling during germination and seedling growth of rice. *The Plant Cell*, 19(8), 2484-2499.

Lu, Q. S., Dela Paz, J., Pathmanathan, A., Chiu, R. S., Tsai, A. Y. L., and Gazzarrini, S. (2010). The C-terminal domain of FUSCA3 negatively regulates mRNA and protein levels, and mediates sensitivity to the hormones abscisic acid and gibberellic acid in *Arabidopsis*. *The Plant Journal*, 64(1), 100-113.

Luo, X., Chen, Z., Gao, J., and Gong, Z. (2014). Abscisic acid inhibits root growth in *Arabidopsis* through ethylene biosynthesis. *The Plant Journal*, 79(1), 44-55.

Mahmood, T., and Yang, P. C. (2012). Western blot: technique, theory, and trouble shooting. *North American journal of medical sciences*, 4(9), 429.

Maillard, A., Diquélou, S., Billard, V., Laîné, P., Garnica, M., Prudent, M., Garcia-Mina, J., Yvin, J., and Ourry, A. (2015). Leaf mineral nutrient remobilization during leaf senescence and modulation by nutrient deficiency. *Frontiers in plant science*, 6, 317.

Margalha, L., Confraria, A., and Baena-González, E. (2019). SnRK1 and TOR: modulating growth–defense trade-offs in plant stress responses. *Journal of experimental botany*, 70(8), 2261-2274.

Mayta, M. L., Lodeyro, A. F., Guiamet, J. J., Tognetti, V. B., Melzer, M., Hajirezaei, M. R., and Carrillo, N. (2018). Expression of a plastid-targeted flavodoxin decreases chloroplast reactive oxygen species accumulation and delays senescence in aging tobacco leaves. *Frontiers in plant science*, 9, 1039.

McCready, K., Spencer, V., and Kim, M. (2020). The Importance of TOR Kinase in Plant Development. *Frontiers in Plant Science*, 11, 16.

Milla, M. A. R., Uno, Y., Chang, F., Townsend, J., Maher, E. A., Quilici, D., and Cushman, J. C. (2006). A novel yeast two-hybrid approach to identify CDPK substrates: Characterization of the interaction between AtCPK11 and AtDi19, a nuclear zinc finger protein1. *FEBS letters*, 580(3), 904-911.

Miller, G. A. D., Suzuki, N., Ciftci-Yilmaz, S. U. L. T. A. N., and Mittler, R. O. N. (2010). Reactive oxygen species homeostasis and signalling during drought and salinity stresses. *Plant, cell & environment*, 33(4), 453-467.

Mittler, R. (2002). Oxidative stress, antioxidants and stress tolerance. *Trends in plant science*, 7(9), 405-410.

- Mittler, R., Vanderauwera, S., Gollery, M., and Van Breusegem, F. (2004). Reactive oxygen gene network of plants. *Trends in plant science*, 9(10), 490-498.
- Mohammadkhani, N., and Heidari, R. (2008). Drought-induced accumulation of soluble sugars and proline in two maize varieties. *World Applied Sciences Journal*, 3(3), 448-453.
- Moore, B., Zhou, L., Rolland, F., Hall, Q., Cheng, W. H., Liu, Y. X., Hwang, I., Jone, T., and Sheen, J. (2003). Role of the Arabidopsis glucose sensor HXK1 in nutrient, light, and hormonal signaling. *Science*, 300(5617), 332-336.
- Morkunas, I., Borek, S., Formela, M., and Ratajczak, L. (2012). Plant responses to sugar starvation. *Carbohydrates-Comprehensive Studies on Glycobiology and Glycotechnology*, 409-438.
- Moreau, M., Azzopardi, M., Clément, G., Dobrenel, T., Marchive, C., Renne, C., et al., and Meyer, C. (2012). Mutations in the Arabidopsis homolog of LST8/GβL, a partner of the target of rapamycin kinase, impair plant growth, flowering, and metabolic adaptation to long days. *The Plant Cell*, 24(2), 463-481.
- Munemasa, S., Hauser, F., Park, J., Waadt, R., Brandt, B., and Schroeder, J. I. (2015). Mechanisms of abscisic acid-mediated control of stomatal aperture. *Current opinion in plant biology*, 28, 154-162.
- Nakabayashi, R., and Saito, K. (2015). Integrated metabolomics for abiotic stress responses in plants. *Current opinion in plant biology*, 24, 10-16.
- Nakagawara, E., Sakuraba, Y., Yamasato, A., Tanaka, R., and Tanaka, A. (2007). Clp protease controls chlorophyll b synthesis by regulating the level of chlorophyllide a oxygenase. *The Plant Journal*, 49(5), 800-809.
- Nakashima, K., Yamaguchi-Shinozaki, K., and Shinozaki, K. (2014). The transcriptional regulatory network in the drought response and its crosstalk in abiotic stress responses including drought, cold, and heat. *Frontiers in plant science*, 5, 170.
- Nishimura, K., and van Wijk, K. J. (2015). Organization, function and substrates of the essential Clp protease system in plastids. *Biochimica et Biophysica Acta (BBA)-Bioenergetics*, 1847(9), 915-930

- Nishimura, K., Kato, Y., and Sakamoto, W. (2016). Chloroplast proteases: updates on proteolysis within and across suborganellar compartments. *Plant Physiology*, 171(4), 2280-2293.
- Nishimura, K., Kato, Y., and Sakamoto, W. (2017). Essentials of proteolytic machineries in chloroplasts. *Molecular plant*, 10(1), 4-19.
- Noctor, G., Mhamdi, A., and Foyer, C. H. (2014). The roles of reactive oxygen metabolism in drought: not so cut and dried. *Plant physiology*, 164(4), 1636-1648.
- Nomura, H., Komori, T., Kobori, M., Nakahira, Y., and Shiina, T. (2008). Evidence for chloroplast control of external Ca²⁺-induced cytosolic Ca²⁺ transients and stomatal closure. *The Plant Journal*, 53(6), 988-998.
- Nuccio, M. L., Wu, J., Mowers, R., Zhou, H. P., Meghji, M., Primavesi, L. F., Paul, M. J., Chen, X., Gao, Y., Haque, E. Basu, S. and Lagrimini, L. M. (2015). Expression of trehalose-6-phosphate phosphatase in maize ears improves yield in well-watered and drought conditions. *Nature biotechnology*, 33(8), 862-869.
- Nukarinen, E., Nägele, T., Pedrotti, L., Wurzinger, B., Mair, A., Landgraf, R., Börnke, F., Hanson, J., Teige, h., Baena-González, E., Weckwerth, W., and Dröge-Laser, W. (2016). Quantitative phosphoproteomics reveals the role of the AMPK plant ortholog SnRK1 as a metabolic master regulator under energy deprivation. *Scientific Reports*, 6, 31697.
- Nxele, X., Klein, A., and Ndimba, B. K. (2017). Drought and salinity stress alters ROS accumulation, water retention, and osmolyte content in sorghum plants. *South African Journal of Botany*, 108, 261-266.
- O'Hara, L. E., Paul, M. J., and Wingler, A. (2013). How do sugars regulate plant growth and development? New insight into the role of trehalose-6-phosphate. *Molecular plant*, 6(2), 261-274.
- Paul, M., Pellny, T., and Goddijn, O. (2001). Enhancing photosynthesis with sugar signals. *Trends in plant science*, 6(5), 197-200.
- Pott, D. M., Osorio, S., and Vallarino, J. G. (2019). From central to specialized metabolism: An overview of some secondary compounds derived from the primary

metabolism for their role in conferring nutritional and organoleptic characteristics to fruit. *Frontiers in plant science*, 10.

Price, J., Laxmi, A., Martin, S. K. S., and Jang, J. C. (2004). Global transcription profiling reveals multiple sugar signal transduction mechanisms in Arabidopsis. *The Plant Cell*, 16(8), 2128-2150.

Ramon, M., Rolland, F., and Sheen, J. (2008). Sugar sensing and signaling. *The Arabidopsis book American Society of Plant Biologists*, 6, e0117.

Ren, M., Qiu, S., Venglat, P., Xiang, D., Feng, L., Selvaraj, G., and Datla, R. (2011). Target of rapamycin regulates development and ribosomal RNA expression through kinase domain in Arabidopsis. *Plant physiology*, 155(3), 1367-1382.

Riaño-Pachón, D. M., Ruzicic, S., Dreyer, I., and Mueller-Roeber, B. (2007). PlnTFDB: an integrative plant transcription factor database. *BMC bioinformatics*, 8(1), 42.

Robaglia, C., Thomas, M., and Meyer, C. (2012). Sensing nutrient and energy status by SnRK1 and TOR kinases. *Current opinion in plant biology*, 15(3), 301-307.

Rodrigues, A., Adamo, M., Crozet, P., Margalha, L., Confraria, A., Martinho, C., Elias, A., Rabissi, A., Lumbreras, V., González-Guzmán, M., Rodriguez, P., Baena-González, e., and Antoni, R. (2013). ABI1 and PP2CA phosphatases are negative regulators of Snf1-related protein kinase1 signaling in Arabidopsis. *The Plant Cell*, 25(10), 3871-3884.

Rolland, F., and Sheen, J. (2005). Sugar sensing and signalling networks in plants. *Biochemical Society Transactions*, 33 (1): 269–271.

Rolland, F., Baena-González, E., and Sheen, J. (2006). Sugar sensing and signaling in plants: conserved and novel mechanisms. *Annual Review of Plant Biology*, 57, 675-709.

Rolland, F., Moore, B., and Sheen, J. (2002). Sugar sensing and signaling in plants. *The plant cell*, 14(suppl 1), S185-S205.

Rosa, M., Hilal, M., González, J. A., and Prado, F. E. (2004). Changes in soluble carbohydrates and related enzymes induced by low temperature during early

developmental stages of quinoa (*Chenopodium quinoa*) seedlings. *Journal of plant physiology*, 161(6), 683-689.

Rosa, M., Prado, C., Podazza, G., Interdonato, R., González, J. A., Hilal, M., and Prado, F. E. (2009). Soluble sugars: Metabolism, sensing and abiotic stress: A complex network in the life of plants. *Plant signaling & behavior*, 4(5), 388-393.

Rosenberger, C. L., and Chen, J. (2018). To grow or not to grow: TOR and SnRK2 coordinate growth and stress response in *Arabidopsis*. *Molecular cell*, 69(1), 3-4.

Roux, P. P., and Topisirovic, I. (2012). Regulation of mRNA translation by signaling pathways. *Cold Spring Harbor perspectives in biology*, 4(11), a012252.

Rudenko, N. N., Fedorchuk, T. P., Terentyev, V. V., Dymova, O. V., Naydov, I. A., Golovko, T. Borisova-Mubarakshina, M., and Ivanov, B. N. (2020). The role of carbonic anhydrase α -CA4 in the adaptive reactions of photosynthetic apparatus: the study with α -CA4 knockout plants. *Protoplasma*, 257(2), 489-499.

Ryabova, L. A., Robaglia, C., and Meyer, C. (2019). Target of Rapamycin kinase: Central regulatory hub for plant growth and metabolism. *Journal of experimental botany*, 70(8), 2211.

Sacks, M. M., Silk, W. K., and Burman, P. (1997). Effect of water stress on cortical cell division rates within the apical meristem of primary roots of maize. *Plant physiology*, 114(2), 519-527.

Salehi-Lisar, S. Y., and Bakhshayeshan-Agdam, H. (2016). Drought stress in plants: causes, consequences, and tolerance. *In Drought Stress Tolerance in Plants*, Vol 1 (pp. 1-16). Springer, Cham.

Schmalenbach, I., Zhang, L., Reymond, M., and Jiménez-Gómez, J. M. (2014). The relationship between flowering time and growth responses to drought in the *Arabidopsis Landsberg erecta* x Antwerp-1 population. *Frontiers in plant science*, 5, 609.

Scholl, R. L., May, S. T., and Ware, D. H. (2000). Seed and molecular resources for *Arabidopsis*. *Plant physiology*, 124(4), 1477-1480.

- Scossa, F., Brotman, Y., de Abreu e Lima, F., Willmitzer, L., Nikoloski, Z., Tohge, T. and Fernie, A.R. (2016) Genomics-based strategies for the use of natural variation in the improvement of crop metabolism. *Plant Science*. 242, 47 –64.
- Seo, M., and Koshiba, T. (2002). Complex regulation of ABA biosynthesis in plants. *Trends in plant science*, 7(1), 41-48.
- Shelton, D., Stranne, M., Mikkelsen, L., Pakseresht, N., Welham, T., Hiraka, H., Tabata, S., Sato, S., Paquette, S., Wang, T., Martin, C., and Bailey, P. (2012). Transcription factors of Lotus: regulation of isoflavonoid biosynthesis requires coordinated changes in transcription factor activity. *Plant Physiology*, 159(2), 531-547.
- Shi, L., Wu, Y., and Sheen, J. (2018). TOR signaling in plants: conservation and innovation. *Development*, 145(13).
- Shinozaki, K., Yamaguchi-Shinozaki, K., and Seki, M. (2003). Regulatory network of gene expression in the drought and cold stress responses. *Current opinion in plant biology*, 6(5), 410-417.
- Shulaev, V., Cortes, D., Miller, G., and Mittler, R. (2008). Metabolomics for plant stress response. *Physiologia plantarum*, 132(2), 199-208.
- Simon, M., Lee, M. M., Lin, Y., Gish, L., and Schiefelbein, J. (2007). Distinct and overlapping roles of single-repeat MYB genes in root epidermal patterning. *Developmental biology*, 311(2), 566-578.
- Simon, N. M., Sawkins, E., and Dodd, A. N. (2018). Involvement of the SnRK1 subunit KIN10 in sucrose-induced hypocotyl elongation. *Plant signaling & behavior*, 13(6), e1457913.
- Sjögren, L. L., Stanne, T. M., Zheng, B., Sutinen, S., and Clarke, A. K. (2006). Structural and functional insights into the chloroplast ATP-dependent Clp protease in Arabidopsis. *The Plant Cell*, 18(10), 2635-2649.
- Slaymaker, D. H., Navarre, D. A., Clark, D., del Pozo, O., Martin, G. B., and Klessig, D. F. (2002). The tobacco salicylic acid-binding protein 3 (SABP3) is the chloroplast carbonic anhydrase, which exhibits antioxidant activity and plays a role in the

hypersensitive defense response. *Proceedings of the national academy of sciences*, 99(18), 11640-11645.

Smeeckens, S. (2000). Sugar-induced signal transduction in plants. *Annual review of plant biology*, 51(1), 49-81.

Smeeckens, S., Ma, J., Hanson, J., and Rolland, F. (2010). Sugar signals and molecular networks controlling plant growth. *Current opinion in plant biology*, 13(3), 273-278.

Soneson, C., Love, M. I., and Robinson, M. D. (2016) Differential analyses for RNA-seq: transcript-level estimates improve gene-level inferences. *F1000Research*, 4, 1521.

Song, L., Huang, S. S. C., Wise, A., Castanon, R., Nery, J. R., Chen, H., Watanabe, M., Thomas, J., Bar-Joseph, Z., and Ecker, J. R. (2016). A transcription factor hierarchy defines an environmental stress response network. *Science*, 354(6312).

Song, Y., Yang, C., Gao, S., Zhang, W., Li, L., and Kuai, B. (2014). Age-triggered and dark-induced leaf senescence require the bHLH transcription factors PIF3, 4, and 5. *Molecular plant*, 7(12), 1776-1787.

Soto-Burgos, J., and Bassham, D. C. (2017). SnRK1 activates autophagy via the TOR signaling pathway in *Arabidopsis thaliana*. *PLoS One*, 12(8), e0182591.

Sussmilch, F. C., Brodribb, T. J., and McAdam, S. A. (2017). Up-regulation of NCED3 and ABA biosynthesis occur within minutes of a decrease in leaf turgor but AHK1 is not required. *Journal of Experimental Botany*, 68(11), 2913-2918.

Takahashi, F., Kuromori, T., Sato, H., and Shinozaki, K. (2018). Regulatory gene networks in drought stress responses and resistance in plants. In *Survival Strategies in Extreme Cold and Desiccation* (pp. 189-214). Springer, Singapore.

Takahashi, Y., Ebisu, Y., and Shimazaki, K. I. (2017). Reconstitution of abscisic acid signaling from the receptor to DNA via bHLH transcription factors. *Plant physiology*, 174(2), 815-822.

Thalmann, M., and Santelia, D. (2017). Starch as a determinant of plant fitness under abiotic stress. *New Phytologist*, 214(3), 943-951.

Tischer, S. V., Wunschel, C., Papacek, M., Kleigrew, K., Hofmann, T., Christmann, A., and Grill, E. (2017). Combinatorial interaction network of abscisic acid receptors and coreceptors from *Arabidopsis thaliana*. *Proceedings of the National Academy of Sciences*, 114(38), 10280-10285.

Tomé, F., Nägele, T., Adamo, M., Garg, A., Marco-Illorca, C., Nukarinen, E., Pedrotti, L., Peviani, A., Simeunovic, A., Tatkiewicz, A., Tomar, M. and Gamm, M. (2014). The low energy signaling network. *Frontiers in plant science*, 5, 353.

Uno, Y., Milla, M. A. R., Maher, E., and Cushman, J. C. (2009). Identification of proteins that interact with catalytically active calcium-dependent protein kinases from *Arabidopsis*. *Molecular Genetics and Genomics*, 281(4), 375-390.

Untergasser, A., Cutcutache, I., Koressaar, T., Ye, J., Faircloth, B. C., Remm, M., and Rozen, S. G. (2012). Primer3—new capabilities and interfaces. *Nucleic acids research*, 40(15), e115-e115.

Usadel, B., Bläsing, O. E., Gibon, Y., Retzlaff, K., Höhne, M., Günther, M., and Stitt, M. (2008). Global transcript levels respond to small changes of the carbon status during progressive exhaustion of carbohydrates in *Arabidopsis* rosettes. *Plant Physiology*, 146(4), 1834-1861.

Vainonen, J. P., Sakuragi, Y., Stael, S., Tikkanen, M., Allahverdiyeva, Y., Paakkarinen, V., *et al.* and Aro, E. M. (2008). Light regulation of CaS, a novel phosphoprotein in the thylakoid membrane of *Arabidopsis thaliana*. *The FEBS journal*, 275(8), 1767-1777.

Villar-Fernández, M. A., da Silva, R. C., Firlej, M., Pan, D., Weir, E., Sarembe, A., Raina, V., Bange, T., Weir, J. R., and Vader, G. (2020). Biochemical and functional characterization of a meiosis-specific Pch2/ORC AAA+ assembly. *Life Science Alliance*, 3(11).

Walter, A., Liebisch, F., and Hund, A. (2015). Plant phenotyping: from bean weighing to image analysis. *Plant methods*, 11(1), 1-11.

Wang, C., Yang, A., Yin, H., and Zhang, J. (2008). Influence of water stress on endogenous hormone contents and cell damage of maize seedlings. *Journal of Integrative Plant Biology*, 50(4), 427-434.

- Wang, L., Jin, X., Li, Q., Wang, X., Li, Z., and Wu, X. (2016). Comparative proteomics reveals that phosphorylation of β carbonic anhydrase 1 might be important for adaptation to drought stress in *Brassica napus*. *Scientific reports*, 6(1), 1-16.
- Wang, L., Li, H., Zhao, C., Li, S., Kong, L., Wu, W., Kongm W., Liu, Y., Wei, Y., Zhu, J., and Zhang, H. (2017). The inhibition of protein translation mediated by AtGCN1 is essential for cold tolerance in *Arabidopsis thaliana*. *Plant, cell & environment*, 40(1), 56-68.
- Wang, W. H., Chen, J., Liu, T. W., Chen, J., Han, A. D., Simon, M., Dong, X., He, J., and Zheng, H. L. (2014). Regulation of the calcium-sensing receptor in both stomatal movement and photosynthetic electron transport is crucial for water use efficiency and drought tolerance in *Arabidopsis*. *Journal of experimental botany*, 65(1), 223-234.
- Wang, W. H., Yi, X. Q., Han, A. D., Liu, T. W., Chen, J., Wu, F. H., Dong, X., He, J., Pei, Z., and Zheng, H. L. (2012). Calcium-sensing receptor regulates stomatal closure through hydrogen peroxide and nitric oxide in response to extracellular calcium in *Arabidopsis*. *Journal of Experimental Botany*, 63(1), 177-190.
- Wang, Y., and Liu, Y. (2013). Autophagic degradation of leaf starch in plants. *Autophagy*, 9(8), 1247-1248.
- Welsch, R., Zhou, X., Yuan, H., Álvarez, D., Sun, T., Schlossarek, D., Yang, Y., Zhang, H., Rodriguez-Concepcion, M., Li, L., and Thannhauser, T. W. (2018). Clp protease and OR directly control the proteostasis of phytoene synthase, the crucial enzyme for carotenoid biosynthesis in *Arabidopsis*. *Molecular plant*, 11(1), 149-162.
- Williams, S. P., Rangarajan, P., Donahue, J. L., Hess, J. E., and Gillaspay, G. E. (2014). Regulation of sucrose non-fermenting related kinase 1 genes in *Arabidopsis thaliana*. *Frontiers in plant science*, 5, 324.
- Wingett, S. W., and Andrews, S. (2018). FastQ Screen: A tool for multi-genome mapping and quality control. *F1000Research*, 7.
- Wingler, A., Fritzius, T., Wiemken, A., Boller, T., and Aeschbacher, R. A. (2000). Trehalose induces the ADP-glucose pyrophosphorylase gene, ApL3, and starch synthesis in *Arabidopsis*. *Plant Physiology*, 124(1), 105-114.

Wong, J. H., Alfatah, M., Sin, M. F., Sim, H. M., Verma, C. S., Lane, D. P., and Arumugam, P. (2017). A yeast two-hybrid system for the screening and characterization of small-molecule inhibitors of protein–protein interactions identifies a novel putative Mdm2-binding site in p53. *BMC biology*, 15(1), 108.

Wu, F. H., Shen, S. C., Lee, L. Y., Lee, S. H., Chan, M. T., and Lin, C. S. (2009). Tape-Arabidopsis Sandwich-a simpler Arabidopsis protoplast isolation method. *Plant methods*, 5(1), 16.

Xiong, F., Zhang, R., Meng, Z., Deng, K., Que, Y., Zhuo, F., Feng, L., Guo, S., Datla, R., and Ren, M. (2017). Brassinosteroid Insensitive 2 (BIN2) acts as a downstream effector of the Target of Rapamycin (TOR) signaling pathway to regulate photoautotrophic growth in Arabidopsis. *New Phytologist*, 213(1), 233-249.

Xiong, L., and Zhu, J. K. (2002). Molecular and genetic aspects of plant responses to osmotic stress. *Plant, Cell & Environment*, 25(2), 131-139.

Xiong, Y., and Sheen, J. (2012). Rapamycin and glucose-target of rapamycin (TOR) protein signaling in plants. *Journal of Biological Chemistry*, 287(4), 2836-2842.

Xiong, Y., and Sheen, J. (2015). Novel links in the plant TOR kinase signaling network. *Current opinion in plant biology*, 28, 83-91.

Xiong, Y., McCormack, M., Li, L., Hall, Q., Xiang, C., and Sheen, J. (2013). Glucose–TOR signalling reprograms the transcriptome and activates meristems. *Nature*, 496(7444), 181-186.

Yamada, K., and Osakabe, Y. (2018). Sugar compartmentation as an environmental stress adaptation strategy in plants. In *Seminars in Cell & Developmental Biology* (Vol. 83, pp. 106-114). Academic Press.

Yang, J., Worley, E., and Udvardi, M. (2014). A NAP-AAO3 regulatory module promotes chlorophyll degradation via ABA biosynthesis in Arabidopsis leaves. *The Plant Cell*, 26(12), 4862-4874.

Yang, T., Wang, L., Li, C., Liu, Y., Zhu, S., Qi, Y., Liu, X., Lin, Q., Luan, S., and Yu, F. (2015). Receptor protein kinase FERONIA controls leaf starch accumulation by

interacting with glyceraldehyde-3-phosphate dehydrogenase. *Biochemical and biophysical research communications*, 465(1), 77-82.

Yoon, Y., Seo, D. H., Shin, H., Kim, H. J., Kim, C. M., and Jang, G. (2020). The Role of Stress-Responsive Transcription Factors in Modulating Abiotic Stress Tolerance in Plants. *Agronomy*, 10(6), 788.

Yoshida, T., Fujita, Y., Maruyama, K., Mogami, J., Todaka, D., Shinozaki, K., and Yamaguchi-Shinozaki, K. A. Z. U. K. O. (2015). Four A rabidopsis AREB/ABF transcription factors function predominantly in gene expression downstream of SnRK2 kinases in abscisic acid signalling in response to osmotic stress. *Plant, cell & environment*, 38(1), 35-49.

You, J., and Chan, Z. (2015). ROS regulation during abiotic stress responses in crop plants. *Frontiers in plant science*, 6, 1092.

YUAN, T. T., XU, H. H., ZHANG, K. X., GUO, T. T., and LU, Y. T. (2014). Glucose inhibits root meristem growth via ABA INSENSITIVE 5, which represses PIN1 accumulation and auxin activity in A rabidopsis. *Plant, cell & environment*, 37(6), 1338-1350.

Zaynab, M., Fatima, M., Sharif, Y., Zafar, M. H., Ali, H., and Khan, K. A. (2019). Role of primary metabolites in plant defense against pathogens. *Microbial pathogenesis*, 137, 103728.

Zhang Y, Li Q, Wang Y, Sun L, shi W. (2018). Biological Function of Calcium-Sensing Receptor (CAS) and Its Coupling Calcium Signaling in Plants. *Preprints.org*; 2018. DOI: 10.20944/preprints201812.0028.v1.

Zhang, B., Zhang, C., Liu, C., Jing, Y., Wang, Y., Jin, L., Yang, L., Fu, A., Shi, J., Zhao, F., Lan, W., and Luan, S. (2018). Inner envelope CHLOROPLAST MANGANESE TRANSPORTER 1 supports manganese homeostasis and phototrophic growth in Arabidopsis. *Molecular plant*, 11(7), 943-954.

Zhang, J., Jia, W., Yang, J., and Ismail, A. M. (2006). Role of ABA in integrating plant responses to drought and salt stresses. *Field Crops Research*, 97(1), 111-119.

Zhu, S. Y., Yu, X. C., Wang, X. J., Zhao, R., Li, Y., Fan, R. C., *et al.* and Xu, Y. H. (2007). Two calcium-dependent protein kinases, CPK4 and CPK11, regulate abscisic acid signal transduction in Arabidopsis. *The Plant Cell*, 19(10), 3019-3036.

Appendices

Appendix A

Nicotiana benthamiana homologous proteins from *Arabidopsis thaliana*

1. Glyceraldehyde-3- phosphate dehydrogenase, **NbGAPDH-A** (A0A0A8IBT8)

Score	Expect	Method	Identities	Positives	Gaps
311 bits(796)	2e-107	Compositional matrix adjust.	175/399(44%)	241/399(60%)	17/399(4%)
Query 7	SVANSSLQVSNKGFSE-----FSGLR TSSAIPFGRKTNDDL SVVAFQTSVIGGGNKR				60
Sbjct 25	S N S S+ GFS FSG +A+ G+ + + A T + R				80
Query 61	GVVEAKLKVAINGFGRIGRNFLRCWHGRKDSPLDVIAINDTG-GVKQASHLLKYDSTLGI				119
Sbjct 81	K KV INGFGRIGR LR R D ++V+A+ND K +++ KYDST G				136
Query 120	FDADV KPVGTDGISVDGKVIQVSDRNPVNL PWGDLGIDLVI EGTGVFVDREGAGKHIQA				179
Sbjct 137	+ + + + ++GK ++VVS R+P +PW DLG + V+E +GVF A H++				196
Query 180	GAKKVLITAPGKGDIPYVVGVNADLYNPDESII SNASCTTNCLAPFVKVLDQKFGIIGK				239
Sbjct 197	GAKKV+I+AP D P +VVGVN Y P+ I+SNASCTTNCLAP KV+ ++FGI++G				255
Query 240	TMTTTHSYTG DQRLDA-SHRDLRRARAALNIVPTSTGA AKAVLV LPSLKGKLNGLIAL				298
Sbjct 256	MTT H+ T Q+ +D S +D R R A+ NI+P+STGA AKAV VLP L GKL G+A				315
Query 299	RVPTPNVSVVDLWVQVSKKTF AEEVNAAFREAADKELKGILDVCD EPLVSVDFRCS DVSS				358
Sbjct 316	RVPTPNVSVVDL ++ K E+V AA + A++ L+GIL +E +VS DF SS				375
Query 359	TVDASLTMVMGDDMVKVI AWYDNEWGYSQRVVDLADIVA				397
Sbjct 376	DA+ + + +K+++WYDNEWGYS RV+DL + +A				414


2. Chloroplast ATP-dependent Clp protease protein, NbClpC1B (A0A088F8F4)

Q9FI56	CLPC1_ARATH - Chaperone protein ClpC1, chloroplastic	Arabidopsis thaliana (Mouse-ear cress)	
E-value: 0.0			
Score: 3982			
Ident.: 87.0%			
Positives : 90.9%			
Query Length: 923			
Match Length: 929			
A0A088F8F4	A0A088F8F4_NICBE3	RALVQSTNIPSSVAGEMTRQFSGSGKNNKTKVMKLCN-VQPPSIRLTNFTGLRGCNAIDTL	61
Q9FI56	CLPC1_ARATH	R L QST PS + GSG++++VKM+C+ +Q +R+ F GLRG NA+DTL	64
A0A088F8F4	A0A088F8F4_NICBE62	VKSGQTLHSKVAAATSVRRPKGCRFVKAMFERFTEKAIKIVIMLAQEEARRLGHNFVGT	121
Q9FI56	CLPC1_ARATH	KS Q HSKV A +V + K RF KAMFERFTEKAIKIVIMLAQEEARRLGHNFVGT	124
A0A088F8F4	A0A088F8F4_NICBE122	QILLGLIGEGTGIAAKILLGLIGEGTGIAAKVLKSMGINLKDARVEVEKIIGRSGGFVAV	181
Q9FI56	CLPC1_ARATH	QILLGLIGE-----GTGIAAKVLKSMGINLKDARVEVEKIIGRSGGFVAV	169
A0A088F8F4	A0A088F8F4_NICBE182	EIPFTPRAKRVLESLLEEARQLGHNVYIGSEHLLGLLREGEVVAARV-----	228
Q9FI56	CLPC1_ARATH	EIPFTPRAKRVLESLLEEARQLGHNVYIGSEHLLGLLREGEVVAARV	229
A0A088F8F4	A0A088F8F4_NICBE229	--IRMVGSNEAVGASVGGGTSQKMFTEEEYGTNLTKLAEEGKLDPVVGRQPQIERVTQ	286
Q9FI56	CLPC1_ARATH	IRMVGE+NE V A+VGGG+S KMFTEEEYGTNLTKLAEEGKLDPVVGRQPQIERV Q	288
A0A088F8F4	A0A088F8F4_NICBE287	ILGRRTKNNPCLIGEPGVGKTAIAEGLAQRIANGDVPETIEGKRVITLDMGLLVAGTKYR	346
Q9FI56	CLPC1_ARATH	ILGRRTKNNPCLIGEPGVGKTAIAEGLAQRIA+GDVPETIEGKRVITLDMGLLVAGTKYR	348
A0A088F8F4	A0A088F8F4_NICBE347	GEFEERLKKLMEEIRQSDEIILFIDEVHTLIGAGAAEGIDAANILKPALARGELQCIGA	406
Q9FI56	CLPC1_ARATH	GEFEERLKKLMEEI+QSDEIILFIDEVHTLIGAGAAEGIDAANILKPALARGELQCIGA	408
A0A088F8F4	A0A088F8F4_NICBE407	TTLDEYRKHIEKDPALERFPQVVKVPEFTVDETIQILKGLRERYEIHKKLRYTDEALEAA	466
Q9FI56	CLPC1_ARATH	TTLDEYRKHIEKDPALERFPQVVKVPEFTVDETIQILKGLRERYEIHKKLRYTDE+L AA	468
A0A088F8F4	A0A088F8F4_NICBE467	AQLSYQYISDRFLPDKAIDLIDEAGSRVRLRHAQLPEEARELEKELRQITKEKNEAVRQ	526
Q9FI56	CLPC1_ARATH	AQLSYQYISDRFLPDKAIDLIDEAGSRVRLRHAQ+PEEARELEKELRQITKEKNEAVRQ	528
A0A088F8F4	A0A088F8F4_NICBE527	DFEKAGELRDREMDLKAQISALIDKKNKEMSKAESEAGDTGPIVTEADIQHIVSSWTGIPV	586
Q9FI56	CLPC1_ARATH	DFEKAG LRDRE++L+A++SA+ K KEMSKAESE G+ GP+VTE+DIQHIVSSWTGIPV	588
A0A088F8F4	A0A088F8F4_NICBE587	EKVSTDESDDLKMEETLHRIIGQDEAVKAIIRAIRARVGLKPNRPIASFIIFSGPTG	646
Q9FI56	CLPC1_ARATH	EKVSTDESDDLKMEETLH RIIGQDEAVKAIIRAIRARVGLKPNRPIASFIIFSGPTG	648
A0A088F8F4	A0A088F8F4_NICBE647	VGKSELAKALAAAYFGSEEMIRLDMSEFMERHTVSKLIGSPFGYVGYTEGGQLTEAVRR	706
Q9FI56	CLPC1_ARATH	VGKSELAKALAAAYFGSEEMIRLDMSEFMERHTVSKLIGSPFGYVGYTEGGQLTEAVRR	708
A0A088F8F4	A0A088F8F4_NICBE707	RFYTVVLFDEIEKAHFDVFNQMLQILEDGRLTDSKGRVDFKNTLLIMTSNVGSSVIEKG	766
Q9FI56	CLPC1_ARATH	RFYTVVLFDEIEKAHFDVFNQMLQILEDGRLTDSKGRVDFKNTLLIMTSNVGSSVIEKG	768
A0A088F8F4	A0A088F8F4_NICBE767	GRRIGFDLDYDEKDS SYNRIKSLVTEELKQYFRPEFLNRLDEMIVFRQLTKLEVREIADI	826
Q9FI56	CLPC1_ARATH	GRRIGFDLDYDEKDS SYNRIKSLVTEELKQYFRPEFLNRLDEMIVFRQLTKLEVREIADI	828
A0A088F8F4	A0A088F8F4_NICBE827	MLKEVFERLKNKEIELQVTERFRDVRVDEGYNPSYGARPLRRAIMRLLEDMAEKMLAGE	886
Q9FI56	CLPC1_ARATH	+LKEVFERLK KEIELQVTERF++RVVDEGYNPSYGARPLRRAIMRLLEDMAEKMLA E	888
A0A088F8F4	A0A088F8F4_NICBE887	IKEGDSVIVDSDGNVTVLNGTSGTFSDPAPE	919
Q9FI56	CLPC1_ARATH	IKEGDSVIVDSD++GNVTVLNG SGTF+ E	921

3. Calcium-sensing receptor, NbCAS (K7ZLE1)

Q9FN48 CAS_ARATH - Calcium sensing receptor, chloroplastic *Arabidopsis thaliana* (Mouse-ear cress)


E-value: 2.4e-171
 Score: 1260
 Ident.: 67.1%
 Positives : 82.7%
 Query Length: 394
 Match Length: 387



K7ZLE1	K7ZLE1_NICBE	27	PTLSQKPEFTSNVSUSLSTSTALFLFFLTAT-HEARA-LSLPKEDIVSSLNQVESAVN	64
Q9FN48	CAS_ARATH	19	P+ S K + VSVSL TST++ L LF + HEA+A +S+FK+ IVSSL +VE +N	78
K7ZLE1	K7ZLE1_NICBE	85	QAQEVGSNIFDARSRVIGPVIEFVKPGIDVALPLVKQAGEEVLKNASFWISDATKKAQEA	144
Q9FN48	CAS_ARATH	79	Q QE GS++FDA RV V + +KP +D ALP+ KQAGEE +K ASP S+A+KKAQEA	138
K7ZLE1	K7ZLE1_NICBE	145	MQSAGMDRQPVMTAARTVVDAAQQTSKVIEGAKFIASSTVETISSADFAIIAVAGGTLFL	204
Q9FN48	CAS_ARATH	139	MQS+G D++FV AAKTV D AQQTSK IE AKFIASST++TISSADF++I VA G FL	198
K7ZLE1	K7ZLE1_NICBE	205	AYLLFPFVLSALSFSRLRGYKGLTPAQTLTDMCSKNYVLIDIRTEKDKKAGIPRLPSSA	264
Q9FN48	CAS_ARATH	199	AYLL FPV SA+SF+ RGYKG+LTPAQTLTLD +C+KNY+++DIR+EKDK+KAGIPRLPS+A	258
K7ZLE1	K7ZLE1_NICBE	265	KNKMIQIPLEDLPSKLRSLVRNNAKKEAELVALKISYLKINKGNSNIVIMDSYSDSAKT	324
Q9FN48	CAS_ARATH	259	KN++I IPLE+LP+K++ +VRN+K+VEAE+ ALKISYLKINKGNSNI+I+DSY+DSAK V	318
K7ZLE1	K7ZLE1_NICBE	325	ARTLTLGLFKNCWIMIDGFSGGRWLQSKLGTDSYNFSFAQVLSFSPRVIPAAARRFGTTG	384
Q9FN48	CAS_ARATH	319	ARTL LG+KNC+I+IDGFSGGRWLQS+LGTDSYNFSFAQVLSFSPR+IPAA+R FGT	378
K7ZLE1	K7ZLE1_NICBE	385	TVKLL	389
Q9FN48	CAS_ARATH	379	K L	383
			GTKFL	

4. Carbonic anhydrase, CA (A4D0J9)


P27140		BCA1_ARATH - Beta carbonic anhydrase 1, chloroplastic Arabidopsis thaliana (Mouse-ear cress)	
E-value: 1.2e-96			
Score: 740			
Ident.: 80.6%			
Positives : 88.9%			
Query Length: 177			
Match Length: 347			



A4D0J9	A4D0J9_NICBE	3	YMFACSDSRVCPHILNFPQGEAFVVRNINAMVFPAYDKTRYSGVGAARIEYAVLHLKVEN	62
P27140	BCA1_ARATH	162	YMFACSDSRVCPH+L+PQPG+AFVVRNINAMVFP +DK +Y GVGAAIEYAVLHLKVEN	221
A4D0J9	A4D0J9_NICBE	63	IIVIGHSACGGIKGLMSLPADGSESTAFIEDWVKIGLPAKARVQGDHVDKCFADQCTACE	122
P27140	BCA1_ARATH	222	IIVIGHSACGGIKGLMS P DG+ ST FIEDWVKI LPAK+KV + D F DQC CE	281
A4D0J9	A4D0J9_NICBE	123	KEAVNVSLNLLTYPFVREGLVKKTLALKGGHYDFVNGGFELWGLEFGLSPSLSV	177
P27140	BCA1_ARATH	282	REAVNVSLANLLTYPFVREGLVKGTLALKGGYYDFVKGAFELWGLEFGLSETSSV	336

5. Phosphoglycerate kinase, PRK (E5LLE7)

Q9SAJ4		PGKY3_ARATH - Phosphoglycerate kinase 3, cytosolic Arabidopsis thaliana (Mouse-ear cress)	
E-value: 0.0			
Score: 1756			
Ident.: 86.2%			
Positives : 94.0%			
Query Length: 481			
Match Length: 401			



E5LLE7	E5LLE7_NICBE	78	KKSUGDLTAELKGRNVFVRADLNVLDDNQNIITDDTRIRAAVPTIKHLMANGAKVILST	137
Q9SAJ4	PGKY3_ARATH	4	K+SVG L A+LKGK+VFVR DLNVPLDDN NITDDTRIRAAVPTIK+LM NG++V+L +	63
E5LLE7	E5LLE7_NICBE	138	HLGRPKGVTPKYSLAPLVPRLSELLGIQVVKVEDCIGPEVEKLVASLPEGGVLLLENVRF	197
Q9SAJ4	PGKY3_ARATH	64	HLGRPKGVTPKYSL FLVPRLSLELG++VV D IG EV+KLVA LPEGGVLLLENVRF	123
E5LLE7	E5LLE7_NICBE	198	YKEEEKNEPEFAKKLASLADLYVNDAPFGTAHRAHASTEGLVTKFLKPSVAGFLLQKELDYL	257
Q9SAJ4	PGKY3_ARATH	124	YAEEEKNDPEFAKKLAALADLVVNDAPFGTAHRAHASTEGLVAKFLKPSVAGFLMQKELDYL	183
E5LLE7	E5LLE7_NICBE	258	VGAVSNPKRPFARIVGGSKVSSKIGVIESLLEKCDILLGGGMIFTFYKAQGLSVGSSLV	317
Q9SAJ4	PGKY3_ARATH	184	VGAVANPKRPFARIVGGSKVSTKIGVIESLLNTVDILLGGGMIFTFYKAQGLSVGSSLV	243
E5LLE7	E5LLE7_NICBE	318	EEDKLELATSLLERAKAKGVSLLLPSDVVIADKFAFDANSKIVPASAIPDGMGLDIGPD	377
Q9SAJ4	PGKY3_ARATH	244	EEDKLDLAKSLMERAKAKGVSLLLPTDVVIADKFAFDANSKIVPATAIPDGMGLDIGPD	303
E5LLE7	E5LLE7_NICBE	378	SUKTFNDALDITTKIIVWNGPMGVFEFDRFVAGTEAIAKKLADLSGKGVTTIIGGGDSVAA	437
Q9SAJ4	PGKY3_ARATH	304	S+KTF++ALDITTKI+IWNNGPMGVFEFDRFAAGTEAVAKQLAELSGKGVTTIIGGGDSVAA	363
E5LLE7	E5LLE7_NICBE	438	VEKVGASVMSHISTGGGASLELLEGGKVLPGVVALDEA	475
Q9SAJ4	PGKY3_ARATH	364	VEKVG+A MSHISTGGGASLELLEGGK LPGA+ALDEA	401

6. Chloroplast elongation factor Tu (D5LT98)

Q56ZD8	Q56ZD8_ARATH - Translation elongation factor EF-Tu, chloroplast <i>Arabidopsis thaliana</i> (Mouse-ear cress)			
E-value: 8.1e-23				
Score: 210				
Ident.: 88.8%				
Positives : 89.5%				
Query Length: 38				
Match Length: 45				
D5LT98	D5LT98_NICBE	1	VNMVVELIMPVACEQGMRFAIREGGKIVGAGVIGKILE	38
			V +VVELI PVACEQGMRFAIREGGKIVGAGVI ILE	
Q56ZD8	Q56ZD8_ARATH	8	VRIVVELIVPVACEQGMRFAIREGGKIVGAGVIGIILE	45

Appendix B

The full output sequencing for the Stop codon (TGA) were detected in

pNAT:DUF:GFP.

(1884 bp)

```

CCGGGGGAAGGACCCCCAGGGAAAAACAACCTCCCCCAAGGGGGCGGAACCCCC
CCAGGCCCCCAGAGCCCCACGGGCCCCGGGCCCCCCCCCCCGGGAGGGTGGTCCC
GCCCAAAAAAGGGCCCCCGGAAACCCTCGCCAGGGACTAAAAATCGGCCCTCAGGG
CCGGGACCGCCAACCCCCCCCCCAAGGAAGTGCCCCGAGGTGCCCGGCCCGGCACC
TTCCGTGGGCAATAAATTTTTTTTCTCCTTCTTTTGTCCGAGTCCCCGTTTC
GCGAGATCTCTCCGATCGATTGAGTGTATTAGTCAAGGGTTATGAGAGGATGGCTAC
GGTTTCGGCGATGGACGCCAGAGATTTGCCTGGTGTAAAGAATCCGAAATCGAGATTG
TACTGGCAATTCTCAGCTCCGGTGAAAGAAGACTACAAGATTAGCAGAGAGGAGGAAG
AAGAAGAAGAAGAAGATAAGCAGAGTACTACGTGAATATGGGTCACGCCGTTTCGTAG
TATCAGAGAAGAGTTTCTCTGTTGTTCTACAAAGAGCTTAATTTTGACATTTACAGGTT
TGATGAAGATTCTCGATTTAAATTGAACTGCTCTCTGATTAGCTCTCTCAAAGAATCTTTT
TGCTTCAGAGTCATGCTTATATCCCAAATTTGATCTGTTCTTGTTAGGTTTCTTAGAGA
ATGATCTGTTTTATCAGTTGGTGATTAGCTCTTTCTTTGTCTAATTCGCAGGGATGAT
ATTGTTTTCAAAGACCCTATGAACACTTTCATGGGAATTGATAACTACAAATCCATATTT
GGGGCCTTACGTTTCCATGGAAGGATCTTCTTCAGAGCACTATGTGTGGACATTGTTAG
TGTTTGGCAACCCACAGAGAACACTCTGATGATACGATGGACTGTTTCATGGAATTCCTC
GTGGTCCGTGGGAGACTCGTGGTCGATTGATGGTACTTCTGAGTATAAATTCGATAAG
AATGGCAAGATTTATGAGCATAAAGTCGATAACATAGCCATTAATTCGCCTCCAAAGTTT
CAAATGCTCACTGTTCAAGAGCTTGTGGAAGCCATTAGCTGCCCTTCGACTCCCAAGCC
GACCTACTTTGAGTTCGGAGATTGAAAGGGTGGGGCGCGCCGACCCAGCTTTCTTGAC
AAAGTGGTGATCATGGTGAGCAAGGGCGAGGAGCTGTTACCCGGGGTGGTGCCCATC
CTGGTCGAGCTGGACGGCGACGTAACGGCCACAAGTTCAGCGTGTCCGGCGAGGGC
GAGGGCGATGCCACCTACGGCAAGCTGACCCTGAAGTTCATCTGCACCACCGGCAAG
CTGCCCCGTGCCCTGGCCCACCCTCGTGACCACCTTACCTACGGCGTGCAGTGCTTCA
GCCGCTACCCCGACCACATGAAGCAGCACGACTTCTCAAGTCCGCCATGCCCGAAGG
CTACGTCCAGGAGCGCACCATCTTCTTCAAGGACGACGGCAACTACAAGACCCGCGCC
GAGGTGAAGTTCGAGGGCGACACCCTGGTGAACCGCATCGAGCTGAAGGGCATCGAC
TTCAAGGAGGACGGCAACATCCTGGGGCACAAGCTGGAGTACAACACTACAACAGCCACA
ACGTCTATATCATGGCCGACAAGCAGAAGAACGGCATCAAGGTGAACTTCAAGATCCG
CCACAACATCGAGGACGGCAGCGTGCAGCTCGCCGACCACTACCAGCAGAACACCCC
CATCGGCGACGGCCCCGTGCTGCTGCCCGACAACCACTACCTGAGCACCCAGTCCGC
CCTGAGCAAAGACCCCAACGAGAAGCGCGGATCACATGGTCCTGCTGGAGTTCGTGA
CCGCCGCCGGGATCACTCACGGC

```

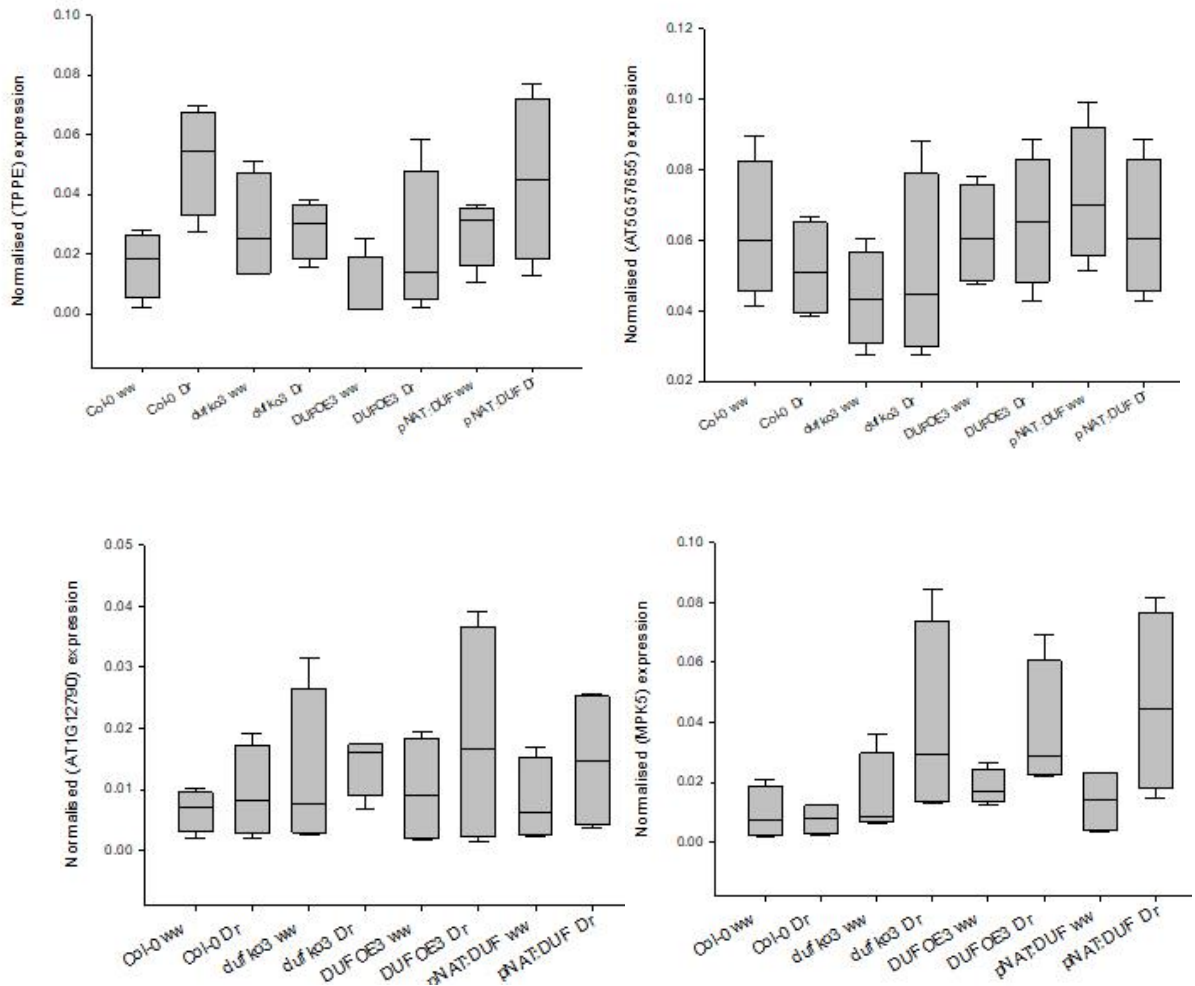

Appendix C

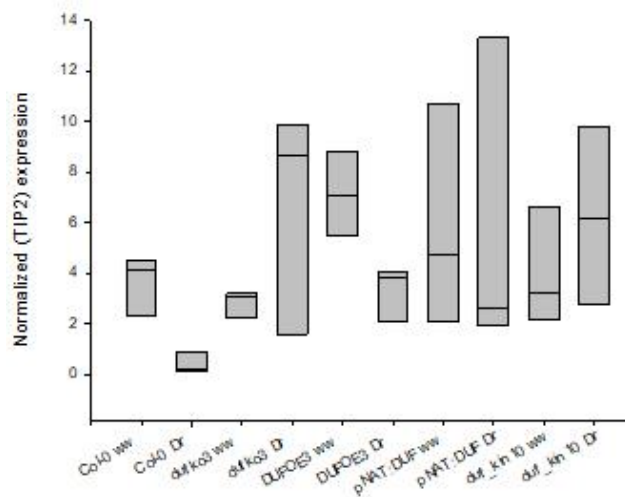
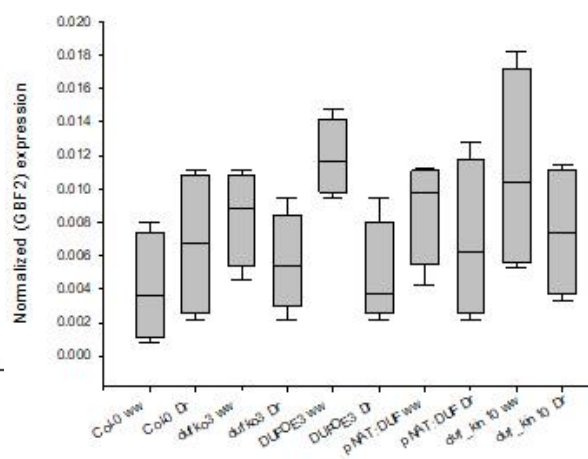
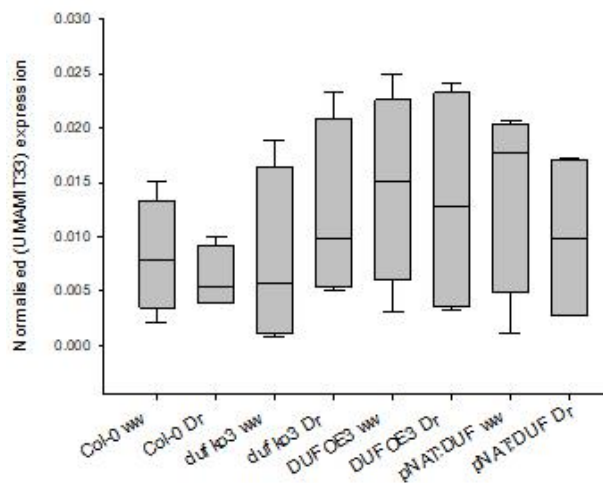
Summary averages of Arabidopsis growth stages under normal condition for Col-0 and mutants.

	Col-0	dufKO3	DUFOE2	DUFOE3	DUFOE4	DUF1	DUF4	kin10-2	KIN11
germination	4.917	4.800	4.667	3.455	3.857	4.500	5.333	4.000	5.250
1.02	10.333	10.600	10.500	9.000	10.000	10.800	11.556	9.750	10.875
1.03	13.500	13.900	14.167	12.455	12.833	14.100	14.000	13.500	13.375
1.04	14.917	14.900	15.667	13.636	14.167	15.000	15.444	14.333	14.875
1.05	17.083	17.100	17.167	15.091	15.667	16.300	17.222	15.500	16.875
1.06	18.500	18.200	18.167	16.545	17.333	17.800	18.556	17.250	18.125
1.07	19.333	19.500	19.167	17.909	18.333	19.000	19.333	18.500	19.250
1.08	20.667	20.400	20.000	19.000	19.333	20.200	20.444	19.583	20.375
1.09	21.917	21.600	21.000	20.091	20.833	21.400	21.778	20.417	21.500
1.1	23.417	23.100	22.167	21.182	22.167	22.600	23.222	21.750	22.875
1.11	24.333	24.800	23.667	22.545	23.333	23.700	24.333	22.833	24.375
1.12	25.583	25.900	24.833	23.636	24.667	25.000	25.556	24.167	25.625
1.13	26.500	26.900	25.833	24.909	25.200	26.500	26.000	25.000	27.000
1.14	27.917	28.200	27.000	26.000	26.000	27.556	27.375	26.417	27.714
1.15	28.636	29.333	28.167	27.182	27.000	28.286	28.875	27.091	28.000
0.16	29.000	29.167	28.750	27.625	27.600	28.600	29.000	27.667	28.667

Appendix D

Different gene expression in Col-0 and mutants which does not show any significant differences under well-watered and drought conditions





Appendix E

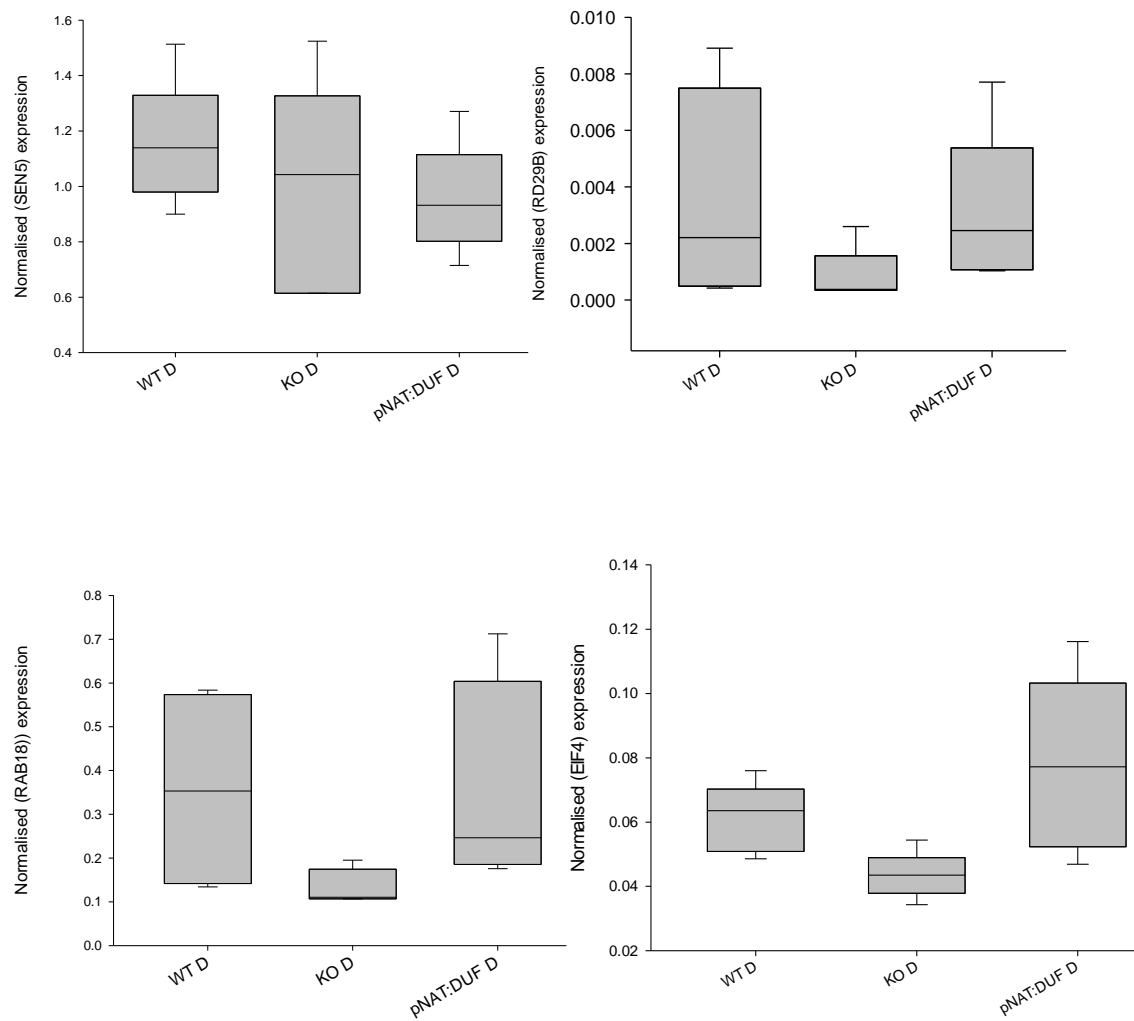
Significant differences between different mutants under well-watered and drought conditions.

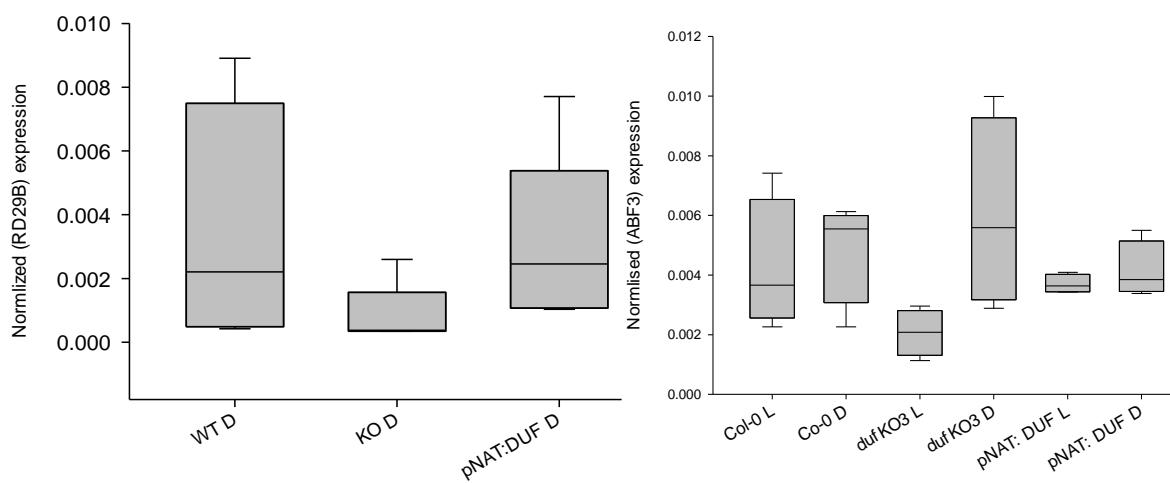
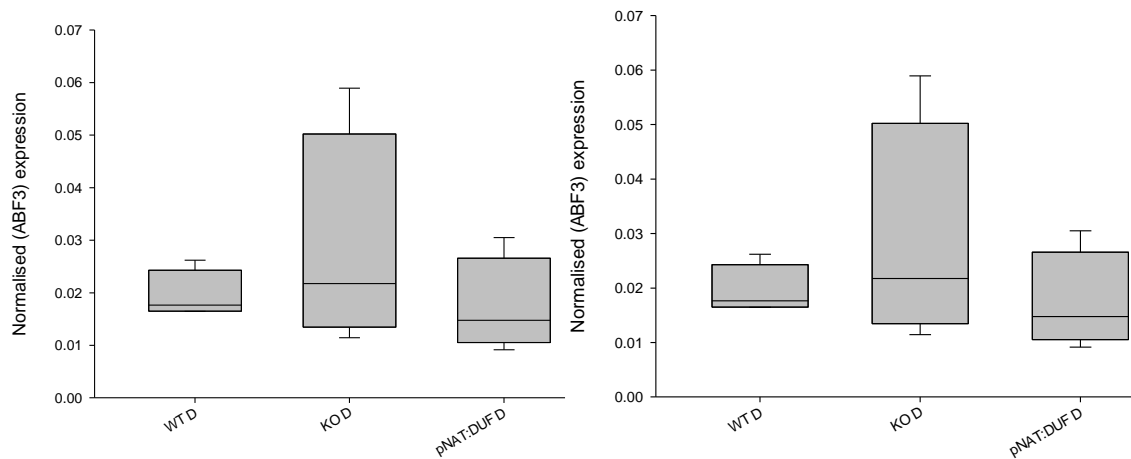
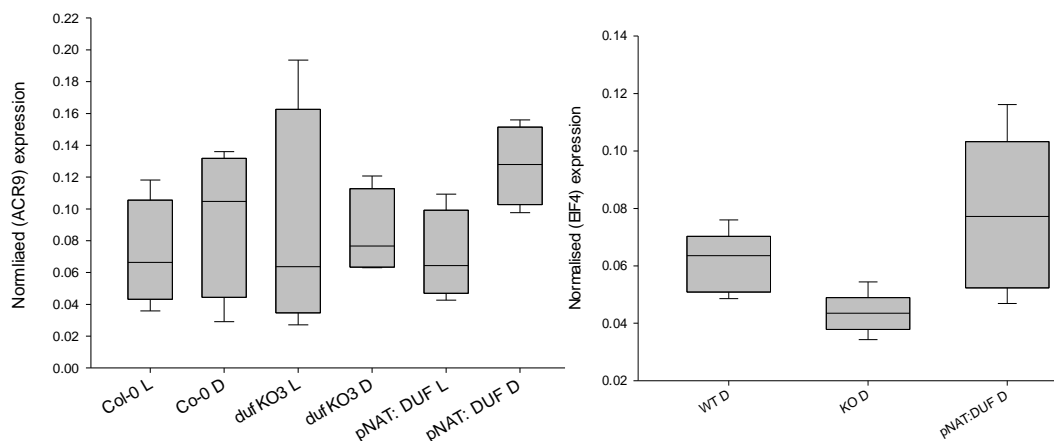
Gene	Compared genotype	condition	Adjust p-Value
DUF2358	<i>DUFOE3 vs dufko3</i>	drought	2.23E-03
	<i>DUFOE3 vs dufko3</i>	Well-watered	2.1E-05
	<i>pNAT:DUF vs dufko3</i>	drought	3.914E-03
	<i>pNAT:DUF vs dufko3</i>	Well-watered	3.80E-03
	<i>DUFOE3 vs duf_kin10-2</i>	drought	2.68E-04
	<i>DUFOE3 vs duf_kin10-2</i>	Well-watered	4.13E-03
	<i>DUFOE3 vs kin10-2</i>	drought	2.98E-04
	<i>pNAT:DUF vs duf_kin10-2</i>	drought	3.17E-03
	<i>pNAT:DUF vs duf_kin10-2</i>	Well-watered	7.99E-04
KIN10	<i>DUFOE3 vs kin10-2</i>	Well-watered	3.57E-03
	<i>DUFOE3 vs kin10-2</i>	drought	2.68E-03
	<i>pNAT:DUF vs duf_kin10-2</i>	drought	1.68E-03
	<i>pNAT:DUF vs duf_kin10-2</i>	Well-watered	2.66E-03
ABF3	<i>DUFOE3 vs duf_kin10-2</i>	Well-watered	1.50E-03
	<i>pNAT:DUF vs duf_kin10-2</i>	Well-watered	1.58E-03
ABI5	<i>dufko3 vs duf_kin10-2</i>	drought	2.89E-03
	<i>pNAT:DUF vs kin10-2</i>	Well-watered	4.02E-03
	<i>kin10-2 VS duf_kin10-2</i>	drought	8.07E-04
ACR5	<i>pNAT:DUF vs kin10-2</i>	drought	1.03E-03
	<i>DUFOE3 vs kin10-2</i>	drought	2.78E-03
	<i>duf_kin10-2 vs kin10-2</i>	drought	3.53E-04
ATTPS5	<i>dufko3 vs kin10-2</i>	drought	1.29E-03
	<i>pNAT:DUF vs dufko3</i>	drought	3.24E-03
CYP71B4	<i>DUFOE3 vs dufko3</i>	Well-watered	3.13E-03
	<i>DUFOE3 vs kin10-2</i>	Well-watered	6.09E-04
AT4G25580	<i>dufko3 vs duf_kin10-2</i>	Well-watered	2.20E-03
	<i>dufko3 vs duf_kin10-2</i>	drought	3.66E-03
	<i>pNAT:DUF vs duf_kin10-2</i>	Well-watered	3.41E-03
	<i>dufko3 vs kin10-2</i>	drought	4.43E-03
AtHXK2	<i>dufko3 vs duf_kin10-2</i>	drought	8.03E-04
	<i>dufko3 vs kin10-2</i>	drought	4.91E-04

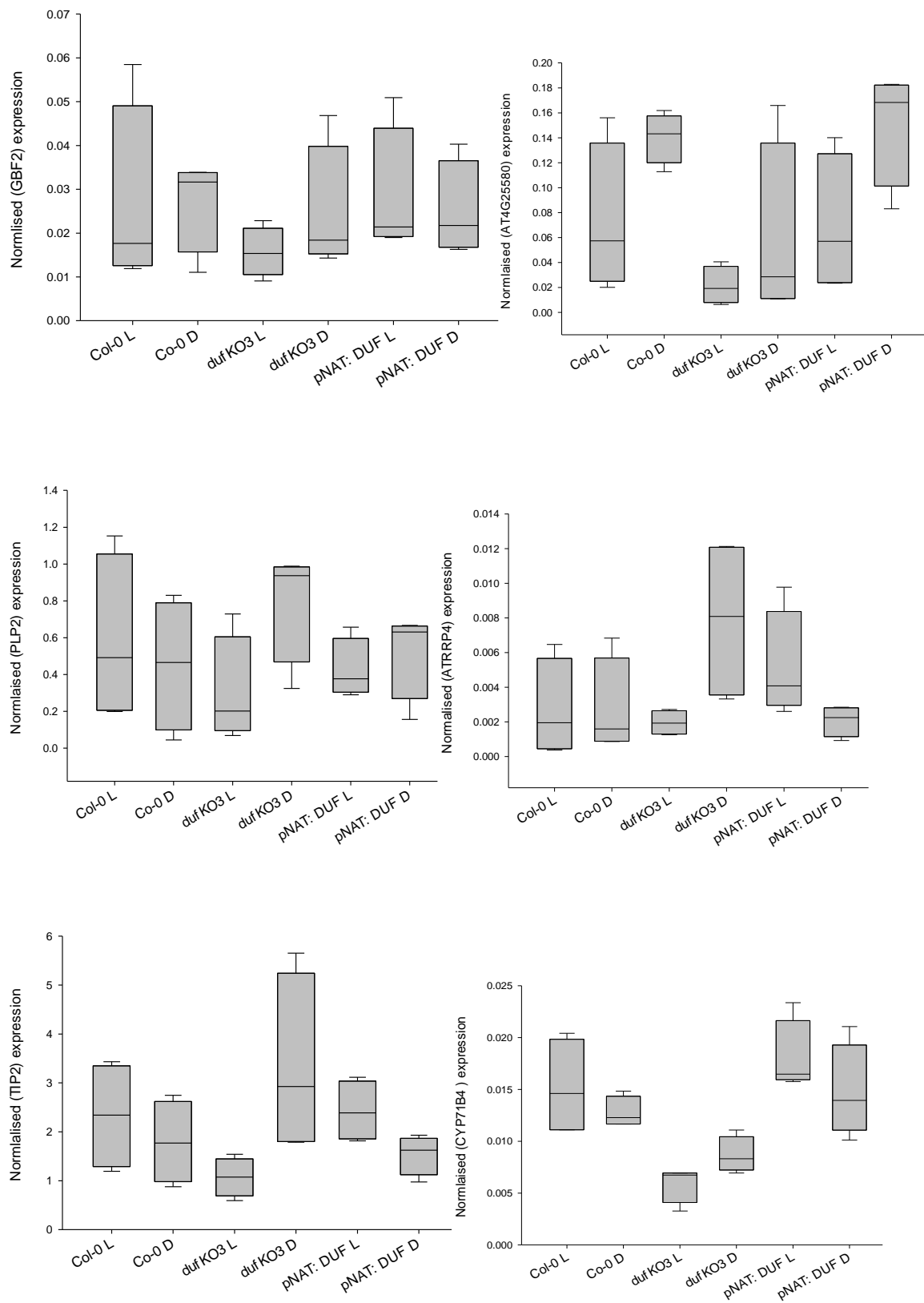
PLP2	<i>dufko3</i> vs <i>duf_kin10-2</i>	Well-watered	9.02E-07
	<i>dufko3</i> vs <i>duf_kin10-2</i>	drought	2.44E-03
	<i>DUFOE3</i> vs <i>duf_kin10-2</i>	Well-watered	2.12E-04
	<i>DUFOE3</i> vs <i>duf_kin10-2</i>	drought	7.09E-04
	<i>pNAT:DUF</i> vs <i>duf_kin10-2</i>	Well-watered	5.65E-05
	<i>pNAT:DUF</i> vs <i>duf_kin10-2</i>	drought	1.54E-03
ATTRP4	<i>DUFOE3</i> vs <i>pNAT:DUF</i>	drought	8.96E-05
	<i>DUFOE3</i> vs <i>kin10-2</i>	drought	2.19E-04
	<i>DUFOE3</i> vs <i>dyf_kin10-2</i>	drought	3.19E-04
	<i>pNAT:DUF</i> vs <i>duf_kin10-2</i>	drought	1.91E-03

Appendix F

Different gene expression in Col-0 and mutants which does not show any significant differences under light/dark and dark conditions







Appendix G

Significant differences between different mutants under light/dark and dark conditions.

Gene	Compared genotype	condition	Adjust p-Value
DUF2358	<i>pNAT:DUF</i> vs <i>dufko3</i>	Light/dark	1.9E-05
	<i>pNAT:DUF</i> vs <i>dufko3</i>	dark	3.84E-05
KIN10	<i>pNAT:DUF</i> vs <i>dufko3</i>	Light/dark	3.46E-04
AT2G36220	<i>pNAT:DUF</i> vs <i>dufko3</i>	dark	3.03E-03
DSP4	<i>pNAT:DUF</i> vs <i>dufko3</i>	dark	4.42E-03

Appendix H

Significant metabolites $p < 0.01$

Metabolite	f.value	p.value	$-\log_{10}(p)$	FDR	Tukey's HSD
1.122	5.3413	0.003497	2.4564	0.008796	5-1
1.2	11.468	4.35E-05	4.3612	0.000729	5-1; 5-3; 5-4; 6-5
1.28	9.1027	0.000187	3.7278	0.001475	4-2; 4-3; 5-4
1.622	10.26	8.91E-05	4.0503	0.000911	5-1; 5-2; 5-4; 6-5
1.679	7.723	0.000494	3.3061	0.002747	5-1; 5-3; 5-4
1.99	6.6126	0.00117	2.9316	0.004357	5-1
5.571	7.6662	0.000515	3.2878	0.002747	5-1; 5-2; 5-3
5.641	10.364	8.36E-05	4.078	0.000911	5-1; 5-3; 5-4; 6-5
6.144	5.8531	0.002217	2.6543	0.006601	5-4
8.18	10.83	6.31E-05	4.2002	0.000845	5-1; 5-3; 5-4; 6-5
8.353	5.2442	0.003822	2.4177	0.009145	5-1
8.436	6.0057	0.001943	2.7115	0.006168	5-1; 6-5
8.565	8.7059	0.000245	3.611	0.001823	5-1; 5-2; 5-3; 5-4
8.68	5.7566	0.002412	2.6177	0.007025	5-4
8.813	5.5449	0.002909	2.5362	0.007814	5-4
9.146	6.4946	0.001289	2.8897	0.004546	5-1; 5-3; 6-5
9.692	10.152	9.52E-05	4.0214	0.000911	5-1; 5-3
9.73	6.549	0.001233	2.9091	0.004465	5-1; 5-4
9.832	11.64	3.95E-05	4.4036	0.000729	5-1; 5-3; 5-4; 6-5
9.922	5.2483	0.003807	2.4194	0.009145	5-1
9.961	9.443	0.000149	3.8254	0.001323	4-2; 4-3; 5-4; 6-4
11.115	6.1934	0.001656	2.7809	0.005691	5-1; 5-3
11.523	6.0952	0.0018	2.7447	0.005903	5-4
11.565	7.7553	0.000482	3.3165	0.002747	2-1; 5-1; 4-2; 5-4
11.779	7.1366	0.000772	3.1127	0.003446	5-3; 6-5
11.92	5.9574	0.002025	2.6935	0.006168	5-2
11.954	11.171	5.17E-05	4.2869	0.000769	5-1; 4-2; 4-3; 5-4
12.419	7.6189	0.000534	3.2724	0.002747	5-1; 5-3
12.576	5.3263	0.003545	2.4504	0.008796	
12.961	7.4808	0.000592	3.2273	0.002747	4-3; 5-4
13.134	7.4763	0.000594	3.2259	0.002747	4-2
13.381	9.3589	0.000158	3.8015	0.001323	5-1; 5-3; 5-4; 6-5
13.461	5.4914	0.003052	2.5154	0.008019	5-1; 6-5
13.79	7.7206	0.000495	3.3054	0.002747	4-2; 5-4
14.27	6.8103	0.000998	3.0009	0.004052	5-2
15.22	5.5424	0.002916	2.5352	0.007814	4-2
16.16	6.6458	0.001139	2.9434	0.004357	4-2; 5-4
16.166	8.0534	0.000388	3.4112	0.002599	5-1; 5-4
16.342	6.6467	0.001139	2.9436	0.004357	5-1

1.865_Rhamnose-1	5.3757	0.003389	2.47	0.008733	5-1
12.144_Galactose	14.918	7.33E-06	5.1347	0.000381	4-1; 4-2; 4-3; 5-4; 6-4
12.15_Mannose	11.48	4.32E-05	4.3642	0.000729	2-1; 4-2; 4-3
12.344_Glucose	5.7159	0.0025	2.6021	0.007126	4-2; 5-4
12.888_Glucuronic acid	5.9627	0.002016	2.6955	0.006168	4-2; 4-3; 5-4
12.924_Both glucorinicgalacturonic acid	14.339	9.66E-06	5.0149	0.000381	2-1; 3-1; 4-2; 6-2; 4-3; 6-3
16.723_Sucrose	6.939	0.000901	3.0453	0.003894	4-2; 5-4
17.365_Maltose	5.6812	0.002577	2.5888	0.007195	6-5
6.357_AA	7.8638	0.000445	3.3512	0.002747	5-1; 5-3; 5-4
6.637_Valine	10.473	7.82E-05	4.1068	0.000911	5-1; 5-3
6.823_Urea	8.6169	0.00026	3.5843	0.001837	5-1; 5-3
7.13_Leucine	11.844	3.52E-05	4.4534	0.000729	5-1; 5-2; 5-3; 5-4; 6-5
7.34_Isoleucine	29.014	5.13E-08	7.29	6.87E-06	4-1; 5-1; 6-1; 5-2; 5-3; 6-3; 5-4
7.9_Serine	14.004	1.14E-05	4.9441	0.000381	5-1; 5-2; 5-3; 5-4; 6-5
8.52_Aspartic acid 2	6.885	0.00094	3.0267	0.003937	5-4; 6-5
9.299_Aspartic acid 1	6.0912	0.001806	2.7433	0.005903	5-1
9.9_Malic acid	7.5567	0.00056	3.2522	0.002747	5-4; 6-5

Appendix I

Significant metabolites $p < 0.025$

Metabolite	f.value	p.value	$-\log_{10}(p)$	FDR	Tukey's HSD
1.122	5.3413	0.003497	2.4564	0.008796	5-1; 5-3
1.2	11.468	4.35E-05	4.3612	0.000729	5-1; 5-3; 5-4; 6-5
1.238	3.9578	0.013473	1.8705	0.021852	5-1; 5-3; 5-4
1.28	9.1027	0.000187	3.7278	0.001475	4-2; 6-2; 4-3; 5-4
1.342	4.4779	0.007942	2.1001	0.015423	5-1
1.532	4.3829	0.00873	2.059	0.015527	5-5
1.622	10.26	8.91E-05	4.0503	0.000911	5-1; 5-2; 5-3; 5-4; 6-5
1.679	7.723	0.000494	3.3061	0.002747	5-1; 5-3; 5-4
1.79	4.4846	0.00789	2.1029	0.015423	5-1; 5-4
1.99	6.6126	0.00117	2.9316	0.004357	5-1; 6-1; 5-3
5.571	7.6662	0.000515	3.2878	0.002747	5-1; 5-2; 5-3
5.641	10.364	8.36E-05	4.078	0.000911	5-1; 5-3; 5-4; 6-5
6.144	5.8531	0.002217	2.6543	0.006601	4-2; 5-4; 6-5
7.751	3.8693	0.014783	1.8302	0.022909	
7.833	4.6111	0.006967	2.157	0.014144	5-1; 5-4; 6-5
7.97	4.3438	0.009078	2.042	0.015798	5-4; 6-5
8.18	10.83	6.31E-05	4.2002	0.000845	2-1; 5-1; 5-3; 5-4; 6-5
8.24	3.9412	0.01371	1.863	0.02187	
8.327	4.3049	0.009441	2.025	0.016013	5-1; 5-4
8.353	5.2442	0.003822	2.4177	0.009145	5-1; 5-4
8.436	6.0057	0.001943	2.7115	0.006168	5-1; 5-4; 6-5
8.565	8.7059	0.000245	3.611	0.001823	5-1; 5-2; 5-3; 5-4
8.68	5.7566	0.002412	2.6177	0.007025	4-3; 5-4
8.813	5.5449	0.002909	2.5362	0.007814	5-1; 5-4; 6-5
9.119	4.4002	0.00858	2.0665	0.015527	5-1; 5-4
9.146	6.4946	0.001289	2.8897	0.004546	5-1; 5-3; 5-4; 6-5
9.436	5.0604	0.004533	2.3437	0.010656	5-1; 5-4
9.656	4.4035	0.008552	2.0679	0.015527	6-5
9.692	10.152	9.52E-05	4.0214	0.000911	4-1; 5-1; 5-2; 5-3
9.73	6.549	0.001233	2.9091	0.004465	5-1; 5-4
9.769	4.7432	0.006128	2.2127	0.01283	5-1; 5-4
9.832	11.64	3.95E-05	4.4036	0.000729	5-1; 5-2; 5-3; 5-4; 6-5
9.922	5.2483	0.003807	2.4194	0.009145	2-1; 5-1
9.961	9.443	0.000149	3.8254	0.001323	4-2; 4-3; 5-4; 6-4
11.115	6.1934	0.001656	2.7809	0.005691	5-1; 5-3; 5-4
11.145	4.1689	0.010837	1.9651	0.018152	2-1
11.16	4.4064	0.008527	2.0692	0.015527	5-1
11.292	4.5079	0.00771	2.113	0.01542	5-1; 6-5
11.368	4.3999	0.008582	2.0664	0.015527	5-1; 5-3; 5-4
11.523	6.0952	0.0018	2.7447	0.005903	4-2; 6-2

11.565	7.7553	0.000482	3.3165	0.002747	2-1; 5-1; 4-2; 5-4
11.662	4.3741	0.008806	2.0552	0.015527	5-5
11.699	4.4591	0.008092	2.092	0.015489	5-4
11.779	7.1366	0.000772	3.1127	0.003446	5-1; 3-2; 5-3; 6-5
11.82	4.9104	0.005221	2.2822	0.01166	5-1
11.92	5.9574	0.002025	2.6935	0.006168	4-2; 6-2; 5-4
11.954	11.171	5.17E-05	4.2869	0.000769	2-1; 5-1; 4-2; 4-3; 5-4; 6-5
12.419	7.6189	0.000534	3.2724	0.002747	5-1; 5-2; 5-3
12.428	5.0341	0.004646	2.333	0.010733	5-1; 5-3
12.498	4.3197	0.009301	2.0315	0.015979	6-5
12.576	5.3263	0.003545	2.4504	0.008796	5-1; 5-4
12.653	3.8635	0.014874	1.8276	0.022909	4-5
12.961	7.4808	0.000592	3.2273	0.002747	4-3; 5-4
13.134	7.4763	0.000594	3.2259	0.002747	4-2; 5-2; 6-2
13.291	4.662	0.006629	2.1785	0.013666	5-1; 5-4
13.381	9.3589	0.000158	3.8015	0.001323	5-1; 6-2; 5-3; 5-4; 6-5
13.431	4.1295	0.011282	1.9476	0.018664	5-1
13.461	5.4914	0.003052	2.5154	0.008019	5-1; 5-2; 5-3; 5-4; 6-5
13.54	4.7846	0.005888	2.2301	0.012523	5-1; 5-4; 6-5
13.79	7.7206	0.000495	3.3054	0.002747	4-2; 6-2; 5-4; 6-5
14.17	4.8364	0.005603	2.2516	0.012307	4-2; 5-4
14.27	6.8103	0.000998	3.0009	0.004052	2-1; 4-2; 4-3; 5-4
15.22	5.5424	0.002916	2.5352	0.007814	5-1; 5-4
16.16	6.6458	0.001139	2.9434	0.004357	4-2; 5-4
16.166	8.0534	0.000388	3.4112	0.002599	5-1; 5-4; 6-5
16.342	6.6467	0.001139	2.9436	0.004357	2-1; 5-1; 6-5
16.663	3.9034	0.014263	1.8458	0.022485	5-1
1.865_Rhamnose-1	5.3757	0.003389	2.47	0.008733	5-1; 5-4; 6-5
11.628_Citric acid	4.8003	0.0058	2.2366	0.012523	4-2; 4-3
12.144_Galactose	14.918	7.33E-06	5.1347	0.000381	4-1; 4-2; 4-3; 5-4; 6-4
12.15_Mannose	11.48	4.32E-05	4.3642	0.000729	2-1; 3-1; 4-2; 4-3; 6-4
12.344_Glucose3	5.7159	0.0025	2.6021	0.007126	4-2; 5-4; 6-4
12.888_Glucuronic acid	5.9627	0.002016	2.6955	0.006168	4-2; 4-3; 5-4
12.924_Both glucorinicgalacturonic acid	14.339	9.66E-06	5.0149	0.000381	2-1; 3-1; 4-2; 6-2; 4-3; 6-3; 5-4
13.14_Galacturonic acid	4.9143	0.005202	2.2838	0.01166	4-3
16.723_Sucrose	6.939	0.000901	3.0453	0.003894	4-2; 4-3; 5-4
17.365_Maltose	5.6812	0.002577	2.5888	0.007195	6-2; 6-5
6.357_AA	7.8638	0.000445	3.3512	0.002747	5-1; 5-2; 5-3; 5-4
6.637_Valine	10.473	7.82E-05	4.1068	0.000911	4-1; 5-1; 6-1; 5-3; 6-3
6.823_Urea	8.6169	0.00026	3.5843	0.001837	5-1; 6-1; 5-3
7.13_Leucine	11.844	3.52E-05	4.4534	0.000729	5-1; 5-2; 5-3; 5-4; 6-5

7.34_Isoleucine	29.014	5.13E-08	7.29	6.87E-06	2-1; 4-1; 5-1; 6-1; 5-2; 5-3; 6-3; 5-4; 6-5
7.36_Threonine	3.9535	0.013535	1.8685	0.021852	
7.9_Serine	14.004	1.14E-05	4.9441	0.000381	5-1; 6-1; 5-2; 5-3; 5-4; 6-5
8.52_Aspartic acid 2	6.885	0.00094	3.0267	0.003937	5-1; 5-4; 6-5
9.299_Aspartic acid 1	6.0912	0.001806	2.7433	0.005903	2-1; 5-1; 6-1
9.9_Malic acid	7.5567	0.00056	3.2522	0.002747	5-4; 6-5

Appendix J

Contribution of metabolites to each principal component.

	PC1	PC2	PC3	PC4	PC5	PC6	PC7	PC8
Valine	0.066817	-0.1711	-0.0613	0.0456	-0.079	0.0006	-0.056	0.10402
Urea	0.092924	-0.1202	-0.0689	0.1023	0.0468	-0.0297	-0.054	-0.06111
Tyrosine-1	0.087209	-0.0235	-0.0673	0.0276	0.1049	0.0041	0.1168	0.000791
Trehalose	0.062432	0.02996	-0.2757	-0.134	0.0311	-0.1089	0.0903	0.020021
Threonine_2	0.093881	-0.0926	-0.0378	-0.083	0.0926	0.0306	0.0057	0.080436
Threonine	0.10498	-0.0427	-0.0485	0.026	0.0322	0.1448	0.099	0.019076
Threonic acid	0.072993	-0.002	0.1155	-0.055	-0.108	-0.1757	0.0835	0.008415
Sucrose	0.089101	0.13646	0.0284	0.112	-0.031	-0.0144	0.0907	-0.03053
Succinic acid	0.070788	0.09861	-0.1001	-0.15	-0.037	0.0365	-0.117	-0.14357
Serine_2	0.097024	-0.1325	-0.0465	0.0093	0.0766	-0.0668	-0.068	0.048208
Serine	0.092146	-0.1126	-0.0854	0.025	0.0849	0.0207	0.1136	-0.09914
Rhamnose-1	0.095419	-0.0644	-0.013	-0.012	0.1572	0.0811	0.0288	2.30E-05
Phenylalanine	0.078595	0.01354	0.0724	-0.042	-0.037	0.0802	0.0859	-0.18449
N-acetyl-hexosamine 2	0.06003	0.06258	0.0491	-0.091	0.0574	-0.2862	-0.148	0.038571
N-acetyl-hexosamine	0.081281	-0.0727	0.1776	-0.001	-0.152	-0.1145	0.0015	0.057828
Myo-Inositol	0.079408	0.08822	-0.0619	0.0028	-0.149	-0.0471	0.0387	0.15179
Mannose	0.06017	0.2061	-0.0485	0.1528	-0.014	0.0233	-0.004	0.008629
Maltose	0.08249	0.05359	-0.0617	-0.19	-0.109	-0.1246	-0.082	0.052287
Malic acid	0.078696	0.07396	0.0452	-0.128	0.1552	-0.0666	0.0235	-0.14382
Leucine	0.079714	-0.1627	-0.0101	0.0166	0.0795	0.0058	-0.051	-0.08804
Isoleucine	0.082973	-0.1898	0.0105	0.0925	-0.018	-0.0117	-0.009	-0.03747
Glycine	0.087484	0.07873	-0.0562	-0.026	0.0395	0.1763	0.0826	-0.03042
Glyceric acid	0.084653	0.08506	-0.1327	-0.154	0.0424	-0.0346	0.1076	0.003815
Glucose3	0.069378	0.06478	0.2	0.1479	0.1231	-0.013	0.1291	0.012456
Glucose-1-Phosphate-2	0.091585	0.01071	-0.101	0.1101	-0.026	0.0996	-0.025	0.012892
Glucose-1-Phosphate_1	0.062366	-0.0557	0.1697	-0.097	-0.04	0.1849	-0.079	0.085487
Glucose1	0.091754	0.02291	-0.0756	0.0242	0.1011	-0.0732	0.0631	-0.10348
Galacturonic acid	0.062646	0.19368	0.0638	0.0359	-0.096	0.0653	0.0716	-0.04275
Galacturonic acid	0.071027	0.11283	-0.0461	0.1608	0.0168	-0.0509	0.0085	-0.09237
Galactose	0.079687	0.16285	0.0404	0.0388	0.0258	-0.034	0.0695	-0.04514
Fumaric acid	0.081391	0.09812	0.0394	0.0633	-0.075	0.0522	0.1753	-0.01894
Fructose2	0.07935	0.12399	-0.0825	-0.115	-0.073	0.1546	0.0266	0.1131
Fructose1	0.097594	0.04713	-0.1067	-0.111	0.0891	-0.0266	0.0383	-0.10455
Citric acid	0.052248	0.14806	-0.0025	0.1321	0.0592	-0.0334	-0.04	-0.1175
Aspartic acid 2	0.11288	0.03898	0.0082	-0.051	0.0709	-0.0723	0.0641	-0.13564

Aspartic acid 1	0.095393	-0.0872	-0.0703	0.144	-0.077	-0.0246	0.0732	0.077232
Arabinose	0.082707	-0.076	0.0396	0.0077	-0.113	-0.1612	0.0403	0.039839
AA_2	0.098383	-0.0254	-0.1173	0.0456	-0.01	0.0769	0.0038	-0.11774
AA_1	0.10415	-0.096	0.0585	0.0482	-0.037	-0.0496	-0.027	0.053907
19.225	0.08874	0.02633	-0.0413	-0.152	-0.064	0.0304	0.1967	0.085085
16.663	0.1078	-0.0332	-0.0634	0.0102	0.0538	-0.08	0.0615	-0.01294
16.489	0.094033	0.00495	0.0694	0.0126	-0.081	-0.0246	-0.192	0.065157
16.342	0.086081	0.0427	-0.0485	-0.041	-0.116	-0.1238	-0.134	-0.24425
16.166	0.10865	-0.0127	0.1254	0.0578	-0.097	-0.1118	-0.047	-0.07372
14.834	0.084645	-0.0696	-0.0109	-0.037	0.0231	0.0485	0.0407	0.1952
14.627	0.089602	-0.0065	-0.1494	0.0857	0.059	0.0723	0.0643	-0.10267
14.547	0.091484	-0.0084	0.004	-0.06	-0.114	0.0767	-0.093	0.16224
14.27	0.081977	0.10772	0.053	0.1429	-0.081	0.0516	-0.039	-0.05556
14.17	0.069873	0.12958	0.1133	-0.043	-0.038	-0.1409	-0.12	0.079998
13.54	0.10418	-0.0066	0.0868	-0.135	0.0078	0.0334	0.0612	-0.0728
13.461	0.068397	-0.095	0.1658	-0.165	0.0378	0.0839	-0.048	-0.19553
13.431	0.1088	0.01731	-0.0462	0.1026	-0.043	-0.0228	-0.02	-0.03178
13.381	0.10397	-0.0178	0.0427	-0.183	0.0403	-0.0656	-0.065	0.085699
13.291	0.098684	0.00118	0.0873	0.0484	0.0633	0.043	-0.168	-0.0715
13.134	0.04341	0.2102	-0.0352	-0.046	-0.008	0.0636	0.0951	0.11079
12.961	0.077865	0.06376	0.1563	0.0837	0.167	-0.0074	-0.147	-0.18613
12.851	0.058392	0.06203	-0.0469	0.2061	-0.056	-0.1937	0.0856	0.12138
12.678	0.067773	0.04824	0.0253	0.0499	-0.318	0.1642	-0.042	0.00575
12.653	0.030334	0.20696	-0.0971	0.0467	0.0631	0.0612	-0.106	0.11446
12.576	0.10522	0.07242	0.0527	0.0502	0.0605	0.0451	-0.05	0.058315
12.498	0.091361	0.00124	0.0228	-0.18	0.0241	0.0506	-0.071	0.17538
12.428	0.085884	-0.1205	-0.0788	0.1097	-0.042	0.0464	-0.006	0.040682
12.419	0.092902	-0.1438	-0.0871	-0.013	-0.073	0.0234	0.0014	0.009822
12.251	0.06687	0.16419	-0.1261	0.0203	-0.056	0.0511	-0.107	-0.00644
11.954	0.10662	0.09265	0.0512	0.0352	-0.013	0.0594	0.0679	-0.04703
11.92	0.086672	0.10692	-0.0874	-0.123	-0.034	-0.065	0.0686	0.10797
11.871	0.08244	0.01782	-0.1237	-0.039	0.048	0.1079	-0.211	-0.10896
11.82	0.10148	0.01164	-0.02	-0.013	-0.062	0.1023	0.044	-0.02217
11.779	0.095248	-0.0045	-0.0803	-0.13	-0.048	-0.0783	-0.025	0.028821
11.699	0.087922	0.07535	0.1758	-0.034	0.1383	0.0046	0.1085	0.062001
11.662	0.090458	-0.0123	-0.0637	-0.111	0.1227	-0.0619	0.1282	0.023611
11.523	0.088622	0.16274	-0.0395	-0.002	0.0105	0.0129	-0.038	0.036761
11.52	0.072426	0.11484	0.0377	0.0908	0.1012	0.0421	-0.027	0.18574
11.478	0.054239	-0.1302	-0.0586	0.1223	-0.079	-0.0034	0.1423	-0.1391
11.318	0.094415	-0.0523	0.005	-0.037	0.0646	0.1521	0.1162	0.023778
11.292	0.10435	-0.0755	0.0569	-0.029	0.0743	-0.0291	-0.046	0.15387
11.212	0.075383	-0.0119	0.004	0.1547	-0.119	-0.1634	-0.068	-0.09395
11.16	0.077447	-0.108	-0.0927	0.0668	0.0503	-0.152	-0.102	0.16064
11.145	0.083686	0.03044	-0.0824	0.2087	-0.074	-0.1909	0.0305	0.022229

11.115	0.084179	-0.1086	-0.0133	0.0452	-0.03	0.0397	0.1463	0.071224
9.961	0.084269	0.09419	0.2006	0.122	0.0826	0.0598	0.0625	0.025519
9.922	0.10258	-0.045	-0.0819	0.0578	-0.029	0.0494	0.1002	0.045221
9.832	0.10835	-0.038	0.1154	0.019	-0.049	-0.0324	0.0213	-0.0738
9.816	0.10488	-0.0077	-0.0776	-0.024	-0.006	0.026	0.1326	0.037764
9.769	0.10005	-0.0428	0.0635	0.0841	0.0999	0.0542	-0.121	0.014021
9.73	0.10748	0.03609	0.0477	0.0249	-0.065	-0.0962	-0.091	-0.02534
9.692	0.082923	-0.1567	-0.0109	-0.02	-0.172	0.0681	-0.015	-0.01388
9.656	0.087726	0.02193	0.0116	-0.162	0.1077	-0.1003	0.1044	0.017238
9.436	0.095098	0.00102	0.1979	-0.062	0.0177	0.0397	0.0632	0.13236
9.399	0.035786	-0.0215	-0.0591	0.0663	0.1642	0.2345	-0.276	0.063387
9.35	0.086436	-0.0641	-0.0628	-0.082	-0.16	-0.0177	0.0912	-0.13135
9.236	0.088439	-0.0487	-0.0757	0.0999	0.1214	-0.0954	-0.061	0.062974
9.179	0.083224	0.091	0.1248	0.01	-0.047	0.1016	-0.046	0.050001
9.146	0.093734	-0.0775	0.0921	-0.062	0.0297	-0.0907	0.0312	-0.10568
9.119	0.1023	0.01026	-0.0705	0.0014	-0.13	0.0254	-0.138	-0.08609
8.896	0.079701	-0.0007	0.1916	-0.021	-0.145	-0.0435	-0.109	-0.02974
8.813	0.10053	0.00543	0.0397	-0.011	0.2304	-0.0024	-0.065	0.00595
8.68	0.099592	0.10997	-0.0239	0.0115	0.0427	0.044	-0.116	0.056118
8.565	0.10186	-0.0787	0.0937	0.1019	0.028	0.0022	-0.018	0.032858
8.53	0.09473	0.02299	-0.1881	-0.021	-0.053	0.0267	-0.088	-0.06261
8.436	0.11444	-0.0109	-0.0526	-0.045	-6E-04	0.07	0.0511	0.063793
8.353	0.1066	-0.0237	0.0198	0.0958	-0.041	-0.0271	0.0392	0.002488
8.327	0.095133	-0.0324	0.0722	-0.011	-0.045	0.2018	0.0277	0.031562
8.24	0.066601	0.15068	-0.0496	-0.019	-0.165	0.0638	0.0658	-0.06278
8.18	0.11349	-0.0295	0.0401	0.017	-0.002	-0.109	-0.034	-0.01459
8.13	0.08603	-0.0573	-0.0019	-0.083	-0.147	-0.0431	0.1378	-0.06838
7.97	0.10385	0.04777	0.0915	-0.068	-0.006	-0.0067	-0.012	0.14892
7.833	0.10999	0.03284	0.0121	-0.057	0.0893	-0.0344	-0.111	0.013179
7.751	0.09391	0.09552	-0.0517	-0.007	0.1051	-0.1837	-0.069	0.12826
6.447	0.096492	0.02424	-0.0588	-0.037	0.038	-0.1117	-0.069	-0.02353
6.144	0.098479	0.08135	-0.0018	-0.04	0.1329	-0.0716	0.0797	-0.01959
5.571	0.083261	-0.1656	0.0207	-0.037	0.0487	0.0042	-0.082	0.035447
1.99	0.10216	-0.1018	-0.0583	0.1222	0.0531	0.0292	0.0011	0.09886
1.959	0.060799	0.03696	0.1785	-0.086	-0.156	0.0424	-0.052	-0.10799
1.79	0.10537	-0.0652	0.0695	0.0023	0.1055	0.0626	0.0762	-0.01109
1.735	0.094761	0.01874	-0.0446	-0.085	0.0065	0.159	-0.07	-0.12882
1.679	0.097597	-0.1042	0.0585	0.0617	0.0006	-0.0664	0.0423	0.087101
1.622	0.088181	-0.0895	0.0999	0.0134	0.134	0.0595	0.0296	-0.15721
1.62	0.084064	0.03016	-0.1689	0.0893	0.0055	-0.0141	-0.104	-0.11852
1.56	0.041833	-0.1109	0.0471	-0.182	-0.143	-0.0264	-0.093	0.002572
1.532	0.1009	-0.0388	-0.0204	-0.122	0.0088	-0.0964	0.0579	-0.11048
1.485	0.097573	-0.0024	0.0635	0.1408	-0.108	0.0715	0.0637	0.10127
1.342	0.085944	-0.0951	-0.0862	0.0567	-0.021	0.0904	-0.078	0.086439

1.28	0.0954	0.15726	0.048	-0.045	-0.016	0.0222	-0.024	0.000521
1.238	0.094796	-0.0772	0.0794	0.0057	0.0421	0.0391	0.1351	-0.0391
1.2	0.11789	-0.0086	0.0232	0.0472	-0.006	0.0388	-0.054	-0.04828
1.122	0.091741	-0.0752	-0.1274	-0.088	-0.076	0.091	-0.144	0.023659

	PC9	PC10	PC11	PC12	PC13	PC14	PC15	PC16
Valine	-0.1492	-0.0746	0.01379	-0.03662	0.07037	0.0252	0.01451	-0.1502
Urea	0.0251	0.095	0.01075	0.05291	-	0.008681	-0.0471	0.05774
Tyrosine-1	0.1271	-0.2194	0.11704	0.01404	-	0.016867	-0.2447	-0.0479
Trehalose	-0.0224	-0.0978	-0.0145	0.0694	-	0.096045	-0.0369	0.06019
Threonine_2	-0.0659	0.00745	0.01929	-0.17381	-	0.068665	-0.0953	0.1908
Threonine	-0.0307	0.10966	-0.1487	0.06473	-	0.012228	0.0093	0.0644
Threonic acid	0.1485	0.00133	-0.0838	0.08683	-	-0.12516	-0.1748	-0.2187
Sucrose	0.0057	-0.0261	-0.0907	-0.07986	-	0.003396	-0.0365	-0.0446
Succinic acid	0.0893	-0.2168	-0.044	0.15404	-	0.068917	0.0372	0.02581
Serine_2	0.0671	0.10115	0.0107	-0.08552	-	0.034738	-0.0056	-0.0437
Serine	0.0005	-0.134	0.01226	0.05829	-	0.037989	-0.0596	-0.1375
Rhamnose-1	-0.0026	0.1466	-0.0278	0.07159	-	0.036324	0.1937	-0.0952
Phenylalanine	-0.0215	-0.0658	-0.2752	0.09888	-	0.057067	-0.085	-0.0194
N-acetyl-hexosamine 2	-0.1115	0.08002	0.12792	-0.05784	-	0.078639	0.0516	-0.049
N-acetyl-hexosamine	-0.0794	-0.0726	-0.03	0.06715	-	0.080621	-0.0159	-0.0988
Myo-Inositol	-0.1253	0.14692	0.0146	0.05869	-	0.07159	-0.0469	0.1534
Mannose	-0.0284	-0.0194	0.01907	0.09044	-	0.013568	0.0118	-0.0169
Maltose	0.0579	0.12123	-0.1108	-0.02788	-	0.088815	0.1459	-0.0845
Malic acid	0.0233	0.05593	-0.1352	0.05795	-	0.15543	0.0896	0.10612
Leucine	0.0208	0.03201	0.0085	0.04057	-	0.12617	0.0064	-0.0233
Isoleucine	0.0886	0.05918	0.06246	0.0054	-	0.056555	0.0252	0.01795
Glycine	0.0976	-0.0973	0.09218	-0.00829	-	-0.12185	-0.0711	-0.0327
Glyceric acid	-0.0418	-0.1288	0.04906	-0.02403	-	0.18437	0.034	-0.0991
Glucose3	-0.0738	0.06644	0.06066	-0.03829	-	0.061936	-0.1759	-0.1271
Glucose-1-Phosphate-2	-0.1234	-0.1649	0.00397	0.01902	-	0.067634	0.0319	0.09234
Glucose-1-Phosphate_1	-0.1028	0.06902	0.0968	0.0502	-	-0.23267	-0.1208	-0.1094
Glucose1	-0.05	0.09744	-0.1548	0.17141	-	0.023459	-0.1378	0.12245
Galacturonic acid	0.0466	0.09954	0.09011	0.06703	-	0.079946	0.0223	0.02937
Galacturonic acid	-0.0713	0.2061	0.07487	0.05323	-	0.038715	0.0318	-0.1516
Galactose	-0.0387	-0.1205	0.17826	-0.12957	-	0.081764	0.04	0.01254
Fumaric acid	-0.1172	-0.0294	-0.167	-0.13508	-	0.046855	0.0348	0.0993

Fructose2	0.0536	0.04897	-0.0544	0.05346	0.060356	0.0455	-0.0071	-0.1606	
Fructose1	0.0692	0.08091	0.02428	-0.12456	0.10277	-0.1281	0.12639	0.01816	
Citric acid	0.1162	0.08759	-0.019	0.06191	0.12724	0.1976	0.06229	0.14657	
Aspartic acid 2	-0.0784	-0.0864	-0.0155	0.03169	-	0.023587	0.0268	-0.0157	0.01842
Aspartic acid 1	0.1395	0.08148	-0.0045	-0.00318	-	0.043715	-0.0008	0.13049	0.02439
Arabinose	-0.1621	-0.1913	-0.1696	-0.02834	0.043276	0.0714	0.01966	-0.0329	
AA_2	-0.0284	-0.0656	0.11475	-0.05902	-0.02569	-0.1073	0.06191	0.13578	
AA_1	0.006	0.00042	0.09144	0.05026	0.10065	-0.0573	0.09466	0.12303	
19.225	-0.0067	-0.1025	-0.0953	-0.01084	0.16512	0.1171	-0.0101	-0.0239	
16.663	0.1844	-0.1424	0.03189	-0.04783	0.025072	0.0456	0.00643	-0.0975	
16.489	-0.0969	-0.0912	-0.0661	-0.04436	0.16888	-0.1069	0.14046	-0.046	
16.342	0.0352	0.04965	0.07155	0.08364	0.013941	0.096	-0.0303	0.00395	
16.166	0.1034	0.01181	-0.0917	-0.00533	0.023392	-0.0119	-0.0553	0.00955	
14.834	0.2543	-0.0849	0.04917	-0.1497	0.031937	-0.0134	0.08216	0.00087	
14.627	0.1503	0.10711	0.049	-0.03069	0.16378	-0.0555	0.01696	-0.0151	
14.547	0.018	-0.0432	0.1265	0.1843	0.090105	0.0042	0.05402	-0.0839	
14.27	-0.0768	-0.0927	0.1472	0.0534	-	0.091687	0.0523	0.07171	0.16087
14.17	-0.198	-0.0699	0.05813	0.05112	0.032848	-0.181	-0.0538	-0.0223	
13.54	0.0978	-0.0019	0.09183	-0.00403	-	0.047002	-0.0891	-0.0909	0.04685
13.461	-0.0033	-0.0012	0.1214	-0.01406	-	0.064692	0.0233	0.00431	0.05584
13.431	-0.0148	-0.0159	-0.0649	-0.0028	-	0.084144	0.0329	-0.0173	-0.2573
13.381	-0.0882	-0.004	0.01694	-0.00075	-	-0.15234	0.006	0.06586	-0.0108
13.291	0.0305	-0.0299	-0.2114	-0.14277	-	0.030547	-0.0135	-0.0175	-0.0266
13.134	0.049	0.07792	0.02894	-0.06125	0.010657	-0.2012	-0.0654	0.05012	
12.961	0.0401	-0.0557	0.00209	-0.06051	0.038273	-0.0173	0.08972	0.01702	
12.851	0.0547	0.0717	-0.1741	-0.00451	-0.19796	-0.0848	-0.0545	0.05655	
12.678	0.1208	-0.049	-0.068	0.11354	0.045319	0.016	-0.0084	-0.0006	
12.653	0.0598	-0.0101	0.07879	-0.1014	0.035378	0.1332	-0.1169	0.11126	
12.576	-0.0216	-0.0043	-0.056	0.07221	-	0.037051	-0.0921	-0.0071	0.0873
12.498	0.0883	0.04695	-0.1	-0.03663	-	0.014427	0.097	-0.0117	0.04084
12.428	-0.0547	0.02603	-0.0355	-0.03983	0.005212	0.13	-0.09	0.1096	
12.419	0.0821	-0.0046	0.0627	0.10668	0.058899	0.0071	0.0705	-0.0162	
12.251	0.0491	0.0877	0.10817	0.03009	-0.05215	-0.136	0.18228	-0.0386	
11.954	-0.0359	0.11289	0.03766	-0.07382	-	0.019541	0.0667	-0.0618	-0.0456
11.92	-0.0097	0.12337	0.08594	0.0234	0.01505	0.043	0.03604	-0.0999	
11.871	-0.0474	0.09232	0.06681	-0.15634	-	0.007838	0.0463	-0.1187	0.12081
11.82	0.0745	0.2099	-0.0773	0.02544	-	0.094225	0.0901	-0.1483	0.04224
11.779	-0.0479	0.04611	-0.129	-0.11438	0.038866	-0.0043	-0.0287	0.01256	

11.699	0.0159	0.09077	0.07445	0.01572	0.018803	0.1092	0.01875	0.07397
11.662	-0.0046	-0.0635	0.09613	0.21037	0.098199	-0.049	-0.0505	0.05091
11.523	-0.077	-0.0799	-0.0933	0.06796	-	0.039252	0.1292	0.01749
11.52	0.1754	-0.075	0.04273	-0.09808	0.031925	-0.002	-0.0887	-0.1199
11.478	-0.1693	-0.1168	0.07515	0.02411	-	0.058712	0.1416	0.06162
11.318	-0.0638	0.09944	-0.1098	-0.04249	-0.16277	-0.0264	-0.0284	-0.094
11.292	0.0182	-0.1263	-0.095	0.03899	-0.01515	-0.0193	0.04317	0.01386
11.212	0.2086	-0.0016	0.00721	-0.17223	-	0.098876	0.0932	0.16378
11.16	-0.0273	0.09462	-0.0742	0.10245	-0.1159	-0.0026	-0.0687	0.10443
11.145	0.0766	-0.035	-0.0702	-0.08005	-	0.053267	0.0096	0.07543
11.115	-0.1692	0.04661	0.10106	-0.08892	0.16786	0.0695	-0.1085	0.07456
9.961	-0.0127	0.00573	0.10832	0.0645	0.029163	0.0141	-0.038	-0.1568
9.922	0.058	0.04972	-0.0727	0.05345	-	0.041188	-0.0789	-0.2049
9.832	-0.0241	-0.0019	0.07259	0.04603	-	0.010077	0.111	-0.0261
9.816	0.07	0.04957	0.02819	0.02915	-	0.064504	-0.0771	0.14874
9.769	0.0804	-0.1443	-0.0633	-0.13826	0.03024	-0.0891	0.09076	-0.073
9.73	-0.1162	0.0215	0.11644	-0.10743	-	0.065853	-0.0338	-0.017
9.692	-0.0245	0.06932	0.0849	-0.04309	0.002541	0.0074	-0.0849	-0.0266
9.656	0.0752	0.00807	0.04016	0.06599	-0.22488	0.0446	0.06658	0.01967
9.436	-0.0097	-0.0079	0.09317	-0.09944	0.028688	0.0336	0.04672	0.04352
9.399	0.0347	-0.1069	-0.1998	0.1493	-	0.045472	-0.014	-0.0086
9.35	-0.0279	-0.0429	0.16271	-0.09388	-0.14884	0.0869	0.02728	0.11936
9.236	-0.0173	0.00671	-0.006	0.00688	-	0.070682	0.1594	-0.146
9.179	0.0006	0.05722	0.16662	0.19237	0.03682	0.0254	0.19444	0.04139
9.146	0.0301	-0.08	0.00153	0.07373	-0.17603	-0.0935	-0.085	-0.0413
9.119	0.0172	0.02404	0.0733	0.00668	0.057006	-0.1135	-0.1564	-0.0573
8.896	0.1829	0.00864	0.08789	0.06557	-0.17239	-0.0019	0.03821	-0.1282
8.813	-0.0463	-0.0176	-0.0496	-0.09793	0.010483	0.1411	-0.0765	0.04673
8.68	0.035	-0.0224	0.09352	0.07047	-0.09952	0.1556	-0.0152	-0.094
8.565	0.0336	0.06497	0.01744	0.029	0.13615	0.0442	0.15781	0.05074
8.53	-0.1722	-0.0976	0.05983	-0.07254	0.013401	-0.0978	-0.0836	0.04753
8.436	-0.0987	0.09918	-0.0288	0.04565	-	0.080083	0.0944	-0.0799
8.353	0.048	-0.0649	-0.0016	0.11473	0.19521	-0.0186	-0.0799	0.11055
8.327	-0.017	-0.0204	-0.0215	-0.22932	0.067243	-0.0744	-0.0812	0.05042
8.24	0.0461	-0.0206	-0.1457	-0.09124	-	0.082357	0.0788	0.07903
8.18	-0.1443	-0.0564	-0.0256	0.12175	0.012325	0.0702	0.04988	-0.0743
8.13	0.071	0.07247	-0.0077	-0.2562	-	0.043357	-0.0135	0.01928

7.97	-0.036	0.0077	-0.1055	0.04448	-5.69E-05	-0.0277	0.06913	0.20638
7.833	-0.0349	-0.0956	-0.0512	-0.09168	-0.16441	-0.0609	0.00143	0.06438
7.751	0.0685	-0.0536	0.02585	-0.08224	0.046502	0.0435	-0.1081	0.00465
6.447	-0.0753	0.1619	0.01186	-0.09129	-0.00567	-0.2101	0.21263	-0.0307
6.144	-0.1943	0.03668	-0.0255	0.04317	-	0.044058	-0.0464	0.12529
5.571	0.0611	0.06223	-0.0381	-0.1077	-	0.013279	0.0365	0.01549
1.99	0.0284	-0.0135	0.01559	0.04093	0.020532	-0.0837	-0.0604	0.14126
1.959	-0.027	0.07768	-0.1415	-0.1699	0.19679	-0.1451	-0.1043	0.07549
1.79	0.088	-0.1176	0.0616	0.07359	0.10514	-0.0445	0.03728	0.07711
1.735	-0.1037	0.01816	-0.075	-0.09264	-0.10079	0.0457	0.09276	-0.0292
1.679	0.044	0.15863	0.05572	0.09174	0.0444	-0.0329	0.05955	0.14855
1.622	0.0153	0.13785	-0.12	0.07439	0.026916	0.0492	0.11077	0.02985
1.62	-0.0963	0.03656	0.02008	0.05496	0.077215	-0.2076	-0.1995	0.01076
1.56	0.113	-0.0317	0.00913	0.12697	0.21723	0.0277	-0.0138	-0.0155
1.532	0.1282	-0.1298	0.03958	0.01902	-	0.016684	0.1054	-0.0571
1.485	-0.0856	-0.1891	-0.0977	0.01702	0.019127	0.0666	0.0438	0.00748
1.342	-0.0714	-0.0615	0.17345	-0.10646	-0.03878	0.1415	0.00264	-0.0642
1.28	0.042	-0.0741	-0.0402	-0.00214	0.087695	0.0606	-0.0543	0.07194
1.238	-0.1996	0.03605	0.04702	0.00062	-	0.015764	0.0785	0.018
1.2	0.0222	0.01299	-0.0296	0.06809	-	0.057961	0.0352	-0.1045
1.122	-0.0524	0.13107	-0.018	0.09419	0.062389	-0.1213	0.05156	-0.0053

	PC17	PC18	PC19	PC20	PC21	PC22	PC23	PC24
Valine	0.14872	0.05395	0.13271	0.06505	0.077	0.0467	-0.11909	-0.0341
Urea	-0.0197	-0.2008	0.056329	0.11142	0.053	0.0298	0.10976	-0.1107
Tyrosine-1	0.0146	0.04692	0.11199	-0.1101	0.028	-0.072	-0.02197	0.02238
Trehalose	0.03811	0.04874	0.047649	0.04588	-0.236	0.102	0.08121	0.07945
Threonine_2	-0.1503	-0.0482	-0.006856	0.00157	-0.125	0.049	-0.03146	-0.0427
Threonine	-0.0125	-0.0774	0.049336	-0.0894	-0.035	-0.113	-0.12606	0.0802
Threonic acid	-0.0967	0.02802	-0.059265	0.1231	-0.017	0.0658	0.099938	-0.0058
Sucrose	0.03755	0.17421	0.15	-0.092	-0.045	0.0889	-0.05959	0.04851
Succinic acid	-0.0238	0.02413	0.058606	0.07153	-0.079	0.086	-0.00496	-0.1998
Serine_2	0.11971	0.00629	-0.0051	0.10897	0.004	0.0277	-0.15172	0.13179
Serine	-0.0203	-0.1102	0.039434	0.03032	0.059	-0.151	0.10669	-0.1231
Rhamnose-1	-0.0305	0.03654	0.082097	-0.1938	0.094	0.089	-0.10066	-0.0976
Phenylalanine	-0.2105	0.05908	-0.016013	-0.1741	-0.041	0.0538	-0.11828	0.00297
N-acetyl-hexosamine 2	-0.0012	-0.1536	0.055137	-0.2385	-0.019	0.0666	-0.04357	-0.126
N-acetyl-hexosamine	0.08867	-0.1486	0.074008	0.03234	-0.237	-0.047	-0.01486	0.03856
Myo-Inositol	-0.159	0.08409	0.082052	-0.0693	0.023	0.0168	0.11517	0.04009
Mannose	-0.1078	0.00056	-0.057652	0.12878	-0.102	0.0664	-0.01582	0.10637

Maltose	-0.0922	-0.0839	0.10313	-0.0052	0.027	-0.053	-0.00961	-0.0394
Malic acid	0.03958	0.09338	-0.031425	0.15749	-0.045	0.1905	0.13983	0.11889
Leucine	0.06585	-0.0133	0.078908	0.0245	-0.102	-0.024	-0.15511	0.08665
Isoleucine	-0.0386	0.07475	0.063285	0.01622	0.029	0.0429	-0.01965	-0.1076
Glycine	-0.0076	-0.0514	-0.12156	-0.1495	0.069	0.0289	0.10966	-0.0368
Glyceric acid	0.03676	-0.0459	-0.025275	-0.089	0.074	-0.156	-0.05495	-0.0166
Glucose3	-0.0658	-0.0392	0.06847	0.12562	-0.002	0.1207	-0.05983	-0.0043
Glucose-1-Phosphate-2	0.12262	0.02069	-0.10432	-0.0455	0.016	0.1921	-0.05385	0.03064
Glucose-1-Phosphate_1	0.06737	-0.0886	0.14787	0.03161	-0.027	-0.119	0.095105	0.02937
Glucose1	0.05409	0.0079	-0.14898	0.04541	0.148	-0.158	-0.00792	-0.1269
Galacturonic acid	-0.0058	0.04992	0.12139	0.02297	-0.024	0.0322	-0.17835	0.05607
Galacturonic acid	-0.1538	-0.1798	-0.0986	0.0034	-0.12	-0.076	-0.03845	-0.0933
Galactose	0.02641	0.08034	0.067351	0.03701	0.027	-0.037	0.006144	-0.12
Fumaric acid	0.01326	0.06219	-0.084299	-0.0655	-0.111	-0.075	0.024116	-0.2284
Fructose2	-0.0645	0.13758	-0.063388	0.10458	-0.027	-0.086	-0.06889	0.01962
Fructose1	-0.0855	0.00327	0.10549	0.06154	-0.035	0.0331	-0.04042	0.05022
Citric acid	0.26607	0.01202	-0.071116	0.00353	0.072	0.0489	-0.07794	-0.0363
Aspartic acid 2	-0.0985	-0.0902	-0.0696	-0.0144	-0.023	0.0209	-0.06015	0.01104
Aspartic acid 1	0.04896	0.09136	0.063611	0.10816	0.044	0.0119	0.065677	-0.0617
Arabinose	0.0601	0.04213	-0.13855	-0.0057	-0.088	-0.023	-0.01244	0.02256
AA_2	0.11719	-0.1867	-0.14023	0.02398	-0.063	-0.078	-0.1171	0.07287
AA_1	0.02684	0.04613	0.081229	-0.1183	0.039	-0.143	0.12966	-0.2057
19.225	0.02233	-0.1704	-0.052716	0.09286	0.03	-0.024	-0.03418	-0.0259
16.663	-0.0042	-0.0117	0.031527	0.0178	0.077	0.0644	-0.0729	0.03235
16.489	-0.092	-0.0984	-0.051077	-0.1301	0.055	-0.007	0.037595	-0.0542
16.342	-0.0684	-0.0205	0.065878	0.15181	-0.056	-0.06	-0.06146	0.01134
16.166	0.02128	-0.04	-0.015683	0.07391	-0.061	0.0066	0.061353	0.03739
14.834	-0.0786	0.00573	-0.056324	-0.0707	-0.103	0.0295	-0.04792	-0.012
14.627	-0.0238	-0.0247	0.17798	-0.0065	-0.157	-0.122	0.014974	0.02115
14.547	0.13001	-0.0535	0.073297	0.05993	0.041	-0.073	-0.22766	-0.0417
14.27	0.01095	0.14869	-0.002915	0.06447	0.128	0.0145	-0.15842	-0.0974
14.17	-0.0419	-0.0338	0.076033	0.02347	0.054	0.0538	-0.01372	0.01223
13.54	0.04078	-0.1705	-0.10282	-0.1204	0.096	-0.032	-0.02936	0.04269
13.461	0.02669	0.13362	0.15636	0.0601	0.035	-0.039	-0.14743	-0.0596
13.431	0.10842	-0.0115	-0.083974	0.03597	-0.02	-0.061	0.13644	0.01372
13.381	-0.0134	-0.1039	-0.054917	0.07816	0.017	-0.025	-0.03594	-0.0535
13.291	0.04405	-0.0283	-0.060764	-0.0043	0.133	0.0082	0.096654	-0.0208
13.134	0.02549	0.05483	0.013924	0.18107	0.05	0.1243	0.039921	-0.0805
12.961	0.0467	0.07997	0.0024798	0.04165	0.191	-0.016	0.014464	0.08268
12.851	0.01997	-0.0047	0.14256	-0.0125	0.087	-0.005	-0.1572	0.04269
12.678	0.00435	-0.0963	-0.008717	-0.005	-0.073	-0.089	-0.07754	-0.0298

12.653	0.00046	-0.0556	-0.08616	-0.1521	-0.061	-0.092	-0.06157	-0.0061
12.576	-0.0123	-0.024	0.24483	0.04535	0.101	-0.18	0.075855	-0.0209
12.498	0.07748	0.04084	-0.2169	0.06483	0.137	-0.046	-0.07623	-0.0489
12.428	0.20606	-0.0027	0.072955	-0.1503	-0.009	0.1322	0.19486	0.06112
12.419	-0.033	0.00315	-0.15042	-0.1039	0.102	0.1088	0.014499	-0.0619
12.251	-0.0253	-0.0255	-0.14686	-0.0061	-0.065	0.1006	0.046931	0.05798
11.954	-0.1355	0.06334	0.025689	-0.092	0.128	0.0601	-0.03771	0.02311
11.92	0.16304	0.09903	-0.085314	0.1794	0.033	-0.01	-0.06729	-0.05
11.871	-0.0674	0.05273	-0.085404	-0.0249	-0.194	-0.076	-8.89E-05	-0.0528
11.82	0.07044	0.01326	0.1485	-0.1058	-0.039	-0.028	0.07145	0.00776
11.779	0.22506	-0.0886	0.19552	-0.0712	0.154	0.1164	0.048999	-0.0199
11.699	-0.1068	-0.1209	0.050437	-0.0553	-0.073	0.1159	0.1116	0.06302
11.662	0.1871	0.09066	0.091013	-0.058	0.019	0.0583	0.092235	0.07647
11.523	0.05365	0.02899	0.035929	-0.0294	-0.027	0.1995	0.039149	0.06607
11.52	-0.0178	-0.0672	0.065869	0.14339	-0.22	0.0327	-0.04577	-0.0213
11.478	-0.1991	0.01756	0.067797	0.08397	0.103	-0.013	-0.11546	0.00581
11.318	0.08465	-0.1458	0.052558	-0.0275	0.049	0.0959	-0.20952	-0.0443
11.292	-0.0399	0.05666	0.027388	0.0156	-0.105	-0.177	-0.04376	0.06432
11.212	0.03527	-0.0304	0.048317	-0.0505	-0.038	0.03	-0.04789	-0.0688
11.16	-0.0743	0.13277	-0.013989	-0.0161	-0.123	-0.074	-0.03571	-0.0463
11.145	-0.0138	-0.1813	0.037384	0.0173	0.124	0.099	-0.05708	-0.0287
11.115	0.00321	0.07328	-0.11989	0.11857	-0.031	0.0177	-0.01841	0.03244
9.961	0.00868	0.01826	0.0030298	-0.0769	-9E-04	0.0476	0.1188	0.05781
9.922	-0.0966	0.09363	-0.11517	0.13668	0.134	-0.004	0.048281	-0.0384
9.832	0.00775	-0.0504	-0.10414	0.0489	0.002	0.11	-0.09764	-0.0201
9.816	-0.0687	-0.1675	-0.067721	-0.1921	-0.041	0.1494	-0.09311	0.00651
9.769	0.02961	0.06448	-0.08552	-0.062	-0.01	-0.034	0.071941	0.04966
9.73	-0.0806	0.08897	-0.032969	-0.1577	0.075	-0.087	0.012441	-0.0813
9.692	-0.1432	0.04865	-0.054789	-0.0412	0.089	0.0952	0.064787	-0.0018
9.656	-0.0293	0.20034	-0.024741	-0.0829	0.007	-0.184	-0.06546	0.0383
9.436	0.00197	-0.1404	0.0005324	0.18591	0.101	0.0769	0.025956	0.02633
9.399	-0.0839	-0.0345	0.042694	0.00308	-0.04	0.1432	0.05055	0.00609
9.35	0.00791	-0.0314	-0.05579	0.07351	-0.1	-0.007	0.15056	0.0958
9.236	-0.2104	-0.1029	-0.12755	0.01265	0.181	-0.079	0.16495	0.07034
9.179	0.1009	-0.0605	-0.05591	-0.0874	0.029	-0.003	0.17112	0.05815
9.146	0.15132	0.08226	-0.1469	0.04516	0.002	0.1565	0.049087	-0.0566
9.119	0.0745	0.0679	-0.15292	0.02981	-0.109	-0.057	0.05901	-0.042
8.896	-0.0221	0.0037	-0.084977	-0.0588	-0.081	0.0526	-0.09892	-0.0174
8.813	-0.0862	0.05814	-0.089811	0.12959	-0.038	-4E-04	0.015246	0.02658
8.68	0.04816	0.03013	0.0012482	0.0027	0.046	-0.176	0.04081	0.07639
8.565	0.01525	0.10997	0.11663	-0.0104	-0.119	-0.116	0.087505	0.01637
8.53	0.05717	-0.0047	0.11297	0.03648	0.021	0.0075	-0.03037	-0.0029
8.436	0.0334	0.06802	-0.045363	-0.1444	0.009	0.0058	-0.00276	0.06686
8.353	-0.0507	-0.1099	-0.058594	0.06195	0.033	-0.197	0.025176	0.02747

8.327	-0.0039	0.03711	-0.082108	0.05693	0.184	0.0474	-0.11415	0.00137
8.24	-0.0826	-0.1578	0.056971	0.12432	0.108	-0.056	0.16145	-0.0274
8.18	-0.0313	-0.0274	-0.008818	0.10103	0.044	-0.057	-0.01441	0.39751
8.13	0.00143	0.17753	0.018113	-0.0376	-0.002	-0.123	0.16516	0.16773
7.97	-0.0971	0.14038	0.017836	-0.035	-0.027	0.0093	0.023751	-0.0196
7.833	-0.0285	-0.0108	0.011199	-0.0116	-0.034	-0.075	-0.14163	0.02966
7.751	-0.0239	0.0138	-0.005289	-0.0154	0.046	0.0085	-0.10803	0.0098
6.447	-0.0418	0.05062	-0.095724	-0.0632	0.067	-0.065	-0.01738	0.26437
6.144	0.02904	0.07822	-0.006999	0.05874	-0.081	-0.028	0.0986	-0.464
5.571	0.01596	-0.0932	0.032852	0.0997	-0.157	0.1219	0.072533	-0.1823
1.99	0.06567	0.07124	-0.042812	0.03616	-0.121	0.0095	-0.03296	0.00498
1.959	0.15974	0.07361	-0.055732	-0.0666	-0.108	-0.025	-0.01908	0.0265
1.79	-0.1014	-0.0745	0.040589	0.02799	0.023	0.0242	0.10485	0.02229
1.735	-0.0311	-0.0777	0.23132	0.14807	0.02	0.0127	0.049935	0.05089
1.679	0.09929	0.00527	-0.097954	0.00344	0.003	0.0744	0.02919	-0.0275
1.622	-0.0012	0.02546	-0.070371	0.02172	-0.067	-0.138	-0.14388	-0.0188
1.62	-0.0131	0.0785	0.017535	-0.1115	-0.029	0.1714	-0.05077	0.04006
1.56	-0.2899	0.12857	0.060249	-0.0168	0.039	0.2293	-0.08322	-0.0297
1.532	0.02489	-0.0179	0.096713	-0.1829	0.051	-0.015	0.075623	0.03365
1.485	-0.0333	0.05689	0.014272	-0.0978	-0.055	-0.046	-0.01324	0.03487
1.342	-0.1427	0.17614	0.077016	0.08881	0.014	0.051	0.094796	-0.0169
1.28	0.04997	-0.037	0.098259	-0.0474	-0.059	-0.012	0.13252	0.02378
1.238	0.03562	-0.1132	-0.069373	-0.0543	-0.248	0.0886	-0.00438	0.03773
1.2	0.0593	0.16419	-0.04749	0.003	0.022	0.03	0.097623	-0.0367
1.122	0.0069	-0.0977	8.91E-05	0.03743	0.133	0.0164	0.055447	0.06176

Appendix K

1. The unique upregulated genes under dark/light conditions in *dufko3* mutant

test_id	log2(fold_change)	q_value	test_id	log2(fold_change)	q_value
AT2G26010	4.03738	0.004325	AT1G34060	1.32433	0.004325
AT4G24340	3.91949	0.004325	AT3G57240	1.32357	0.004325
AT5G44430	3.33609	0.004325	AT1G15125	1.31742	0.007757
AT2G26020	3.11114	0.004325	AT5G52760	1.31665	0.004325
AT5G19470	2.88093	0.004325	AT1G52410	1.31077	0.004325
AT2G24210	2.78264	0.004325	AT5G59670	1.30895	0.004325
AT5G44420	2.60938	0.004325	AT4G23230	1.30835	0.004325
AT2G43590	2.58273	0.004325	AT2G46430	1.30834	0.004325
AT4G08570	2.38383	0.004325	AT5G42530	1.28747	0.004325
AT1G21310	2.27288	0.004325	AT2G39330	1.28627	0.004325
AT1G66960	2.15788	0.007757	AT1G54020	1.28206	0.004325
AT1G65790	2.10757	0.004325	AT5G52750	1.27819	0.004325
AT3G11010	2.00243	0.004325	AT4G23220	1.27792	0.004325
AT5G42800	1.99427	0.004325	AT3G48080	1.27397	0.004325
AT5G22545	1.98077	0.007757	AT1G21250	1.27387	0.004325
AT1G09080	1.97844	0.004325	AT1G52400	1.26882	0.013702
AT1G67000	1.91831	0.004325	AT2G43150	1.26119	0.004325
AT4G23140	1.9052	0.004325	AT5G55450	1.24734	0.004325
AT4G04500	1.90482	0.004325	AT1G76790	1.24487	0.007757
AT1G35710	1.89653	0.004325	AT4G18440	1.23445	0.004325
AT4G23310	1.88218	0.004325	AT5G10760	1.23443	0.004325
AT2G15040	1.84033	0.007757	AT2G31880	1.22851	0.004325
AT2G15042	1.80152	0.004325	AT4G01010	1.22708	0.004325
AT1G58225	1.78917	0.004325	AT2G17040	1.2262	0.004325
AT4G23150	1.78733	0.004325	AT1G30900	1.22557	0.004325
AT5G61160	1.72691	0.004325	AT3G07520	1.21275	0.004325
AT1G03940	1.71276	0.004325	AT4G23180	1.20991	0.004325
AT3G25010	1.69598	0.004325	AT5G45380	1.20347	0.004325
AT3G09940	1.68928	0.004325	AT1G61120	1.19256	0.004325
AT5G24780	1.66153	0.004325	AT3G61990	1.18777	0.004325
AT1G21240	1.65696	0.004325	AT1G72830	1.18586	0.007757
AT5G24770	1.64673	0.004325	AT5G60800	1.18443	0.004325
AT4G37140	1.63544	0.004325	AT1G24070	1.18141	0.004325
AT2G32680	1.63119	0.004325	AT4G21850	1.17964	0.004325
AT5G07990	1.5955	0.004325	AT3G16470	1.17737	0.004325
AT2G18660	1.58258	0.004325	AT1G64360	1.17181	0.004325
AT4G18250	1.58121	0.004325	AT5G05460	1.16934	0.004325
AT2G24160	1.58077	0.004325	AT2G20340	1.16843	0.004325
AT5G27060	1.56881	0.013702	AT5G24530	1.16552	0.004325
AT1G13470	1.56461	0.004325	AT1G23840	1.14163	0.010872

AT3G23120	1.5619	0.004325	AT1G58270	1.139	0.004325
AT4G22880	1.54345	0.004325	AT4G27860	1.13707	0.004325
AT5G48850	1.5367	0.004325	AT5G39670	1.13655	0.010872
AT5G22380	1.53591	0.010872	AT2G24600	1.13453	0.004325
AT1G03495	1.52273	0.004325	AT5G58940	1.13265	0.004325
AT5G15500	1.51059	0.004325	AT2G46400	1.13161	0.004325
AT4G24450	1.49208	0.004325	AT2G43530	1.13144	0.004325
AT1G56600	1.48888	0.004325	AT4G24350	1.12817	0.004325
AT1G68600	1.48395	0.004325	AT4G23130	1.12725	0.004325
AT5G38210	1.48073	0.007757	AT4G16590	1.11535	0.004325
AT2G04460	1.47345	0.004325	AT4G27300	1.11278	0.004325
AT5G54060	1.46149	0.004325	AT2G31865	1.10649	0.004325
AT1G76960	1.45233	0.004325	AT1G66880	1.10233	0.004325
AT4G17470	1.44633	0.004325	AT1G28230	1.0995	0.004325
AT1G24145	1.4353	0.004325	AT1G07620	1.08886	0.010872
AT3G50280	1.43501	0.004325	AT3G28270	1.08512	0.007757
AT2G39030	1.41826	0.004325	AT4G02520	1.07805	0.004325
AT3G08860	1.4127	0.004325	AT3G48090	1.07654	0.004325
AT5G64810	1.4067	0.013702	AT1G22160	1.07192	0.004325
AT3G25510	1.40451	0.004325	AT1G54010	1.06784	0.004325
AT3G45860	1.3679	0.004325	AT2G28940	1.0666	0.010872
AT3G28220	1.36702	0.004325	AT2G39800	1.06398	0.010872
AT1G34420	1.36612	0.007757	AT1G18710	1.06064	0.004325
AT3G26210	1.36506	0.004325	AT5G53550	1.06007	0.004325
AT3G61280	1.36023	0.004325	AT1G21400	1.03397	0.004325
AT1G62540	1.35372	0.004325	AT4G13900	1.01786	0.004325
AT5G22570	1.34623	0.004325	AT4G08850	1.01388	0.013702
AT4G38340	1.33938	0.007757	AT4G39210	1.00368	0.007757

2. The unique upregulated genes under dark conditions in *dufko3* mutant

gene_id	log2(fold_change)	q_value	gene_id	log2(fold_change)	q_value
AT2G41850	4.709	0.003	AT4G32810	1.684	0.003
AT2G36780	4.549	0.003	AT4G37370	1.648	0.003
AT1G11190	4.325	0.003	AT4G37010	1.619	0.006
AT1G03790	4.178	0.003	AT2G23170	1.614	0.003
AT2G29470	4.094	0.003	AT3G06420	1.578	0.003
AT5G45890	3.939	0.003	AT2G31945	1.545	0.003
AT1G09500	3.929	0.003	AT4G00700	1.519	0.006
AT4G18425	3.914	0.003	AT5G48180	1.511	0.003
AT3G02480	3.746	0.003	AT2G33380	1.506	0.003
AT3G01420	3.713	0.003	AT2G15220	1.479	0.003

AT1G20180	3.650	0.003	AT1G47510	1.424	0.003
AT1G14880	3.591	0.003	AT4G24000	1.419	0.003
AT3G05400	3.472	0.003	AT5G19520	1.418	0.006
AT3G28210	3.427	0.003	AT2G29350	1.406	0.003
AT1G09380	3.269	0.003	AT3G22370	1.402	0.003
AT5G45630	3.125	0.003	AT4G31970	1.373	0.003
AT5G50260	3.122	0.003	AT2G29940	1.365	0.003
AT3G05630	3.070	0.003	AT3G49120	1.365	0.003
AT5G40690	2.995	0.003	AT1G17020	1.363	0.003
AT1G68450	2.880	0.008	AT3G55500	1.350	0.003
AT4G37390	2.873	0.003	AT3G14440	1.336	0.003
AT1G05100	2.806	0.003	AT2G22470	1.307	0.003
AT2G45570	2.797	0.003	AT1G26380	1.294	0.013
AT2G01890	2.749	0.003	AT1G55020	1.248	0.003
AT1G61800	2.718	0.003	AT1G08920	1.246	0.003
AT3G19615	2.681	0.013	AT1G20630	1.210	0.003
AT1G02390	2.552	0.003	AT4G10120	1.183	0.008
AT2G25460	2.510	0.003	AT4G13250	1.179	0.003
AT1G19200	2.480	0.003	AT1G28130	1.176	0.003
AT1G30700	2.461	0.003	AT1G74020	1.176	0.003
AT1G15520	2.384	0.003	AT5G16360	1.158	0.003
AT1G13520	2.334	0.003	AT3G14770	1.154	0.003
AT2G25625	2.249	0.003	AT1G62570	1.141	0.003
AT3G60140	2.233	0.003	AT4G25000	1.128	0.008
AT4G39670	2.168	0.003	AT2G19970	1.117	0.013
AT1G29640	2.143	0.003	AT4G32250	1.090	0.003
AT5G43580	2.102	0.003	AT1G78230	1.090	0.008
AT3G21500	2.075	0.003	AT1G74010	1.065	0.003
AT5G50760	2.057	0.003	AT5G05410	1.013	0.008
AT4G33467	1.989	0.003	AT1G26390	1.010	0.003
AT1G58340	1.986	0.003	AT5G20830	1.007	0.003
AT5G18270	1.966	0.003	AT2G26560	0.988	0.003
AT1G01560	1.944	0.003	AT1G05340	0.954	0.003
AT4G01430	1.944	0.003	AT3G44300	0.922	0.008
AT1G54570	1.939	0.003	AT5G59220	0.859	0.008
AT1G62760	1.888	0.003	AT2G19950	0.825	0.003
AT2G27389	1.862	0.013	AT1G32450	0.824	0.006
AT4G37430	1.857	0.003	AT4G02940	0.817	0.003
AT5G48410	1.844	0.008	AT4G22920	0.816	0.003
AT1G52690	1.841	0.011	AT5G17460	0.808	0.003
AT1G48260	1.816	0.003	AT3G15500	0.804	0.006
AT5G28237	1.799	0.003	AT2G41190	0.794	0.003
AT5G13080	1.784	0.003	AT1G77770	0.786	0.013
AT4G18980	1.773	0.003	AT3G50970	0.782	0.003

AT5G04200	1.764	0.008	AT1G73260	0.779	0.003
AT1G32350	1.728	0.003	AT5G11520	0.779	0.003
AT4G37990	1.710	0.003	AT4G14400	0.744	0.003
AT1G01480	1.700	0.003	AT5G52310	0.733	0.003

Appendix L

1. The unique downregulated genes under dark conditions in *dufko3* mutant

gene_id	log2 (fold_change)	q_value	gene_id	log2 (fold_change)	q_value
AT3G19680	-0.605	0.013	AT3G15210	-1.310	0.003
AT4G36900	-0.616	0.013	AT4G11320	-1.323	0.003
AT4G38970	-0.638	0.013	AT5G07460	-1.331	0.003
AT2G47730	-0.664	0.008	AT5G05440	-1.335	0.003
AT5G06870	-0.678	0.006	AT1G21500	-1.338	0.003
AT4G39980	-0.682	0.006	AT1G24100	-1.366	0.003
AT4G28750	-0.689	0.011	AT1G67750	-1.378	0.006
AT4G34881	-0.697	0.006	AT1G21440	-1.393	0.003
AT3G20470	-0.699	0.008	AT2G38870	-1.402	0.003
AT3G25760	-0.711	0.011	AT1G17420	-1.403	0.003
AT4G38680	-0.726	0.006	AT1G44575	-1.409	0.003
AT4G31800	-0.726	0.008	AT3G21080	-1.412	0.006
AT1G80180	-0.732	0.003	AT1G52040	-1.423	0.003
AT1G30380	-0.733	0.003	AT3G49110	-1.428	0.003
AT3G03780	-0.735	0.003	AT1G76930	-1.428	0.003
AT1G61890	-0.739	0.003	AT2G24600	-1.451	0.003
AT4G08950	-0.755	0.006	AT5G22500	-1.483	0.003
AT1G79850	-0.766	0.008	AT5G58390	-1.492	0.003
AT3G16400	-0.769	0.003	AT2G29890	-1.500	0.006
AT2G47910	-0.776	0.006	AT4G12480	-1.509	0.003
AT3G25770	-0.780	0.006	AT5G41040	-1.518	0.013
AT1G64500	-0.789	0.003	AT4G18440	-1.527	0.003
AT1G28400	-0.798	0.013	AT2G42840	-1.536	0.003
AT2G06050	-0.809	0.003	AT4G08870	-1.556	0.003
AT2G41100	-0.824	0.003	AT2G39030	-1.581	0.003
AT1G70370	-0.835	0.006	AT2G33850	-1.585	0.003
AT2G43530	-0.841	0.003	AT1G52400	-1.602	0.003
AT2G45070	-0.851	0.003	AT4G21650	-1.607	0.003
AT1G64660	-0.853	0.003	AT1G54020	-1.609	0.003
AT4G38740	-0.856	0.003	AT1G72520	-1.620	0.003
AT2G14750	-0.859	0.011	AT4G04610	-1.622	0.003
AT5G13220	-0.868	0.006	AT4G30280	-1.643	0.008
AT2G01080	-0.873	0.006	AT5G44420	-1.649	0.003
AT3G45140	-0.874	0.013	AT4G29700	-1.653	0.003
AT3G16460	-0.875	0.003	AT1G61120	-1.653	0.003
AT4G27520	-0.885	0.003	AT5G24420	-1.696	0.003
AT1G67870	-0.908	0.003	AT3G17840	-1.701	0.003
AT5G55120	-0.913	0.003	AT4G28780	-1.727	0.003

AT3G59930	-0.919	0.003	AT4G24570	-1.746	0.003
AT1G64390	-0.922	0.008	AT3G59220	-1.767	0.006
AT3G10985	-0.930	0.003	AT1G52030	-1.773	0.003
AT5G02940	-0.945	0.003	AT4G17470	-1.803	0.003
AT5G66200	-0.950	0.003	AT1G26770	-1.806	0.011
AT5G65390	-0.951	0.013	AT5G16250	-1.833	0.006
AT1G52000	-0.956	0.003	AT5G05340	-1.853	0.006
AT2G47840	-0.960	0.003	AT4G22517	-1.871	0.011
AT5G05600	-0.974	0.003	AT3G04290	-1.899	0.003
AT1G35140	-1.005	0.003	AT1G72260	-1.917	0.003
AT1G54010	-1.007	0.003	AT5G55730	-1.941	0.003
AT4G31500	-1.008	0.003	AT4G37450	-1.980	0.006
AT2G02100	-1.011	0.003	AT2G39330	-1.989	0.003
AT2G38750	-1.020	0.006	AT4G39510	-2.008	0.003
AT3G16470	-1.030	0.003	AT5G09530	-2.010	0.003
AT3G54400	-1.031	0.006	AT5G22880	-2.044	0.003
AT2G28950	-1.037	0.003	AT5G28490	-2.072	0.006
AT3G44720	-1.040	0.003	AT1G19670	-2.085	0.003
AT3G50770	-1.049	0.003	AT4G15210	-2.085	0.003
AT3G23290	-1.061	0.003	AT3G63200	-2.110	0.006
AT3G63390	-1.064	0.003	AT1G18590	-2.119	0.003
AT3G45060	-1.072	0.011	AT5G09600	-2.178	0.011
AT1G52410	-1.074	0.003	AT3G07320	-2.190	0.006
AT1G20510	-1.078	0.003	AT2G16060	-2.224	0.013
AT2G36830	-1.083	0.003	AT4G38950	-2.225	0.003
AT1G30530	-1.092	0.003	AT3G12145	-2.230	0.003
AT2G21140	-1.093	0.006	AT5G13930	-2.298	0.003
AT5G09440	-1.102	0.003	AT5G45670	-2.328	0.003
AT1G56580	-1.110	0.003	AT4G37800	-2.359	0.013
AT5G38410	-1.113	0.003	AT4G22505	-2.361	0.003
AT2G34600	-1.115	0.006	AT4G39940	-2.377	0.003
AT2G34420	-1.116	0.003	AT1G29910	-2.404	0.003
AT1G10960	-1.132	0.003	AT1G08560	-2.443	0.006
AT3G23810	-1.133	0.003	AT5G23010	-2.472	0.003
AT4G21850	-1.154	0.003	AT1G09200	-2.503	0.003
AT1G19610	-1.162	0.003	AT5G20740	-2.520	0.006
AT1G66100	-1.167	0.003	AT5G44430	-2.583	0.003
AT5G60890	-1.192	0.008	AT5G24780	-2.593	0.003
AT4G36360	-1.206	0.003	AT5G10390	-2.593	0.008
AT2G22330	-1.216	0.003	AT2G46650	-2.651	0.003
AT3G21055	-1.216	0.003	AT3G53190	-2.722	0.003
AT1G15820	-1.218	0.003	AT1G24070	-2.764	0.003
AT2G23130	-1.219	0.003	AT1G22480	-2.861	0.013
AT2G43540	-1.221	0.003	AT2G28790	-2.908	0.003

AT4G04840	-1.223	0.013	AT1G45191	-2.920	0.011
AT1G29920	-1.223	0.003	AT5G23940	-2.940	0.003
AT2G20610	-1.227	0.003	AT3G54600	-3.143	0.003
AT4G23210	-1.229	0.003	AT2G03090	-3.276	0.003
AT2G35930	-1.236	0.011	AT5G14200	-3.293	0.003
AT2G38530	-1.244	0.003	AT4G30140	-3.294	0.003
AT3G51450	-1.246	0.003	AT5G59870	-3.363	0.003
AT1G74100	-1.254	0.003	AT4G28250	-3.369	0.003
AT5G24770	-1.271	0.006	AT4G13770	-3.584	0.003
ATMG01390	-1.272	0.003	AT4G12030	-3.737	0.003
AT1G17380	-1.275	0.003	AT1G16410	-3.877	0.003
AT5G14180	-1.284	0.003	AT3G19710	-4.208	0.003
AT3G25780	-1.284	0.006	AT5G47500	-4.240	0.013
AT4G37750	-1.289	0.003	AT1G78370	-4.322	0.003
AT4G29020	-1.289	0.003	AT1G62560	-4.463	0.003
AT1G72970	-1.289	0.003	AT1G24020	-4.987	0.003
AT3G28220	-1.301	0.003	AT3G58990	-4.997	0.003
AT1G06360	-1.303	0.003	AT2G43100	-5.026	0.003
AT1G25275	-1.309	0.003	AT1G65860	-5.158	0.003
AT5G11550	-1.309	0.003	AT1G70260	-5.278	0.003
			AT3G02020	-5.326	0.003

Appendix M

Most proteins detected after co-immunoprecipitation with GFP antibody. Yes indicates the presence in the sample, No indicates absence in the sample.

Protein	Ct-DUF	Wt	Nt-SS4	P19
A0A088F9I1	Yes	Yes	No	No
A0A0A7HI84	Yes	No	Yes	Yes
A0A0A8IBT8	Yes	No	Yes	Yes
A0A0A8K9V3	Yes	Yes	Yes	Yes
A0A0H5B1M3	Yes	No	Yes	Yes
A0A0S4IJL0	No	No	Yes	Yes
A4D0J9	Yes	No	No	No
B2C7Y6	Yes	No	Yes	No
C9DFA3	Yes	No	Yes	No
D2DMF5	No	Yes	No	Yes
D5LT98	Yes	No	No	No
E0X584	Yes	No	No	Yes
E5LLE7	Yes	No	No	Yes
F8WQS2	Yes	No	No	No
A0A088F8F4	Yes	No	No	No
I0B7J5	Yes	No	No	Yes
I0B7J6	Yes	No	No	No
I0B7J8	Yes	No	No	No
K7ZLE1	Yes	No	No	Yes
Q2LAH0	No	No	No	Yes
Q4TVR0	No	No	No	Yes
Q5EEQ1	No	No	No	Yes
Q6XX19	Yes	Yes	No	Yes
R9W4N2	No	No	No	Yes
U3MY90	No	Yes	No	Yes